Self-nanoemulsifying drug delivery systems (SNEDDS) for solubility enhancement - new approaches for determining appropriate formulations for liquid SNEDDS and their conversion to solid SNEDDS

INAUGURALDISSERTATION

zur Erlangung des akademischen Grades eines

Doktors der Naturwissenschaften (Dr. rer. nat.)

der

Mathematisch-Naturwissenschaftlichen Fakultät

der

Universität Greifswald

vorgelegt von

Fabian-Pascal Schmied

Greifswald, 07.12.2022

Dekan: Prof. Dr. Gerald Kerth

1. Gutachter: Prof. Dr. Sandra Klein

2. Gutachter: Prof. Dr. Thomas Rades

Tag der Promotion: 09.05.2023

Table of contents

List of abbreviations

API	active pharmaceutical ingredient
ASD	amorphous solid dispersion
BCS	biopharmaceutics classification system
CTA	chain-transfer-agent
DAoI	designated area of interest
DoE	design of experiment
DSC	differential scanning calorimetry
e.g.	*exempli gratia* (for the sake of example)
HLB	hydrophilic lipophilic balance
HME	hot melt extrusion
ICH	international conference on harmonization
i.e.	*id est* (that is)
kDa	kiloDalton (unit)
LFCS	lipid formulation classification system
LBDDS	lipid-based drug delivery system
LNP	lipid nanoparticle
LogP	n-octanol-water partition coefficient
L-SNEDDS	liquid self-nanoemulsifying drug delivery system
M-GA	cellulose-based microparticle with gum arabic
M-MC	cellulose-based microparticle with methylcellulose
ModE	"modified EUDRAGIT E PO" (aminomethacrylate-based copolymer)
M_n	number-average molecular weight
M_w	weight-average molecular weight

mg	milligram (unit)
ml	milliliter (unit)
nm	nanometer (unit)
PDI	polydispersity index
pH	decimal logarithm of reciprocal of hydrogen ion activity in a solution
Ph. Eur.	European Pharmacopoeia
RSD	relative standard deviation
S-SEDDS	solid self-emulsifying drug delivery system
SMEDDS	self-microemulsifying drug delivery system
SNEDDS	self-nanoemulsifying drug delivery system
S-SNEDDS	solid self-nanoemulsifying drug delivery system
T_g	glass transition temperature
T_m	melting temperature
USP	United States Pharmacopeia
XRPD	x-ray powder diffraction

1. Introduction

The oral administration of drugs is the most popular way to achieve pharmacological effects for adequate disease treatment as it exhibits a painless application route accompanied with high patient acceptance and convenience (1-3). A highly challenging feature of many orally administered drugs is their poor aqueous solubility that can be responsible for limited as well as strongly variable drug absorption (3-11). Limited absorption of the unprocessed drugs which ultimately leads to low bioavailability, essentially complicates achieving the minimum threshold concentration that is necessary for establishing therapeutic drug plasma levels (11-16). The question therefore arises as to how to meet the growing challenge of developing suitable formulations that provide pronounced solubility enhancement of poorly water-soluble active pharmaceutical ingredients (APIs) after their oral administration.

According to recent studies, about 40% of the drugs on the market and up to 75% of the drugs in the state of development are poorly water-soluble (17). Drugs associated with poor aqueous solubility can be further distinguished into "grease ball" and "brick dust" molecules (18, 19). Whereas the aqueous solubility of "grease ball" molecules is limited due to their pronounced lipophilic character (LogP > 3), "brick dust" molecules are characterized by very high melting points (T_m > 200 °C) accompanied by a high crystal lattice energy that substantially impedes the drugs' solubility (18, 19). The growing number of drug candidates that are poorly water-soluble proves the necessity to establish formulation approaches in order to counteract the solubility issue.

Basically, there are different approaches to classify the solubility of drugs, which can simplify the identification of challenging drug candidates. Based on the solubility criteria of the European Pharmacopoeia (Ph. Eur.) as well as the United States Pharmacopeia (USP), drugs are categorized according to their saturation solubility. Drugs associated with the descriptive terms "very slightly soluble" or "practically insoluble (solubility < 0.1 mg/ml)" in water are usually referred to as the critical ones that require improvement of aqueous solubility to achieve adequate drug plasma levels after oral administration.

The Biopharmaceutics Classification System (BCS) implemented by Gordon Amidon in 1995 categorizes drugs according to their expected bioavailability. The concept is based on the principle that the oral bioavailability of a drug is essentially determined by its solubility and its permeation properties. According to the BCS, drugs are categorized into four different classes (Class I - IV) (Figure 1). Class II includes drugs that exhibit a low solubility and high permeability whereas Class IV involves drugs being poorly soluble as well as poorly permeable (Figure 1). Hence, drugs assigned to Class II or IV are attractive drug candidates for solubility improvement

studies, especially drugs assigned to Class II as they are often subjected to dissolution rate limited absorption.
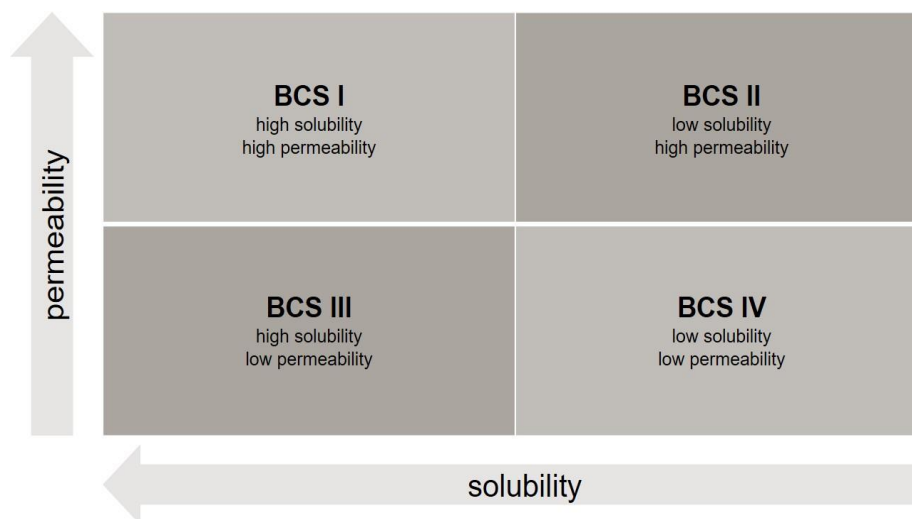

Figure 1: Visualization of the Biopharmaceutics Classification System (BCS).

The solubility of drugs is further influenced by a multitude of factors resulting in high complexity which may be overcome by various solubility enhancement strategies (20). Different approaches for solubility enhancement of drugs may be selected when considering the individual properties of a drug, the route of application and dose of a drug as well as the dosage form used.

Improved solubility in water can be achieved by affecting the crystal lattice structure or nanoencapsulation of the drug substance (21, 22). Furthermore, reducing the drugs' lipophilicity by chemical reaction such as linkage to hydrophilic groups (prodrug synthesis) is a conceivable, alternative strategy (22, 23). In order to successfully manage the challenge of drugs' poor aqueous solubility and/or dissolution, strategies such as salt formation, particle size reduction, micellar solutions, complexation using cyclodextrins, nanoemulsions and amorphization leading to supersaturation of the drug in aqueous media can be applied (1, 11, 12, 16, 17, 24). The recent increase in the number of publications regarding lipid-based drug delivery systems (LBDDSs), for instance lipid nanoparticles (LNPs), liposomes and especially self-nanoemulsifying drug delivery systems (SNEDDS) emphasizes the major importance of developing these formulation systems for the pharmaceutical science as well as industry (2, 7, 25). As an approach to categorize compositions and characteristics of lipid-based formulations resulting in micro- or nanoemulsions when dispersed in an aqueous medium, the Lipid Formulation Classification System (LFCS) by Porter *et al.* (25), which distinguishes four different types of lipid-based formulations has been proposed (Table 1) (25, 26). LFCS Type I formulation approaches comprise triglycerides or mixed mono-, di- and triglycerides, whereas LFCS Type II describes a group of formulations that consists of glycerides combined with water-insoluble surfactants having a hydrophilic lipophilic balance (HLB) < 12 (25). Compared to the LFCS Type I and II, the more

advanced LFCS Type III formulation approach envisions the replacement of water-insoluble surfactants with water-soluble surfactants (HLB > 12) and enables additional use of hydrophilic co-solvents (25).

Table 1

Lipid Formulation Classification System (LFCS) adapted from Porter *et al.* (25).

Components and properties	Type I	Type II	Type IIIa	Type IIIb	Type IV
Triglycerides or mixed glycerides [%]	100	40 - 80	40 - 80	< 20	-
Water-insoluble surfactants (HLB < 12) [%]	-	20 - 60	-	-	0 - 20
Water-soluble surfactants (HLB > 12) [%]	-	-	20 - 40	20 - 50	30 - 80
Hydrophilic co-solvents	-	-	0 - 40	20 - 50	0 - 20
Particle size [nm]	coarse	100 - 250	100 - 250	50 - 100	< 50
Significance of aqueous dilution	limited importance	solvent capacity unaffected	some loss of solvent capacity	significant phase changes and potential loss of solvent capacity	significant phase changes and potential loss of solvent capacity
Significance of digestibility	crucial requirement	not crucial but likely to occur	not crucial but may be inhibited	not required	not required

Furthermore, Porter *et al.* (25) subdivide the LFCS Type III formulations into categories a and b, which include the same types of components, but different quantity ranges for each of these components (25). The different quantity ranges for components mentioned in the LFCS affect parameters such as particle/droplet size as well as the significance of aqueous dilution and digestibility (Table 2), that have been studied for all LFCS formulation types listed in the LFCS by Porter *et al.* (25). The LFCS is completed by the LFCS Type IV formulations, which are free of triglycerides or mixed glycerides and present with reduced particle/droplet size upon contact with an aqueous medium as stated for LFCS Type III formulations (25). Considering the LFCS system, the question now arises which LFCS type the SNEDDS can be assigned to. Due to composition and resulting droplet size after dispersion in an aqueous medium, SNEDDS could be assigned LFCS Type IIIb formulations. Basically, SNEDDS consist of an oil or a lipid that is combined with a surfactant or a blend of surfactants, a co-solvent, if required, and can incorporate a lipophilic drug substance (Figure 2) (27-29). As multi-component, homogeneous, and anhydrous liquids, orally administered SNEDDS spontaneously form translucent nanoemulsions when in contact with gastrointestinal fluids under agitation of digestive motility (28, 30).
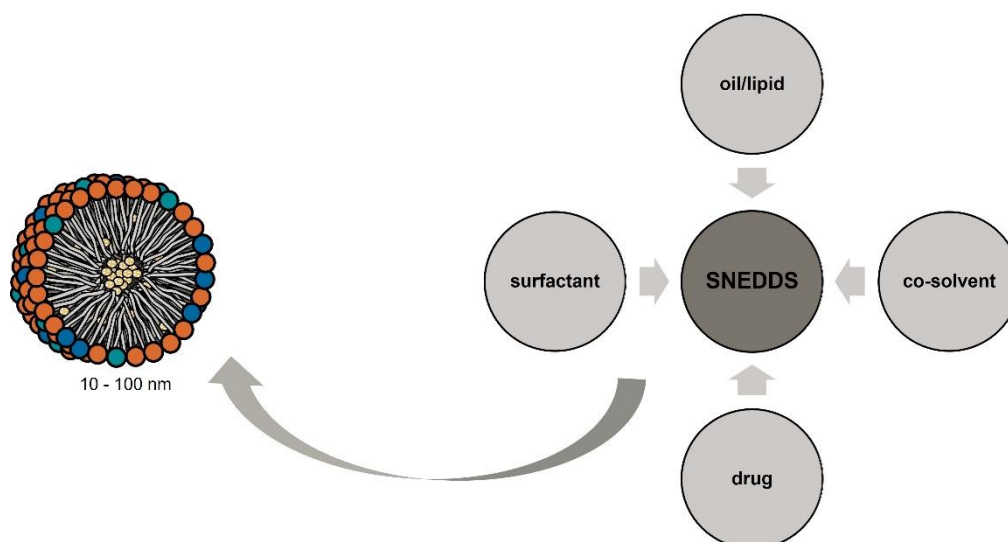
Figure 2: Multi-component structure of drug-loaded SNEDDS (mixed micelle) comprising oil/lipid (colored yellow), surfactant(s) (colored orange, blue and green), co-solvent (not colored, surrounding the mixed micelle) and incorporated drug (white dots) resulting preferably in a droplet size range of 10 - 100 nm.

In fact, the principal of SNEDDS or self-microemulsifying drug delivery systems (SMEDDS), that emerged during the last two decades, reveals a promising formulation approach in the research field of solubility enhancement (2, 31). Mixing of the individual components and, if necessary, melting during the mixing process in the case of semi-solid or solid SNEDDS' excipients proves to be a simple manufacturing technique with the possibility to scale up the process (2, 11, 32). In addition, the manufacturing process can be performed continuously and without organic solvents (2, 11, 32). Referring to the nomenclature of these systems, so far it is not completely assured how to technically differentiate between SNEDDS and SMEDDS. There is a general discussion about whether it is reasonable to categorize the two self-emulsifying systems according to their droplet size (SNEDDS < 100 nm, SMEDDS 100 - 250 nm) (22, 27). Another reported approach for distinction refers to different stability theories indicating that SNEDDS may be kinetically and SMEDDS thermodynamically stable (10, 33).

Essentially, there are several advantages linked to the SNEDDS technology. The comparatively low free energy and a minimum interfacial tension of the instantaneously forming, optically translucent nano-emulsifying systems are responsible for the pronounced stability of SNEDDS (10, 11, 25, 34). Compared to conventional dosage forms (e.g., tablets), additional benefits of SNEDDS such as an omitted dissolution step of a solid drug prior to drug absorption in the intestine as the drug is already dissolved in a water-free preconcentrate as well as obtained droplet sizes in the lower nanometer range after dispersion in an aqueous fluid may facilitate intestinal drug absorption (22, 23, 35, 36). A certain risk of precipitation of the drug still exists since it must leave the SNEDDS formulation again, immediately before absorption in order to exert its pharmacological effect. Depending on the properties of the excipients that comprise a

SNEDDS formulation, drugs that are prone to enzymatic degradation in the gastrointestinal tract such as peptides or proteins, might be properly delivered due to the ability of SNEDDS to provide drug protection by preventing contact to enzymes (2, 11, 32, 37). Furthermore, efflux transporters which limit the intestinal absorption of drugs and are located in the gut wall can be inhibited by components of SNEDDS formulations (10, 11). Additional benefits such as a high solubilization capacity for poorly water-soluble drugs, improved bioavailability resulting in lower administered doses and encapsulation of aggressive drugs damaging the gastric mucosa might be accomplished with SNEDDS (2, 11, 20, 25, 32, 37).

The origin of the beneficial aspects mentioned may be related to the individual excipients or their combination. Structural details of the excipients may provide information about the expected properties of the SNEDDS formulation (38).

Commonly, the oily or lipid phase of SNEDDS consists of triglycerides or a mixture of mono-, di- and triglycerides (11, 25, 37, 38). These glycerides can comprise long-chain, medium-chain or short-chain fatty acids that are linked to glycerol (11). The (partial) esterification of glycerol with different fatty acids can result in different types of mono-, di- or triglycerides with specified properties including polarity, density, viscosity, aqueous solubility and chemical stability (11, 25, 26). Due to their substantial size, long-chain triglycerides that present with fatty acids of more than twelve carbon atoms esterified with glycerol may be suitable to stimulate the lymphatic drug absorption in order to circumvent the first-pass effect that may result in higher drug plasma levels (11, 22, 27, 33, 39, 40). In addition, a SNEDDS formulation further requires the presence of a surfactant or a mixture of surfactants that possess the ability to emulsify an oily with an aqueous phase resulting in a nanoemulsion (11, 25, 37). Hydrophilic surfactants are essential elements for providing effective self-emulsifying properties of SNEDDS (25, 33). Lipophilic surfactants can act as potential co-surfactants to support the emulsification process in aqueous fluids and may lead to a higher saturation solubility of the drug that is incorporated in a SNEDDS formulation (25). Furthermore, type and concentration of surfactants could strongly affect the emulsion droplet size (22, 33). Conventionally, non-ionic surfactants are used to prepare SNEDDS to ensure a certain stability and limit the impact of pH value changes, ionic strength, and ionic interaction on SNEDDS formulations' stability (33, 37). Considering that anionic or cationic drugs incorporated in SNEDDS can easily interact with oppositely charged excipients that are used together in the same SNEDDS formulation, there is a potential risk for drugs to precipitate irreversibly (41). Another group of potential components to be used in a SNEDDS formulation is represented by the co-solvents (11, 25, 26, 37). Co-solvents reduce the interfacial tension, stabilize the dispersed phase, and can contribute to a more hydrophobic environment

by lowering the dielectric constant of water to improve the emulsification performance of SNEDDS (11, 42).

Since a SNEDDS formulation is intended to solubilize a drug with poor aqueous solubility in gastrointestinal fluids upon oral administration, it can be considered as a fundamental specification that a sufficient solubility of the drug in both the individual components (oil/lipid, surfactant, co-solvent) of SNEDDS as well as in the complex mixture of these individual components is guaranteed (30, 43). The analysis of the saturation solubility of a lipophilic drug in the individual components can be performed to identify a suitable mixture of constituents for the development of a SNEDDS formulation (10, 28, 30, 43-47). High saturation solubilities determined for a certain drug may be linked to a selection of promising candidates of components for SNEDDS (10, 25). Furthermore, miscibility as well as compatibility of all the individual constituents are required for developing a SNEDDS formulation (10, 25). Once a promising, compatible mixture of components for SNEDDS with high drug loading has been identified, a ternary phase diagram is typically used to determine the self-emulsifying region as well as the best performing mixing ratio of the selected components including the drug (43, 48). The performance of a certain SNEDDS formulation is often characterized based on analytical methods, for instance the droplet size as well as the transmittance of the nanoemulsion that is formed after dispersion in water (8, 11, 43, 48-50). Once, drug-loaded SNEDDS formulations that have a small droplet size with narrow distribution as well as a high transmittance are determined, they can be selected for advanced analyses such as drug release as well as storage stability studies (51-57).

Commercial products based on SNEDDS technology (e.g., Neoral® or Aptivus®) are available in different dosage forms such as oily solutions or soft capsules (4). As mentioned earlier in this section, once they are developed, SNEDDS formulations can be manufactured quickly and easily by mixing a lipophilic drug with selected excipient components. However, SNEDDS formulations in a liquid state tend to be linked to a couple of major drawbacks (25, 50). The majority of Liquid-SNEDDS (L-SNEDDS) formulations reveals a poor storage stability, very limited shelf life and can suffer from chemical instability as well as drug precipitation (20, 22, 27, 50, 58, 59). The reported poor dosing accuracy of these liquid systems may be compensated by filling L-SNEDDS into soft capsules (22, 50, 58). However, besides the fact that the production of filled soft capsules is a costly process and presents a technical challenge, the potential of L-SNEDDS to interact with or even leach through the soft capsule is a major concern. Consequently, soft capsule filling may not resolve the indicated drawbacks of L-SNEDDS (7, 22, 27, 50, 58). Due to several drawbacks and limitations that are accompanied by L-SNEDDS technology, conversion to a solid dosage form as an innovative formulation approach may be advisable. Converting L-SNEDDS into a solid

dosage form, that is referred to as Solid-SNEDDS (S-SNEDDS) formulation in the following, could lead to a substantial improvement on aspects such as stability and shelf life of the formulation, production costs in comparison to soft capsule manufacturing and dosing accuracy (58). Various manufacturing methods, such as conventional wet granulation, spray drying, application of supercritical fluid technology, freeze drying, and adsorption to a solid carrier, might be used to efficiently perform this conversion step (17, 27, 44, 50, 60-62). When focussing now on the technology approach using adsorptive carriers, a huge variety of materials could act as adsorbent for L-SNEDDS formulations. Promising materials that are already used for adsorption processes can either originate from biological source or chemical synthesis (60-62). The varying, individual physicochemical properties of adsorptive carriers with regard to surface area, morphology, density, polarity, porosity, particle size and distribution resulting from different chemical compositions as well as manufacturing methods may be of major interest for a suitable selection of carriers for S-SNEDDS preparation (17, 60, 63). Material-specific properties of the different adsorptive carriers used to prepare S-SNEDDS may affect the loading capacity for L-SNEDDS, the processing and the drug release performance (63-66). Carriers that can be used for S-SNEDDS manufacturing include materials that are based on silicon dioxide, calcium silicate, other inorganic salts and different polysaccharides, among others (5, 17, 27, 61, 62, 67, 68). Adsorption to a solid carrier is an elementary approach, mainly based on capillary forces and chemical or physical interactions. Gentle adsorption processing into a solid dosage form constitutes a major advantage, as SNEDDS are neither exposed to high temperatures nor to strong mechanical forces as can be the case with other manufacturing technologies (17). Many solid carriers loaded with L-SNEDDS induce a reduction of both, rate and extent of drug release compared to the corresponding L-SNEDDS as a result of pronounced chemical interactions (63-66). The identification of suitable solid carriers with a high loading capacity that do not substantially impact the release of the adsorbed L-SNEDDS formulation and the incorporated drug respectively, remains a challenge.

As an alternative manufacturing process, the preparation of S-SNEDDS may also be conducted using a hot melt extrusion (HME) co-processing that combines L-SNEDDS with an appropriate, thermoplastic polymer (58). However, using HME technology for converting L-SNEDDS into S-SNEDDS based on a polymeric compound is still a largely unexplored area in the SNEDDS manufacturing field. Basically, HME is a well-established technology that induces thermal as well as mechanical input in order to process a polymer or blends of polymers together with other liquid or solid substances to obtain a solid dosage form (Figure 3).
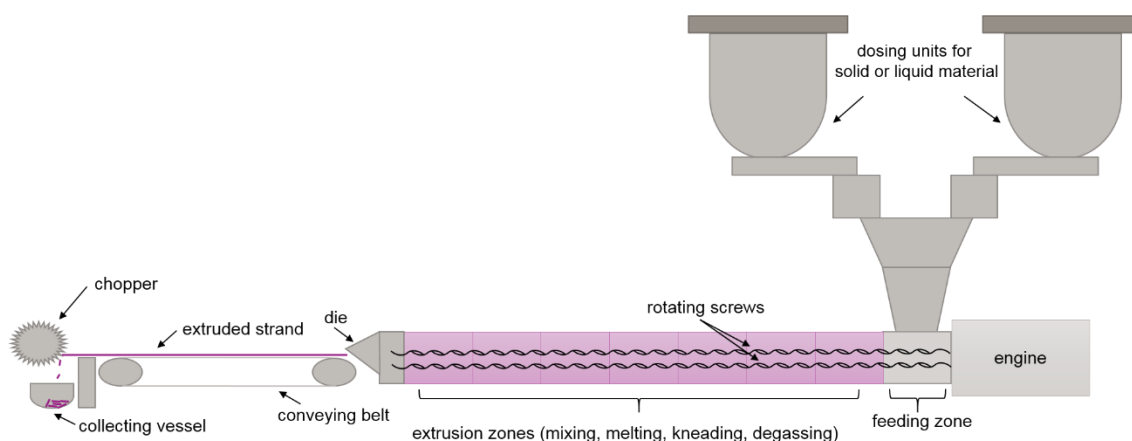
Figure 3: Visualization of a hot melt extrusion (HME) process.

Before entering the feeding zone of an extruder, liquid and solid materials can be dosed separately or as mixtures for the HME process. A flowable melt is then generated inside the extruder (extrusion zones) due to elevated temperatures as well as the impact of mixing and kneading elements. The molten material is conveyed via rotating screws towards the extruder die where it leaves the extruder and cools down, shaped as a homogenous strand that can be further chopped into granules of different particle sizes. HME is a continuous, solvent-free process that is easy to scale-up and less time-consuming compared to other technologies that are suitable for the transformation into a solid dosage form (58). Essential characteristics of the polymeric material that is supposed to be processed via HME for the preparation of S-SNEDDS may be the glass transition temperature (T_g), the weight-average molecular weight (M_w) and the number-average molecular weight (M_n), the binding and solubilizing capacity for oily formulations (e.g., L-SNEDDS) as well as the decomposition temperature, flexibility and hardness (1, 21, 69, 70). Due to a lack of literature examples in this context as well as a large number of potential impact factors considering material- and process-specific parameters, S-SNEDDS manufacture by means of HME certainly remains a major challenge.

From this perspective, there is a wide scope for research activities in the technology field of S-SNEDDS to exploit its great potential for solubility enhancement of poorly water-soluble drugs focusing on the development of promising formulation excipients, novel carrier materials, and combinations thereof using different, suitable manufacturing techniques.

2. Objectives

When screening the published studies in the field of solubility enhancement of poorly water-soluble drugs, it became evident that many different technology approaches can be used to counteract the growing solubility issue of drugs.

The aim of the present work was to investigate the SNEDDS technology approach for improving the solubility as well as the release performance of BCS class II drugs. When administered orally, the drugs to be selected for formulation development should have a pH-independent solubility within a pH range that is physiologically relevant in order to enable a better assessment of the impact of the SNEDDS formulation on drug release.

In the first part of the work, a novel screening approach for rapid development of SNEDDS formulations should be developed to streamline the process of conventional methods by reducing the time and experimental effort. The screening approach to be established should be used, in particular, for the development and characterization of drug-loaded and rapidly releasing L-SNEDDS formulations. However, since some disadvantages, such as limited stability and dosing accuracy, were already disclosed for L-SNEDDS formulations, the elaboration of a technical approach to overcome these limitations represented another central goal of the present work. One consideration to address this challenge was to convert L-SNEDDS into a solid dosage form (S-SNEDDS) that may resolve stability issues. The aim was to evaluate suitable technology approaches such as adsorption to solid carriers as well as HME with regard to the conversion step into S-SNEDDS formulations. In this context, established excipients for the preparation of solid (amorphous) oral dosage forms should be investigated, but beyond that, in particular novel materials, e.g., porous carriers for adsorption processing or thermoplastic (co-)polymers for HME should be developed and evaluated for the successful preparation of S-SNEDDS. To evaluate the suitability of new and established materials for the preparation of S-SNEDDS by HME, the performance of drug-loaded S-SNEDDS should be compared with that of the corresponding amorphous solid dispersions (ASDs), which are co-extrudates of (co-)polymers and drugs. In this context, different *in vitro* characterization approaches should be applied to evaluate the properties and performance of drug-loaded S-SNEDDS and ASDs. These should include amorphicity/crystallinity-, drug release- and storage stability studies.

3. Discussion

The first part of the discussion relates to the content of the publication "A customized screening tool approach for the development of a self-nanoemulsifying drug delivery system (SNEDDS)" (71).

This screening approach aimed the establishment of a tool that was supposed to streamline the development of rapid-releasing SNEDDS formulations. As a starting point, a comprehensive series of experiments on the solubility of BCS Class II substances in potential SNEDDS components has been performed to identify three model drug substances, which should be used throughout the study.
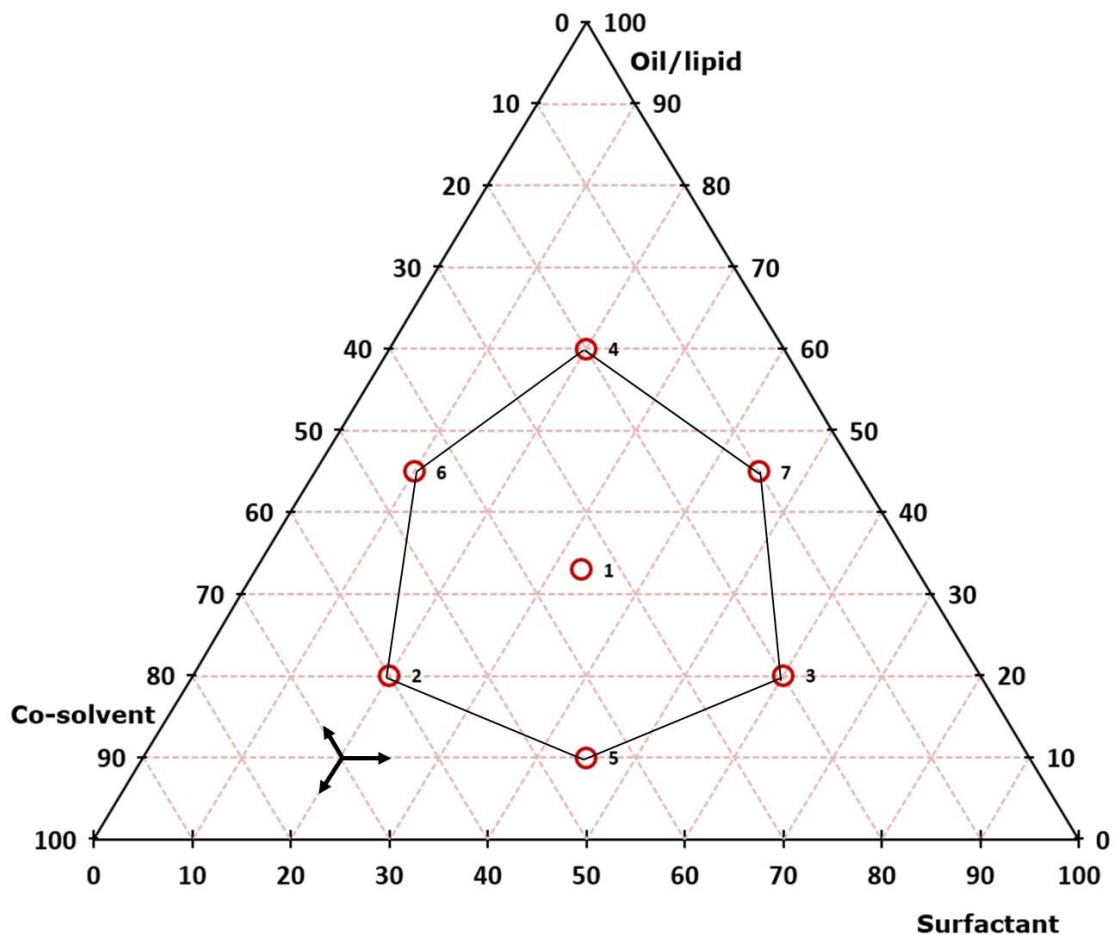

Figure 4: Example for the basic layout of the triangular mixture design applied in determining optimal SNEDDS mixtures for the drug substances celecoxib and fenofibrate (71).

The drugs of interest were expected to have a high solubility in the excipients and a pH-independent solubility in the physiological pH range that is relevant for the oral administration of drugs. Based on these requirements, which were investigated for a multitude of drugs, celecoxib, efavirenz and fenofibrate turned out to be suitable model drugs and thus were

selected for SNEDDS development. In addition, a pre-selection of excipients that might be suitable for SNEDDS formulations has resulted from these experiments. Since SNEDDS resulted from a combination of multiple excipients, initial ideas for developing a methodology for evaluating these excipients and different mixing ratios using a fixed drug load were proposed. For this reason, a special triangular mixture design (Figure 4) for screening and determining appropriate excipient ratios for SNEDDS formulations was established to streamline their development. As the selected excipients were of liquid or semisolid state, the developed screening approach was applied for the development of L-SNEDDS formulations and was distinct from the conventional 10% increment procedure which has been used in several SNEDDS studies (43, 48) that ultimately aimed the solubility enhancement of poorly water-soluble drug substances. This novel screening approach in a special triangular design (Figure 4) was supposed to save time and resources as well as to substantially diminish the number of individual trials from about 50 to less than 15 for L-SNEDDS development. While reducing the experimental effort, stringent self-imposed requirements for L-SNEDDS such as a droplet size < 50 nm, a PDI < 0.15, and a transmittance > 99% after dispersing the L-SNEDDS formulation in water were defined (71). The requirements set for L-SNEDDS aimed not only to distinguish between good and bad mixing ratios, but also to determine such mixing ratios that in the end really yield nanoemulsions. Figure 4 maps the basic layout of the special triangular mixture design including the center point (sample 1) of the triangle and a hexagon-shaped mixture region (samples 2 to 7) around this center point representing varying quantity ratios of potential L-SNEDDS compositions (71). For identifying the designated area of interest (DAoI) (i.e., the area within the triangular mixture design that provided L-SNEDDS that were closest to the above self-imposed specifications), potential L-SNEDDS compositions were analyzed regarding their droplet size, PDI, transmittance and emulsification performance. Analyzing additional L-SNEDDS samples representing quantity ratios of the excipients in the DAoI enabled the most promising L-SNEDDS formulation candidate to be determined (71). The analytical results obtained for the best L-SNEDDS formulations that met the self-imposed specifications were compared with literature data from various L-SNEDDS studies, focusing on the droplet size and PDI of the nanoemulsions analyzed after dispersion. These parameters were considered essential in literature as L-SNEDDS with much smaller droplet sizes and PDIs after dispersion in aqueous fluids indicated an improved physical stability (72) demonstrated by emulsification performance tests. Apart from that, results of better drug absorption and increased bioavailability associated with a decrease in droplet size and PDI were reported in several research studies (36, 73). The selected L-SNEDDS formulation incorporating celecoxib provided better results with regard to droplet size and/or PDI than achieved in several other studies (44, 52, 54, 56, 57). In addition, also the fenofibrate

L-SNEDDS presented with smaller droplet sizes and/or PDIs when dispersed in an aqueous medium compared to many results that were reported in literature (29, 49, 51, 55, 74). The methodology for analyzing droplet size and PDI was robust as low standard deviations (RSD < 5%) were determined when performing the experiments in triplicate. Furthermore, when screening the drug release performance of the selected celecoxib- efavirenz- and fenofibrate L-SNEDDS in a standard paddle setup (500 ml, 100 rpm), rapid and complete drug release was observed (100% of test dose released in < 15 min) independent of the pH conditions (pH 1, 4.5 and 6.8) (71).

Based on the results obtained with L-SNEDDS incorporating either the drug substance celecoxib, efavirenz or fenofibrate as well as the efficiency of the L-SNEDDS development process, the novel screening approach can be considered as a promising alternative to conventional methods in order to obtain a good performing L-SNEDDS formulation in a more manageable time. Concluding, this customized tool can be seen as an initial screening approach to enable a very rapid development of L-SNEDDS formulations with a substantially reduced number of experiments. There is no question that using conventional methods, even finer gradations can certainly be achieved and a better basic understanding regarding the formulations can be obtained. In addition, an absolutely optimal L-SNEDDS formulations may be identified. However, the focus of the presented work was on speeding up the screening process while also meeting very stringent specifications for L-SNEDDS.

The presented screening approach for the L-SNEDDS development has not yet been fully exploited, as considerations for instance choosing a broader range of potential L-SNEDDS' excipients and increasing the drug load of the formulations could be additionally incorporated. Since these L-SNEDDS formulations resulted from a first screening approach, the doses of the selected drug substances were lower than their therapeutic doses and the performed release studies were conducted at three different pH values without further addressing intraluminal contents of the gastrointestinal tract. Furthermore, analyzing the impact of digestive processes that may be simulated in advanced *in vitro* studies as well as an evaluation of L-SNEDDS' *in vivo* behavior could extend the content of information provided by the screening tool.

The next part of the discussion focuses on research activities that are highlighted in the publication "Development and characterization of celecoxib solid self-nanoemulsifying drug delivery systems (S-SNEDDS) prepared using novel cellulose-based microparticles as adsorptive carriers" (75).

As L-SNEDDS formulations could also have some drawbacks related to their stability after they have been successfully developed, the idea was to overcome these by converting L-SNEDDS into a solid dosage form. As a first manufacturing approach to convert L-SNEDDS into S-SNEDDS, a technique of adsorbing celecoxib L-SNEDDS onto a solid carrier was investigated. For this purpose, a selection of commercially available adsorptive carriers was tested with respect to their ability of adsorbing L-SNEDDS. The different loading capacities of the carriers for L-SNEDDS were identified as a key material property when characterizing and comparing the adsorptive carrier candidates. As a first experiment, celecoxib loaded L-SNEDDS were prepared and subsequently combined with different carrier materials to generate S-SNEDDS (75). Initially, adsorption for S-SNEDDS preparation was performed with the silica-based adsorbent Aeroperl® 300 Pharma, and the celecoxib release of the obtained S-SNEDDS formulation was investigated. Drug release experiments with S-SNEDDS formulations were performed in the same way as already described for L-SNEDDS to determine if the drug release was rapid and complete. When analyzing the drug release of Aeroperl® 300 Pharma-based S-SNEDDS in 500 ml of acidic dissolution medium (pH 1), the celecoxib release was < 40% of the test dose. Thereafter, S-SNEDDS based on adsorptive carriers different from Aeroperl® 300 Pharma were prepared and the celecoxib release of these S-SNEDDS formulations was studied as well. As a result, the fraction of dose released differed significantly among the formulations when using different adsorptive carriers. All S-SNEDDS formulations that were prepared with commercially available carriers such as silica-, calcium silicate- as well as cellulose-based materials presented with an incomplete celecoxib release. The incomplete drug release determined for S-SNEDDS, regardless of the commercial adsorptive carrier used, turned into a major challenge during the development process. Other research groups have also reported about the challenge of incomplete drug release from S-SNEDDS formulations based on the approach of adsorption to solid carriers including silica (44,76), but also other materials such as hypromellose and maltodextrin (76). However, it was not possible to compare the obtained release data with those of other research groups because the test conditions were not the same (44, 76). Overall, the results of the different studies confirm the complexity of carrier properties that could be responsible for varying and incomplete drug releases for S-SNEDDS (44, 75, 76). Hence, the selection, manufacture and evaluation of adsorptive carriers is an important step in the development process of S-SNEDDS formulations in this context. With respect to the goal of developing an adsorptive carrier-based S-SNEDDS formulation, that resulted in a rapid and complete drug release, the development of a tailor-made carrier was initiated. The prerequisites of developing such a carrier included that this new carrier was supposed to be based on cellulose or cellulose derivatives (issued as a specification by the supporting company). For comparative

reason, a marketed cellulose-based material, Avicel® PH-101, was also evaluated for its suitability as a carrier for S-SNEDDS formulations in this context.

The novel carrier should be linked to a rapid and complete L-SNEDDS/drug release, a high loading capacity (loading factor > 1) for L-SNEDDS and simple processing. Different cellulose types and excipients were screened for their suitability to be processed into an adsorptive microparticle carrier. It was determined that a certain binder was required to obtain a stable cellulose-based microparticle for subsequent L-SNEDDS adsorption. Ultimately, using a multi-step manufacturing process (completed by spray-drying), a novel adsorptive carrier material for S-SNEDDS manufacturing that presented with a microparticle structure derived from native cellulose in combination with a certain binder (gum arabic or methylcellulose) was established (75). Two variants of the cellulose-based microparticles referred to as M-GA (cellulose-based microparticle with gum arabic) and M-MC (cellulose-based microparticle with methylcellulose) in the following were loaded with celecoxib L-SNEDDS and subjected to drug release studies. A set of drug release studies analogous to those of the underlying L-SNEDDS formulation were performed for S-SNEDDS using different pH conditions. M-GA- as well as M-MC S-SNEDDS presented with rapid (< 15 min) and complete (100% of test dose) celecoxib release regardless of the selected dissolution medium (75). As a comparison, S-SNEDDS based on Avicel® PH-101 presented with a drug release of approximately 90% of the celecoxib dose using the same dissolution test conditions, that was substantially lower than determined for S-SNEDDS based on M-GA and M-MC.

In addition, it could be noted that the L-SNEDDS' loading capacity of M-GA and M-MC was significantly higher than for Avicel® PH-101, however, it was lower compared to that of the corresponding silica-based carriers studied earlier (75)

Overall, M-GA proved to be the preferred variant of the two novel cellulose-based microparticles as it showed an improved processibility towards S-SNEDDS compared to M-MC. The spherical particle shape of M-GA may be one reason for the different processing behavior (75). Furthermore, the adsorption process of L-SNEDDS using Avicel® PH-101 was more complicated when compared to the application of the carriers M-GA and M-MC, as Avicel® PH-101 showed some sticking issues during the adsorption process.

Finally, the storage stability of all S-SNEDDS formulations prepared in the context of this study was tested. Based on the International Conference on Harmonisation (ICH) guidelines, the intermediate storage conditions of 30°C/65% RH over a period of three months were selected for testing (75). After three months of storage, test criteria were met if visual inspection of S-

SNEDDS resulted in no change of formulation and the deviation of the extent of drug release was < 3% compared to that at the time of manufacture. Sufficient storage stability was determined for all S-SNEDDS formulations, as no visual change was noticeable, and the extent of the drug release had changed by less than 3% after the three months storage period.

In conclusion, developing a suitable carrier for converting L-SNEDDS into S-SNEDDS was a major step in the value chain towards the ultimate goal of obtaining a rapidly and completely releasing S-SNEDDS formulation. S-SNEDDS based on M-GA and M-MC prepared via adsorption technology met the predefined requirements, with M-GA being preferred over M-MC due to its beneficial morphology and facilitated processing.

Apart from the adsorption process, a technical approach which has been described in the literature already, there are currently only very few alternative approaches for manufacturing of S-SNEDDS. In the present work, therefore, hot melt extrusion was investigated as a novel approach for the production of S-SNEDDS. With a change in the technological approach for manufacturing of S-SNEDDS from adsorption technique to HME process, the final part of the discussion now deals with the content of the publications "A novel aminomethacrylate-based copolymer for solubility enhancement - from radical polymer synthesis to manufacture and characterization of amorphous solid dispersions" (77) as well as "Preparation of solid self-nanoemulsifying drug delivery systems (S-SNEDDS) by co-extrusion of liquid SNEDDS and polymeric carriers - a new and promising approach to improve the solubility of poorly water-soluble drugs" (78).

For the preparation of S-SNEDDS using HME as an alternative transforming step, L-SNEDDS were combined with different thermoplastic (co-)polymers that are well-known in the context of solubility enhancement of poorly water-soluble drugs. Since examples on S-SNEDDS manufacturing via HME processing are not available in literature, initial HME trials with drug-loaded L-SNEDDS combined with different (co-)polymers were conducted to get an understanding of critical process- (e.g., temperature and screw speed) as well as material-specific parameters. In that context, the mechanical as well as physicochemical properties of the applied (co-)polymer materials such as flexibility, hardness and brittleness of the final polymer strand, the M_w and T_g of the (co-)polymer as well as the binding capacity for L-SNEDDS were identified as elementary factors for proper S-SNEDDS manufacturing (77, 78). Initial HME trials for S-SNEDDS manufacturing revealed technically limited applicability of the selected (co-)polymers that are currently available on the market such as EUDRAGIT® E PO, Soluplus®, Kollidon® VA 64, Kollidon® 17 PF, Affinisol® HPMC 100 LV, AQOAT® AS-MMP. Challenges such as a lack of linkage between drug-loaded L-SNEDDS and (co-)polymer, inappropriate melt

viscosities leading to clogging of the extruder die, high flexibilities and insufficient rigidity of the extruded polymer strands emerged during the preliminary trials. These observations further led to the idea of developing a tailor-made (co-)polymer for the S-SNEDDS application field. Except for the excessive flexibility of the extruded polymer strand, EUDRAGIT® E PO proved to be a good starting material for the development of a new copolymer for preparation of S-SNEDDS via HME. In addition, as methacrylate chemistry is a core business of the supporting company, it was reasonable to extend the research activities in this area. The aim was to develop a (co-)polymer related to EUDRAGIT® E PO with modified properties. With a focus on radical polymer synthesis, first approaches with different monomer compositions compared to EUDRAGIT® E PO were performed to develop a customized copolymer that is suitable for S-SNEDDS manufacturing using HME.
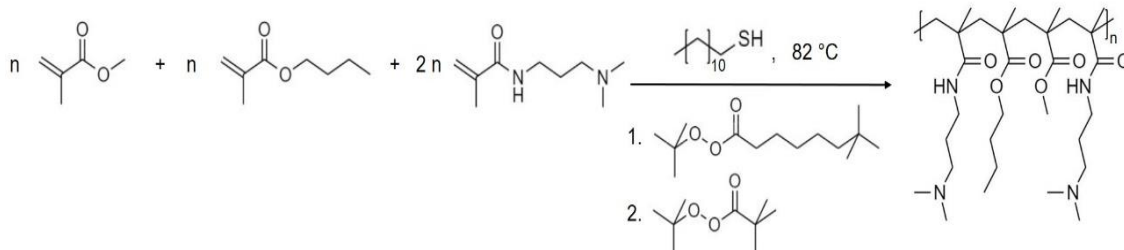
Figure 5: Radical copolymer synthesis of modified EUDRAGIT® E PO (ModE) including monomers, chain-transfer-agent (CTA), initiators (1. tert-butyl peroxyneodecanoate, and 2. tert-butyl peroxypivalate) and reaction conditions (77).

The radical polymer synthesis including the different monomers, two radical initiators, a chain-transfer-agent (CTA) and the reaction conditions that was applied to finally obtain this customized copolymer for S-SNEDDS formulation development is shown in Figure 5. This novel aminomethacrylate-based copolymer, the dimethylaminopropyl methacrylamide-butyl methacrylate-methyl methacrylate (ModE), can be described as a structural modification of dimethylaminoethyl methacrylate-butyl methacrylate-methyl methacrylate (EUDRAGIT® E PO). A comparison of the chemical structures of both ModE as well as EUDRAGIT® E PO clearly indicate the modifications within the amino-functional monomer unit (Figure 6).
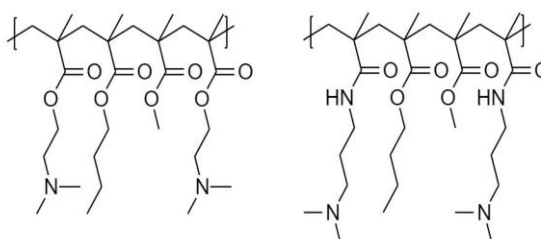

Figure 6: Section of the chemical structure of EUDRAGIT® E PO (left) and ModE (right) (77).

As already indicated, the rationale for modifying the commercialized copolymer EUDRAGIT® E PO for S-SNEDDS manufacturing involved an increased T_g, that should enable higher L-SNEDDS loading capacities, improved processability via HME as well as a better storage stability. The radical polymerization process (Figure 5) was performed with high monomer conversion rates resulting in low residual monomer contents, so that the final ModE copolymer only required a short time for further purification. Different ModE types with varying M_w, T_g and PDI respectively were synthesized and evaluated first for drug release performance when combined with drug-loaded L-SNEDDS. As previous studies (71, 79) had confirmed that the three model drugs (celecoxib, efavirenz and fenofibrate) used in the study revealed pH-independent solubility, the dissolution medium should not have a notable effect on their dissolution. Based on the results of the dissolution tests in an acidic medium (pH 1) using drug-loaded S-SNEDDS prepared with ModE, a trend towards better drug release performance with decreasing M_w and T_g of ModE was observed. Thus, the impact of ModE's M_w and T_g on rate and extent of drug release was inversely proportional independent of whether the drug substance celecoxib, efavirenz or fenofibrate was incorporated in the S-SNEDDS formulation (78). The same correlation was observed when ModE was used for preparing drug-loaded ASDs via HME (77). A similar effect for a certain polymer type with varying M_ws was detected by Knopp *et al.* (80) working with polyvinylpyrrolidone-based ASDs. As a decrease of a copolymer's M_w usually entails a higher flexibility and lower viscosity, both effects may contribute to a better solubilization of the drug and higher drug releases (77, 78, 80). When investigating the drug release performance of drug-loaded S-SNEDDS and the corresponding ASDs that were produced analogous in the presented studies (77, 78) it turned out that all S-SNEDDS presented with both, a higher rate and extent of drug release in acidic medium (pH 1) compared to the corresponding ASD. With focus on the drug release performance of the different S-SNEDDS formulations, S-SNEDDS based on ModE variant 173 kDa showed the best results among S-SNEDDS prepared with selected commercially available (co-)polymers or other ModE variants.

Apart from investigation on drug release, a series of differential scanning calorimetry (DSC) and x-ray powder diffraction (XRPD) studies was performed to investigate amorphicity/crystallinity of the drug in S-SNEDDS or ASD formulations. Whereas some ASDs showed evidence of drug recrystallization and substantial decrease of drug release after the ASDs had been stored over three months at 30°C/65% RH according to the ICH guidelines, the drug incorporated in S-SNEDDS remained in the amorphous state regardless of the drug/(co-)polymer combination.

As an additional benefit from the process point of view, S-SNEDDS could be prepared at lower extrusion temperatures than the corresponding ASDs, since the combination with L-SNEDDS facilitated the co-processing of almost all (co-)polymers tested (78).

Although ModE is currently considered a prototype copolymer and not yet commercially available, the S-SNEDDS formulations based on ModE also showed promising results in terms of their storage stability (78). In most cases, the storage stability data of ModE-based S-SNEDDS was even better than that of S-SNEDDS based on the commercial (co-)polymers tested in this study (78). As no studies of S-SNEDDS prepared by HME are yet available, a comparison of these S-SNEDDS results with reasonable data sets in the literature was not possible.

Based on drug release, amorphicity/crystallinity and storage stability data of drug-loaded S-SNEDDS as well as ASDs, the most promising ModE type that was synthesized had a M_w of 173 kDa and a T_g of 77 °C and at the same time was the variant with the lowest M_w and T_g in the present study (78). It may certainly be obvious to further decrease M_w and T_g of ModE in order to achieve even better drug release performances when using this copolymer. However, the synthesis of another ModE type with even lower M_w and T_g was not considered, since this change would most likely have a negative impact on the loading capacity for L-SNEDDS, the processability of S-SNEDDS via HME and its storage stability. In contrast, a further increase of the drug release in an acidic dissolution medium (pH 1) would be negligible, since it was already complete (100% of test dose released), at least for celecoxib- and efavirenz S-SNEDDS using ModE variant 173 kDa (78).

As a brief conclusion of the final part of the discussion, a novel technology concept, that highlighted the preparation of (co-)polymer-based S-SNEDDS formulations via HME processing, was successfully developed. Since the use of most commercially available (co-)polymers, which are already used for solubility enhancement of poorly water-soluble drugs, did not present with the expected results, a new tailor-made copolymer "ModE" was synthesized and turned out to be the most promising (co-)polymer for S-SNEDDS development. Moreover, all S-SNEDDS formulations presented with superior performance regarding drug release and formulation stability when compared to the corresponding ASDs.

Overall, it can be concluded L-SNEDDS formulations with the intended *in vitro* performance were rapidly developed using the novel customized screening tool approach that saved time, resources as well as experimental effort for the L-SNEDDS development process. Furthermore, the transformation step into S-SNEDDS was achieved applying different technology approaches in the related field. New, tailor-made materials developed specifically for the preparation of S-

SNEDDS were found to be more suitable in terms of investigated formulation properties than many commercially available materials studied in this context. As a result, pronounced solubility enhancement of the poorly water-soluble model drug substances celecoxib, efavirenz and fenofibrate was achieved using the SNEDDS technology approach. Promising formulation candidates for both liquid and solid dosage forms have been developed.

Providing a brief outlook on potential trends in the SNEDDS technology field, developing sustainable materials that are biocompatible, biodegradable, and suitable for various manufacturing processes at the same time may be of great importance in the future. Looking at new excipients as well as extending the selection of excipients for the screening approach at the very beginning of the L-SNEDDS development procedure will certainly increase the number of possible combinations and promising formulation candidates. In addition, combining carrier materials with different characteristics to further tailor the properties of S-SNEDDS as well as extending S-SNEDDS studies to other poorly water-soluble drug substances could be of great interest.

4. Summary

The poor aqueous solubility of many drug substances has been addressed using different solubility enhancement approaches in the pharmaceutical technology field over the last decades. In this context, advanced drug delivery systems based on lipids referred to as SNEDDS were used to overcome solubility limitations of drugs, that are often associated with a low bioavailability after oral administration. There are numerous examples in the literature for the development of L-SNEDDS, which have led to some pharmaceutical products available on the market. As L-SNEDDS development using conventional methods requires a lot of time and experimental effort, a streamlining of this procedure was aimed in the first part of the presented work.

Starting with the development of L-SNEDDS formulations for solubility enhancement of poorly-water soluble drugs, extensive solubility studies with different BCS Class II drugs were performed in various excipients to determine drugs with high solubilities in these excipients as well as to evaluate multiple excipients for their suitability to be used in L-SNEDDS formulations. Celecoxib, efavirenz and fenofibrate were selected as model drugs and a pre-selection of excipients for further development was made. In a next step, a novel screening approach for L-SNEDDS formulation development based on a customized mapping method in a special triangular mixture design was established. This customized tool for L-SNEDDS development comprised the systematic analysis of results obtained with different *in vitro* characterization methods such as droplet size analysis and distribution, transmittance measurement and emulsification performance assessment. Furthermore, the novel approach streamlined the procedure for L-SNEDDS development as a reduction of experimental effort and time compared to conventional methods was achieved. The most promising L-SNEDDS formulations determined via the customized screening tool approach showed high drug release of celecoxib, efavirenz as well as fenofibrate, and clearly indicated that this method was suitable for efficiently designing stable and rapidly releasing L-SNEDDS formulations incorporating poorly water-soluble drugs.

After the successful development of L-SNEDDS formulations with different drug substances using the novel screening approach, a further aspect of this work dealt with conversion of L-SNEDDS into S-SNEDDS, since a limited storage stability has been reported for many L-SNEDDS formulations. The conversion into S-SNEDDS required the determination of appropriate solid carriers with different material properties depending on the manufacturing process. As a first technological approach, adsorption to a solid carrier was investigated by adding a carrier to drug-loaded L-SNEDDS applying a defined mixing ratio resulting in a solid, particulate formulation. When performing drug release studies, S-SNEDDS based on different commercial

carrier materials revealed major limitations due to incomplete drug release. Thus, a tailor-made microparticulate carrier material based on cellulose was developed for the purpose of adsorbing L-SNEDDS and presented with superior performance compared to conventional adsorbents based on cellulose or silica. Based on the obtained results, this novel cellulose-based microparticle prepared with gum arabic as a binder was determined to be the most promising material amongst all adsorptive carriers that were investigated.

In addition to the technology approach of adsorption, another manufacturing process was considered in the course of the present work, which focused on the preparation of S-SNEDDS by means of HME. As a successful conversion of L-SNEDDS into S-SNEDDS using HME processing requires at least one additional polymeric component, a selection of marketed (co-)polymers that were frequently used in the field of solubility enhancement were evaluated for their suitability in this context. Critical process parameters and target properties of the (co-)polymers were determined, ultimately leading to the idea of developing a novel, customized polymer in order to perform the conversion step via HME in a more suitable and effective manner. In this context, a new copolymer referred to as ModE, as it disclosed a structural association with the commercially available copolymer EUDRAGIT® E PO, was developed. The novel copolymer ModE was evaluated for its suitability for different formulation technologies and showed promising results when used for S-SNEDDS and ASD formulations prepared by the HME process. Different variants of ModE in terms of M_w, T_g and PDI were synthesized via radical polymerization and it was found that the modification of M_w, T_g and PDI of the novel aminomethacrylate-based copolymer had significant effects on drug release as well as storage stability of S-SNEDDS and ASDs. The ModE copolymer type with a M_w of 173 kDa turned out to be the most suitable candidate for S-SNEDDS development using HME technology. In addition, drug-loaded S-SNEDDS based on the ModE variant 173 kDa were storage stable and presented with the highest drug release among all S-SNEDDS formulations tested.

In conclusion, a novel screening tool approach for efficient L-SNEDDS development was established in order to streamline the process for obtaining stable and rapidly releasing L-SNEDDS formulations which improved the solubility of poorly water-soluble drugs. Apart from the L-SNEDDS development process, the conversion from L-SNEDDS into S-SNEDDS was successfully performed using the technology approaches of adsorption to a solid carrier and HME processing. An improved storage stability compared to L-SNEDDS as well as high drug release were achieved for several S-SNEDDS formulations, especially for those prepared with tailor-made materials. Based on the results obtained for S-SNEDDS formulations produced via adsorption, especially in terms of drug release performance, the new cellulose-based

26

microparticle carriers (M-GA and M-MC) turned out to be the most suitable materials. S-SNEDDS that were manufactured via HME presented with a superior performance regardless of the incorporated drug when comparing the results of S-SNEDDS with those of the corresponding ASDs regarding drug release performance, amorphicity/crystallinity and storage stability. In this context, among all S-SNEDDS formulations prepared via HME, S-SNEDDS based on the ModE variant 173 kDa showed the best results, especially when using the drug substances celecoxib and efavirenz. Although the S-SNEDDS formulation approach is still largely unexplored, based on the research results generated in the present work, it represents a promising technology platform that should definitely be further developed in future experiments.

5. Bibliography

1. Rumondor ACF, Dhareshwar SS, Kesisoglou F. Amorphous solid dispersions or prodrugs: Complementary strategies to increase drug absorption. J Pharm Sci. 2016;105(9):2498-508. doi: 10.1016/j.xphs.2015.11.004.

2. Vithani K, Jannin V, Pouton CW, Boyd BJ. Colloidal aspects of dispersion and digestion of self-dispersing lipid-based formulations for poorly water-soluble drugs. Adv Drug Deliv Rev. 2019. doi: 10.1016/j.addr.2019.01.008.

3. Fatouros DG, Deen GR, Arleth L, Bergenstahl B, Nielsen FS, Pedersen JS, et al. Structural development of self nano emulsifying drug delivery systems (SNEDDS) during in vitro lipid digestion monitored by small-angle X-ray scattering. Pharm Res. 2007;24(10):1844-53. doi: 10.1007/s11095-007-9304-6.

4. Kalepu S, Nekkanti V. Insoluble drug delivery strategies: Review of recent advances and business prospects. Acta Pharm Sin B. 2015;5(5):442-53. doi: 10.1016/j.apsb.2015.07.003.

5. Borkar N, Xia D, Holm R, Gan Y, Mullertz A, Yang M, et al. Investigating the correlation between in vivo absorption and in vitro release of fenofibrate from lipid matrix particles in biorelevant medium. Eur J Pharm Sci. 2014;51:204-10. doi: 10.1016/j.ejps.2013.09.022.

6. Siqueira Jorgensen SD, Al Sawaf M, Graeser K, Mu H, Mullertz A, Rades T. The ability of two in vitro lipolysis models reflecting the human and rat gastro-intestinal conditions to predict the in vivo performance of SNEDDS dosing regimens. Eur J Pharm Biopharm. 2018;124:116-24. doi: 10.1016/j.ejpb.2017.12.014.

7. Vithani K, Hawley A, Jannin V, Pouton C, Boyd BJ. Solubilisation behaviour of poorly water-soluble drugs during digestion of solid SMEDDS. Eur J Pharm Biopharm. 2018;130:236-46. doi: 10.1016/j.ejpb.2018.07.006.

8. Siqueira SDVS, Mullertz A, Graeser K, Kasten G, Mu H, Rades T. Influence of drug load and physical form of cinnarizine in new SNEDDS dosing regimens: In vivo and in vitro evaluations. AAPS J. 2017;19(2):587-94. doi: 10.1208/s12248-016-0038-4.

9. Michaelsen MH, Wasan KM, Sivak O, Mullertz A, Rades T. The effect of digestion and drug load on halofantrine absorption from self-nanoemulsifying drug delivery system (SNEDDS). AAPS J. 2016;18(1):180-6. doi: 10.1208/s12248-015-9832-7.

10. Larsen AT, Ogbonna A, Abu-Rmaileh R, Abrahamsson B, Ostergaard J, Mullertz A. SNEDDS containing poorly water soluble cinnarizine; Development and in vitro characterization of dispersion, digestion and solubilization. Pharmaceutics. 2012;4(4):641-65. doi: 10.3390/pharmaceutics4040641.

11. Akula S, Gurram AK, Devireddy SR. Self-microemulsifying drug delivery systems: An attractive strategy for enhanced therapeutic profile. Int Sch Res Notices. 2014;2014:1-11. doi: 10.1155/2014/964051.

12. Kawabata Y, Wada K, Nakatani M, Yamada S, Onoue S. Formulation design for poorly water-soluble drugs based on biopharmaceutics classification system: Basic approaches and practical applications. Int J Pharm. 2011;420(1):1-10. doi: 10.1016/j.ijpharm.2011.08.032.

13. Lipinski CA. Drug-like properties and the causes of poor solubility and poor permeability. J Pharmacol Toxicol Methods. 2000;44(1):235-49. doi: 10.1016/s1056-8719(00)00107-6.

14. Ueda K, Higashi K, Yamamoto K, Moribe K. The effect of HPMCAS functional groups on drug crystallization from the supersaturated state and dissolution improvement. Int J Pharm. 2014;464(1-2):205-13. doi: 10.1016/j.ijpharm.2014.01.005.

15. Ullrich A, Schiffter HA. The influence of polymer excipients on the dissolution and recrystallization behavior of ketoconazole: Application, variation and practical aspects of a pH shift method. Eur J Pharm Biopharm. 2018;133:20-30. doi: 10.1016/j.ejpb.2018.09.018.

16. Williams HD, Trevaskis NL, Charman SA, Shanker RM, Charman WN, Pouton CW, et al. Strategies to address low drug solubility in discovery and development. Pharmacological Reviews. 2013;65(1):315-499. doi: 10.1124/pr.112.005660.

17. Hanada M, Jermain SV, Williams III RO. Enhanced dissolution of a porous carrier-containing ternary amorphous solid dispersion system prepared by a hot melt method. J Pharm Sci. 2018;107:362-71. doi: 10.1016/j.xphs.2017.09.025.

18. Bergstrom CAS, Charman WN, Porter CJH. Computational prediction of formulation strategies for beyond-rule-of-5 compounds. Adv Drug Deliv Rev. 2016;101:6-21. doi: 10.1016/j.addr.2016.02.005.

19. Koehl NJ, Holm R, Kuentz M, Griffin BT. New insights into using lipid based suspensions for 'brick dust' molecules: case study of nilotinib. Pharm Res. 2019;36(56):1-13. doi: 10.1007/s11095-019-2590-y.

20. Yetukuri K, Sudheer P. Approaches to development of solid - self micron emulsifying drug delivery system: formulation techniques an dosage forms: A review. Int J Pharm Sci Res. 2012;3(10):3550-8.

21. Jain S, Patel N, Lin S. Solubility and dissolution enhancement strategies: current understanding and recent trends. Drug Dev Ind Pharm. 2015;41(6):875-87. doi: 10.3109/03639045.2014.971027.

22. Chatterjee B, Almurisi SH, Dukhan AAM, Mandal UK, Sengupta P. Controversies with self-emulsifying drug delivery system from pharmacokinetic point of view. Drug Deliv. 2016;23(9):3639-52. doi: 10.1080/10717544.2016.1214990.

23. de Smidt PC, Campanero MA, Troconiz IF. Intestinal absorption of penclomedine from lipid vehicles in the conscious rat: contribution of emulsification versus digestibility. Int J Pharm. 2004;270(1-2):109-18. doi: 10.1016/j.ijpharm.2003.10.036.

24. Kaur H, Kaur G. A critical appraisal of solubility enhancement techniques of polyphenols. J Pharm (Cairo). 2014;2014:1-14. doi: 10.1155/2014/180845.

25. Porter CJH, Pouton CW, Cuine JF, Charman WN. Enhancing intestinal drug solubilisation using lipid-based delivery systems. Adv Drug Deliv Rev. 2008;60(6):673-91. doi: 10.1016/j.addr.2007.10.014.

26. Pouton CW. Lipid formulations for oral administration of drugs: Non-emulsifying, self-emulsifying and 'self-microemulsifying' drug delivery systems. Eur J Pharm Sci. 2000;11(2):93-8. doi: 10.1016/s0928-0987(00)00167-6.

27. Dokania S, Joshi AK. Self-microemulsifying drug delivery system (SMEDDS) - Challenges and road ahead. Drug Deliv. 2015;22(6):675-90. doi: 10.3109/10717544.2014.896058.

28. Kamble RN, Mehta PP, Kumar A. Efavirenz self-nano-emulsifying drug delivery system: In vitro and in vivo evaluation. AAPS PharmSciTech. 2016;17(5):1240-7. doi: 10.1208/s12249-015-0446-2.

29. Mohsin K, Alamri R, Ahmad A, Raish M, Alanazi FK, Hussain MD. Development of self-nanoemulsifying drug delivery systems for the enhancement of solubility and oral bioavailability of fenofibrate, a poorly water-soluble drug. Int J Nanomedicine. 2016;11:2829-38. doi: 10.2147/IJN.S104187.

30. Thomas N, Holm R, Mullertz A, Rades T. In vitro and in vivo performance of novel supersaturated self-nanoemulsifying drug delivery systems (super-SNEDDS). J Control Release. 2012;160(1):25-32. doi: 10.1016/j.jconrel.2012.02.027.

31. Fule R, Dhamecha D, Maniruzzaman M, Khale A, Amin P. Development of hot melt co-formulated antimalarial solid dispersion system in fixed dose form (arlumelt): Evaluating amorphous state and in vivo performance. Int J Pharm. 2015;496:137-56. doi: 10.1016/j.ijpharm.2015.09.069.

32. Singh AK, Chaurasiya A, Singh M, Upadhyay SC, Mukherjee R, Khar RK. Exemestane loaded self-microemulsifying drug delivery system (SMEDDS): Development and optimization. AAPS PharmSciTech. 2008;9(2):628-34. doi: 10.1208/s12249-008-9080-6.

33. Čerpnjak K, Zvonar A, Gašperlin M, Vrečer F. Lipid-based systems as a promising approach for enhancing the bioavailability of poorly water-soluble drugs. Acta Pharm. 2013;63:427-45. doi: 10.2478/acph-2013-0040.

34. Qi X, Wang L, Zhu J, Hu Z, Zhang J. Self-double-emulsifying drug delivery system (SDEDDS): A new way for oral delivery of drugs with high solubility and low permeability. Int J Pharm. 2011;409:245-51. doi: 10.1016/j.ijpharm.2011.02.047.

35. Tarr BD, Yalkowsky SH. Enhanced intestinal absorption of cyclosporine in rats through the reduction of emulsion droplet size. Pharm Res. 1989;6(1):40-3. doi: 10.1023/a:1015843517762.

36. Yap SP, Yuen KH. Influence of lipolysis and droplet size on tocotrienol absorption from self-emulsifying formulations. Int J Pharm. 2004;281(1-2):67-78. doi: 10.1016/j.ijpharm.2004.05.015.

37. Nigade PM, Patil SL, Tiwari SS. Self emulsifying drug delivery system (SEDDS): A review. Int J Pharm Biol Sci. 2012;2(2):42-52.

38. Mahmoud EA, Bendas ER, Mohamed MI. Preparation and evaluation of self-nanoemulsifying tablets of carvedilol. AAPS PharmSciTech. 2009;10(1):183-92. doi: 10.1208/s12249-009-9192-7.

39. Trevaskis NL, Charman WN, Porter CJH. Lipid-based delivery systems and intestinal lymphatic drug transport: A mechanistic update. Adv Drug Deliv Rev. 2008;60(6):702-16. doi: 10.1016/j.addr.2007.09.007.

40. Williams HD, Ford L, Igonin A, Shan Z, Botti P, Morgen MM, et al. Unlocking the full potential of lipid-based formulations using lipophilic salt/ionic liquid forms. Adv Drug Deliv Rev. 2019. doi: 10.1016/j.addr.2019.05.008.

41. Song Y, Zemlyanov D, Chen X, Su Z, Nie H, Lubach JW, et al. Acid-base interactions in amorphous solid dispersions of lumefantrine prepared by spray-drying and hot-melt extrusion using X-ray photoelectron spectroscopy. Int J Pharm. 2016;514:456-64. doi: 10.1016/j.ijpharm.2016.06.126.

42. Wadhwa J, Nair A, Kumria R. Emulsion forming drug delivery system for lipophilic drugs. Acta Pol Pharm. 2012;69(2):179-91.

43. Senapati PC, Sahoo SK, Sahu AN. Mixed surfactant based (SNEDDS) self-nanoemulsifying drug delivery system presenting efavirenz for enhancement of oral bioavailability. Biomed Pharmacother. 2016;80:42-51. doi: 10.1016/j.biopha.2016.02.039.

44. Chavan RB, Modi SR, Bansal AK. Role of solid carriers in pharmaceutical performance of solid supersaturable SEDDS of celecoxib. Int J Pharm. 2015;495(1):374-84. doi: 10.1016/j.ijpharm.2015.09.011.

45. Shono Y, Jantratid E, Janssen N, Kesisoglou F, Mao Y, Vertzoni M, et al. Prediction of food effects on the absorption of celecoxib based on biorelevant dissolution testing coupled with

physiologically based pharmacokinetic modeling. Eur J Pharm Biopharm. 2009;73:107-14. doi: 10.1016/j.ejpb.2009.05.009.

46. Spernath A, Aserin A. Microemulsions as carriers for drugs and nutraceuticals. Adv Colloid Interface Sci. 2006;128-130:47-64. doi: 10.1016/j.cis.2006.11.016.

47. Subramanian N, Ray S, Ghosal SK, Bhadra R, Moulik SP. Formulation design of self-microemulsifying drug delivery systems for improved oral bioavailability of celecoxib. Biol Pharm Bull. 2004;27(12):1993-9. doi: 10.1248/bpb.27.1993.

48. Chen Y, Li G, Wu X, Chen Z, Hang J, Qin B, et al. Self-microemulsifying drug delivery system (SMEDDS) of vinpocetine: Formulation development and in vivo assessment. Biol Pharm Bull. 2008;31(1):118-25.

49. Alshamsan A, Kazi M, Badran MM, Alanazi FK. Role of alternative lipid excipients in the design of self-nanoemulsifying formulations for fenofibrate: Characterization, in vitro dispersion, digestion and ex vivo gut permeation studies. Front Pharmacol. 2018;9:1-15. doi: 10.3389/fphar.2018.01219.

50. Vithani K, Hawley A, Jannin V, Pouton C, Boyd BJ. Inclusion of digestible surfactants in solid SMEDDS formulation removes lag time and influences the formation of structured particles during digestion. AAPS J. 2017;19(3):754-64. doi: 10.1208/s12248-016-0036-6.

51. Bahloul B, Lassoued MA, Sfar S. A novel approach for the development and optimization of self emulsifying drug delivery system using HLB and response surface methodology: application to fenofibrate encapsulation. Int J Pharm. 2014;466(1-2):341-8. doi: 10.1016/j.ijpharm.2014.03.040.

52. Shaji J, Lodha S. Response surface methodology for the optimization of celecoxib self-microemulsifying drug delivery system. Indian J Pharm Sci. 2008;70(5):585-90. doi: 10.4103/0250-474X.45395.

53. Shen HR, Zhong MK. Preparation and evaluation of self-microemulsifying drug delivery systems (SMEDDS) containing atorvastatin. J Pharm Pharmacol. 2006;58(9):1183-91. doi: 10.1211/jpp.58.9.0004.

54. Song WH, Park JH, Yeom DW, Ahn BK, Lee KM, Lee SG, et al. Enhanced dissolution of celecoxib by supersaturating self-emulsifying drug delivery system (S-SEDDS) formulation. Arch Pharm Res. 2013;36(1):69-78. doi: 10.1007/s12272-013-0011-z.

55. Tran T, Siqueira SDVS, Amenitsch H, Mullertz A, Rades T. In vitro and in vivo performance of monoacyl phospholipid-based self-emulsifying drug delivery systems. J Control Release. 2017;255:45-53. doi: 10.1016/j.jconrel.2017.03.393.

56. Yakushiji K, Sato H, Ogino M, Suzuki H, Seto Y, Onoue S. Self-emulsifying drug delivery system of celecoxib for avoiding delayed oral absorption in rats with impaired gastric motility. AAPS PharmSciTech. 2020;21(135):1-8. doi: 10.1208/s12249-020-01686-0.

57. Salem HF, Kharshoum RM, Sayed OM, Abdel Hakim LF. Formulation development of self-nanoemulsifying drug delivery system of celecoxib for the management of oral cavity inflammation. J Liposome Res. 2019;29(2):195-205. doi: 10.1080/08982104.2018.1524484.

58. Silva LAD, Almeida SL, Alonso ECP, Rocha PBR, Martins FT, Freitas LAP, et al. Preparation of a solid self-microemulsifying drug delivery system by hot-melt extrusion. Int J Pharm. 2018;541:1-10. doi: 10.1016/j.ijpharm.2018.02.020.

59. Heshmati N, Cheng X, Dapat E, Sassene P, Eisenbrand G, Fricker G, et al. In vitro and in vivo evaluations of the performance of an indirubin derivative, formulated in four different self-emulsifying drug delivery systems. J Pharm Pharmacol. 2014;66(11):1567-75. doi: 10.1111/jphp.12286.

60. Kim DS, Yang ES, Yong CS, Youn YS, Oh KT, Li DX, et al. Effect of inorganic mesoporous carriers on 1-palmitoyl-2-linoleoyl-3-acetyl-rac-glycerol-loaded solid self-emulsifying drug delivery system: Physicochemical characterization and bioavailability in rats. Colloids Surf B Biointerfaces. 2017;160:331-6. doi: 10.1016/j.colsurfb.2017.09.041.

61. Milović M, Djuriš J, Djekić L, Vasiljević D, Ibrić S. Characterization and evaluation of solid self-microemulsifying drug delivery systems with porous carriers as systems for improved carbamazepine release. Int J Pharm. 2012;436(1-2):58-65. doi: 10.1016/j.ijpharm.2012.06.032.

62. Sander C, Holm P. Porous magnesium aluminometasilicate tablets as carrier of a cyclosporine self-emulsifying formulation. AAPS PharmSciTech. 2009;10(4):1388-95. doi: 10.1208/s12249-009-9340-0.

63. Yeom DW, Chae BR, Kim JH, Chae JS, Shin DJ, Kim CH, et al. Solid formulation of a supersaturable self-microemulsifying drug delivery system for valsartan with improved dissolution and bioavailability. Oncotarget. 2017;8(55):94297-316. doi: 10.18632/oncotarget.21691.

64. Hu X, Lin C, Chen D, Zhang J, Liu Z, Wu W, et al. Sirolimus solid self-microemulsifying pellets: Formulation development, characterization and bioavailability evaluation. Int J Pharm. 2012;438:123-33. doi: 10.1016/j.ijpharm.2012.07.055.

65. Sohn Y, Lee SY, Lee GH, Na YJ, Kim SY, Seong I, et al. Development of self-microemulsifying bilayer tablets for pH-independent fast release of candesartan cilexetil. Pharmazie. 2012;67:917-24.

66. Tung NT, Tran CS, Pham TMH, Nguyen HA, Nguyen TL, Chi SC, et al. Development of solidified self-microemulsifying drug delivery systems containing l-tetrahydropalmatine: Design of experiment approach and bioavailability comparison. Int J Pharm. 2018;537:9-21. doi: 10.1016/j.ijpharm.2017.12.027.

67. Li T, Chen X, Liu Y, Fan L, Lin L, Xu Y, et al. pH-Sensitive mesoporous silica nanoparticles anticancer prodrugs for sustained release of ursolic acid and the enhanced anti-cancer efficacy for hepatocellular carcinoma cancer. Eur J Pharm Sci. 2017;96:456-63. doi: 10.1016/j.ejps.2016.10.019.

68. Stjern L, Voittonen S, Weldemichel R, Thuresson S, Agnes M, Benkovics G, et al. Cyclodextrin-mesoporous silica particle composites for controlled antibiotic release. A proof of concept toward colon targeting. Int J Pharm. 2017;531:595-605. doi: 10.1016/j.ijpharm.2017.05.062.

69. Wyttenbach N, Janas C, Siam M, Lauer ME, Jacob L, Scheubel E, et al. Miniaturized screening of polymers for amorphous drug stabilization (SPADS): Rapid assessment of solid dispersion systems. Eur J Pharm Biopharm. 2013;84(3):583-98. doi: 10.1016/j.ejpb.2013.01.009.

70. Wegiel LA, Mauer LJ, Edgar KJ, Taylor LS. Crystallization of amorphous solid dispersions of resveratrol during preparation and storage - Impact of different polymers. J Pharm Sci. 2013;102(1):171-84. doi: 10.1002/jps.23358.

71. Schmied FP, Bernhardt A, Engel A, Klein S. A customized screening tool approach for the development of a self-nanoemulsifying drug delivery system (SNEDDS). AAPS PharmSciTech. 2022;23(1):39. doi: 10.1208/s12249-021-02176-7.

72. Di Costanzo A, Angelico R. Formulation strategies for enhancing the bioavailability of silymarin: The state of the art. Molecules. 2019;24(11):1-29. doi: 10.3390/molecules24112155.

73. Anuar N, Sabri AH, Bustami Effendi TJ, Abdul Hamid K. Development and characterisation of ibuprofen-loaded nanoemulsion with enhanced oral bioavailability. Heliyon. 2020;6(7):1-10. doi: 10.1016/j.heliyon.2020.e04570.

74. Eleftheriadis GK, Mantelou P, Karavasili C, Chatzopoulou P, Katsantonis D, Irakli M, et al. Development and characterization of a self-nanoemulsifying drug delivery system comprised of rice bran oil for poorly soluble drugs. AAPS PharmSciTech. 2019;20(78):1-14. doi: 10.1208/s12249-018-1274-y.

75. Schmied FP, Bernhardt A, Baudron V, Beine B, Klein S. Development and characterization of celecoxib solid self-nanoemulsifying drug delivery systems (S-SNEDDS) prepared using novel cellulose-based microparticles as adsorptive carriers. AAPS PharmSciTech. 2022;23(6):213. doi: 10.1208/s12249-022-02347-0.

76. Čerpnjak K, Zvonar A, Vrečer F, Gašperlin M. Characterization of naproxen-loaded solid SMEDDSs prepared by spray drying: The effect of the polysaccharide carrier and naproxen concentration. Int J Pharm. 2015;485:215-28. doi: 10.1016/j.ijpharm.2015.03.015.

77. Schmied FP, Bernhardt A, Moers C, Meier CE, T., Klein S. A novel aminomethacrylate-based copolymer for solubility enhancement – from radical polymer synthesis to manufacture and characterization of amorphous solid dispersions. Polymers (Basel). 2022;14(7):1281. doi: 10.3390/polym14071281.

78. Schmied FP, Bernhardt A, Klein S. Preparation of solid self-nanoemulsifying drug delivery systems (S-SNEDDS) by co-extrusion of liquid SNEDDS and polymeric carriers – a new and promising approach to improve the solubility of poorly water-soluble drugs. Pharmaceuticals. 2022;15(9):1135. doi: 10.3390/ph15091135.

79. Cristofoletti R, Nair A, Abrahamsson B, Groot DW, Kopp S, Langguth P, et al. Biowaiver monographs for immediate release solid oral dosage forms: efavirenz. J Pharm Sci. 2013;102(2):318-29. doi: 10.1002/jps.23380.

80. Knopp MM, Nguyen JH, Becker C, Francke NM, Jorgensen EB, Holm P, et al. Influence of polymer molecular weight on in vitro dissolution behavior and in vivo performance of celecoxib: PVP amorphous solid dispersions. Eur J Pharm Biopharm. 2016;101:145-51. doi: 10.1016/j.ejpb.2016.02.007.

6. Published manuscripts

6.1 A customized screening tool approach for the development of a self-nanoemulsifying drug delivery system (SNEDDS)*
(*AAPS PharmSciTech*, 2022, 23(1): 39)

The presented study described the establishment of a novel screening approach that was designed in order to streamline the development of rapidly releasing self-nanoemulsifying drug delivery systems (SNEDDS) for solubility enhancement of poorly water-soluble drugs. Appropriate excipients and mixtures thereof providing a high saturation solubility for the lipophilic drug substances celecoxib as well as fenofibrate were individually identified for SNEDDS development and a special triangular mixture design was applied for ratio optimization of the excipients. When dispersed in water, suitable SNEDDS formulation candidates were characterized by a very small droplet size, a low PDI, a high transmittance as well as an excellent emulsification performance. For each drug substance, the most promising SNEDDS composition was determined individually. In addition, *in vitro* drug release studies at pH values 1, 4.5 and 6.8, that simulated different pH values along the human gastrointestinal tract, were performed. Those drug release studies were considered as another criterion for the determination of suitable SNEDDS formulation candidates in order to assess the effect on the solubilization behavior of the drug achieved by the SNEDDS formulations. The *in vitro* release experiments indicated a remarkable increase in both rate and extent of drug release when the performance of the selected celecoxib and fenofibrate SNEDDS formulation was compared with that of the corresponding, pure drug substance. Based on the obtained results, the novel screening tool proved to be a promising approach for efficiently developing stable and rapidly releasing SNEDDS formulations.

Own contributions:
Development of the scientific concept, performance of the laboratory experiments and the calculations, preparation of the manuscript

Alexander Bernhardt and Dr. Andrea Engel:
Contribution in the development of the scientific concept

Prof. Dr. Sandra Klein:
Contribution in the development of the scientific concept, revision of the manuscript

_____   _____
Fabian-Pascal Schmied   Prof. Dr. Sandra Klein

*reproduced with permission from Springer Nature

Research Article

A Customized Screening Tool Approach for the Development of a Self-Nanoemulsifying Drug Delivery System (SNEDDS)

Fabian-Pascal Schmied,[1,2] Alexander Bernhardt,[2] Andrea Engel,[2] and Sandra Klein[1,3]

Abstract. The present study focused on establishing a novel, (pre-)screening approach that enables the development of promising performing self-nanoemulsifying drug delivery systems (SNEDDSs) with a limited number of experiments. The strategic approach was based on first identifying appropriate excipients (oils/lipids, surfactants, and co-solvents) providing a high saturation solubility for lipophilic model compounds with poor aqueous solubility. Excipients meeting these requirements were selected for SNEDDS development, and a special triangular mixture design was applied for determining excipient ratios for the SNEDDS formulations. Celecoxib and fenofibrate were used as model drugs. Formulations were studied applying a specific combination of *in vitro* characterization methods. Specifications for a promising SNEDDS formulation were self-imposed: a very small droplet size (< 50 nm), a narrow size distribution of these droplets ($PDI < 0.15$) and a high transmittance following SNEDDS dispersion in water ($> 99\%$ in comparison with purified water). Excipients that provided a nanoemulsion after dispersion were combined, and ratios were optimized using a customized mapping method in a triangular mixture design. The best performing formulations were finally studied for their *in vitro* release performance. Results of the study demonstrate the efficiency of the customized screening tool approach. Since it enables successful SNEDDS development in a short time with manageable resources, this novel screening tool approach could play an important role in future SNEDDS development.

INTRODUCTION

The majority of new drug candidates in current research and development pipelines are associated with poor aqueous solubility. This may lead to low bioavailability (1–3) and is thus one of the main limitations for oral drug delivery. According to recent reports, currently, about 40% of the drugs on the market and about 75% of the drugs in the state of development are poorly water-soluble (4). Drugs with poor aqueous solubility can be further distinguished into "grease ball" and "brick dust" molecules. The aqueous solubility of "grease ball" molecules is substantially limited by their pronounced lipophilic character ($\mathrm{Log}P > 3$), while "brick dust" molecules are characterized by very high melting points

($T_m > 200\ {}^\circ$C) resulting in a high crystal lattice energy that severely impedes the drugs' solubility behavior (5, 6). In view of this growing number of poorly soluble drug candidates, it is proving necessary to establish formulation approaches to counteract the solubility issues of these drugs. Lipid-based drug delivery systems possess the ability to address an inadequate aqueous solubility (7). Especially for "grease ball" molecules, numerous studies applying lipid-based drug delivery systems have been published, while corresponding studies on "brick dust" molecules are sort of lacking (5). One of the lipid-based drug delivery systems that address the challenge of solubility enhancement of poorly water-soluble drugs is referred to as self-nanoemulsifying drug delivery system (SNEDDS) (2, 8). SNEDDSs are multicomponent, homogeneous, anhydrous liquids that, after oral administration, under the mild agitation of digestive motility, spontaneously form translucent emulsions upon contact with gastrointestinal fluids (3, 9). They consist of an oil or a lipid that is combined with a surfactant or a blend of surfactants, a co-solvent, if required, and can incorporate a lipophilic drug (3, 8, 10–12). The variety of components that can be used for SNEDDS reveals the complexity of these systems and the

---

[1] Department of Pharmacy, Institute of Biopharmaceutics and Pharmaceutical Technology, University of Greifswald, Felix-Hausdorff-Straße 3, 17489, Greifswald, Germany.

[2] Research, Development & Innovation, Evonik Operations GmbH, Kirschenallee, 64293, Darmstadt, Germany.

[3] To whom correspondence should be addressed. (e–mail: Sandra.Klein@uni-greifswald.de)

almost endless number of possible combinations with each other (13). On the one hand, this innumerable combination variety tremendously increases the possibilities to develop a functioning SNEDDS formulation. On the other hand, the high number of conceivable combinations also requires a lot of time and experimental effort when it comes to finding the right formulation approach. It would therefore be desirable to develop a screening tool that allows successful formulation approaches to be determined in a short time and with manageable experimental effort. The screening tool should target on selecting those SNEDDS components that in an appropriate mixing ratio provide excellent emulsification properties (*i.e.*, the formation of a nanoemulsion) for the drug compound of interest. Dissolving the drug in a water-free preconcentrate and obtaining a stable nanoemulsion after dispersion in an aqueous medium avoids the dissolution step of the solid prior to drug absorption and thus can facilitate drug absorption in the intestine. Particularly for highly permeable drug compounds, this can present with a higher bioavailability, which in this case is also often accompanied by more reliable *in vivo* plasma levels (14, 15).

Since a SNEDDS formulation is intended to solubilize a drug with poor aqueous solubility in the contents of the gastrointestinal tract, solubility of the drug both in the individual components of the SNEDDS as well as in the complex mixture of these components is a fundamental requirement. It is essential that the individual components of SNEDDS are also miscible with each other. As a first step in determining an appropriate mixture of constituents for a SNEDDS formulation, the saturation solubility of a lipophilic drug in the individual components that would generally be suitable for SNEDDS development should be investigated (3, 7, 9, 16–20). Components that present with a high saturation solubility for the drug of interest are promising candidates for the application in mixtures for SNEDDS (8, 16). However, the successful use of an excipient in a SNEDDS formulation requires the compatibility of all individual constituents with each other (8, 16). Moreover, as stated before, to ensure proper dispersion and to prevent drug precipitation in gastrointestinal fluids, SNEDDS should provide stable and transparent nanoemulsions after dispersion. Usually, ternary phase diagrams are constructed to determine the self-emulsifying region of a certain excipient mixture, and if a compatible excipient mixture enabling a high drug loading has been determined, a number of characterization methods such as droplet size analysis and transmittance measurement of SNEDDS after dispersion in water are applied to determine an appropriate mixing ratio of the components including the drug (20–25).

The conventional way of optimizing a ternary mixture requires about 50 individual experiments since the composition is usually varied in 10% increments to determine the optimal SNEDDS formulation.

A novel, customized screening approach distinct from the 10% increment procedure, might reduce the number of trials for developing SNEDDS formulations and could thus help to streamline the screening process for SNEDDS development. The aim of the present study was thus to establish a novel and tailored screening tool approach for the initial, rapid development of promising SNEDDS formulations which should be based on the triangular mixture design

and provide SNEDDS mixtures that fit with a set of self-imposed specifications such as providing very small nanodroplets (< 50 nm) that are narrowly distributed (polydispersity index (PDI) < 0.15) and provide a highly translucent (> 99%), stable nanoemulsion after dispersion in aqueous fluids. If these requirements are met, the resulting SNEDDS formulations should lead to improved solubility and higher dissolution rates of the investigated active pharmaceutical ingredients (APIs) and also ensure long-term stability of the formulation.

MATERIALS AND METHODS

Materials

Celecoxib and fenofibrate were used as model drug substances. Celecoxib was obtained from Aarti Drugs Ltd. (Mumbai, India) and fenofibrate from D.K. Pharma Chem PVT Ltd. (Maharashtra, India). Polyoxyethylene (80) sorbitan monooleate (Tween® 80), d-α-tocopherol polyethylene glycol 1000 succinate (d-TPGS, Tocophersolan), isopropyl myristate (IPM-100), polyoxyl-(23) lauryl ether (Brij® 35), castor oil, oleic acid, corn oil, olive oil, peanut oil, soybean oil, polyoxyl-40 hydrogenated castor oil (Cremophor® RH 40), sorbitan sesquioleate (Span® 83), polyoxyethylene sorbitan monolaurate (Tween® 20), and tetraethylene glycol (Tetra EG) were purchased from Sigma Aldrich (Steinheim, Germany). Lauroyl polyoxyl-32 glycerides (Gelucire® 44/14), oleoyl polyoxyl-6 glycerides (Labrafil® M 1944 CS), linoleoyl polyoxyl-6 glycerides (Labrafil® M 2125 CS), caprylocaproyl polyoxyl-8 glycerides (Labrasol®), propylene glycol monolaurate (type II) (lauroglycol™ 90), propylene glycol monolaurate (type I) (Lauroglycol™ FCC), glyceryl monolinoleate (Maisine™ CC), glyceryl monooleate (Peceol™), polyglyceryl-3 dioleate (Plurol® Oleique CC 497), glyceryl tricaprylate/tricaprate (Labrafac™ lipophile WL 1349), propylene glycol dicaprylate/dicaprate (Labrafac™ PG) and diethylene glycol monoethyl ether (Transcutol® HP) were kindly donated by Gattefossé S.A.S (Saint Priest, France). Medium-chain triglycerides (Miglyol® 812) and polyethylene glycol 400 were obtained from Caesar & Loretz GmbH (Hilden, Germany). Ethyl oleate (Crodamol™ EO), sorbitan monolaurate (Span® 20), sorbitan monooleate (Span® 80) and propane-1,2,3-triol were provided by Merck KGaA (Darmstadt, Germany). Polyoxyl-35 hydrogenated castor oil (Kolliphor® EL) and polyoxyl-15 hydroxystearate (Kolliphor® HS 15) were obtained from BASF SE (Ludwigshafen, Germany). Propylene glycol was purchased from VWR International GmbH (Darmstadt, Germany). Fish oil (EPA/DHA) is an in-house product of Evonik Operations GmbH (Hanau, Germany). All other chemicals and solvents were of analytical grade and purchased commercially.

HPLC Equipment for Analyzing Drug Substances

A high-performance liquid chromatography (HPLC) system (Agilent 1260 Infinity) was used for the quantification of the model drug substances. The system consisted of a quaternary pump (G1311B), autosampler (G1329B), column oven (G1316A), and UV detector (G1314C), all from Agilent

Technologies (Frankfurt am Main, Germany). The validation of the applied analytical methods was conducted according to USP specifications.

HPLC Method for Analyzing Celecoxib

Separation of all samples containing celecoxib was achieved using a Knauer Nucleosil 100–7 C18 (125 × 4.6 mm, 7 µm) column maintained at 40 °C. The mobile phase consisted of an acetonitrile:water:triethylamine mixture (300:300:0.9 v/v), adjusted to pH 3.00 with phosphoric acid. The flow rate was set to 1.8 ml/min. An injection volume of 5 µl was applied, and celecoxib was detected at 254 nm. In the concentration range of 0.13–542 µg/ml, the analytical curve was linear (r^2 = 0.999995). The method was found to be accurate (100.2–102.1%) and precise (CV 2.46%) with a quantification limit of 0.05 µg/ml. Run time was defined as 7 min.

HPLC Method for Analyzing Fenofibrate

Separation of all samples containing fenofibrate was achieved using a Symmetry 300 C18 (150 × 4.6 mm, 5 µm) column maintained at 22 °C. The mobile phase consisted of an acetonitrile:water mixture (70:30 v/v), adjusted to pH 2.50 with phosphoric acid. The flow rate was set to 2.0 ml/min. An injection volume of 20 µl was applied, and fenofibrate was detected at 286 nm. In the concentration range of 0.13–526 µg/ml, the analytical curve was linear (r^2 = 0.999992). The method was found to be accurate (101.2–101.4%) and precise (CV 2.42%) with a quantification limit of 0.05 µg/ml. Run time was defined as 6 min.

For both HPLC methods, the selectivity for the respective drug substances was determined (in the presence of each of the excipients used in the formulations). No interference was observed in drug retention time, and the peak area did not change.

Solubility Studies of Celecoxib and Fenofibrate in Various Excipients

The saturation solubility of each drug in each of the individual excipients was investigated in triplicate by the following procedure: first, drug and excipients were blended in 2-ml safe lock test tubes (17, 23, 26). After short, intense vortex mixing, the mixtures were agitated at 1000 rpm for 24 h at 37 °C under light protection using a ThermoMixer® C (Eppendorf AG, Hamburg, Germany) to achieve an equilibrium state (7, 12, 16, 17, 23, 26, 27). Subsequently, the samples were centrifuged for 1 min at 9300 relative centrifugation forces (rcf) in a preheated (37 °C) centrifuge to remove drug substance that had not dissolved (16, 17, 19, 26–28). After centrifugation at 37 °C, a defined mass (50 mg) of the supernatant was withdrawn and transferred to a 25-ml volumetric flask, and the sample was diluted with methanol to a total volume of 25.0 ml. Finally, a sample of 1 ml was analyzed using one of the previously described drug-specific HPLC methods.

Excipient Compatibility Assessment

Following the solubility studies, the excipients were tested for their miscibility or compatibility. For this purpose, binary mixtures in different mixing ratios were prepared in each case and visually inspected (data not shown). The miscibility of the individual excipients as well as the solubility of the specific drug in the individual excipients were considered as decisive criteria for the compatibility evaluation of promising excipient candidates for further SNEDDS production. Consequently, only excipients that successfully passed the compatibility test (*i.e.*, resulted in a single-phase stable system without detectable droplets, particles, or even complete phase separation) were used in the following experiments.

Triangular Mixture Design

Once a mixture of compatible excipients was identified for a given drug compound, in the presence of the API of interest, a systematic optimization of the excipient mixing ratio was performed with respect to the set specifications, namely a droplet size < 50 nm, a PDI < 0.15, and a transmittance > 99% after dispersing the SNEDDS formulation in water. For this purpose, a triangular mixture design, in which the three individual components must sum up to 100% was applied. Prior to assessing the emulsion performance, celecoxib or fenofibrate was dissolved in each individual SNEDDS mixture prepared in the screening experiments. The drug load applied in these experiments was calculated based on API solubility in the individual components of the SNEDDS mixture using the following equation:

$$Drug\ load\ [\%] = f * \frac{\sum_{i=1}^{n}(c_s)_i}{n} * 0.1 \tag{1}$$

Equation (1) contains a drug-specific factor f to ensure that the drug is completely dissolved in the mixture of the individual components even at varying quantity ratios, the determined saturation solubility c_s (in mg/g) of the drug in the individual components, and the number of individual components n used for the SNEDDS formulation. Experiments were performed as follows: in both cases, as a first step, a mixture comprising equal portions of all components, represented by the center point of the triangle, was prepared (sample 1). Then, a hexagon-shaped mixture region around this center point was mapped (Fig. 1), whereas only those mixtures described by the vertices of the hexagon were prepared and analyzed (samples 2–7). With the information obtained from the analyzed SNEDDS mixtures, attention for further formulation optimization was focused on the so-called designated area of interest (DAOI) (*i.e.*, the area within the triangular mixture design that provided SNEDDS that were closest to the above self-imposed specifications). For this step, other geometric figures such as parallelograms and trapezoids were placed into the DAOI, and the SNEDDS mixtures described by the vertices (parallelogram) or the vertices plus one or two more mixing ratios along the parallel sides (trapezoid) of these geometric structures were analyzed
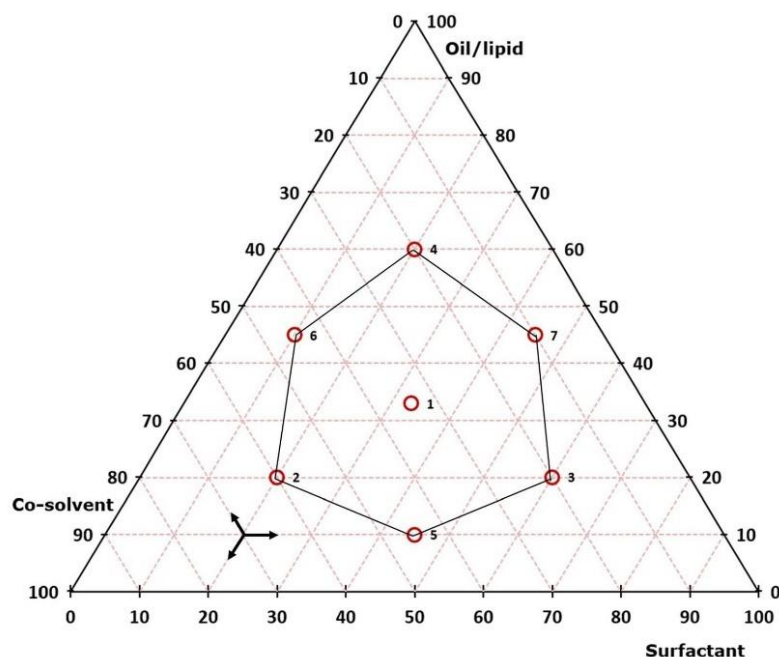
Fig. 1. Example for the basic layout of the triangular mixture design applied in determining optimal SNEDDS mixtures for celecoxib and fenofibrate

(samples 8–11 or 8–14, respectively) until a SNEDDS formulation meeting all specifications was identified.

Emulsification Performance (Visual Observation)

To ensure that SNEDDS mixtures capable of forming a stable and translucent nanoemulsion after dispersion in gastrointestinal fluids are determined, emulsification performance tests were performed as follows: a volume of 300 μl SNEDDS containing 25 mg of the specific drug was added to 500 ml water in a 600-ml low type borosilicate glass beaker. The mixture was stirred on a magnetic stirrer for 120 min at 37 ± 0.5 °C. A stirring speed of 150 rpm was set to ensure sufficient mixing, but to prevent vortex formation. All emulsification experiments were conducted using the same settings. Whether a translucent nanoemulsion had formed was visually assessed within the first 5 min of these 120 min. Visual assessment of the emulsions was performed using a grading system, with grade I representing excellent emulsifying properties and grade V indicating that no emulsion had formed (29). All SNEDDS mixtures that did not provide a nanoemulsion after dispersion were discarded. All nanoemulsions were tested for their stability over 120 min. The appearance of turbidity and precipitation of the drug substance and/or the excipients within these 120 min also led to the rejection of the respective SNEDDS mixture. All samples that provided a stable nanoemulsion after dispersion in water were retested for emulsification performance in 0.1 N hydrochloric acid using the same procedure.

Droplet Size Analysis and Zeta Potential

Besides visual inspection, samples obtained in the emulsification experiments with water as the emulsification medium were subjected to investigation of droplet size distribution by dynamic light scattering (DLS) technology and surface charge analysis (zeta potential) using a Zetasizer Nano ZS (Malvern Analytical Ltd., Malvern, UK). For these experiments, an aliquot of 1 ml was withdrawn after 10 min of stirring as described in the section "Emulsification Performance" and analyzed for droplet size and size distribution.

Transmittance Measurement

The transmittance of the samples was analyzed to identify stable nanoemulsions. A high transmittance (> 99%) indicated promising sample candidates with a small droplet size, a low chance for drug precipitation, and the potential for a high drug release. Like for the droplet size analysis, after stirring aqueous SNEDDS dispersions in the emulsification performance tests for 10 min, another aliquot (150.0 μl) was removed for transmittance measurement. The aliquot was transferred to a polystyrene 96-well plate (Cellstar, Greiner Bio-One, Kremsmuenster, Austria), and transmittance was measured at 650 nm by UV/Vis spectroscopy using a multiplate reader (Tecan Infinite M200 Pro, TECAN Group Ltd., Männedorf, Switzerland) using purified water as a blank (24, 30, 31).

Proof of Concept via Statistical Analysis

For proving the concept of the customized mapping method in a triangular mixture design, a statistical analysis of the values linked to droplet size, transmittance and emulsification performance of the analyzed celecoxib and fenofibrate SNEDDS samples was performed using Umetrics software MODDE 9.1.1 from MKS Instruments AB (Malmö, Sweden). Coefficient plots, scatter plots, and contour plots were established to investigate the impacts of varying the SNEDDS composition according to the scheme shown in Figs. 3 and 4 on droplet size, transmittance, and emulsification. As a final, statistical analysis, which essentially required the identification of statistically significant terms, main terms (*e.g.*, "Mig") and alternating terms (*e.g.*, "Mig*PS8") were implemented for the dataset of fenofibrate SNEDDS and for celecoxib SNEDDS; also, quadratic terms (*e.g.*, "Mig*Mig") were implemented to identify statistically significant trends in a coefficient diagram. In the established coefficient diagram, a significant term is represented by a large distance to the line $y = 0$ and an uncertainty level that does not cross $y = 0$. By contrast, a non-significant model term is a model term close to the line $y = 0$ and with an uncertainty level that extends beyond $y = 0$. The statistical analysis was extended by applying observed *vs.* predicted scatter plots to demonstrate the goodness of fit of the collected data. A high R^2 value indicates a good correlation, where ideally all sample points are very close to a regression diagonal.

Finally, contour plots were used to visualize the three-dimensional datasets for celecoxib and fenofibrate SNEDDS in two-dimensional plots for droplet size, transmittance, and emulsification grade. The range of all values of interest (droplet size in nm, transmittance in %, and emulsification grade according to Singh et al.(29)) was divided into a specific number of subranges by contour lines, and each subrange was assigned a color. The color assignment across the triangle geometry was used to visualize the values for droplet size, transmittance, and emulsification grade at each point of the triangle, whereby each individual point in the diagram can be assigned to a defined mixing ratio of the excipients used. In the present case, the target range for droplet size (< 50 nm) and emulsification grade (I) is in the purple area of the respective diagrams, and that for transmittance in the orange area of the related diagram.

Encapsulation Efficiency

To determine the encapsulation efficiency of the selected celecoxib and fenofibrate SNEDDS, a quantity of 1.0 g of each of the corresponding SNEDDS formulations was used. SNEDDS samples were transferred to a small safe-lock tube and centrifuged for 1 min at 9300 rcf and defined quantities of the supernatants (~ 25.0 mg, exactly weighed) were transferred into a 50-ml volumetric flask. Then, first, to each SNEDDS sample was added 10–15 ml mobile phase described in the sections "HPLC Method for Analyzing Celecoxib" and "HPLC Method for Analyzing Fenofibrate", and the mixture was subjected to ultrasonic treatment for 5 min. Then, each sample was filled up to a total volume of 50.0 ml with mobile phase, thoroughly mixed and analyzed via HPLC. Finally, encapsulation efficiency for celecoxib and

fenofibrate was calculated based on the experimentally determined drug load and the theoretical drug load of the corresponding celecoxib and fenofibrate SNEDDS.

Dissolution Studies with Drug-Loaded SNEDDS

Dissolution experiments were performed with selected celecoxib and fenofibrate SNEDDS formulations. All experiments were performed in triplicate with 25 mg of the specific drug, or an equivalent amount of drug-loaded SNEDDS (300 µl) using USP apparatus II (DT 800 LH, ERWEKA GmbH, Langen, Germany). Dissolution was studied in 0.1 N hydrochloric acid (pH 1.0), acetate buffer USP (pH 4.5), and phosphate buffer USP (pH 6.8). All experiments were performed in a media volume of 500 ml at 37 $\pm$ 0.5 °C using a paddle speed of 100 rpm. All samples were withdrawn automatically using a fraction collector, equipped with cannula filters of 10 µm pore size and manually diluted 1:1 (v/v) with acetonitrile before HPLC analysis.

Stability Studies

Quantities of 10 g each of the selected celecoxib and fenofibrate SNEDDS samples were placed into a 30-ml amber glass jar which was closed with a screw cap and stored at constant and controlled conditions (30 °C/65% RH) in a climatic chamber from Binder GmbH (Tuttlingen, Germany) for 3 months. After 3 months, aliquots from each sample were removed and again studied for encapsulation efficiency, dissolution performance, as well as droplet size, PDI, and surface charge (zeta potential) after dispersion. Results from these studies were compared with those obtained immediately after manufacture.

RESULTS

Solubility Data

The solubility data (expressed as weight percent) of the model drug substances in a selection of excipients are depicted in Fig. 2a and b. The excipients are sorted according to their function highlighted by different colors in the bar chart.

SNEDDS Formulation Design

Excipient mixtures were selected based on the solubility of the drug substance in the individual excipients and the compatibility of the excipients with each other and with the drug substance. The compatibility referred to the miscibility of the excipients with each other and the drug. Another selection criterion was the emulsification performance of the drug–excipient mixture in water. For celecoxib, an excipient mixture of Miglyol® 812, Gelucire® 44/14, Tween® 80, and d-TPGS was selected for further development. Even though celecoxib showed a high solubility in some of the co-solvents (*e.g.*, Tetra EG, Transcutol® HP, Carbowax™ PEG 400) (Fig. 2a), the emulsification properties of these candidates were inappropriate when combined with several oily components and surfactants. Therefore, they were not considered for SNEDDS formulation. By contrast, Miglyol®
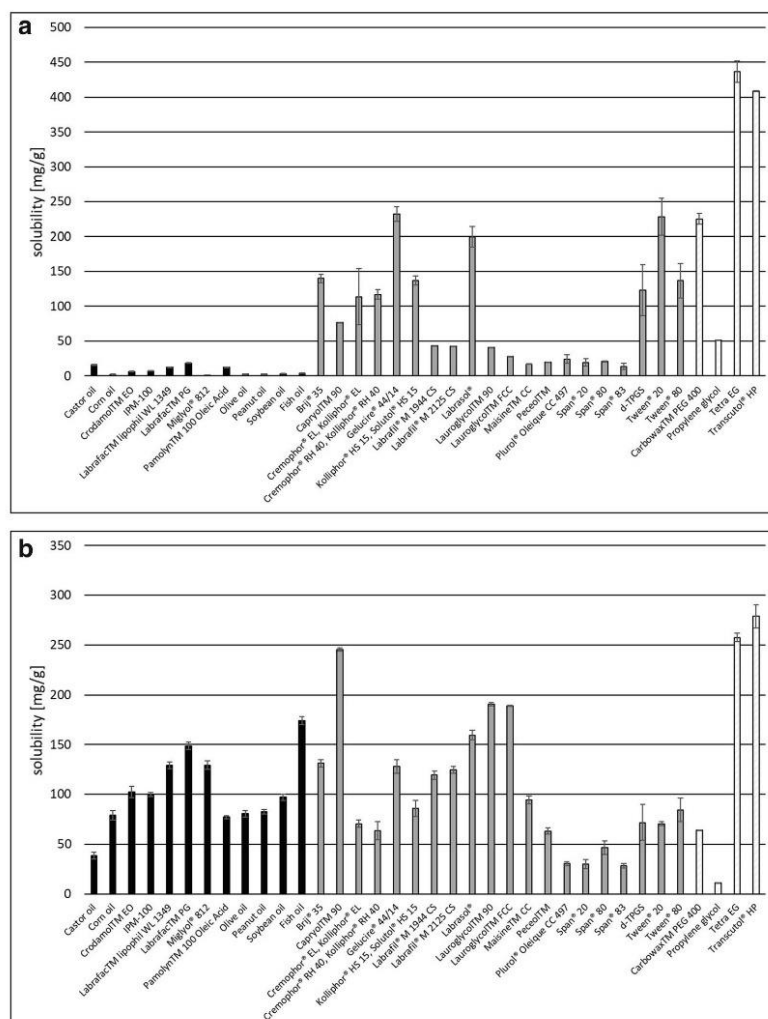
Fig. 2. Solubility of celecoxib **a** and fenofibrate **b** in various excipients. Each value designates the mean ± S.D. of $n = 3$. The oils/lipids are colored black, the surfactants grey, and the co-solvents light grey with diagonal stripes

812, which revealed exceptionally low solubility for the drug substance celecoxib, was quite easy to emulsify with the surfactant mixture selected in the prescreening experiments and thus, regardless of the solubility data, used for SNEDDS development. For both model drugs assessed in the present study, the combination of Tween® 80 and d-TPGS in a mixture ratio of 8:1 (w/w) or 5:1 (w/w) respectively, represented a well-working surfactant mixture for SNEDDS development. These two excipients were thus part of all formulations and two more compounds, selected from oils/lipids, surfactants, or a surfactant–co-solvent mixture, were added. Fenofibrate SNEDDS consisting of Miglyol®

812, Brij® 35, Tween® 80, and d-TPGS were selected for further assessment. In several other surfactants (*e.g.*, Capryol™ 90, Labrasol®, Lauroglycol™ 90, Lauroglycol™ FCC), an increased solubility of the fenofibrate (Fig. 2b) had been observed, but the respective surfactants were not suitable for establishing a stable nanoemulsion. Similar observations were made for the co-solvents Transcutol® HP and Tetra EG, which also presented with a high solubility of fenofibrate, but were not able to establish a stable nanoemulsion and thus not considered in further formulation steps. The compositions of the final SNEDDS formulations for each of the drug compounds are depicted in Table I.

Table I. Final Composition of SNEDDS Formulations Incorporating Celecoxib and Fenofibrate

Drug-SNEDDS formulation	Compound 1 (%)	Compound 2 (%)	Compound 3 (%)	Compound 4 (%)	Drug substance (%)
Celecoxib SNEDDS	Miglyol® 812 30.27	Tween® 80 49.85	Gelucire® 44/14 4.55	d-TPGS 6.24	Celecoxib 9.09
Fenofibrate SNEDDS	Miglyol® 812 18.96	Brij® 35 9.48	Tween® 80 55.29	d-TPGS 11.06	Fenofibrate 5.21

SNEDDS, self-nanoemulsifying drug delivery system

Individual Designs of the SNEDDS Optimization Approach and Proof of Concept Via Statistical Analysis

The SNEDDS development process using a triangular mixture design targeted to determine a SNEDDS composition for each drug substance that after dispersion provided a droplet size < 50 nm, a PDI < 0.15, and a transmittance > 99%. SNEDDS formulations with different mixing ratios of the selected excipients were prepared. Each formulation exhibited a drug load of 9.09% celecoxib or 5.21% fenofibrate, respectively. The proportional composition of the excipient mixtures analyzed in this initial screening approach can be obtained by reading out the triangular mixture designs provided in Figs. 3 and 4 for each sample by following the arrow directions in the lower left of the graph. Results of the droplet size analysis, PDI, and transmittance of all formulations are shown in Table II. Some mixtures did not form an emulsion after dispersion in water. For each of the two drug substances, results obtained with the majority of the excipient mixtures turned out to be in a reasonable range for the SNEDDS development studies.

When investigating promising excipient mixture ratios for celecoxib (Fig. 3), results from analyzing mixtures 1–7 indicated a DAOI in the vicinity of mixtures 1 and 6 in the triangular mixture diagram. To screen additional mixing ratios in this area for optimizing the SNEDDS composition, a parallelogram providing mixtures 8–11 was inserted for mapping this area in more detail (Fig. 3). Compared with mixtures 1 and 6, the mixtures 10 and 11 showed the desired results in terms of the droplet size and the transmittance, while mixture 11 also showed a considerably lower PDI. The best performing SNEDDS formulation for celecoxib obtained by applying this initial screening approach was thus mixture 11, which after dispersion presented itself as a stable nanoemulsion with the smallest droplet size and the lowest PDI and met all self-imposed specifications. In determining the best SNEDDS compositions for fenofibrate, results from analyzing mixtures 1–7 indicated a DAOI in the vicinity of mixtures 1, 2, 3, and 5. This area was thus mapped in more detail by inserting a trapezoid providing mixtures 8–14 (Fig. 4). In contrast to mixtures 2 and 5 which met the requirements for droplet size and transmittance, most of these additional mixtures did not meet with any of the three specifications. By contrast, mixture 8 which was in close vicinity to mixture 2 provided the best results meeting all specifications.

Statistical analysis performed to prove the concept of the tailored screening approach successfully identified significant terms for the celecoxib (Fig. 5a) and fenofibrate SNEDDS (Fig. 6a) datasets using coefficient plots. The celecoxib SNEDDS dataset proved to be more complex in this regard as compared with that of fenofibrate SNEDDS, since implementation of additional quadratic terms was required to determine significant terms for statistical analysis. The scatter plots showed linear regressions for both celecoxib (Fig. 5b) and fenofibrate SNEDDS (Fig. 6b), each with high R^2 values, indicating a sound statistical model. The contour plots (Figs. 5c and 6c) displayed target ranges for droplet size (purple region), transmittance (orange region), as well as for emulsification grade (purple region), which all met the self-imposed specifications for SNEDDS. The contour plot for celecoxib SNEDDS (Fig. 5c) showed that a concentration of Miglyol® 812 between 30 and 40% would be needed to meet the self-imposed specifications for SNEDDS, especially for droplet size and transmittance. The contour plot for fenofibrate SNEDDS (Fig. 6c) indicated that an amount of at least 50% of the Tween® 80: d-TPGS 5:1 blend would be required to achieve the relevant specifications. The mixing ratio of the selected celecoxib (sample 11) and fenofibrate (sample 8) SNEDDS formulations chosen using the new screening tool were each within the statistically determined target range. The statistical analysis thus confirmed the suitability of the tailored screening approach using a specific mapping method in a triangular design for the rapid determination of promising SNEDDS candidates.

Encapsulation Efficiency

The encapsulation efficiency was > 99% for both celecoxib and fenofibrate SNEDDS (Table III) (*i.e.*, the actual drug load was almost identical to the theoretical one shown in Table I).

Dissolution Performance of Drug-Loaded SNEDDS

Whereas the dissolution experiments confirmed the poor solubility of the two model drugs, both celecoxib and fenofibrate SNEDDS formulations showed fast and complete dissolution in media of pH 1, 4.5, and 6.8, and no precipitation was observed over the test duration of 120 min. (Fig. 7a–b).

Stability Studies

For the celecoxib SNEDDS, all results obtained in the 3-month stability study at 30 °C/65% RH were similar to those obtained immediately after manufacture (Table III) (*i.e.*, encapsulation efficiency, as well as droplet size, PDI and
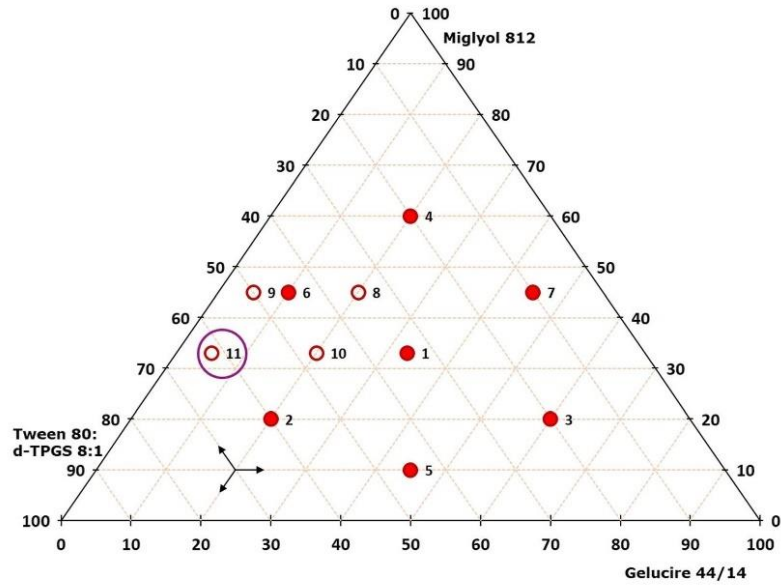
Fig. 3. Triangular mixture design applied for the SNEDDS mixture optimization for celecoxib. The filled symbols (symbols numbered 1 to 7) demonstrate the basic structure including the center point and the surrounding hexagon shape. The unfilled symbols (symbols numbered 8 to 11) show a parallelogram structure for further optimization in the DAOI. The circled symbol (symbol numbered 11) represents the final, optimized mixture ratio of excipients for celecoxib SNEDDS
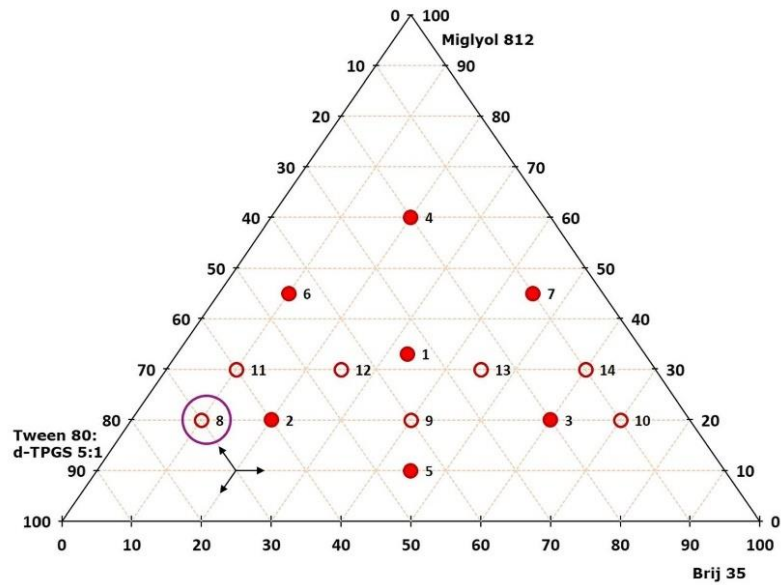

Fig. 4. Triangular mixture design applied for the SNEDDS mixture optimization for fenofibrate. The filled symbols (symbols numbered 1 to 7) demonstrate the basic structure including the center point and the surrounding hexagon shape. The unfilled symbols (symbols numbered 8 to 14) show a trapezoid structure for further optimization in the DAOI. The circled symbol (symbol numbered 8) represents the final, optimized mixture ratio of excipients for fenofibrate SNEDDS

Table II. Size Average, PDI, and Transmittance of Different Celecoxib and Fenofibrate SNEDDS Formulations Following Dispersion in Water. Sample Numbers Refer to the Corresponding Data Point (Excipient Ratio) Plotted in the Triangle Diagrams (Figs. 3 and 4). Each Value Designates the Mean ± S.D. of $n = 3$

Drug substance	Sample number	Size average (nm) ± S.D.	PDI ± S.D.	Transmittance (%) ± S.D.	Emulsification grade**
Celecoxib	1	58.8 ± 0.5	0.27 ± 0.01	98.9 ± 0.4	II
	2	N/D*	N/D*	N/D*	V
	3	N/D*	N/D*	N/D*	V
	4	150.9 ± 35.1	0.34 ± 0.07	93.5 ± 0.2	IV
	5	N/D*	N/D*	N/D*	V
	6	140.1 ± 41.6	0.20 ± 0.03	99.0 ± 0.1	II
	7	169.2 ± 2.3	0.28 ± 0.02	86.2 ± 0.4	IV
	8	133.3 ± 1.9	0.18 ± 0.01	96.9 ± 0.3	III
	9	83.3 ± 1.6	0.22 ± 0.01	99.2 ± 0.4	II
	10	38.9 ± 0.5	0.23 ± 0.01	99.9 ± 0.4	II
	11	24.4 ± 0.2	0.11 ± 0.01	99.8 ± 0.0	I
Fenofibrate	1	137.5 ± 0.7	0.16 ± 0.01	97.1 ± 0.0	III
	2	34.2 ± 0.2	0.29 ± 0.00	99.8 ± 0.2	I
	3	119.7 ± 1.3	0.20 ± 0.01	98.1 ± 0.2	III
	4	175.6 ± 1.4	0.30 ± 0.00	77.4 ± 0.3	IV
	5	34.7 ± 0.1	0.29 ± 0.00	99.2 ± 0.1	II
	6	143.5 ± 1.3	0.19 ± 0.01	93.6 ± 0.2	III
	7	181.3 ± 3.8	0.23 ± 0.00	87.1 ± 0.6	IV
	8	18.6 ± 0.3	0.06 ± 0.01	99.9 ± 0.1	I
	9	96.3 ± 0.6	0.24 ± 0.01	99.1 ± 0.2	II
	10	114.6 ± 1.2	0.17 ± 0.01	99.1 ± 0.2	III
	11	86.9 ± 0.7	0.19 ± 0.00	99.6 ± 0.1	II
	12	107.4 ± 1.4	0.21 ± 0.01	98.8 ± 0.1	III
	13	156.3 ± 1.5	0.18 ± 0.01	94.6 ± 0.3	III
	14	161.0 ± 2.7	0.17 ± 0.01	92.7 ± 0.7	III

N/D, not determined (composition did not form an emulsion); **assessment according to the grading system by Singh et al. (2008)

surface charge (zeta potential) after dispersion did barely change. Results for fenofibrate SNEDDS were mostly similar but presented with a slight decrease of the surface charge (zeta potential) and a slight increase of the PDI of the droplets after dispersion (Table III).

Storage conditions did not have an impact on the dissolution performance of both celecoxib and fenofibrate SNEDDS. As observed in the initial set of dissolution experiments, drug release was fast and complete with > 90% of the dose released within the first 15 min of the experiment in all media (Figs. 7a–b and 8a–b), and no drug precipitation was observed over the duration (120 min) of the experiments.

DISCUSSION

In this study, a special triangular mixture design was applied for determining appropriate excipient ratios for SNEDDS formulations of two poorly water-soluble drug compounds. The presented development and optimization approach for SNEDDS distinct from the conventional 10% increment procedure offered the opportunity to substantially diminish the number of trials from about 50 to 11 or 14 individual experiments, respectively. Based on reducing the number of screening experiments, this approach is very efficient in saving time and resources. Several analytical methods were strategically combined to determine the best SNEDDS composition for a given drug compound. Each analytical method on its separate basis

provided limited utility for SNEDDS development, but the combination of selected analytical results provided information on key properties, particularly emulsification performance, droplet size, PDI, and transmittance after dispersing the drug-loaded SNEDDS in water. The target drug loads for the SNEDDS formulations were calculated based on Eq. (1). A drug-specific factor f was applied to circumvent a limitation due to the saturation solubility of the drug in the excipient mixtures, especially when varying the excipient quantity ratios, since in the concentration range close to the saturation solubility of the drug in the excipient mixture, the risk of generating unstable emulsions that fail in the emulsification performance evaluation and then could not be further utilized was likely to be high. By considering the varying excipient mixture ratios as regarded from the center point of the mapping method in the triangular mixture design, value 0.7 was chosen as drug-specific factor f for celecoxib SNEDDS and 0.5 for fenofibrate SNEDDS. As a result of the initial observations in the emulsification performance experiments, a smaller value for the factor f was applied for fenofibrate than in the case of celecoxib to ensure that both celecoxib and fenofibrate SNEDDS formulations formed stable emulsions. However, three SNEDDS formulations of celecoxib did not provide stable emulsions as shown in Table II so that the information level for the mapping method in the triangular design was limited for the development of celecoxib SNEDDS. Since these three
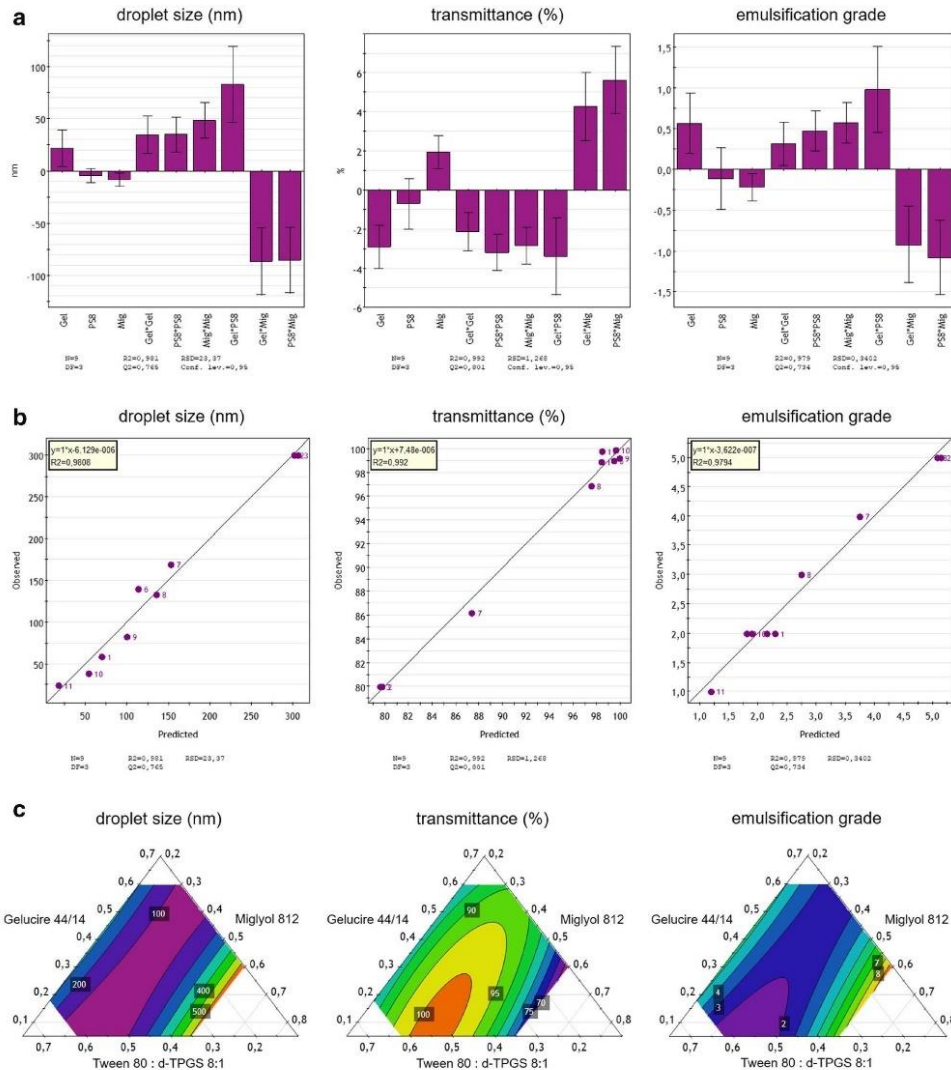
Fig. 5. Statistical modelling of the analyzed celecoxib SNEDDS samples applying a coefficient plot **a** ("Gel" = Gelucire® 44/14, "PS8" = Tween® 80: d-TPGS 8:1, "Mig" = Miglyol® 812), an observed *vs.* predicted scatter plot **b**, and a contour plot **c** for the SNEDDS parameters droplet size, transmittance, and emulsification grade

SNEDDS formulations did not provide stable emulsions for the statistical evaluation, theoretical worst-case assumptions regarding droplet size, transmittance, and emulsification grade were made for these samples to enable establishment of a statistical model. Moreover, in the applied model, results for two samples for each drug substance (samples 4 and 5 for celecoxib SNEDDS and samples 5 and 14 for fenofibrate

SNEDDS) were identified as statistical outliers and therefore excluded from the statistical analysis.

Analytical parameters obtained for the best performing SNEDDS formulations were compared with literature data from various SNEDDS studies. The droplet size of the final SNEDDS composition containing celecoxib was much smaller than the range of the droplet sizes achieved by Song
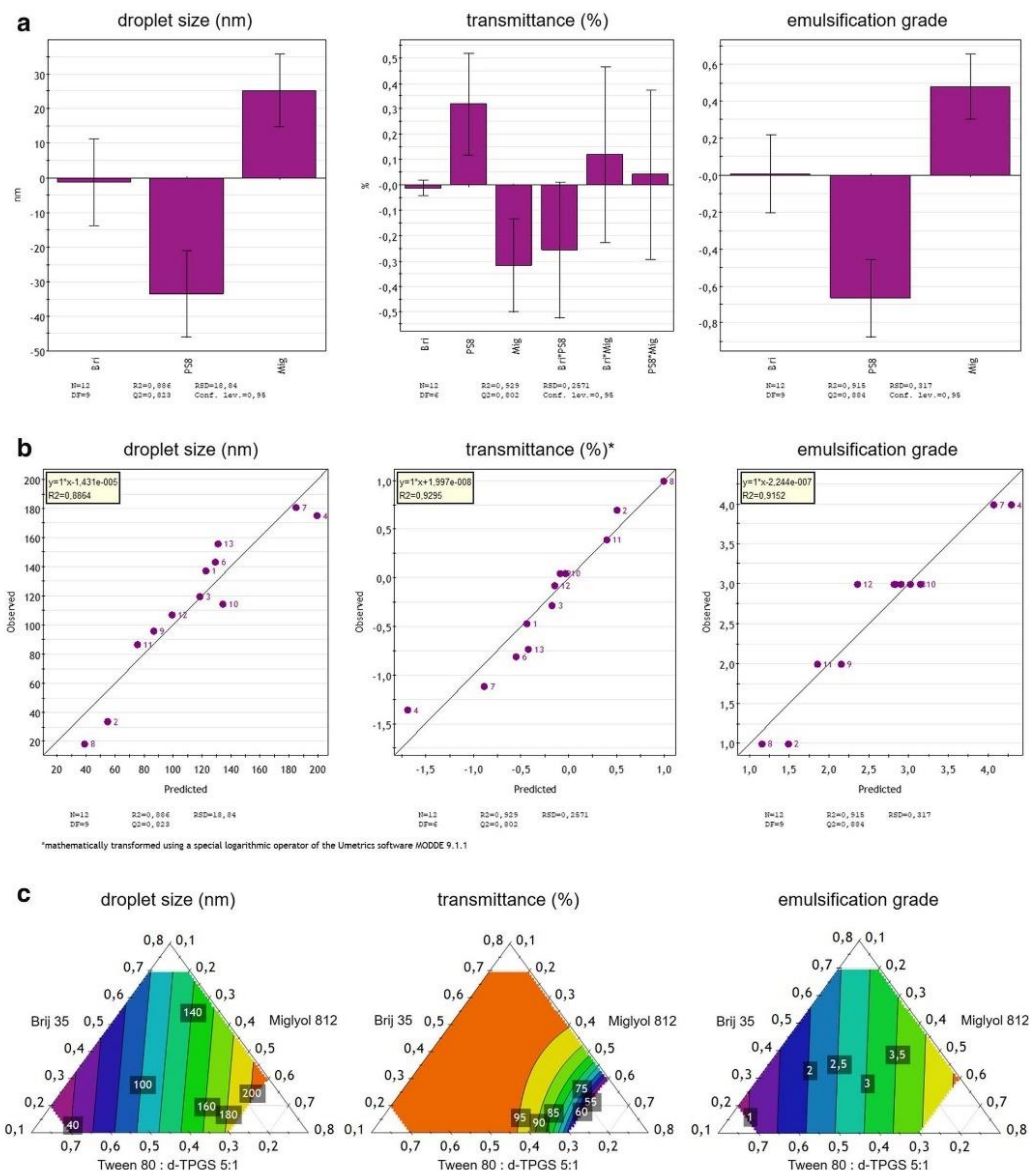
Fig. 6. Statistical modelling of the analyzed fenofibrate SNEDDS samples applying a coefficient plot **a** ("Bri" = Brij® 35, "PS8" = Tween® 80: d-TPGS 5:1, "Mig" = Miglyol® 812), an observed *vs.* predicted scatter plot **b**, and a contour plot **c** for the SNEDDS parameters droplet size, transmittance, and emulsification grade

et al.(32), Shaji et al.(33), and Salem et al.(2). Moreover, both the obtained droplet size and the PDI of celecoxib SNEDDS were smaller than those reported by Chavan et al.(19) and Yakushiji et al.(34). The final fenofibrate SNEDDS formulation revealed both a smaller droplet size and a lower PDI than the SNEDDS formulations developed by Mohsin et al.(12), Eleftheriadis et al.(35), Tran et al.(36), Bahloul

et al.(37), and Alshamsan et al.(25). All results were characterized by low standard deviations indicating the robustness of the methodology. Compared with the cited studies on SNEDDS development for the active ingredients celecoxib and fenofibrate, the approach using a special triangular mixture design provided formulations that might exhibit a better *in vivo* performance. Administering SNEDDS

Table III. Size Average, PDI, and Zeta Potential of Selected SNEDDS Formulations Following Dispersion in Water as well as Encapsulation Efficiency for the Drug Substances Celecoxib (Sample 11) and Fenofibrate (Sample 8) at the Time of Manufacture (0 M) and After 3 Months of Storage at 30 °C/65% RH (3 M). Each Value Designates the Mean ± S.D. of $n = 3$

Sample name	Zeta potential (mV) ± S.D.	Size average (nm) ± S.D.	PDI ± S.D.	Encapsulation efficiency (%) ± S.D.
Celecoxib SNEDDS (0 M)	− 6.62 ± 0.66	24.4 ± 0.2	0.11 ± 0.01	99.98 ± 0.06
Celecoxib SNEDDS (3 M)	− 7.07 ± 0.61	26.1 ± 0.2	0.12 ± 0.01	99.87 ± 0.18
Fenofibrate SNEDDS (0 M)	− 13.10 ± 0.79	18.6 ± 0.3	0.06 ± 0.01	99.90 ± 0.16
Fenofibrate SNEDDS (3 M)	− 9.34 ± 1.72	21.7 ± 0.2	0.11 ± 0.01	99.40 ± 0.13

SNEDDS, self-nanoemulsifying drug delivery system

that provide much smaller droplet sizes after dispersion may lead to better drug absorption associated with increased bioavailability (14, 38). A smaller droplet size also provided an indication of better physical stability (15) over the time as
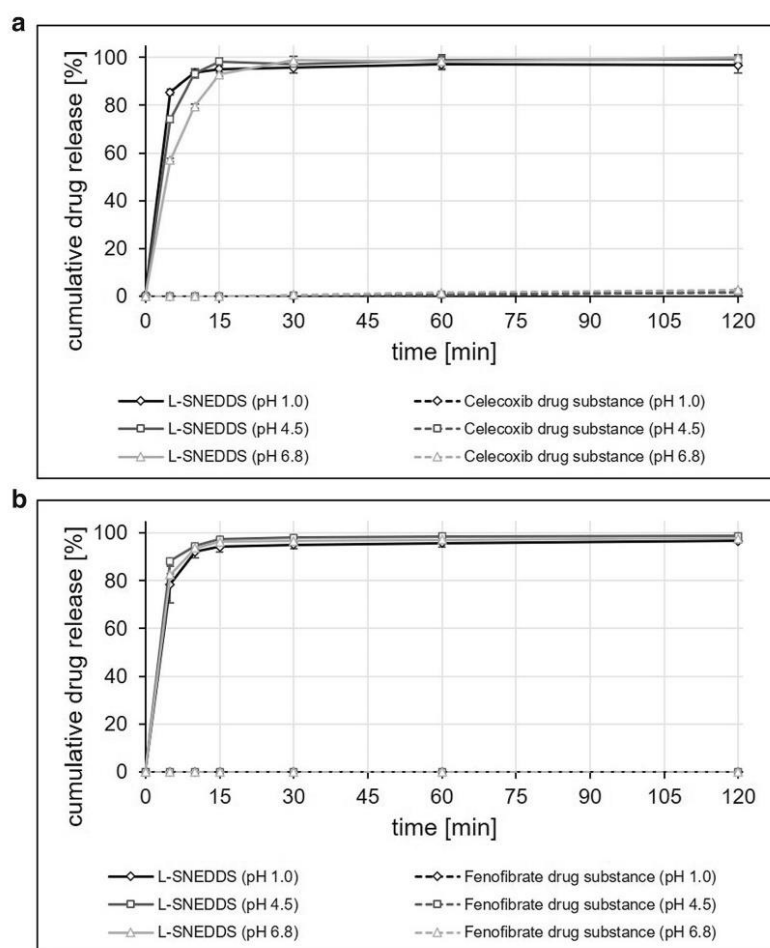
Fig. 7. Drug release profiles of celecoxib SNEDDS **a**, fenofibrate SNEDDS **b**, and the corresponding drug substances at the time of manufacture in 500 ml of 0.1 N hydrochloric acid (pH 1.0), acetate buffer USP (pH 4.5), and phosphate buffer USP (pH 6.8) using USP apparatus II at 100 rpm. Each value designates the mean ± S.D. of $n = 3$
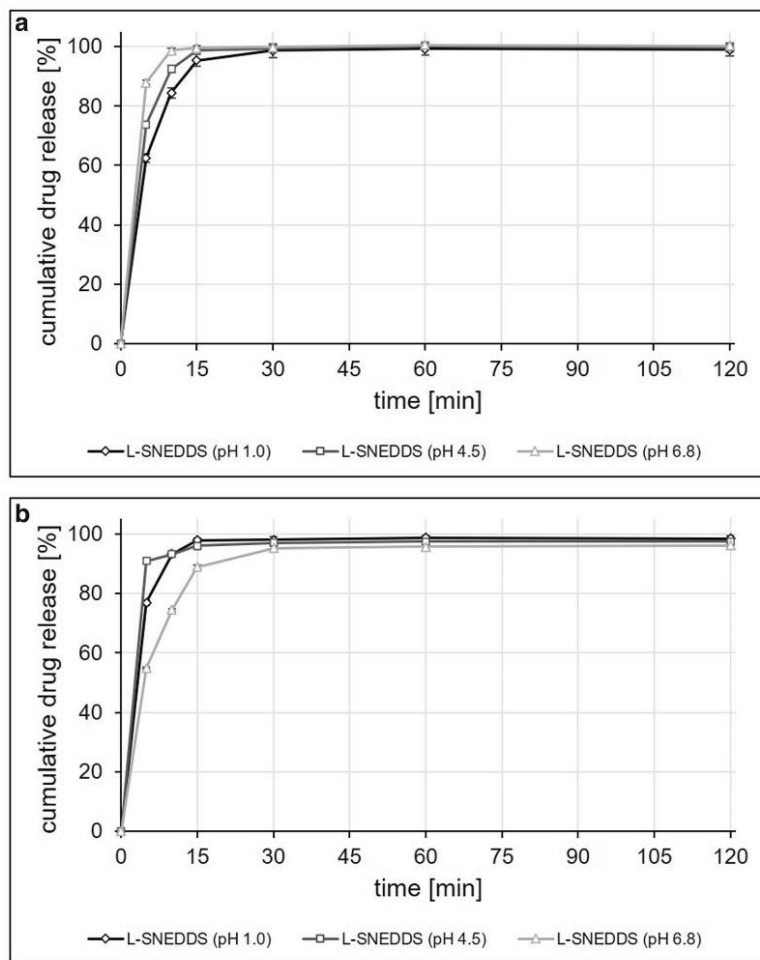
Fig. 8. Drug release profiles of celecoxib SNEDDS **a**, fenofibrate SNEDDS **b**, and the corresponding drug substances after 3 months of storage in 500 ml of 0.1 N hydrochloric acid (pH 1.0), acetate buffer USP (pH 4.5), and phosphate buffer USP (pH 6.8) using USP apparatus II at 100 rpm. Each value designates the mean ± S.D. of $n = 3$

revealed by the emulsification performance tests. Enhanced drug release and absorption as well as increased bioavailability from smaller droplet sizes of two otherwise identical formulations have been demonstrated for emulsions (39) and also for self-emulsifying drug delivery systems (38, 40, 41), although the influence of lipid digestion should not be neglected (41). The slight increase in droplet size of the final fenofibrate-SNEDDS formulation may be related to the slightly decreasing zeta potential of the formulation during the storage period, as a higher zeta potential generally indicates a higher stability of the dispersed system. This hypothesis is supported by the fact that the zeta potential for the selected celecoxib-SNEDDS formulation remained almost unchanged over a 3-month storage period, which was

also true for the corresponding droplet size of the corresponding formulation.

Results from *in vitro* release experiments with the best performing celecoxib and fenofibrate SNEDDS formulation and the corresponding active ingredients (Fig. 7a–b) clearly demonstrated the impact of formulation properties on extent and rate of drug release. Based on results from the emulsification performance tests, SNEDDS formulations rated grade III (or worse) according to the rating system of Singh et al.(29), did not prove to be suitable candidates for drug release studies and were thus not further investigated. The *in vitro* release profiles of the selected SNEDDS formulations shown in Figs. 7 and 8 support the observations made in the emulsification performance tests. The celecoxib

and fenofibrate SNEDDS formulations that immediately after manufacture, but also after 3 months of storage presented with a high encapsulation efficiency, spontaneous emulsification, a small droplet size, and a low PDI (Table III) provided a rapid, complete, and pH-independent drug release for both poorly soluble APIs.

In summary, these data clearly demonstrate the value of the established screening method, which provided a rapid, innovative, and effective (pre-)screening tool approach for the future development of SNEDDS formulations. In order to optimize this screening approach for the development of SNEDDS formulations, which certainly has not yet been fully exploited, consideration could be given to increasing the drug load of the formulations and including a broader range of excipients at the beginning of the screening process. As digestive processes could have a significant impact on the formation of nanoemulsions and therefore theoretically on the bioavailability of the administered SNEDDS formulations, this should be addressed in advanced *in vitro* studies and selected SNEDDS formulations should be finally evaluated *in vivo*.

CONCLUSION

A novel customized screening approach for rapid SNEDDS development was successfully established and applied to the model drugs celecoxib and fenofibrate. Promising SNEDDS formulations were characterized by a very small droplet size, a low PDI, a high transmittance, and excellent emulsification performance. Results from *in vitro* release experiments indicated a huge increase in both rate and extent of drug release when comparing the performance of celecoxib and fenofibrate SNEDDS formulations with that of the corresponding drug compounds. Overall, results obtained in the study indicate that the novel approach represents a promising platform for efficiently designing stable and rapidly releasing SNEDDS formulations incorporating poorly water-soluble drugs. The approach enabled the rapid determination of optimized SNEDDS formulations with a manageable, limited number of experiments. It could thus streamline the screening process for rapid SNEDDS development and will be further refined in the future.

AUTHOR CONTRIBUTION

F-PS was responsible for the methodology, validation, formal analysis, investigation, data curation, writing—original draft, and visualization. AB did the methodology, formal analysis, resources, writing—review & editing, supervision, and project administration. AE was responsible for the conceptualization, resources, and supervision. SK did the methodology, resources, writing—review & editing, supervision, and project administration.

DECLARATIONS

Conflict of interest The authors declare no disclosure of potential conflicts of interest.

REFERENCES

1. Kalepu S, Nekkanti V. Insoluble drug delivery strategies: Review of recent advances and business prospects. Acta Pharm Sin B. 2015;5(5):442–53. https://doi.org/10.1016/j.apsb.2015.07.003.
2. Salem HF, Kharshoum RM, Sayed OM, Abdel Hakim LF. Formulation development of self-nanoemulsifying drug delivery system of celecoxib for the management of oral cavity inflammation. J Liposome Res. 2019;29(2):195–205. https://doi.org/10.1080/08982104.2018.1524484.
3. Kamble RN, Mehta PP, Kumar A. Efavirenz self-nano-emulsifying drug delivery system: *In vitro* and *in vivo* evaluation. American Association of Pharmaceutical Scientists. 2016;17(5):1240–7. https://doi.org/10.1208/s12249-015-0446-2.
4. Hanada M, Jermain SV, Williams RO III. Enhanced dissolution of a porous carrier-containing ternary amorphous solid dispersion system prepared by a hot melt method. J Pharm Sci. 2018;107:362–71. https://doi.org/10.1016/j.xphs.2017.09.025.
5. Koehl NJ, Holm R, Kuentz M, Griffin BT. New insights into using lipid based suspensions for "brick dust" molecules: case study of nilotinib. Pharm Res. 2019;36(56):1–13. https://doi.org/10.1007/s11095-019-2590-y.
6. Bergstrom CAS, Charman WN, Porter CJH. Computational prediction of formulation strategies for beyond-rule-of-5 compounds. Adv Drug Deliv Rev. 2016;101:6–21. https://doi.org/10.1016/j.addr.2016.02.005.
7. Subramanian N, Ray S, Ghosal SK, Bhadra R, Moulik SP. Formulation design of self-microemulsifying drug delivery systems for improved oral bioavailability of celecoxib. Biol

Pharm. Bull. 2004;27(12):1993–9. https://doi.org/10.1248/bpb.27.1993.

8. Porter CJH, Pouton CW, Cuine JF, Charman WN. Enhancing intestinal drug solubilisation using lipid-based delivery systems. Adv Drug Deliv Rev. 2008;60(6):673–91. https://doi.org/10.1016/j.addr.2007.10.014.

9. Thomas N, Holm R, Mullertz A, Rades T. *In vitro* and *in vivo* performance of novel supersaturated self-nanoemulsifying drug delivery systems (super-SNEDDS). J Control Release. 2012;160(1):25–32. https://doi.org/10.1016/j.jconrel.2012.02.027.

10. Dokania S, Joshi AK. Self-microemulsifying drug delivery system (SMEDDS) - Challenges and road ahead. Drug Deliv. 2015;22(6):675–90. https://doi.org/10.3109/10717544.2014.896058.

11. Pouton CW. Lipid formulations for oral administration of drugs: Non-emulsifying, self-emulsifying and "self-microemulsifying" drug delivery systems. Eur J Pharm Sci. 2000;11(2):93–8. https://doi.org/10.1016/s0928-0987(00)00167-6.

12. Mohsin K, Alamri R, Ahmad A, Raish M, Alanazi FK, Hussain MD. Development of self-nanoemulsifying drug delivery systems for the enhancement of solubility and oral bioavailability of fenofibrate, a poorly water-soluble drug. Int J Nanomed. 2016;11:2829–38. https://doi.org/10.2147/IJN.S104187.

13. Mahmoud EA, Bendas ER, Mohamed MI. Preparation and evaluation of self-nanoemulsifying tablets of carvedilol. American Association of Pharmaceutical Scientists. 2009;10(1):183–92. https://doi.org/10.1208/s12249-009-9192-7.

14. Anuar N, Sabri AH, Bustami Effendi TJ, Abdul HK. Development and characterisation of ibuprofen-loaded nanoemulsion with enhanced oral bioavailability. Heliyon. 2020;6(7):1–10. https://doi.org/10.1016/j.heliyon.2020.e04570.

15. Di Costanzo A, Angelico R. Formulation strategies for enhancing the bioavailability of silymarin: The state of the art. Molecules. 2019;24(11):1–29. https://doi.org/10.3390/molecules24112155.

16. Larsen AT, Ogbonna A, Abu-Rmaileh R, Abrahamsson B, Ostergaard J, Mullertz A. SNEDDS containing poorly water soluble cinnarizine; Development and *in vitro* characterization of dispersion, digestion and solubilization. Pharmaceutics. 2012;4(4):641–65. https://doi.org/10.3390/pharmaceutics4040641.

17. Shono Y, Jantratid E, Janssen N, Kesisoglou F, Mao Y, Vertzoni M, et al. Prediction of food effects on the absorption of celecoxib based on biorelevant dissolution testing coupled with physiologically based pharmacokinetic modeling. Eur J Pharm Biopharm. 2009;73:107–14. https://doi.org/10.1016/j.ejpb.2009.05.009.

18. Spernath A, Aserin A. Microemulsions as carriers for drugs and nutraceuticals. Adv Colloid Interface Sci. 2006;128–130:47–64. https://doi.org/10.1016/j.cis.2006.11.016.

19. Chavan RB, Modi SR, Bansal AK. Role of solid carriers in pharmaceutical performance of solid supersaturable SEDDS of celecoxib. Int J Pharm. 2015;495(1):374–84. https://doi.org/10.1016/j.ijpharm.2015.09.011.

20. Senapati PC, Sahoo SK, Sahu AN. Mixed surfactant based (SNEDDS) self-nanoemulsifying drug delivery system presenting efavirenz for enhancement of oral bioavailability. Biomed Pharmacother. 2016;80:42–51. https://doi.org/10.1016/j.biopha.2016.02.039.

21. Akula S, Gurram AK, Devireddy SR. Self-microemulsifying drug delivery systems: An attractive strategy for enhanced therapeutic profile. Int Sch Res Notices. 2014;2014:1–11. https://doi.org/10.1155/2014/964051.

22. Chen Y, Li G, Wu X, Chen Z, Hang J, Qin B, et al. Self-microemulsifying drug delivery system (SMEDDS) of vinpocetine: Formulation development and *in vivo* assessment. Biol Pharm Bull. 2008;31(1):118–25.

23. Siqueira SDVS, Mullertz A, Graeser K, Kasten G, Mu H, Rades T. Influence of drug load and physical form of cinnarizine in new SNEDDS dosing regimens: *In vitro* and *in vivo* evaluations. AAPS J. 2017;19(2):587–94. https://doi.org/10.1208/s12248-016-0038-4.

24. Vithani K, Hawley A, Jannin V, Pouton C, Boyd BJ. Inclusion of digestible surfactants in solid SMEDDS formulation removes lag time and influences the formation of structured particles during digestion. AAPS J. 2017;19(3):754–64. https://doi.org/10.1208/s12248-016-0036-6.

25. Alshamsan A, Kazi M, Badran MM, Alanazi FK. Role of alternative lipid excipients in the design of self-nanoemulsifying formulations for fenofibrate: Characterization, *in vitro* dispersion, digestion and ex vivo gut permeation studies. Front Pharmacol. 2018;9:1–15. https://doi.org/10.3389/fphar.2018.01219.

26. Sagar K, Kendre P, Pande V, Chaudhari V. Design, development and characterization of self-nanoemulsifiying drug delivery system (SNEDDS) of nateglinide. World J Pharm Pharm Sci. 2014;3(8):794–811.

27. Tung NT, Tran CS, Pham TMH, Nguyen HA, Nguyen TL, Chi SC, et al. Development of solidified self-microemulsifying drug delivery systems containing l-tetrahydropalmatine: Design of experiment approach and bioavailability comparison. Int J Pharm. 2018;537:9–21. https://doi.org/10.1016/j.ijpharm.2017.12.027.

28. Jangipuria F, Londhe V. Solubility enhancement of lurasidone hydrochloride by preparing SMEDDS. Int J Pharm Pharm Sci. 2015;7(11):283–8.

29. Singh AK, Chaurasiya A, Singh M, Upadhyay SC, Mukherjee R, Khar RK. Exemestane loaded self-microemulsifying drug delivery system (SMEDDS): Development and optimization. American Association of Pharmaceutical Scientists. 2008;9(2):628–34. https://doi.org/10.1208/s12249-008-9080-0.

30. Nigade PM, Patil SL, Tiwari SS. Self emulsifying drug delivery system (SEDDS): A review. Int J Pharm Biol Sci. 2012;2(2):42–52.

31. Shen HR, Zhong MK. Preparation and evaluation of self-microemulsifying drug delivery systems (SMEDDS) containing atorvastatin. J Pharm Pharmacol. 2006;58(9):1183–91. https://doi.org/10.1211/jpp.58.9.0004.

32. Song WH, Park JH, Yeom DW, Ahn BK, Lee KM, Lee SG, et al. Enhanced dissolution of celecoxib by supersaturating self-emulsifying drug delivery system (S-SEDDS) formulation. Arch Pharmacal Res. 2013;36(1):69–78. https://doi.org/10.1007/s12272-013-0011-z.

33. Shaji J, Lodha S. Response surface methodology for the optimization of celecoxib self-microemulsifying drug delivery system. Indian J Pharm Sci. 2008;70(5):585–90. https://doi.org/10.4103/0250-474X.45395.

34. Yakushiji K, Sato H, Ogino M, Suzuki H, Seto Y, Onoue S. Self-emulsifying drug delivery system of celecoxib for avoiding delayed oral absorption in rats with impaired gastric motility. American Association of Pharmaceutical Scientists. 2020;21(135):1–8. https://doi.org/10.1208/s12249-020-01686-0.

35. Eleftheriadis GK, Mantelou P, Karavasili C, Chatzopoulou P, Katsantonis D, Irakli M, et al. Development and characterization of a self-nanoemulsifying drug delivery system comprised of rice bran oil for poorly soluble drugs. American Association of Pharmaceutical Scientists. 2019;20(78):1–14. https://doi.org/10.1208/s12249-018-1274-y.

36. Tran T, Siqueira SDVS, Amenitsch H, Mullertz A, Rades T. *In vitro* and *in vivo* performance of monoacyl phospholipid-based self-emulsifying drug delivery systems. J Control Release. 2017;255:45–53. https://doi.org/10.1016/j.jconrel.2017.03.393.

37. Bahloul B, Lassoued MA, Sfar S. A novel approach for the development and optimization of self emulsifying drug delivery system using HLB and response surface methodology: application to fenofibrate encapsulation. Int J Pharm. 2014;466(1–2):341–8. https://doi.org/10.1016/j.ijpharm.2014.03.040.

51

38. Yap SP, Yuen KH. Influence of lipolysis and droplet size on tocotrienol absorption from self-emulsifying formulations. Int J Pharm. 2004;281(1–2):67–78. https://doi.org/10.1016/j.ijpharm.2004.05.015.

39. Tarr BD, Yalkowsky SH. Enhanced intestinal absorption of cyclosporine in rats through the reduction of emulsion droplet size. Pharm Res. 1989;6(1):40–3. https://doi.org/10.1023/a:1015843517762.

40. Chatterjee B, Almurisi SH, Dukhan AAM, Mandal UK, Sengupta P. Controversies with self-emulsifying drug delivery system from pharmacokinetic point of view. Drug Deliv. 2016;23(9):3639–52. https://doi.org/10.1080/10717544.2016.1214990.

41. de Smidt PC, Campanero MA, Troconiz IF. Intestinal absorption of penclomedine from lipid vehicles in the conscious rat: contribution of emulsification versus digestibility. Int J Pharm. 2004;270(1–2):109–18. https://doi.org/10.1016/j.ijpharm.2003.10.036.

6.2 Development and characterization of celecoxib solid self-nanoemulsifying drug delivery systems (S-SNEDDS) prepared using novel cellulose-based microparticles as adsorptive carriers*

(*AAPS PharmSciTech*, 2022, 23(6): 213)

This study focused on the conversion of celecoxib loaded L-SNEDDS into S-SNEDDS with improved stability compared to corresponding L-SNEDDS formulations using different adsorptive carrier materials. The aim was to obtain stable S-SNEDDS showing a release behavior similar to that of L-SNEDDS, that should not be affected by measures of the adsorptive carrier. In this context, novel cellulose-based microparticles using different binders (gum arabic or methylcellulose) were prepared via spray drying and investigated for their suitability as adsorbents for L-SNEDDS formulations. The material-specific properties such as particle size and morphology of the novel cellulose-based microparticles as well as various commercially available carriers were screened and the effects of the different carriers' properties on loading capacity for L-SNEDDS and *in vitro* drug release performance were analyzed. The results of the study revealed that it is possible to develop S-SNEDDS without affecting rate and extent of drug release of the corresponding L-SNEDDS when using suitable adsorptive carriers. Amongst all the carriers evaluated in this study the novel cellulose-based microparticle carrier with the binder gum arabic turned out as the most promising candidate for the development of celecoxib loaded S-SNEDDS. In summary, depending on the material-specific properties, adsorptive carriers provide a promising, alternative approach to prepare stable S-SNEDDS formulations.

Own contributions:
Development of the scientific concept, performance of the laboratory experiments and the calculations, preparation of the manuscript

Alexander Bernhardt:
Contribution in the development of the scientific concept, revision of the manuscript

Victor Baudron and Dr. Birte Beine:
Contribution in the development of microparticle carrier

Prof. Dr. Sandra Klein:
Contribution in the development of the scientific concept, revision of the manuscript

_____   _____
           Fabian-Pascal Schmied   Prof. Dr. Sandra Klein

*reproduced with permission from Springer Nature

RESEARCH ARTICLE

Advancements in Amorphous Solid Dispersions to Improve Bioavailability

Development and Characterization of Celecoxib Solid Self-nanoemulsifying Drug Delivery Systems (S-SNEDDS) Prepared Using Novel Cellulose-Based Microparticles as Adsorptive Carriers

Fabian-Pascal Schmied[1,2] · Alexander Bernhardt[2] · Victor Baudron[3] · Birte Beine[4] · Sandra Klein[1]

Abstract

Self-nanoemulsifying drug delivery systems (SNEDDS) represent an interesting platform for improving the oral bioavailability of poorly soluble lipophilic drugs. While Liquid-SNEDDS (L-SNEDDS) effectively solubilize the drug *in vivo*, they have several drawbacks, including poor storage stability. Solid-SNEDDS (S-SNEDDS) combine the advantages of L-SNEDDS with those of solid dosage forms, particularly stability. The aim of the present study was to convert celecoxib L-SNEDDS into S-SNEDDS without altering their release behavior. Various commercially available adsorptive carrier materials were investigated, as well as novel cellulose-based microparticles prepared by spray drying from an aqueous dispersion containing Diacel® 10 and methyl cellulose or gum arabic as a binder prior to their use. Particle size and morphology of the carrier materials were screened by scanning electron microscopy and their effects on the loading capacity for L-SNEDDS were investigated, and comparative *in vitro* dissolution studies of celecoxib L-SNEDDS and the different S-SNEDDS were performed immediately after preparation and after 3 months of storage. Among the adsorptive carrier materials, the novel cellulose-based microparticles were found to be the most suitable for the preparation of celecoxib S-SNEDDS from L-SNEDDS, enabling the preparation of a solid, stable formulation while preserving the *in vitro* release performance of the L-SNEDDS formulation.

Keywords Cellulose · Drug release · L-SNEDDS · Poorly soluble drugs · Scanning electron microscopy

Introduction

Many new drug candidates are characterized by poor water solubility and for this reason often have poor oral bioavailability [1]. Since this trend will certainly continue in the coming decades, the question of how to overcome this limitation is becoming more and more important. Lipid-based drug delivery systems, particularly self-nanoemulsifying drug delivery system (SNEDDS), represent an interesting platform for improving the oral bioavailability of drugs that are poorly soluble in aqueous media but can be well absorbed through the intestinal wall. SNEDDS are made from a combination of different excipients, such as lipids/oils, surfactants and co-solvents and typically present liquid formulations [2–4]. Oral administration of SNEDDS aims to generate a transparent emulsion characterized by an average droplet size of approximately 100 nm upon contact with gastrointestinal fluids at conditions of average gastrointestinal motility [5]. If poorly soluble drugs are formulated in Liquid-SNEDDS (L-SNEDDS), they usually remain dissolved in the inner phase of the resulting emulsion and are solubilized in this way. Currently, several L-SNEDDS formulations are available on the market [1]. However,

✉ Sandra Klein
Sandra.Klein@uni-greifswald.de

1   University of Greifswald, Department of Pharmacy, Institute of Biopharmaceutics and Pharmaceutical Technology, Felix-Hausdorff-Straße 3, 17489 Greifswald, Germany

2   Evonik Operations GmbH, Research, Development & Innovation, Kirschenallee, 64293 Darmstadt, Germany

3   Evonik Operations GmbH, Research, Development & Innovation, Rodenbacher Chaussee 4, 63457 Hanau, Germany

4   Evonik Operations GmbH, Research, Development & Innovation, Paul-Baumann-Str. 1, 55772 Marl, Germany

 aaps

 Springer

while L-SNEDDS, once a suitable excipient combination for a given drug has been determined, are relatively quick and easy to prepare and effectively solubilize the drug *in vivo*, they also have some major drawbacks [6]. These arise, among other factors, from the need for complex processes for their further conversion into suitable dosage forms, such as the filling of L-SNEDDS into soft capsules, or sealed hard capsules, which are often associated with high production costs [2, 6, 7]. In addition, these liquid formulations often have low storage stability as well as limited shelf life [2, 6–8]. Moreover, they pose the risk of interactions with the capsule shell material, leakage from the capsule, and are hardly suitable for the development of controlled release dosage forms [2, 9]. Conversion of L-SNEDDS into Solid-SNEDDS (S-SNEDDS) could be a method of overcoming these drawbacks. Adsorption onto a solid carrier represents a suitable technology for this purpose and various materials with different chemical as well as biological origins can be utilized as adsorptive carriers [2, 10–14].

Due to their different chemical compositions and the methods used for their manufacture, adsorptive carrier materials may differ in terms of many of their properties, such as particle size and particle size distribution, surface area, morphology, density, porosity, plasticity, hardness, acid–base resistance, polarity, and the potential for molecular interactions [10, 11, 15]. These material-specific properties can affect the loading capacity for liquid formulations, further processing (e.g., capsule filling or tableting) and drug release [15–18]. The selection of the right carrier should allow the design of an individual, tailor-made formulation depending on the desired properties of the S-SNEDDS to be produced. By carefully combining specific carrier materials and properties with L-SNEDDS, it would ideally be possible to produce tailor-made S-SNEDDS with predefined properties. Materials that can be considered as solid carriers comprise silicon dioxide, calcium silicate, other inorganic magnesium and calcium salts, cellulose or starch, and their derivatives [2, 10, 12, 13, 19–21].

When L-SNEDDS are adsorbed onto a specific adsorptive carrier material, it is important to maintain their good release behavior, which can be a problem for the obtained S-SNEDDS formulation [14, 22, 23]. For example, studies by Patki *et al*. [23], in which the drug release of fenofibrate S-SNEDDS prepared from L-SNEDDS of this poorly water-soluble drug and various carrier materials, showed a decrease in drug release after adsorption to a solid carrier compared to fenofibrate L-SNEDDS. Although the release studies were conducted in a surfactant-containing medium (900 ml distilled water with 0.75% sodium lauryl sulfate (SLS) added), complete fenofibrate release did not occur, indicating limited drug desorption with respect to the carrier materials used. Carrier materials used in this study comprised hydroxypropyl methyl cellulose (HPMC),

calcium silicate (FLORITE®), polyvinyl alcohol (PVA), magnesium aluminometasilicate (Neusilin® US2), amorphous anhydrous colloidal silica (AEROSIL® 200), and mixtures thereof. Similarly, a decreased celecoxib release was reported by Chavan *et al*. [14], when studying drug release of celecoxib L-SNEDDS in 900 ml of distilled water before and after adsorption onto silica-based carrier materials. Finally, also Cerpnjak *et al*. [22], who used maltodextrin as well as HPMC as adsorptive carriers for celecoxib L-SNEDDS, observed incomplete drug release after adsorbing L-SNEDDS to a solid carrier. Thus, the advantages of converting L-SNEDDS into solid formulations have initially proven to be only theoretical in most cases. The identification of suitable solid carrier materials that can be loaded with L-SNEDDS allows a high loading capacity and does not significantly impair the release of the adsorbed L-SNEDDS formulation or the contained active ingredient remains a challenge.

Although a variety of adsorptive carriers is already available, there is still room for new materials when it comes to overcoming the existing limitations of carriers in the field of L-SNEDDS conversion by adsorption technologies. The aim of the present study was to convert celecoxib L-SNEDDS developed in a previous study by Schmied *et al*. [24] into S-SNEDDS without altering their release behavior. Various commercially available adsorptive carrier materials as well as a novel biodegradable cellulose-based microparticle material should be evaluated for their suitability for S-SNEDDS preparation. Particles with a spherical, porous design should first be produced from the new cellulose-based material to enable good processability and the highest possible loading capacity for L-SNEDDS. To investigate the influence of material and particle characteristics of the different adsorptive carriers on drug release, particle size and morphology and their effects on the loading capacity for L-SNEDDS should be screened. Furthermore, comparative *in vitro* dissolution studies of the celecoxib L-SNEDDS and S-SNEDDS should be performed.

Materials and Methods

Materials

Celecoxib was obtained from Aarti Drugs Ltd. (Mumbai, India). Methyl cellulose, polyoxyethylene (80) sorbitan monooleate (Tween® 80), and d-α-tocopherol polyethylene glycol 1000 succinate (d-TPGS) were purchased from Sigma Aldrich Chemie GmbH (Steinheim, Germany). Gelucire® 44/14 was kindly donated by Gattefossé S.A.S (Saint Priest, France). Miglyol® 812 was purchased from Caesar & Loretz GmbH (Hilden, Germany). Aeroperl® 300 Pharma, Zeopharm® 600, and Sipernat® 160 PQ were in-house

products of Evonik Resource Efficiency GmbH (Hanau, Germany). Syloid® XDP 3050 was kindly donated by W. R. Grace & Co.-Conn. (Worms, Germany). Avicel® PH-101 was obtained from Dow Chemical Company (Schwalbach am Taunus, Germany) and Diacel® 10 was purchased from CFF GmbH & Co. KG (Gehren, Germany). Gum arabic was obtained from Norevo GmbH (Hamburg, Germany). All other chemicals and solvents were of analytical grade and purchased commercially.

Methods

L-SNEDDS

Celecoxib L-SNEDDS were prepared as described by Schmied *et al.* [24] in a previous study based on solubility studies of the specific drug in a variety of excipients selected from lipids, (co)surfactants, and (co)solvents (data not shown). Combining the application of a systematic triangular design approach [24] and multiple analytical methods resulted in the selected celecoxib L-SNEDDS formulations, which were then used for subsequent, further processing into S-SNEDDS. The best-performing excipient composition and mixing ratio for L-SNEDDS were derived from meeting the following self-imposed specifications: the resulting nanoemulsion after dispersion of the L-SNEDDS in water had to have a droplet size < 50 nm, a polydispersity index (PDI) < 0.15, and a transmittance of > 99% (data not shown) [24]. The formulation used for all adsorption experiments in the present study consisted of 30.27% (w/w) Miglyol® 812, 49.85% (w/w) Tween® 80, 4.55% (w/w) Gelucire® 44/14, 6.24% (w/w) d-TPGS, and 9.09% (w/w) celecoxib.

Manufacturing of Cellulose-Based Microparticles as Adsorptive Carrier

Cellulose microparticles were made from native Diacel® 10 cellulose material by spray drying using an aqueous dispersion containing Diacel® 10 and methyl cellulose (MC) or gum arabic (GA) as a binder. The quantities of cellulose, binder, and deionized water were chosen in order to obtain a 10 or 20% (w/w) solid concentration in the dispersion and a 9:1 ratio (w/w) of cellulose to binder in the final dry product. Dispersions were made as follows: first, the binders were dissolved in water. For obtaining a gum arabic solution, gum arabic was stepwise added to the water while stirring with an overhead stirrer at 600 rpm. After completing the addition of gum arabic, stirring was continued for 30 min until a clear solution was obtained. The methyl cellulose colloidal solution was made by heating half of the total water quantity to 80°C before stepwise adding methyl cellulose while stirring as described for gum arabic. The second half of the total water volume was kept at room temperature, then added to

the methyl cellulose dispersion, and the mixture was stirred for another 40 min at 600 rpm. Thereafter, while stirring (600 rpm), the Diacel® 10 cellulose material was added to the binder solution and stirring was continued for another 30 min at 600 rpm. Subsequently, the resulting aqueous cellulose dispersion was spray dried using a Niro Minor spray dryer (GEA Group AG, Düsseldorf, Germany). For this purpose, the dispersion was fed into the nozzle at a flow rate of 2.5 kg/h via a tube connected to a peristaltic pump. The dispersion was atomized into fine droplets using a two-fluid nozzle with a bore diameter of 1 mm. Nitrogen was used as the atomizing gas and the temperature of the drying air at the inlet was 200°C. The process was operated in the top-spray mode and the dry particles, referred to as microcellulose-methyl cellulose particles (M-MC) or microcellulose-gum arabic particles (M-GA), were collected in a vessel after being separated from the gas stream via a cyclone.

Particle Size Distribution Analysis of Adsorptive Carriers by Laser Diffraction

All adsorptive carrier materials applied in the study, *i.e.*, calcium silicate (Zeopharm® 600), silicon dioxide (Aeroperl® 300 Pharma, Sipernat® 160 PQ, Syloid® XDP 3050), and cellulose (Avicel® PH-101, M-MC, and M-GA), were subject to investigation of particle size distribution by laser diffraction analysis using a Mastersizer 3000 from Malvern Panalytical Ltd. (Malvern, UK). The particles were suspended in Milli Q water and the sample concentration was guided by the measured obscuration. All samples were analyzed in an obscuration range of 5–10% to ensure an optimal signal to noise ratio and the average particle size d_{50} of individual samples was determined in triplicate.

Morphology Analysis of Adsorptive Carriers by Scanning Electron Microscopy (SEM)

To get an estimate of the morphology of the solid carrier materials, a representative sample of particles, approximately 30 mg, was sputtered with gold in an argon plasma for 30 s at 40 mA in a Jeol JFC-1300 auto fine coater from Nikon Metrology GmbH (Alzenau, Germany). Subsequently, microscopic images of the particles were taken using the Jeol Neoscope JCM-5000 scanning electron microscope from Nikon Metrology GmbH (Alzenau, Germany) at an accelerating voltage of 10 kV.

Preparation of S-SNEDDS

Celecoxib S-SNEDDS were prepared by adsorption of anhydrous celecoxib L-SNEDDS onto the individual solid carrier

▷ Springer

materials. For this purpose, 1.0 g of the liquid phase, *i.e.*, the celecoxib L-SNEDDS formulation comprising a combination of lipids/oils, surfactants, co-solvents, and the dissolved drug substance, was placed in a 25-ml glass beaker under moderate stirring using a propeller stirrer at 100 rpm. With stirring, a suitable amount of adsorptive material was added to the liquid phase in small portions, depending on the properties of the carrier material. In order to achieve as reproducible an end point as possible, the approximate amount of carrier material needed to adsorb this amount of L-SNEDDS had been determined in a previous step for each individual formulation using the same procedure. The adsorption process was considered complete once a dry, solid, and flowable material was obtained. The end point of the adsorption process and the flowability properties were determined visually. In the present case, the end point was reached when the formulation did not stick to either the wall of the beaker or the propeller stirrer used for mixing. The flowable material obtained was then stirred for an additional 2 min at 100 rpm to ensure the formation of a homogenous S-SNEDDS formulation. In this way, three individual S-SNEDDS formulations were prepared for each adsorptive carrier.

Based on the amount of solid carrier material required for solidifying L-SNEDDS, the loading capacity, expressed as loading factor, for each carrier was determined according to the following equation:

$$loading\ factor = \frac{m(L - SNEDDS)}{m\ (adsorptive\ carrier)} \quad (1)$$

where the calculation of the loading factor for the adsorptive carrier materials is based on L-SNEDDS.

HPLC Method for Celecoxib Quantification

High-performance liquid chromatography (HPLC) was used for celecoxib quantification [24]. The HPLC system (Agilent 1260 Infinity) consisted of a quaternary pump (G1311B), autosampler (G1329B), column oven (G1316A), and UV detector (G1314C), all from Agilent Technologies (Frankfurt am Main, Germany). Separation was achieved using a Knauer Nucleosil 100–7 C18 (125 × 4.6 mm, 7 µm) column maintained at 40°C. The mobile phase consisted of an acetonitrile:water:triethylamine mixture (300:300:0.9 v/v), adjusted to pH 3.0 with phosphoric acid. The flow rate was set to 1.8 ml/min. An injection volume of 5 µl was applied, run time was 7 min, and celecoxib was detected at 254 nm. In the concentration range of 0.13–542 µg/ml, the analytical curve was linear ($r^2 = 0.999995$). The method was found to be accurate (100.2–102.1%) and precise (CV 2.46%) with a quantification limit of 0.05 µg/ml. Selectivity was determined (formulation excipients) and no interference was

observed in drug retention time. Moreover, the celecoxib peak area did not change in the presence of all excipients used in the study.

Drug Load of Celecoxib S-SNEDDS

To determine the drug load of each of the celecoxib S-SNEDDS formulations, a defined quantity of 10.0 mg of celecoxib S-SNEDDS was transferred to a 25-ml volumetric flask, diluted with approximately 20 ml of the mobile phase described in the section "HPLC method for analyzing celecoxib," and subjected to an intense ultrasonic treatment for 10 min. The volumetric flask was then filled with mobile phase to the calibration mark (25.0 ml) and the contents were mixed by manual shaking. Subsequently, 1.0 ml of the resulting mixture was transferred to a small safe-lock tube and centrifuged for 1 min at 9300 relative centrifugation forces (rcf). The supernatant of the centrifugate was transferred into an HPLC vial and analyzed via HPLC. All investigations were performed in triplicate and the actual drug load of the S-SNEDDS was calculated from the celecoxib concentration measured in the sample and the S-SNEDDS weight used for analysis. Using the calculated drug load, the yield of the loading process was also calculated by relating the actual and theoretical drug load.

Differential Scanning Calorimetry Analysis

All celecoxib loaded S-SNEDDSs were analyzed via differential scanning calorimetry (DSC) to determine whether the incorporated drug was in the amorphous or crystalline state. All DSC analyses were conducted using a DSC 3+ (DSC-HC01) from Mettler Toledo (Giessen, Germany). A sample of 5–10 mg each was weighed into a small, aluminum pan with a perforated lid, and exposed to a heating–cooling-heating cycle in a temperature range of 0 to 200°C. The heating/cooling rate was set at 10°C/min and a nitrogen flow of 50 ml/min was applied while running the measurement. For comparison, the melting point of the pure drug substance was investigated. For all analyzed samples, the information on the amorphous or crystalline state was taken from the thermogram obtained from the first heating cycle. Each sample was prepared and analyzed in triplicate.

Dissolution Testing of Celecoxib SNEDDS

Dissolution experiments were performed with 25 mg celecoxib or an equivalent amount of L-/S-SNEDDS using USP apparatus II (DT 800 LH) from ERWEKA GmbH (Langen, Germany). The paddle speed was set to 100 rpm to avoid coning effects and the experiments were performed in 500 ml of 0.1 N hydrochloric acid (HCl) as well as in 500 ml of phosphate buffer 6.8 USP, both maintained at 37 ± 0.5°C.

Samples were withdrawn via a fraction collector, equipped with poroplast cannula filters with a pore size of 10 μm, and were then diluted 1+1 (v/v) with acetonitrile and analyzed by HPLC.

Stability Studies

Quantities of approximately 5 g of L-/S-SNEDDS were added to a 30-ml amber glass jars, closed with a screw cap, and stored at constant and controlled conditions (30°C/65% RH) in a climatic chamber from Binder GmbH (Tuttlingen, Germany) for 3 months. After 3 months, they were again subjected to dissolution experiments and the results of these tests were compared with those obtained immediately after manufacture.

Results and Discussion

Particle Size Distribution and Morphology of the Adsorptive Carriers

Results from the particle size analysis determination are summarized in Table 1. Most of the carrier materials were characterized by a particle size (d_{50}) in the lower micrometer range. With a d_{50} of 8 ± 1 μm, the Zeopharm® 600 calcium silicate particles exhibited the smallest particle size, whereas the largest particle size ($d_{50} = 182 \pm 7$) was measured for the novel M-GA particles.

SEM studies of all adsorptive carrier materials were performed at different magnification levels to analyze whether differences in surface area, morphology, and porosity could be identified. Aeroperl® 300 Pharma (Figs. 1a and 2a) presented with a smooth surface and a donut-like shape while Zeopharm® 600 (Figs. 1b and 2b) and Sipernat® 160 PQ (Figs. 1c and 2c) demonstrated a coarse surface and a flake-like structure with smaller particle agglomerates. Syloid® XDP 3050 (Figs. 1d and 2d) showed a structure of differently sized blocks with a smooth surface. None of the silica-based carriers investigated in this study exhibited a microporous surface, but a mesoporous texture resulting in nanopores (pore size 1–50 nm). Avicel® PH-101 (Figs. 1e and 2e) presented with elongated flake-like fragments of different sizes. The novel cellulose-based microparticles M-MC (Figs. 1f and 2f) and M-GA (Figs. 1g and 2g) exhibited distinctly different particle morphologies. In the case of M-MC, a mixture of spherical and flake-like particles as well as elongated, fibrous structures was identified. In contrast to M-MC, M-GA exhibited spherical particles with a highly porous surface, i.e., the particle structure targeted in this study. Interestingly, the replacement of the binder MC with GA in the preparation of the M-MC and M-GA particles had a significant impact on the morphology and size of the particles, although the same process parameters were used for the preparation of these microparticles. These observations are in accordance with those reported by other researchers, e.g., Alhassan et al. [25] who reported that depending on its concentration used in a formulation gum arabic may tremendously affect mechanical properties such as tensile strength as well as the modulus of elasticity when combined with a polymer. Furthermore, as reported by several research groups, also the viscosity of the spray dispersion either prepared with gum arabic or methyl cellulose may have an impact on the obtained particles' morphology and size [25, 26].

S-SNEDDS Manufacture and Characterization

The L-SNEDDS formulation selected for the manufacturing of S-SNEDDS had been established in a previous study [24] and consisted of 30.27% (w/w) Miglyol® 812, 49.85% (w/w) Tween® 80, 4.55% (w/w) Gelucire® 44/14, 6.24% (w/w) d-TPGS, and 9.09% (w/w) celecoxib. In the cited study, this formulation provided excellent emulsification properties resulting in small droplet sizes and a narrow PDI [24]. Moreover, an initial set of

Table 1 Characteristics of Adsorptive Carriers and S-SNEDDS. Each Value Designates the Mean $\pm$ S.D. of $n = 3$

Trade name	Adsorbent	Particle size d_{50} of adsorbent (μm)	Loading factor (g L-SNEDDS/g adsorbent)	Celecoxib load of S-SNEDDS (%)	Yield of the loading process (%)
Aeroperl® 300 Pharma	Colloidal silicon dioxide	30 ± 4	1.40 ± 0.03	5.30 ± 0.05	98.77 ± 0.9
Zeopharm® 600	Calcium silicate	8 ± 1	2.37 ± 0.03	6.39 ± 0.01	98.91 ± 0.5
Sipernat® 160 PQ	Amorphous silicon dioxide	13 ± 1	2.44 ± 0.04	6.45 ± 0.03	98.76 ± 0.5
Syloid® XDP 3050	Amorphous silicon dioxide	50 ± 3	1.44 ± 0.02	5.36 ± 0.03	98.96 ± 0.4
Avicel® PH-101	Microcrystalline cellulose	50 ± 4	0.90 ± 0.02	4.31 ± 0.06	99.72 ± 0.2
M-MC*	Cellulose + MC	66 ± 2	1.15 ± 0.02	4.86 ± 0.04	99.84 ± 0.2
M-GA*	Cellulose + GA	182 ± 7	1.14 ± 0.02	4.84 ± 0.02	99.68 ± 0.2

Cellulose-based microparticles, no commercial product; MC, methyl cellulose; GA, gum arabic

⚫ Springer

Fig. 1 SEM images (250-fold magnification) of Aeroperl® 300 Pharma (**a**), Zeopharm® 600 (**b**), Sipernat® 160 PQ (**c**), Syloid® XDP 3050 (**d**), Avicel® PH-101 (**e**), M-MC (**f**), M-GA (**g**)
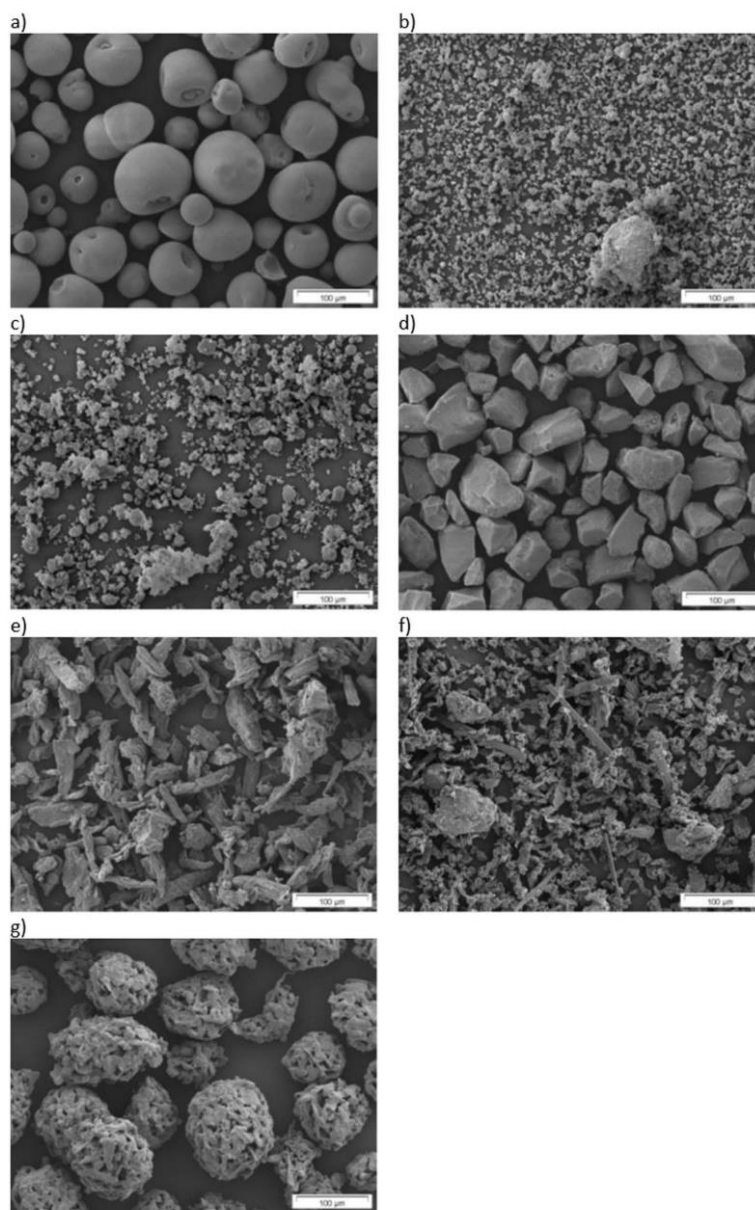
dissolution experiments had indicated fast and complete drug release in conditions of the fasted stomach. In the present study, this L-SNEDDS formulation was prepared and adsorbed to a solid carrier material applying a gentle preparation method protecting the formulations from high temperatures and strong mechanical forces. Mechanisms that are, or can be, involved in such an adsorption process include capillary forces, a synergistic effect of the surface tension of L-SNEDDS, and the interfacial tension between L-SNEDDS and the capillaries of the carrier, and

Fig. 2 SEM images (1000-fold magnification) of Aeroperl® 300 Pharma (**a**), Zeopharm® 600 (**b**), Sipernat® 160 PQ (**c**), Syloid® XDP 3050 (**d**), Avicel® PH-101 (**e**), M-MC (**f**), M-GA (**g**)
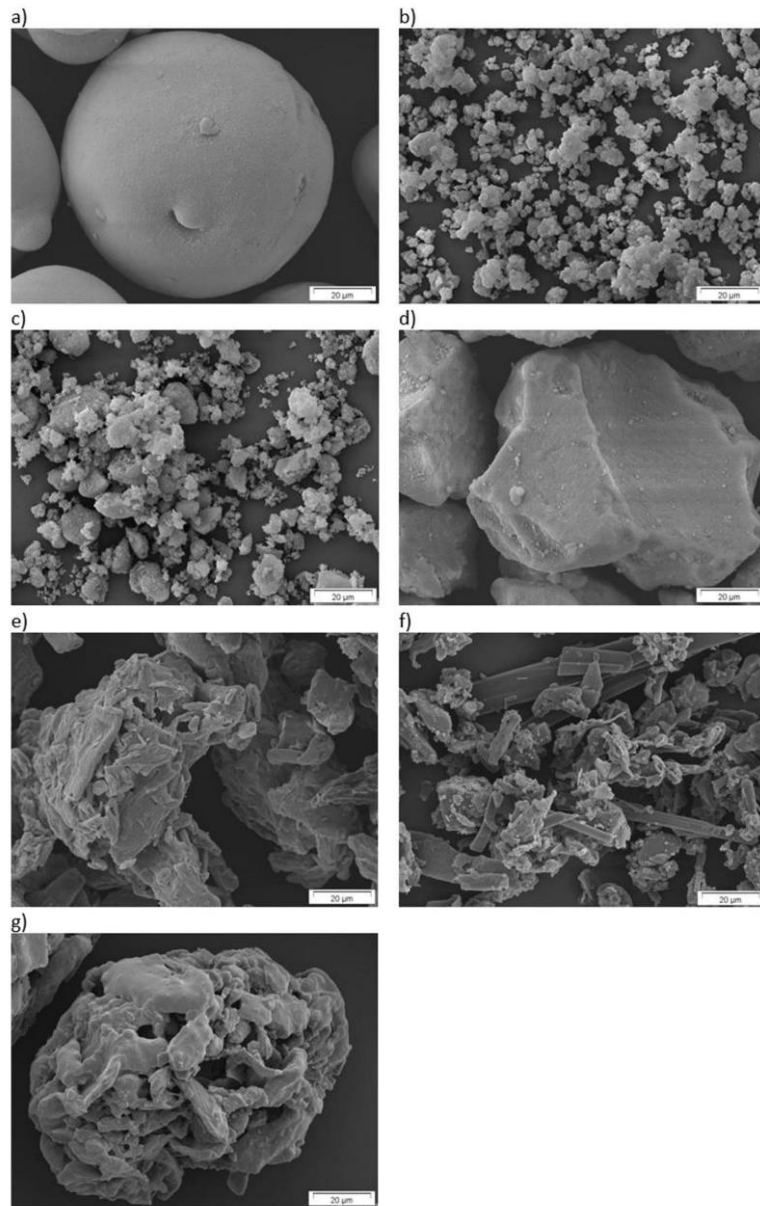
intermolecular adhesion forces triggered by the formation of covalent bonds, hydrogen bonds, dipole–dipole, electrostatic, and hydrophobic interactions when L-SNEDDS and the porous carrier material are combined [20, 21]. L-SNEDDS adsorption to the solid carriers provided powders with (visually assessed) varying flow properties, depending on the carriers' properties.

The evaluation of the loading factors for the adsorptive carrier materials revealed that Sipernat® 160 PQ as well as Zeopharm® 600 exhibited the highest capacity for

L-SNEDDS adsorption and consequently presented the highest drug load (Table 1). These two carriers also demonstrated the smallest particle size of all carriers analyzed (Table 1). This observation suggests that a smaller particle size, which correlates with a larger surface area, may be associated with a higher loading capacity in the case of the silica-based materials. The loading capacity of all cellulose-based carriers was lower than that of silicon-based materials, but the loading capacity of both M-GA and M-MC was higher than that of the commercial Avicel® PH-101, although the Avicel® PH-101 particles were slightly smaller than M-MC particles and significantly smaller than M-GA particles (Table 1). These results underline that not just the average particle diameter, but also the surface area and porosity of the cellulose-based materials are crucial factors for their loading capacity. M-MC may compensate for its lower porosity compared to M-GA by its much smaller particle size and/or its mixture of particles of different morphologies. Interestingly, replacing the binder MC with GA in the preparation of the cellulose-based microparticles M-MC and M-GA revealed to have a tremendous impact both on morphology and size of the particles.

As for the loading capacity, drug load was similar for M-MC ($4.86 \pm 0.04\%$) and M-GA ($4.84 \pm 0.02\%$). Overall, drug load of the S-SNEDDS correlated with the loading capacity and was highest for the Zeopharm® 600 calcium silicate particles ($6.39 \pm 0.01\%$) and lowest for the Avicel® PH-101 particles ($4.31 \pm 0.06\%$). Regardless of the substrate, the yield of the S-SNEDDS preparation was consistently above 98.5%, indicating an effective manufacturing process.

DSC analysis (thermograms displayed in endo up mode) of the celecoxib S-SNEDDS (Fig. 3), as well as the corresponding pure drug substance, indicated amorphous properties (no melting peaks) for all celecoxib S-SNEDDS (Fig. 3), while the crystalline character of the pure drug was demonstrated by a characteristic peak in the corresponding melting range (162–164°C) of the celecoxib (Fig. 3). These results show that the adsorption process of celecoxib-containing L-SNEDDS onto solid carriers, regardless of the carrier material used, had no effect on the amorphicity of celecoxib.

Dissolution Studies of L-/S-SNEDDS

A celecoxib dose of 25 mg or an equivalent amount of L-/S-SNEDDS was screened in the dissolution experiments. Results of the release experiments performed in 0.1 N HCl are shown in Fig. 4. Both L-SNEDDS and S-SNEDDS formulations showed a rapid release, *i.e.*, release profiles reached a plateau within the first 15 min of the experiment and no precipitation was observed until the end of the experiment (120 min). Indicative of the poor solubility of celecoxib, dissolution of the pure drug was poor with less than 5% of the tested dose dissolved at the end of the experiment. Whereas a rapid drug release was observed for all SNEDDS formulations, the fraction of dose released differed significantly among the formulations tested. The celecoxib L-SNEDDS as such showed a release of about 96% in 15 min and the release profile of the L-SNEDDS did not noticeably change after preparing S-SNEDDS by adsorption to M-MC and M-GA. Celecoxib S-SNEDDS made with Avicel® PH-101 also revealed a rapid and high drug release with approximately 90% of the dose released within in the
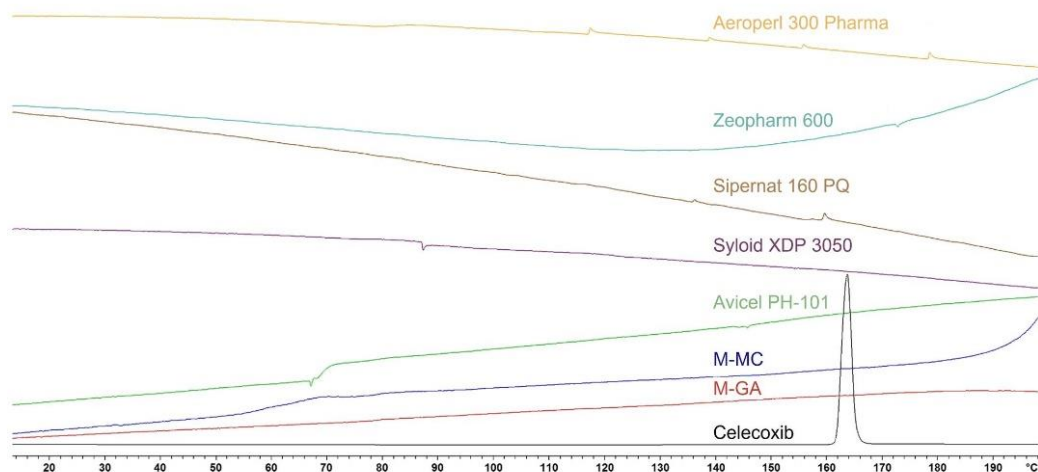
Fig. 3 DSC thermograms of celecoxib drug substance and celecoxib S-SNEDDS (first heating, 0–200°C, 10°C/min)

⚙ Springer

Fig. 5 Dissolution profile of celecoxib L-SNEDDS, celecoxib S-SNEDDS, and celecoxib drug substance in 500 ml phosphate buffer pH 6.8 in USP apparatus II at 100 rpm. Each value designates the mean $\pm$ S.D. of $n = 3$
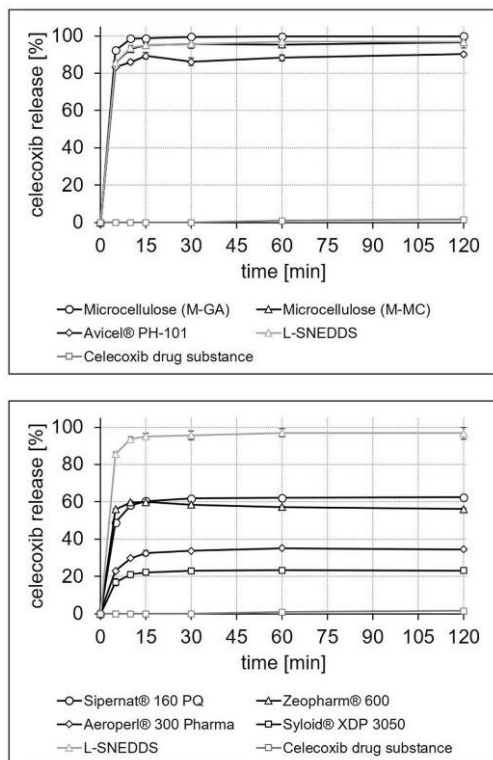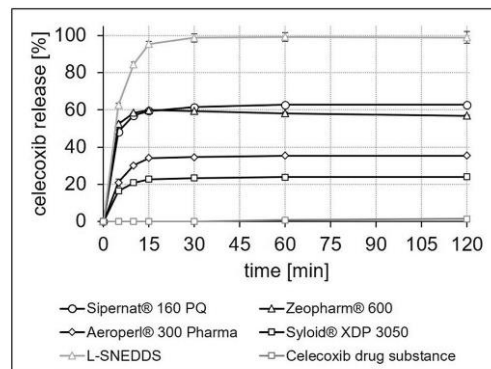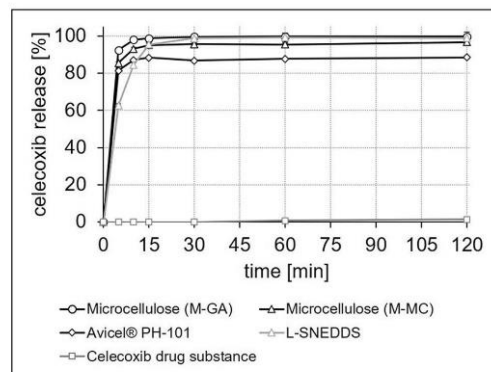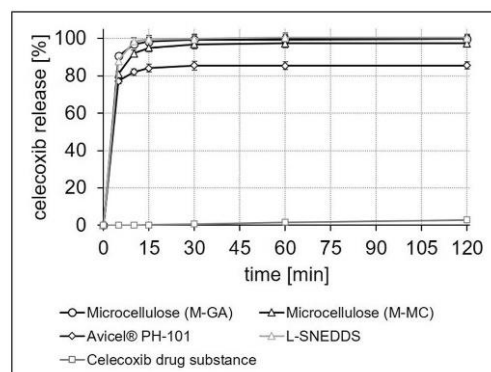

Fig. 4 Dissolution profile of celecoxib L-SNEDDS, celecoxib S-SNEDDS, and celecoxib drug substance in 500 ml of 0.1 N HCl in USP apparatus II at 100 rpm. Each value designates the mean $\pm$ S.D. of $n = 3$

first 15 min of the experiment. By contrast, drug release of all other S-SNEDDS formulations was incomplete. Within the test duration of 120 min, S-SNEDDS made of Sipernat® 160 PQ and Zeopharm® 600 showed a total drug release of about 60%. With a release of 35% and 25% of the dose applied, an even lower release was observed for celecoxib in the experiments with S-SNEDDS containing Aeroperl® 300 Pharma and Syloid® XDP 3050, respectively. These results indicate that silica-based carrier materials retained a proportionally larger fraction of the adsorbed drug formulation than did the cellulose-based carrier materials. Based on these observations, it can be assumed that molecular interactions between the adsorbed drug formulation and the carrier material can have a great impact on the equilibrium between adsorption and desorption processes and thus may have a strong influence on drug release.

Initial screening experiments were performed in 0.1 N HCl. Therefore, the results would indicate whether and to what extent the formulations would release under conditions of fasting stomach. To screen, whether the best-performing S-SNEDDS would also release in small intestinal pH conditions, an additional set of experiments was performed in phosphate buffer pH 6.8 USP. This second set of experiments comprised dissolution studies with cellulose-based celecoxib S-SNEDDS, celecoxib L-SNEDDS, and celecoxib drug substance. As can be seen from Fig. 5, for all formulations tested, dissolution profiles obtained in phosphate buffer pH 6.8 were like those in 0.1 N HCl indicating that that adsorption of L-SNEDDS onto M-MC and M-GA did not affect the original release performance of the L-SNEDDS formulation and also indicate that L-SNEDDS or drug release was not affected by pH conditions that may occur in the fasting stomach and mid-small intestine, respectively.
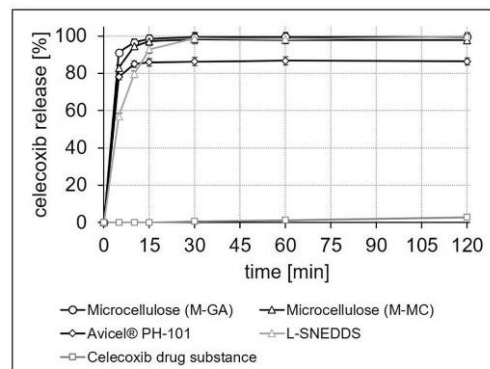
The challenge of releasing a self-emulsifying drug release system from an adsorptive solid carrier material without significantly affecting drug release compared to its liquid state has already been reported from other studies. Chavan et al. [14] studied drug release from silica-based celecoxib S-SEDDS containing 100 mg celecoxib in 900 ml distilled water in USP apparatus II at 200 rpm. Whereas drug release of the L-SNEDDS formulation was complete after 120 min, that of the S-SNEDDS did not exceed 10% of the tested dose for most of the carrier materials within the same test duration. Only for one formulation, a release of 40% of the tested dose could be observed in the same time frame. Results of the cited study thus show into the same direction as those from the present study; however, it should be noted that the silica-based materials used by Chavan et al. [14] were different from those applied in the present study, that the drug load of the tested S-SNEDDS was slightly higher and, that

⚘ Springer

also a higher celecoxib dose (100 mg *vs*. 25 mg) was studied in the dissolution experiments.

Another study assessing the impact of adsorbing self-emulsifying formulations to solid carriers on drug release was published by Cerpnjak *et al.* [22], who adsorbed naproxen liquid self-microemulsifying drug delivery systems (L-SMEDDS) to maltodextrin, hypromellose, and a combination of the two as a solid carrier and studied drug release of the obtained solid SMEDDS (S-SMEDDS) in 900 ml of 0.1 N hydrochloric acid in USP apparatus II at 100 rpm. The drug load of the S-SMEDDS was 6%. Whereas one of the S-SMEDDS formulations tested preserved the self-microemulsifying properties of L-SMEDDS and exhibited dissolution profiles similar to those of L-SMEDDS, the others did not. Overall, results of the study of Cerpnjak *et al.* [22] also confirm the hypothesis that there are several factors that determine the drug release of solid self-emulsifying formulations, including the underlying L-SNEDDS formulation, the material, and a number of other characteristics of the solid carrier. In addition, it should be noted that the drug loads of the formulations in the cited and the present study were similar, but naproxen had a significantly better solubility in the release medium than celecoxib. In the naproxen study, also a higher media volume was used, but nevertheless complete drug release could not be achieved with each of the carrier materials. This underlines the results of the present study, especially those of the dissolution studies with M-MC- and M-GA-based celecoxib S-SNEDDS.

None of the carrier materials used in the present study was soluble in the test medium, leading to the assumption that the release of the drug was solely caused by the detachment of L-SNEDDS from the surface of the carrier and/or its removal from the carriers' pores. Due to these preconditions, the release of active substances seems to be predominantly determined by complex material- and morphology-dependent adsorption and desorption processes, in which not only simple monolayer molecular adsorption, but also effects such as capillary condensation can play a role, especially in mesoporous systems. Differences in the extent and rate of desorption can accordingly have a direct impact on the release characteristics of the formulation and explain the different release profiles obtained in the present study.

Stability Studies of L-/S-SNEDDS

After storing L-/S-SNEDDS at 30°C/65% RH for 3 months, dissolution studies were again performed in 0.1 N HCl and in phosphate buffer pH 6.8. Results are shown in Figs. 6 and 7. In both dissolution media, celecoxib release profiles were similar to those recorded immediately after manufacture of L-SNEDDS and S-SNEDDS. After a total test duration of 120 min, the maximum difference between the total amount of celecoxib release immediately after preparation and that

Fig. 6 Dissolution profile of celecoxib L-SNEDDS, celecoxib S-SNEDDS, and celecoxib drug substance in 500 ml of 0.1 N HCl in USP apparatus II at 100 rpm after 3 months of storage at 30°C/65% RH. Each value designates the mean ± S.D. of $n = 3$

Fig. 7 Dissolution profile of celecoxib L-SNEDDS, celecoxib S-SNEDDS, and celecoxib drug substance in 500 ml phosphate buffer pH 6.8 in USP apparatus II at 100 rpm after 3 months of storage at 30°C/65% RH. Each value designates the mean ± S.D. of $n = 3$

after 3 months of storage was < 1.5% for all formulations tested, which proves the stability of the release mechanism over the storage period.

In summary, the results of the study clearly indicate that of the carrier materials investigated, the cellulose-based microparticles M-MC and M-GA are the most suitable for the production of celecoxib S-SNEDDS from L-SNEDDS, as they allow the preparation of a solid, stable formulation while preserving the *in vitro* release performance of the L-SNEDDS formulation. In the present study, celecoxib was used as a model drug. However, the tested dose was in the non-therapeutic range. Future studies will focus on other poorly soluble drugs whose therapeutic dose is in the investigated dose range, as well as on significantly increasing the drug loading of L-SNEDDS and S-SNEDDS so that they can be used for higher-dose poorly soluble drugs without the need to divide a single dose among multiple dosage forms.

Conclusion

With suitable adsorptive carrier materials, it is possible to formulate drug-loaded L-SNEDDS into S-SNEDDS without affecting the rate and extent of drug release of the L-SNEDDS used. As anticipated, both the carrier material and the particle size and morphology have a crucial impact on the success of this formulation approach. In the present study, a microparticulate carrier based on cellulose and gum arabic which was prepared by spray drying was found to be the most promising candidate among all carrier materials evaluated. This novel adsorptive carrier exhibited the desired spherical particle design, which is essential for good processability and reproducible drug loading and enabled a good drug release performance. The results of the present study give rise to further investigations to evaluate the suitability of the carrier material for loading with other L-SNEDDS, especially those with higher drug contents, to further improve the carrier material in terms of particle size and morphology if necessary, and ultimately to provide an alternative approach for the formulation of poorly soluble drugs.

Declarations

References

1. Kalepu S, Nekkanti V. Insoluble drug delivery strategies: review of recent advances and business prospects. Acta Pharm Sin B. 2015;5(5):442–53. https://doi.org/10.1016/j.apsb.2015.07.003.

2. Dokania S, Joshi AK. Self-microemulsifying drug delivery system (SMEDDS) - challenges and road ahead. Drug Deliv. 2015;22(6):675–90. https://doi.org/10.3109/10717544.2014.896058.

3. Porter CJH, Pouton CW, Cuine JF, Charman WN. Enhancing intestinal drug solubilisation using lipid-based delivery systems. Adv Drug Deliv Rev. 2008;60(6):673–91. https://doi.org/10.1016/j.addr.2007.10.014.

4. Pouton CW. Lipid formulations for oral administration of drugs: non-emulsifying, self-emulsifying and 'self-microemulsifying' drug delivery systems. Eur J Pharm Sci. 2000;11(2):93–8. https://doi.org/10.1016/s0928-0987(00)00167-6.

5. Thomas N, Holm R, Mullertz A, Rades T. *In vitro* and *in vivo* performance of novel supersaturated self-nanoemulsifying drug delivery systems (super-SNEDDS). J Control Release. 2012;160(1):25–32. https://doi.org/10.1016/j.jconrel.2012.02.027.

6. Vithani K, Hawley A, Jannin V, Pouton C, Boyd BJ. Inclusion of digestible surfactants in solid SMEDDS formulation removes lag time and influences the formation of structured particles during digestion. AAPS J. 2017;19(3):754–64. https://doi.org/10.1208/s12248-016-0036-6.

7. Chatterjee B, Almurisi SH, Dukhan AAM, Mandal UK, Sengupta P. Controversies with self-emulsifying drug delivery system from pharmacokinetic point of view. Drug Deliv. 2016;23(9):3639–52. https://doi.org/10.1080/10717544.2016.1214990.

8. Yetukuri K, Sudheer P. Approaches to development of solid - self micron emulsifying drug delivery system: formulation techniques an dosage forms: A review. Int J Pharm Sci Res. 2012;3(10):3550–8.

9. Vithani K, Hawley A, Jannin V, Pouton C, Boyd BJ. Solubilisation behaviour of poorly water-soluble drugs during digestion of solid SMEDDS. Eur J Pharm Biopharm. 2018;130:236–46. https://doi.org/10.1016/j.ejpb.2018.07.006.

10. Hanada M, Jermain SV, Williams RO III. Enhanced dissolution of a porous carrier-containing ternary amorphous solid dispersion system prepared by a hot melt method. J Pharm Sci. 2018;107:362–71. https://doi.org/10.1016/j.xphs.2017.09.025.

Springer

11. Kim DS, Yang ES, Yong CS, Youn YS, Oh KT, Li DX, *et al*. Effect of inorganic mesoporous carriers on 1-palmitoyl-2-linoleoyl-3-acetyl-rac-glycerol-loaded solid self-emulsifying drug delivery system: physicochemical characterization and bioavailability in rats. Colloids Surf B Biointerfaces. 2017;160:331–6. https://doi.org/10.1016/j.colsurfb.2017.09.041.

12. Milović M, Djuriš J, Djekić L, Vasiljević D, Ibrić S. Characterization and evaluation of solid self-microemulsifying drug delivery systems with porous carriers as systems for improved carbamazepine release. Int J Pharm. 2012;436(1–2):58–65. https://doi.org/10.1016/j.ijpharm.2012.06.032.

13. Sander C, Holm P. Porous magnesium aluminometasilicate tablets as carrier of a cyclosporine self-emulsifying formulation. AAPS PharmSciTech. 2009;10(4):1388–95. https://doi.org/10.1208/s12249-009-9340-0.

14. Chavan RB, Modi SR, Bansal AK. Role of solid carriers in pharmaceutical performance of solid supersaturable SEDDS of celecoxib. Int J Pharm. 2015;495(1):374–84. https://doi.org/10.1016/j.ijpharm.2015.09.011.

15 Yeom DW, Chae BR, Kim JH, Chae JS, Shin DJ, Kim CH, *et al*. Solid formulation of a supersaturable self-microemulsifying drug delivery system for valsartan with improved dissolution and bioavailability. Oncotarget. 2017;8(55):94297–316. https://doi.org/10.18632/oncotarget.21691.

16. Hu X, Lin C, Chen D, Zhang J, Liu Z, Wu W, *et al*. Sirolimus solid self-microemulsifying pellets: formulation development, characterization and bioavailability evaluation. Int J Pharm. 2012;438:123–33. https://doi.org/10.1016/j.ijpharm.2012.07.055.

17. Sohn Y, Lee SY, Lee GH, Na YJ, Kim SY, Seong I, *et al*. Development of self-microemulsifying bilayer tablets for pH-independent fast release of candesartan cilexetil. Pharmazie. 2012;67:917–24.

18. Tung NT, Tran CS, Pham TMH, Nguyen HA, Nguyen TL, Chi SC, *et al*. Development of solidified self-microemulsifying drug delivery systems containing l-tetrahydropalmatine: design of experiment approach and bioavailability comparison. Int J Pharm. 2018;537:9–21. https://doi.org/10.1016/j.ijpharm.2017.12.027.

19. Borkar N, Xia D, Holm R, Gan Y, Mullertz A, Yang M, *et al*. Investigating the correlation between *in vivo* absorption and *in vitro* release of fenofibrate from lipid matrix particles in biorelevant medium. Eur J Pharm Sci. 2014;51:204–10. https://doi.org/10.1016/j.ejps.2013.09.022.

20. Li T, Chen X, Liu Y, Fan L, Lin L, Xu Y, *et al*. pH-Sensitive mesoporous silica nanoparticles anticancer prodrugs for sustained release of ursolic acid and the enhanced anti-cancer efficacy for hepatocellular carcinoma cancer. Eur J Pharm Sci. 2017;96:456–63. https://doi.org/10.1016/j.ejps.2016.10.019.

21. Stjern L, Voittonen S, Weldemichel R, Thuresson S, Agnes M, Benkovics G, *et al*. Cyclodextrin-mesoporous silica particle composites for controlled antibiotic release A proof of concept toward colon targeting. Int J Pharm. 2017;531:595–605. https://doi.org/10.1016/j.ijpharm.2017.05.062.

22. Čerpnjak K, Zvonar A, Vrečer F, Gašperlin M. Characterization of naproxen-loaded solid SMEDDSs prepared by spray drying: The effect of the polysaccharide carrier and naproxen. Int J Pharm. 2015;485:215–28. https://doi.org/10.1016/j.ijpharm.2015.03.015.

23. Patki M, Patel K. Development of a solid supersaturated self nanoemulsifying preconcentrate (S-superSNEP) of fenofibrate using dimethylacetamide and a novel co-processed excipient. Drug Dev Ind Pharm. 2018;45(3):405–14. https://doi.org/10.1080/03639045.2018.1546311.

24. Schmied FP, Bernhardt A, Engel A, Klein S. A customized screening tool approach for the development of a self-nanoemulsifying drug delivery system (SNEDDS). AAPS PharmSciTech. 2022;23(1):39. https://doi.org/10.1208/s12249-021-02176-7.

25. Alhassan SI, Mamza PAP, Ja'oAM. Effect of pure and modified gum arabic on the mechanical properties of poly (vinyl chloride). IJSRP. 2015;5(5):1–7.

26. Nasatto PL, Pignon F, Silveira JLM, Duarte MER, Noseda MD, Rinaudo M. Interfacial properties of methylcelluloses: the influence of molar mass. Polymers (Basel). 2014;6:2961–73. https://doi.org/10.3390/polym6122961.

Publisher's Note Springer Nature remains neutral with regard to jurisdictional claims in published maps and institutional affiliations.

6.3 A novel aminomethacrylate-based copolymer for solubility enhancement—from radical polymer synthesis to manufacture and characterization of amorphous solid dispersions*

(*Polymers*, 2022, 14(7): 1281)

This part of the work dealt with the radical synthesis, purification and characterization of a novel aminomethacrylate-based copolymer referred to as ModE that was developed for the advanced manufacturing of enabling formulations such as ASDs and S-SNEDDS in the context of solubility enhancement of poorly water-soluble drugs. ModE can be considered as a structural modification of the conventional and commercialized EUDRAGIT® E PO. ModE types with varying M_w and T_g respectively were synthesized and investigated for their suitability to improve the poor aqueous solubility and the incomplete *in vitro* drug release of the model drug substances celecoxib, efavirenz and fenofibrate when applied as ASD formulations. Drug-loaded ASDs were manufactured via HME and revealed that M_w and T_g substantially affected the drug release performance of the incorporated drug substances when subjected to *in vitro* dissolution studies. ModE with a M_w of 173 kDa, the lowest M_w amongst all different ModE types that were synthesized, was identified as the most promising candidate for formulation development in order to enhance the solubility of poorly water-soluble drugs. Furthermore, ASDs prepared with this specific ModE type showed a better release behavior of the incorporated drug as well as storage stability compared to ASDs based on other marketed (co-)polymers.

Own contributions:
Development of the scientific concept and ModE copolymer, synthesis of ModE copolymer, performance of the laboratory experiments and the calculations, preparation of the manuscript

Alexander Bernhardt:
Contribution in the development of the scientific concept

Dr. Christian Moers, Dr. Christian Meier and Dr. Thomas Endres:
Contribution in the development of ModE copolymer

Prof. Dr. Sandra Klein:
Contribution in the development of the scientific concept, revision of the manuscript

_____   _____
          Fabian-Pascal Schmied   Prof. Dr. Sandra Klein

Article

A Novel Aminomethacrylate-Based Copolymer for Solubility Enhancement—From Radical Polymer Synthesis to Manufacture and Characterization of Amorphous Solid Dispersions

Fabian-Pascal Schmied [1,2], Alexander Bernhardt [2], Christian Moers [2], Christian Meier [3], Thomas Endres [2] and Sandra Klein [1,*] ![ORCID]

[1] Institute of Biopharmaceutics and Pharmaceutical Technology, Department of Pharmacy, University of Greifswald, Felix-Hausdorff-Straße 3, 17489 Greifswald, Germany; fabian-pascal.schmied@stud.uni-greifswald.de or fabian-pascal.schmied@evonik.com

[2] Evonik Operations GmbH, Research, Development & Innovation, Kirschenallee, 64293 Darmstadt, Germany; alexander.bernhardt@evonik.com (A.B.); christian.moers@evonik.com (C.M.); thomas.endres@evonik.com (T.E.)

[3] Evonik Operations GmbH, Research, Development & Innovation, Rodenbacher Chaussee 4, 63457 Hanau, Germany; christian.meier@evonik.com

* Correspondence: sandra.klein@uni-greifswald.de; Tel.: +49-3834-420-4897

Abstract: The present study covers the synthesis, purification and evaluation of a novel aminomethacrylate-based copolymer in terms of its suitability for improving the solubility and in vitro release of poorly water-soluble drug compounds. The new copolymer was synthesized by solvent polymerization with radical initiation and by use of a chain transfer agent. Based on its composition, it can be considered as a modified type of dimethylaminoethyl methacrylate-butyl methacrylate-methyl methacrylate "EUDRAGIT® E PO" (ModE). ModE was specifically developed to provide a copolymer with processing and application properties that exceed those of commercially available (co-)polymers in solubility enhancement technologies where possible. By varying the concentration of the chain transfer agent in the radical polymerization process, the molecular weight of ModE was varied in a range of 173–305 kDa. To evaluate the solubility-enhancing properties of ModE, a series of drug-loaded extrudates were prepared by hot melt extrusion using the novel—as well as several commercially available—(co-)polymers. These extrudates were then subjected to comparative tests for amorphousness, solubility-enhancing properties, storage stability, and drug release. Celecoxib, efavirenz, and fenofibrate were used as model drugs in all experiments. Of all the (co-)polymers included in the study, ModE with a molecular weight of 173 kDa showed the best performance in terms of desired properties and was shown to be particularly suitable for preparing amorphous solid dispersions (ASDs) of the three model drugs, which in a first set of dissolution experiments showed better release behavior under pH conditions of the fasting stomach than higher molecular weight ModE types, as well as a variety of commercially available (co-)polymers. Therefore, the results demonstrate the successful synthesis of a new copolymer, which in future studies will be investigated in more detail for universal application in the field of solubility enhancement.

Keywords: drug release; molecular weight; glass transition; poorly soluble drugs; in vitro dissolution; hot melt extrusion; amorphous solid dispersion; celecoxib; fenofibrate; efavirenz

1. Introduction

Addressing the solubility problem of poorly water-soluble drugs is of particular importance for current research into new active pharmaceutical ingredients [1–5]. The number of potential drug candidates exhibiting poor aqueous solubility, that may lead to insufficient drug absorption in the gastrointestinal tract and subsequently to low bioavailability, has increased considerably in recent years [3,5–8]. To overcome the challenge of a drug's

low aqueous solubility, strategies such as particle size reduction, complexation using cyclodextrins, self-emulsifying systems or amorphization leading to supersaturation of the drug in aqueous media can be used to increase the solubility and/or dissolution rate of poorly water-soluble drugs [3,8]. The amorphous state is characterized by an increased free energy, which can lead to an improved solubility of the drug and thus also improve its bioavailability after oral administration compared to the corresponding crystalline active substance [3,5,8,9]. Recrystallization of the drug from a metastable, amorphous state is widely reported to have an adverse effect on its solubility in aqueous fluids [3,7–9]. To maintain the amorphous state, as well as to prevent recrystallization, drugs are usually embedded in a polymer matrix [9,10].

Several (co-)polymers—such as polyvinyl caprolactam-polyvinyl acetate-polyethylene glycol graft copolymer, polyvinylpyrrolidone-polyvinyl acetate copolymer, dimethylaminoethyl methacrylate-butyl methacrylate-methyl methacrylate, different types of hydroxypropyl methylcellulose (HPMC), as well as hydroxypropyl methylcellulose acetate succinate (HPMCAS)—have proven suitable for the purpose of enhancing the solubility of poorly water-soluble drugs [3,7,9–11]. EUDRAGIT® E PO (EPO) is a copolymer that consists of the three monomers dimethylaminoethyl methacrylate, butyl methacrylate and methyl methacrylate in a ratio of 2:1:1 by weight. It has been a commercial product for several decades and is widely used in many applications, including solubility enhancement strategies [12]. EPO is insoluble in saliva, but soluble in fasted gastric fluid (pH < 5) enabling immediate drug release in the stomach to ensure fast drug absorption in the upper intestine. However, if one wants to use EPO for the preparation of drug-loaded ASDs, this often proves challenging, as it is a flexible copolymer with a moderately high glass transition (T_g), which allows strong movement of the polymer chains. Consequently, when applying high drug loads, a lower storage stability of the formulations due to a further decrease of the copolymers T_g and subsequent recrystallization of the drug can become a major concern [13]. However, some limitations and drawbacks of EPO related to this issue might be compensated by structural modifications. One approach to create a functionally similar but more suitable copolymer for the preparation of stable ASDs is to substitute one or more of the monomers used for EPO synthesis with structurally-related monomers that would contribute to a higher T_g in the final copolymer [14]. Likewise, altering the molecular weight (M_w) of the copolymer might be beneficial [14,15]. Both a change in monomer composition and the aim of changing the molecular weight of the polymer to be produced usually require a change in polymer synthesis and reaction conditions [14,16].

The M_w of a (co-)polymer can be adjusted by different means, for instance, by altering the drip rate of the radical initiator added to the monomer mixture or by adding different concentrations of a chain-transfer-agent (CTA). A CTA is a molecule that has at least one weak chemical bond and that, when added to the reaction mixture, interrupts chain growth by reacting with the free-radical site of a growing polymer chain. CTAs are usually added to control the chain length during the synthesis of a polymer to achieve the desired mechanical and processing properties [15,17]. The impact of CTAs on the average M_w of a (co-)polymer to be synthesized is concentration dependent and the M_w of the resulting (co-)polymer typically decreases with increasing CTA concentration. Regardless of whether a CTA is added or not, it is desirable to achieve a high monomer conversion by choosing suitable reaction conditions for the polymerization process, which at the same time promises a very low number of residual monomers [18]. Altogether, this would not only increase the yield, but also reduce the time required for the purification of the (co-)polymer. By means of a robust synthesis method, (co-)polymers which reflect the mass ratio of the monomers used, and consequently also the ratio of their functional units, can be obtained in a reproducible way [18].

The aim of the present study was the reproducible synthesis of an aminomethacrylate-based copolymer with the lowest possible number of residual monomers. Structural modification of EPO should result in a modified EPO copolymer (ModE) consisting of about 50 wt% of its amino-functional unit, which is suitable for improving the dissolution rate and

the solubility of poorly water-soluble drugs by preparing drug-loaded ASDs. The ASDs produced using the new copolymer and different model drugs should be characterized by a pronounced storage stability; therefore, the effect of varying T_g and M_w of the copolymer on this property should be investigated.

2. Materials and Methods

2.1. Materials

Celecoxib obtained from Aarti Drugs Ltd. (Mumbai, India), efavirenz received from Angene International Ltd. (London, UK) and fenofibrate provided by D.K. Pharma Chem PVT Ltd. (Maharashtra, India) were used as model compounds. Dimethylaminopropyl methacrylamide was purchased from TCI Deutschland GmbH (Eschborn, Germany). Butyl methacrylate and methyl methacrylate were provided by Röhm GmbH (Darmstadt, Germany). Tert-butyl peroxyneodecanoate was received from Nouryon (Amsterdam, The Netherlands) and tert-butyl peroxypivalate was obtained from United Initiators GmbH & Co. KG (Pullach im Isartal, Germany). Polyvinyl caprolactam-polyvinyl acetate-polyethylene glycol graft copolymer (Soluplus®, M_w = 90,000–140,000 g/mol), polyvinylpyrrolidone-polyvinyl acetate copolymer (Kollidon® VA 64, M_w = 45,000–70,000 g/mol) and polyvinylpyrrolidone (Kollidon® 17 PF, M_w = 7000–11,000 g/mol) were purchased from BASF SE (Ludwigshafen, Germany). Hydroxypropyl methylcellulose acetate succinate (AQOAT® AS-MMP, M_w = 18,000 g/mol) was kindly donated by Shin-Etsu Chemical Co., Ltd. (Tokio, Japan). Hydroxypropyl methylcellulose (Affinisol® HPMC 100 LV, M_w = 179,000 g/mol) was provided by Dow Chemical Company (Schwalbach am Taunus, Germany). Dimethylaminoethyl methacrylate-butyl methacrylate-methyl methacrylate (EUDRAGIT® E PO, EUDRAGIT® E 100, M_w = 47,000 g/mol) were from Evonik Operations GmbH (Darmstadt, Germany). n-propanol and n-dodecylmercaptan were obtained from Merck KGaA (Darmstadt, Germany). All other chemicals were of analytical grade and purchased commercially.

2.2. Methods

2.2.1. Preparation of ModE Copolymer

For the preparation of ModE copolymer (dimethylaminopropyl methacrylamide-butyl methacrylate-methyl methacrylate copolymer 2:1:1 (ratios by weight)), the monomers dimethylaminopropyl methacrylamide (500.0 g), butyl methacrylate (250.0 g) and methyl methacrylate (250.0 g) were added into a 3-L round-bottom flask reaction vessel equipped with a propeller stirrer, a reflux condenser and a nitrogen inlet. The reaction vessel was placed in a preheated water bath at 82 °C and the mixture of monomers was stirred at 300 rpm. Immediately after reaching an internal temperature of 65 °C, the CTA n-dodecylmercaptan (either 3.0 g, 5.0 g, 9.0 g or 15.0 g), was added in a 1:1 (*w:w*) mixture with n-propanol as a bolus to control the M_w of the copolymer during the polymerization process. The different amounts of n-dodecylmercaptan indicated were chosen in order to selectively modify the M_w of the synthesized copolymer and then evaluate the effects of the M_w on the desired polymer properties and applications. While stirring the mixture in the reaction vessel, the internal temperature was continuously increased until a temperature of 80 °C was reached. Then, 1000 g of a tert-butyl peroxyneodecanoate (0.6 wt%) solution in n-propanol was added with a continuous flow rate of 5 g/min to initiate a radical polymerization as well as to counteract the increasing viscosity throughout the polymerization process. After approximately 3.5 h at a temperature of 80–85 °C, the second initiator, tert-butyl peroxypivalate (0.5 g) was added to complete the reaction within the following 90 min. Thereafter, the mixture was cooled down to 60 °C and transferred to a drying oven with exhaust air at 40 °C to remove n-propanol over 48 h. This drying process provided a coarse copolymer block to which then 1 L of liquid nitrogen was added to enable grinding (mesh size: 0.25 mm) using an Ultra Centrifugal Mill ZM 200 from Retsch GmbH (Haan, Germany). Subsequently, the ground copolymer was subjected to a purification process for the purpose of extracting residual monomers and organic solvent.

2.2.2. Purification and Drying of ModE

For removing residual monomers and the organic solvent n-propanol, the ground ModE was subjected to a purification procedure. For this purpose, it was transferred to a 5-L beaker and 3 L of deionized water were added. Using an overhead stirrer with a perforated stirring blade, the copolymer-water mixture was stirred at 300 rpm for a total of 36 h. During this procedure, the deionized water was completely replaced every 4 h by separating water and copolymer using a sieve (mesh size: 0.1 mm) before fresh water was added again to the copolymer. The purified copolymer was finally dried for 10 days at 50 °C in a drying cabinet. Since after drying, several agglomerates of the copolymer had formed, it was ground (mesh size: 0.25 mm) one more time using the Ultra Centrifugal Mill ZM 200.

2.2.3. Determination of Water Content of ModE

The water content of ModE was measured after 5 and 10 days of drying using the Moisture Analyzer HC 103 from Mettler Toledo (Giessen, Germany). This device works according to the thermo-gravimetric principle, often referred to as the loss-on-drying (LOD) principle. The device consisted of two components, a heating as well as a balance unit. In order to determine the LOD, a sample of a defined weight (1 g) was placed on the balance. Then, a halogen lamp, which heated and dried the sample, was switched on. During drying, the sample weight was continually recorded via the integrated balance. A temperature of 105 °C was maintained during the entire measurement. The water content was measured automatically, and the result was displayed by the instrument when no change in sample weight was monitored within 10 consecutive seconds. All measurements were performed in triplicate.

2.2.4. Residual Monomer Analysis and Monomer Conversion Rate

Prior to the removal of volatiles immediately after the polymerization process, and also after the completion of the purification and drying process, samples (n = 3) of ModE were withdrawn for the analysis of residual monomers. High performance liquid chromatography (HPLC) was used for the analysis of dimethylaminopropyl methacrylamide and gas chromatography (GC) for the analysis of butyl methacrylate and methyl methacrylate. Results from residual monomer quantification were then used to calculate the amount of polymerized monomers providing the final copolymer composition. For HPLC analysis, an Agilent 1260 Infinity system from Agilent Technologies (Frankfurt am Main, Germany) was used. The GC analysis was conducted using a Clarus 500 GC with a head space sampler (Turbomatrix 40), both from PerkinElmer LAS GmbH (Rodgau, Germany).

2.2.5. Molecular Weight Analysis by Gel Permeation Chromatography

The molecular weight distribution of ModE was determined by gel permeation chromatography (GPC) using an Agilent 1100 Series GPC-SEC Analysis System comprising a pump (G1310A), autosampler (G1313A), column oven (G1316A), RI-detector (G1362A) and a control module (G1323B), all from Agilent Technologies (Frankfurt am Main, Germany). Separation was achieved using a GRAM precolumn (8×50 mm, 10 µm) and another three GRAM columns (8×300 mm, 10 µm) in series, all maintained at 60 °C. The eluent consisted of n,n-dimethylacetamide: lithium bromide: tris(hydroxymethyl)aminomethane (TRIS): water (1000:2:2:10 *w/w*), the flow rate was set to 1 mL/min and an injection volume of 100 µL was applied. The RI-detector was maintained at 40 °C and a polymethylmethacrylate solution (1 g/L eluent) was used as a standard. A solution of ModE (1 g/L eluent) was used for analysis and the number-average molecular weight (M_n), the weight-average molecular weight (M_w), and the polydispersity index (PDI) of ModE was determined in triplicate.

2.2.6. Thermogravimetric Analysis for Studying ModE Decomposition

In order to obtain information on whether the new polymer can be processed with the application of heat without decomposition, which is for instance required for melt extrusion, an isothermal thermogravimetric analysis (TGA) of ModE was performed to measure weight changes of ModE as a function of temperature and time using a TGA Q5000 from TA Instruments (Huellhorst, Germany). Analyses were performed as follows: samples of 20 mg each were placed into the device's sample chamber and preheated for 15 min at a temperature of 100 °C to remove residual water. Thereafter, samples were kept at a fixed temperature of either 150 °C or 165 °C for another 25 min and the copolymers' change in weight was continuously recorded.

2.2.7. Flowability Measurement

The flowability of the ground copolymers ModE and EPO was analyzed using the flowability tester BEP 2 from Copley Scientific (Nottingham, UK). Both the time required for 100 g of each of the copolymers to flow through a 10 mm nozzle and the slope angle of the resulting pile was measured. A high flow rate as well as a low slope angle (<40°) indicated a good flowability. For better comparability, prior to the analysis EPO was also reduced to a particle size of approximately 0.25 mm using the Ultra Centrifugal Mill ZM 200. The flowability measurements were conducted in triplicate.

2.2.8. Preparation of Amorphous Solid Dispersions via Hot Melt Extrusion

To evaluate the suitability of the new ModE copolymer for the preparation of solid ASDs, various ModE copolymers with different M_w were extruded with different model drugs, i.e., celecoxib, efavirenz or fenofibrate, by hot melt extrusion (HME). For comparison, using the same manufacturing process, ASDs were prepared from the same model drug substances with (co-)polymers already established for the purpose of solubility enhancement such as EPO, Soluplus®, Kollidon® VA 64, Kollidon® 17 PF, AQOAT® AS-MMP and Affinisol® HPMC 100 LV. Extrudates were prepared as follows: first, 15 g of a mixture of each of the individual (co-)polymers and one of the poorly soluble model drugs celecoxib, efavirenz, or fenofibrate was prepared in a predetermined mixing ratio by mixing the components in a 100 mL jar sealed with a screw cap for 10 min using a turbular mixer (TURBULA®, WAB Group, Nidderau-Heldenbergen, Germany). Then, the polymer-drug blends were processed via HME technology to obtain ASDs using a co-rotating HAAKE MiniLab twin screw extruder with a conical screw design from Thermo Fisher Scientific (Dreieich, Germany). The HME process was characterized by the set parameters of screw speed and process temperature, and by the torque recorded during the process. The die diameter was 2 mm, and the strand leaving the extruder was allowed to cool during transport via a conveyor belt and was finally ground to coarse granules by a small chopper with a rotating metal gear. The coarse granules were then pulverized using the ZM 200 ultra-centrifugal mill (mesh size: 0.25 mm). The obtained powders were used for all further experiments.

2.2.9. Differential Scanning Calorimetry Analysis

All ASDs were analyzed via differential scanning calorimetry (DSC) to determine whether the incorporated drug was in the amorphous or crystalline state. All DSC analyses were conducted using a DSC 3+ (DSC-HC01) from Mettler Toledo (Giessen, Germany). A sample of 5–10 mg each was weighed into a small, aluminum pan with a perforated lid and exposed to a heating-cooling-heating cycle in a temperature range of 0 °C to 200 °C. The heating/cooling rate was set at 10 °C/min and a nitrogen flow of 50 mL/min was applied while running the measurement. For comparison, the melting point of the pure drug substance as well as the glass transition temperature of the individual (co-)polymers were investigated. For all analyzed samples, T_g was taken from the thermogram obtained from the second heating cycle, and the indicated value represents the mean of n = 3.

2.2.10. X-ray Powder Diffraction Studies

X-ray powder diffraction (XRPD) studies were performed to verify the results of the DSC analysis. For these investigations, all individual samples, i.e., drug substances, (co-)polymers and all ASDs, were first triturated to a fine soft powder in a ceramic mortar, and 500 mg of each sample was packed (back-loaded) into the 16 mm-diameter well of a sample holder. Analyses were then run on a Cubix3 Pharma diffractometer from Malvern Panalytical (Malvern, UK) in Bragg–Brentano geometry using the following components and parameters: X-ray tube: LFF-Cu X-ray tube, Cu Kα, $\lambda = 0.1542$ nm, detector: X'Celerator, generator settings: 40 mA, 40 kV, rotation: 1 revolution/s, 2-Theta(θ) range: $2°$–$40°$ with $0.02°$ steps, applying 200 s per step. The intensity (count) of the diffracted X-rays was recorded as a function of the diffraction angle θ and the resulting diffractogram was displayed as intensity (count) against 2θ. The positions of the angles were determined by the geometry of the unit cell of the crystalline phase. The relative intensities (counts) of the peaks observed were modulated by different diffraction behavior of atoms with different electrons' density function (atomic number) and by the positions of the individual atoms in the unit cell.

2.2.11. Fourier-Transform Infrared Spectroscopy Analysis

Fourier-transform infrared spectroscopy (FT-IR) analysis was performed to investigate potential molecular interactions between the individual model drugs and the ModE copolymer. Therefore, drug substances, ModE copolymer, a physical mixture (PM) of the drug substance and ModE copolymer, as well as the corresponding ASDs, were analyzed using the FT-IR spectrometer "ALPHA" from Bruker Optics (Hanau, Germany). The samples were placed into the light path for recording the spectra, and the selected scanning range was 4000 to 400 cm^{-1}. Characteristic patterns (spikes) related to the chemical structure of the samples were identified by measuring the attenuated total reflection (ATR) of the exposed infrared radiation. The resulting FT-IR spectrogram was obtained by plotting the transmission (%) against the wave number (cm^{-1}).

2.2.12. Determination of Saturation Solubility in Water

Saturation solubility of celecoxib, efavirenz and fenofibrate in water was studied for pure drugs and the corresponding ASDs immediately after preparation. For this purpose, approximately 25 mg of the substance or a quantity of ASD corresponding to this amount of drug substance was added to a volume of 25 mL of distilled water and stirred at controlled temperature in a water bath at 20 °C for 48 h (100 rpm). The resulting suspensions were filtered via a 0.22 µm polytetrafluoroethylene (PTFE) membrane filter with a diameter of 25 mm from Global Biomed Scientific (Forest, VA, USA). The appropriateness of the filter material had been validated for each of the drug compounds before use. All filtrates were diluted with acetonitrile in a predetermined ratio, before the amount of celecoxib, efavirenz, and fenofibrate dissolved was quantified by HPLC.

2.2.13. Dissolution Studies of ASD

Dissolution experiments were conducted in triplicate with 25 mg drug substance or an equivalent amount of ASD using USP apparatus II (DT 800 LH) from ERWEKA GmbH (Langen, Germany). The paddle speed was set to 100 rpm to avoid coning effects and all experiments were performed in 500 mL of 0.1 M hydrochloric acid at 37 ± 0.5 °C. The test duration was 120 min. All samples were withdrawn by a fraction collector, equipped with poroplast cannula filters of 10 µm pore size and manually diluted 1:1 (*v/v*) with acetonitrile, before HPLC analysis.

2.2.14. HPLC Setup

An HPLC system (Agilent 1260 Infinity) was used for the quantification of the three different model drug substances. The system consisted of a quaternary pump (G1311B), an autosampler (G1329B), a column oven (G1316A) and an UV detector (G1314C), all from

Agilent Technologies (Frankfurt am Main, Germany). Prior to use, all analytical methods were validated according to USP requirements.

HPLC Method for Celecoxib

Separation of all samples containing celecoxib was achieved using a Knauer Nucleosil 100-7 C18 (125 × 4.6 mm, 7 μm) column (Knauer-Wissenschaftliche Geräte GmbH, Berlin, Germany) maintained at 40 °C. The mobile phase consisted of an acetonitrile: water: triethylamine mixture (300:300:0.9 *v/v*), adjusted to pH 3.00 with phosphoric acid. The flow rate was set to 1.8 mL/min. An injection volume of 5 μL was applied, the run time was 7 min, and celecoxib was detected at 254 nm. In the concentration range of 0.13–542 μg/mL, the analytical curve was linear (r^2 = 0.999995). The method was found to be accurate (100.2–102.1%) and precise (CV 2.46%) with a quantification limit of 0.05 μg/mL.

HPLC Method for Efavirenz

Separation of the efavirenz samples was achieved using a Symmetry 300 C18 (250 × 4.6 mm, 5 μm) column (Waters GmbH, Eschborn, Germany) maintained at 22 °C. The mobile phase consisted of an acetonitrile: buffer solution (disodium hydrogen phosphate/phosphoric acid adjusted to pH 3.60) mixture (290:210 *v/v*). The flow rate was set to 1.5 mL/min and the injection volume was 20 μL. The run time was 10 min and efavirenz was detected at 247 nm. In the concentration range of 0.13–515 μg/mL, the analytical curve was linear (r^2 = 0.999894). The method was found to be accurate (101.4–103.0%) and precise (CV 4.05%), with a quantification limit of 0.05 μg/mL.

HPLC Method for Fenofibrate

Separation of the fenofibrate samples was achieved on a Symmetry 300 C18 (150 × 4.6 mm, 5 μm) column maintained at 22 °C. The mobile phase consisted of an acetonitrile: water mixture (70:30 *v/v*), adjusted to pH 2.50 with phosphoric acid. The flow rate was set to 2.0 mL/min. The injection volume was set at 20 μL, the run time was 6 min and fenofibrate was detected at 286 nm. In the concentration range of 0.13–526 μg/mL, the analytical curve was linear (r^2 = 0.999992). The method was found to be accurate (101.2–101.4%) and precise (CV 2.42%) with a quantification limit of 0.05 μg/mL.

For all three methods, selectivity was determined (formulation excipients), and no interference was observed in the retention time of celecoxib, efavirenz, or fenofibrate. In addition, the peak area of the specific drug did not change in the presence of all excipients used in the study.

2.2.15. Stability Studies

ASDs were added to 30 mL amber-glass jars, closed with a screw cap, and stored at constant and controlled conditions (30 °C/65% RH) in a climatic chamber from Binder GmbH (Tuttlingen, Germany) for three months. After three months, they were first visually inspected to determine whether they could be easily fluffed up again or stuck together (formation of larger agglomerates). Subsequently, they were subjected to dissolution experiments and DSC analyses using the same conditions as selected for the studies immediately after manufacture, and results of these experiments were compared with those obtained immediately after manufacture.

2.2.16. Data Analysis

All reported data were derived from at least three independent experiments. Significance tests were conducted with SigmaPlot 14.0 from Systat Software GmbH (Erkrath, Germany) using a one-way analysis of variance (ANOVA) test with the Holm–Sidak post-test. Significances are indicated with $p < 0.05$ in brackets.

3. Results and Discussion

3.1. Synthesis of ModE

ModE, a dimethylaminopropyl methacrylamide-butyl methacrylate-methyl methacrylate copolymer, was synthesized by applying four different concentrations of the CTA n-dodecylmercaptan (0.3%, 0.5%, 0.9% and 1.5% by weight). The higher the CTA concentration, the lower the M_w of the ModE type produced. Four copolymers with different weight average M_w of 173 kDa, 254 kDa, 281 kDa and 305 kDa were obtained, which will be referred to in the following as copolymers E-173 kDa, E-254 kDa, E-281 kDa and E-305 kDa. Figure 1a illustrates the radical copolymer synthesis of ModE, and Figure 1b shows the differences in the chemical structure of ModE and EPO. Overall, ModE was obtained by replacing the functional monomer unit of EPO—more precisely the dimethylaminoethyl methacrylate by dimethylaminopropyl methacrylamide.

(a)

(b)
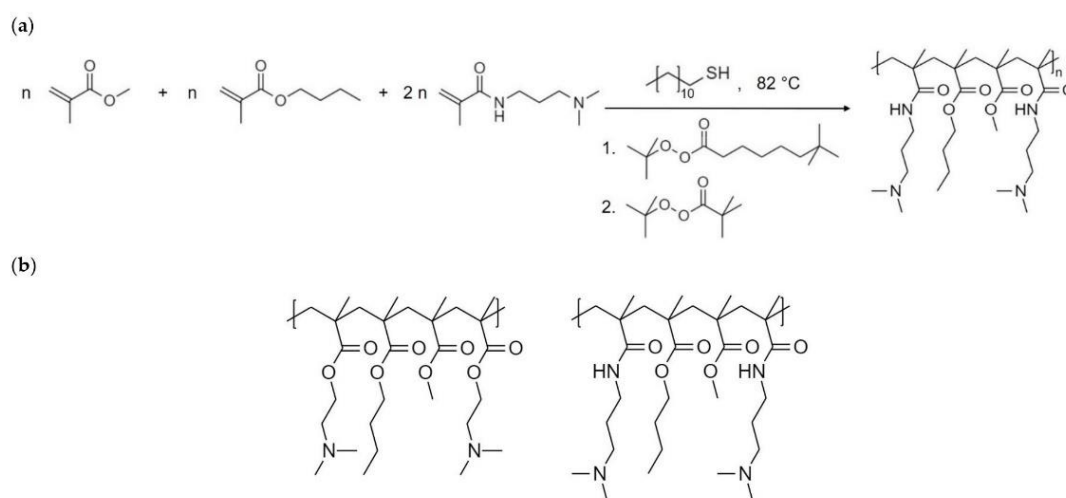
Figure 1. Radical copolymer synthesis of ModE including monomers, chain-transfer-agent (CTA), initiators (1. tert-butyl peroxyneodecanoate, and 2. tert-butyl peroxypivalate) and reaction conditions (**a**), and a section of the chemical structure of EUDRAGIT® E PO (EPO) (left) and ModE (right) (**b**).

3.2. Purification, Residual Monomer Analysis and Water Content of ModE

Based on the results of the residual monomer analysis immediately after polymer synthesis (on average 6.16 wt% for dimethylaminopropyl methacrylamide, 0.002 wt% for butyl methacrylate, and 0.035 wt% for methyl methacrylate), considering a monomer ratio of 2:1:1 (dimethylaminopropyl methacrylamide: butyl methacrylate: methyl methacrylate) by weight, the average monomer conversion rate was calculated as 87.68% for dimethylaminopropyl methacrylamide, 99.99% for butyl methacrylate, and 99.86% for methyl methacrylate (Table 1). Consequently, with the applied radical polymerization process, a high monomer conversion providing a yield >90% was achieved. The results led to a final copolymer composition comprising in average 46.74 wt% dimethylaminopropyl methacrylamide, 26.65 wt% butyl methacrylate, and 26.61 wt% methyl methacrylate (Table 1). Regardless of its M_w, ModE presented with a proportion of its amino methacrylamide functional unit of about 47 wt% which is very close to the targeted value of 50 wt%. The proportion of amino functionality is therefore comparable to that of EPO.

Table 1. Residual monomer content, monomer conversion rate and the final composition of ModE copolymers. Each value designates the mean (n = 3). Since S.D. was <0.04 for DMAPMA and <0.005 for all other reported values, detailed S.D. values are not shown for better overview.

Polymer	Residual Monomer Content			Monomer Conversion Rate			Final Polymer Composition		
	DMAPMA *[%]	BMA *[%]	MMA *[%]	DMAPMA [%]	BMA [%]	MMA [%]	DMAPMA [%]	BMA [%]	MMA [%]
E-173 kDa	6.48	0.002	0.022	87.04	99.99	99.91	46.55	26.74	26.71
E-254 kDa	6.79	0.002	0.037	86.42	99.99	99.85	46.38	26.83	26.79
E-281 kDa	5.59	0.002	0.034	88.82	99.99	99.86	47.06	26.49	26.45
E-305 kDa	5.78	0.002	0.045	88.44	99.99	99.82	46.96	26.54	26.50
average	6.16	0.002	0.035	87.68	99.99	99.86	46.74	26.65	26.61

* DMAPMA = dimethylaminopropyl methacrylamide, BMA = butyl methacrylate, MMA = methyl methacrylate.

The residual monomer content of butyl methacrylate and methyl methacrylate had already been very low immediately after radical polymerization synthesis but could be further reduced by applying a water-based purification process. In particular, the residual monomer content of the dimethylaminopropyl methacrylamide monomer could be significantly ($p < 0.05$) reduced by this purification step. Independent of their M_w, all ModE copolymers finally exhibited a total residual monomer content below 0.05% (Table 2).

Table 2. Residual monomer and water content after purification and drying of ModE. Each value designates the mean $\pm$ S.D. (n = 3).

Polymer	DMAPMA * [%]	BMA * [%]	MMA * [%]	Water Content after 5 Days [%] $\pm$ S.D.	Water Content after 10 Days [%] $\pm$ S.D.
E-173 kDa	0.016 $\pm$ 0.001	<0.002 $\pm$ 0	<0.002 $\pm$ 0	1.11 $\pm$ 0.05	0.60 $\pm$ 0.07
E-254 kDa	0.025 $\pm$ 0.002	<0.002 $\pm$ 0	<0.002 $\pm$ 0	1.31 $\pm$ 0.08	0.90 $\pm$ 0.03
E-281 kDa	0.028 $\pm$ 0.002	<0.002 $\pm$ 0	<0.002 $\pm$ 0	1.10 $\pm$ 0.05	0.90 $\pm$ 0.04
E-305 kDa	0.042 $\pm$ 0.003	<0.002 $\pm$ 0	<0.002 $\pm$ 0	1.11 $\pm$ 0.07	0.80 $\pm$ 0.06

* DMAPMA = dimethylaminopropyl methacrylamide, BMA = butyl methacrylate, MMA = methyl methacrylate.

The residual water content of all ModE copolymers (Table 2) was monitored after 5 and 10 days of drying, respectively. Results indicate that the target residual water content of less than 1% was achieved after 10 days of drying. It was assumed that this specified maximum acceptable water content would effectively prevent agglomeration that could affect processability.

3.3. Molecular Weight Analysis

Results from the GPC analysis of the four ModE copolymers obtained by utilizing different concentrations of the CTA n-dodecylmercaptan in copolymer synthesis (Table 3) indicated that a higher concentration of the CTA led to a decrease of both the M_n and the M_w, as expected for this radical polymerization. By contrast, the PDI slightly increased with increasing CTA concentration (Table 3).

Table 3. M_n, M_w and PDI of the ModE copolymers determined via gel permeation chromatography (GPC) analysis. Each value designates the mean $\pm$ S.D. (n = 3).

Concentration of n-Dodecylmercaptan [%]	Number-Average Molecular Weight (M_n) [kDa]	Weight-Average Molecular Weight (M_w) [kDa]	Polydispersity Index (PDI)
1.5	41.5 $\pm$ 1.8	173 $\pm$ 0.5	4.17 $\pm$ 0.09
0.9	64.1 $\pm$ 0.4	254 $\pm$ 0.5	3.97 $\pm$ 0.02
0.5	71.7 $\pm$ 1.3	281 $\pm$ 1.0	3.92 $\pm$ 0.05
0.3	81.4 $\pm$ 0.1	305 $\pm$ 0.5	3.75 $\pm$ 0.01

3.4. Flowability

Since a good flowability of a powder is an essential prerequisite for easy processing and dose accuracy, immediately after grinding, the flowability of ModE copolymers was measured. With increasing M_w, and inversely with decreasing PDI, the flowability of ModE improved (Table 4). As all copolymers had been ground to a similar particle size of about 0.25 mm immediately before running the flowability test, an impact of the particle size could be neglected. Independent of their M_w, all ModE types demonstrated a slope angle that was substantially smaller than 40°, indicating good flow properties. In contrast to all ModE copolymers, EPO revealed no product flow through the nozzle of the flowability tester.

Table 4. Flowability data of ModE considering different molecular weights (M_w) and EPO. Each value designates the mean ± S.D. (n = 3).

	E-173 kDa	E-254 kDa	E-281 kDa	E-305 kDa	EPO *
polymer [g]	99.90 ± 0.45	99.17 ± 0.54	99.35 ± 0.55	99.87 ± 0.33	99.65 ± 0.41
flow time [s]	30.51 ± 0.60	25.37 ± 0.71	24.09 ± 0.40	23.11 ± 1.46	-
flow rate [g/s]	3.28 ± 0.06	3.91 ± 0.13	4.13 ± 0.09	4.34 ± 0.29	-
slope angle [°]	34.58 ± 0.43	31.33 ± 0.52	31.87 ± 0.54	32.20 ± 1.00	-

* ground to a particle size of approximately 0.25 mm applying EUDRAGIT® E 100.

3.5. Investigation on Decomposition of ModE via TGA

The four different types of ModE copolymers were first dried at 100 °C and then subjected to isothermal TGAs at 150 °C and 165 °C, i.e., the HME process temperatures, to mimic the heat input that the copolymers would be subjected to during the investigation. Based on the results of stability studies with EPO, whose chemical structure is very similar to that of ModE, it might be possible that, at the selected temperatures, decomposition of ModE copolymers might take place in the side chain region. Possible decomposition products in this case would be dimethylamine, trimethylamine, acetaldehyde, and short-chain alcohols, i.e., substances that are volatile at these high temperatures. Accordingly, possible decomposition of ModE could be easily detected in the context of isothermal TGA, since this would be associated with a measurable change in weight due to the escape of volatile compounds.

The time ModE would be exposed to temperatures of 150 °C and 165 °C in the extruder would range from 5–10 min. From the TGA thermograms (Figure S1a,b), it is evident that at both temperatures ModE did not decompose noticeably, for a time period of at least 10 min, since the thermograms showed no significant ($p > 0.05$) weight change (<1% after 10 min in each case) for all ModE copolymers tested. As expected, the weight loss at a temperature of 165 °C (Figure S1b) was slightly higher than at 150 °C (Figure S1a). However, even after 25 min of heat exposure, there were no noticeable changes in weight, which is why the copolymer was regarded as suitable for the HME process.

3.6. ASD Composition and Manufacture

In the next step, the novel ModE copolymers were used to produce ASDs by HME. For comparative purposes, ASDs were also prepared using other (co-)polymers, including EPO, which are commonly used for solubility enhancement. The total drug load, as well as the process parameters applied in the HME process, are displayed in Table 5. The extrusion temperature was chosen individually for each (co-)polymer based on its melt viscosity characteristics when applying thermal and mechanical force input. A high torque indicates a pronounced melt viscosity, which can lead to clogging of the extruder die if the extruded material cools immediately upon leaving the extruder. Torque values higher than 250 N·cm proved to complicate the HME process. The issue of very high torque values could be addressed by increasing the processing temperature if the corresponding (co-)polymers could tolerate higher temperatures. While the same screw speed was used for all other (co-)polymers, Affinisol® HPMC 100 LV was extruded at a lower screw speed, as it would otherwise have clogged the extruder die. A further increase in extrusion temperature was

not an alternative for processing Affinisol® HPMC 100 LV, as this would have led to a loss of integrity. All commercially available (co-)polymers were processed via HME within their recommended temperature range provided by the corresponding manufacturer, if possible [19–21]. For the use of these (co-)polymers, there is also information from other HME studies, in which generally somewhat lower extrusion temperatures were used than indicated in Table 5 [22–26]. This is, however, probably due to differences in drug loads and extruder types used, i.e., parameters that have an influence on both the torque values and the temperature required for a successful extrusion process [23–26].

Table 5. Composition and hot melt extrusion process parameters of ASDs incorporating celecoxib/efavirenz/fenofibrate.

Polymer	Drug Load [%]	Extrusion Temperature [°C]	Torque [N·cm]	Screw Speed [rpm]
Soluplus®	5.1/6.3/4.2	150/150/150	130/105/95	200/200/200
Kollidon® VA 64	5.1/6.3/4.2	160/165/170	70/90/65	200/200/200
Kollidon® 17 PF	5.1/6.3/4.2	180/180/180	55/85/65	200/200/200
AQOAT® AS-MMP	5.1/6.3/4.2	170/175/175	140/200/140	200/200/200
E-173 kDa	5.1/6.3/4.2	150/160/160	200/185/180	200/200/200
E-254 kDa	5.1/6.3/4.2	165/160/165	190/180/180	200/200/200
E-281 kDa	5.1/6.3/4.2	160/160/160	200/200/200	200/200/200
E-305 kDa	5.1/6.3/4.2	165/165/165	230/200/220	200/200/200
Affinisol® HPMC 100 LV	5.1/6.3/4.2	165/165/170	150/150/120	100/100/100
EUDRAGIT® E PO	5.1/6.3/4.2	150/150/150	50/45/45	200/200/200

3.7. Thermal Characterization of the Pure Drugs, (Co-)Polymers and ASDs via DSC Analysis

Immediately after processing, celecoxib- (Figure S2a,b), efavirenz- (Figure S3a,b) and fenofibrate ASDs (Figure S4a,b), as well as the individual (co-)polymers (Table 6), were analyzed via DSC (thermograms displayed in endo up mode). ASDs and (co-)polymers showed, without exception, amorphous properties (no melting peaks) (Figures S2–S4), while the crystalline character of the pure drug substances was revealed by characteristic peaks in the respective melting range of the drug substances (Figures S2–S4). Moreover, the T_g of the corresponding ASD was always lower than that of the pure (co-)polymer. EPO showed a significantly ($p < 0.05$) lower T_g than all other (co-)polymers applied in the study. The T_g of EPO was also lower than that of all ASDs prepared with ModE copolymers. Consequently, the T_gs of the drug loaded EPO ASDs were the lowest of all T_gs measured, which may lead to storage stability issues related to crystallization of the active ingredient and, accordingly, lower drug release.

Table 6. Glass transition temperatures (T_g) of pure (co-)polymers and amorphous solid dispersions (ASDs) incorporating celecoxib, efavirenz or fenofibrate. Each value designates the mean ± S.D. (n = 3).

Polymer	T_g (Polymer) [°C]	T_g (Celecoxib ASD) [°C]	T_g (Efavirenz ASD) [°C]	T_g (Fenofibrate ASD) [°C]
Soluplus®	70 ± 0	67 ± 1	69 ± 0	62 ± 1
Kollidon® VA 64	107 ± 1	100 ± 2	100 ± 1	92 ± 2
Kollidon® 17 PF	136 ± 3	126 ± 3	96 ± 1	90 ± 3
AQOAT® AS-MMP	113 ± 1	106 ± 1	100 ± 2	101 ± 1
E-173 kDa	77 ± 1	77 ± 1	76 ± 1	74 ± 1
E-254 kDa	85 ± 2	79 ± 0	78 ± 1	77 ± 1
E-281 kDa	89 ± 0	84 ± 1	83 ± 2	76 ± 2
E-305 kDa	91 ± 1	84 ± 1	82 ± 1	80 ± 2
Affinisol® HPMC 100 LV	103 ± 2	90 ± 0	87 ± 0	84 ± 1
EUDRAGIT® E PO	42 ± 1	41 ± 1	40 ± 1	34 ± 2

3.8. XRPD Studies of Pure Drugs, (Co-)Polymers and ASDs

XRPD analyses of the pure drug substances celecoxib (Figure 2a,b), efavirenz (Figure 3a,b) and fenofibrate (Figure 4a,b) provided characteristic diffraction peaks indicating crystalline phases. In contrast, the XRPD patterns of both the pure (co-)polymers and all ASD formulations prepared by HME did not exhibit diffraction peaks, regardless of the incorporated drug substance, indicating that these materials were amorphous (Figures 2–4) and proving that the preparation of ASDs by HME was successful in all cases.

3.9. FT-IR Analysis

As a representative of all ModE copolymers, E-173 kDa was selected to investigate the potential interactions between the copolymer and the drugs celecoxib, efavirenz, or fenofibrate, which may occur during HME processing. The selection of only one representative for the FT-IR analysis was considered sufficient for this study, since differences between the ModE polymers are mainly limited to their M_ws.

The spectrum of the celecoxib molecule presented with characteristic peaks of the NH_2 group at 3332 cm^{-1} and 3224 cm^{-1} (N-H stretching vibrations) as a potential H-donor group, as well as a potential H$^+$-acceptor in the SO_2 group at 1345 cm^{-1} (S=O stretching vibrations) (Figure 5a). The copolymer E-173 kDa revealed distinctive peaks between 2950 and 2750 cm^{-1} of its dimethylamino group (N-CH$_3$ stretching vibrations), as well as a peak of its carbonyl groups at 1723 cm^{-1} (C=O stretching vibrations) as a potential H$^+$-acceptor (Figure 5a). The intensity of the characteristic celecoxib peaks in both the ASD and PM formulation spectra decreased significantly compared to those observed in the spectrum of the pure drug which was due to the lower drug concentration in these samples. The fact that celecoxib peaks between 3400 and 3200 cm^{-1} were no longer detectable in the ASD spectrum, but less pronounced, yet still present in the spectrum of the PM, might be attributable to a potential interaction (via hydrogen bonds) between the proton accepting groups (C=O) in ModE and the proton donating groups (NH) of celecoxib. In addition, the disappearance of the characteristic celecoxib peak at 1345 cm^{-1}, which was observed for the ASD but not for the PM formulation (Figure 5a), was considered to indicate a possible further interaction.

The efavirenz spectrum revealed characteristic peaks at 3313 cm^{-1} (N-H stretching vibrations), 2249 cm^{-1} (C≡C stretching vibrations), 1744 cm^{-1} (C=O stretching vibrations) and around 1241 cm^{-1} (C-F stretching vibrations) (Figure 5b). As had been observed for the celecoxib formulations, efavirenz peaks in the ASD- and PM spectra were presented with lower intensities and less details. Furthermore, in the ASD spectrum, the efavirenz peak at 3313 cm^{-1} disappeared and a shift and broadening of the peak at 1744 cm^{-1} was observed in both the ASD- and PM spectra (Figure 5b). These observations might be related to interactions between efavirenz and the ModE copolymer.

In contrast to celecoxib, as well as efavirenz formulations, fenofibrate formulations demonstrated very weak drug–polymer interactions. The FT-IR spectrum of the fenofibrate-ModE ASD showed no obvious differences compared to that of the corresponding physical mixture across the entire scanning range (Figure 5c). Only the characteristic peak of fenofibrate at 2983 cm^{-1} disappeared in both spectra, which is most probably due to the lower drug concentration in the PM, as well as in ASD when compared to the pure drug (Figure 5c).

(**a**)

(**b**)
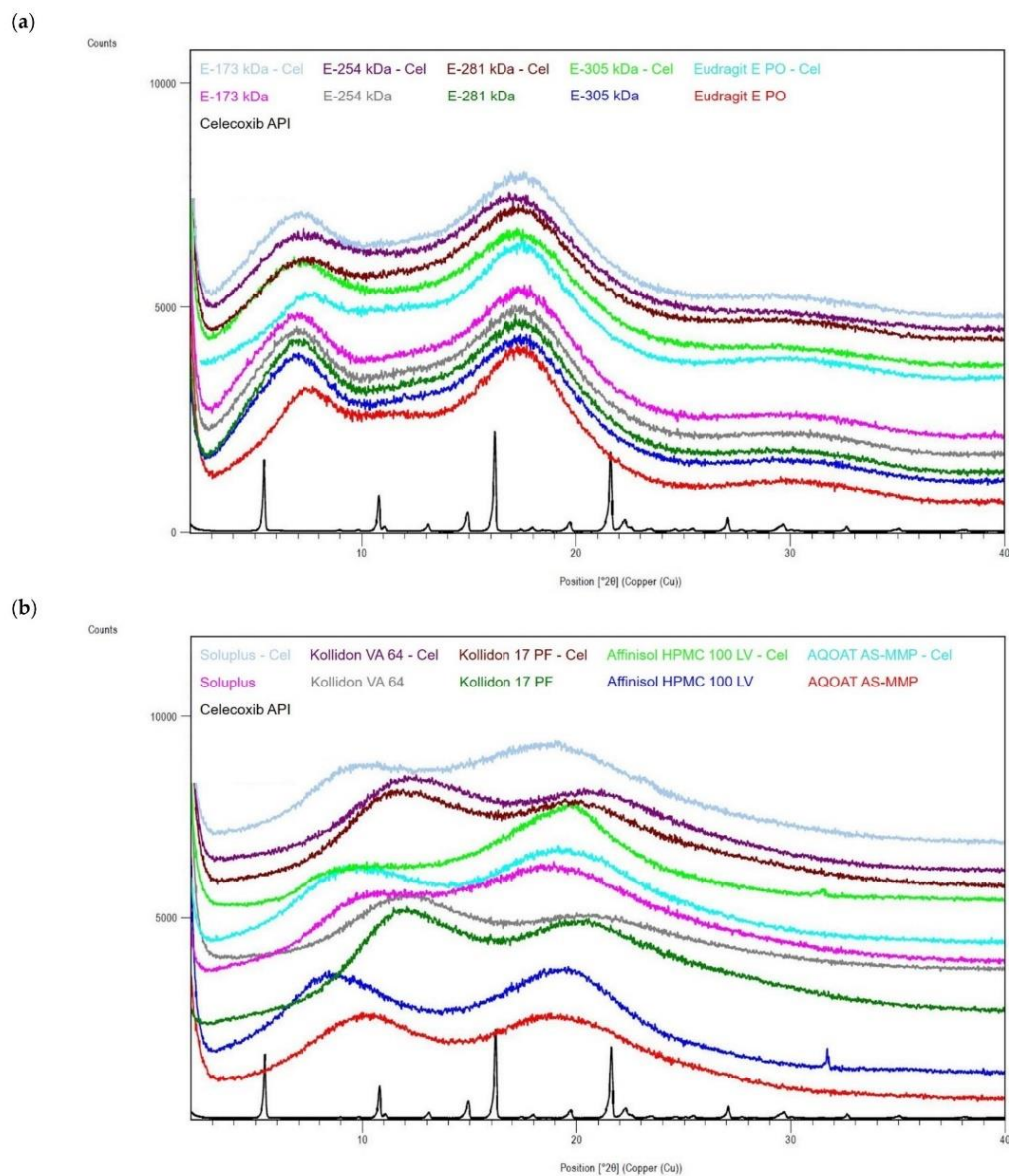
Figure 2. X-ray powder diffraction (XRPD) diffractograms of the drug substance celecoxib, ModE copolymers, EPO and the corresponding ASDs (**a**), as well as celecoxib drug substance, other marketed (co-)polymers (selection) and the corresponding ASDs (**b**).

(**a**)

(**b**)
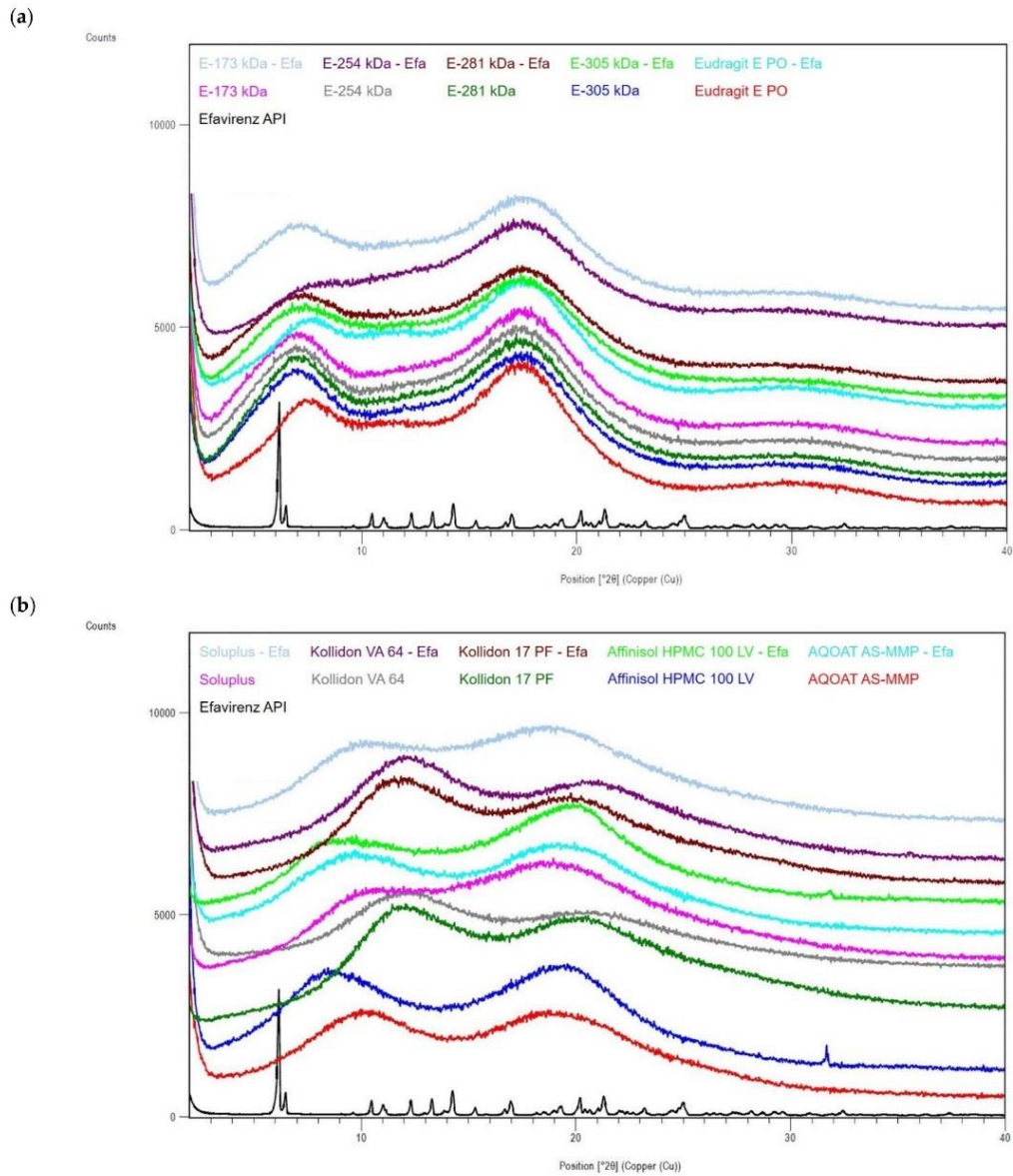
Figure 3. X-ray powder diffraction (XRPD) diffractograms of the drug substance efavirenz, ModE copolymers, EPO and the corresponding ASDs (**a**), as well as efavirenz drug substance, other marketed (co-)polymers (selection) and the corresponding ASDs (**b**).

(**a**)

(**b**)
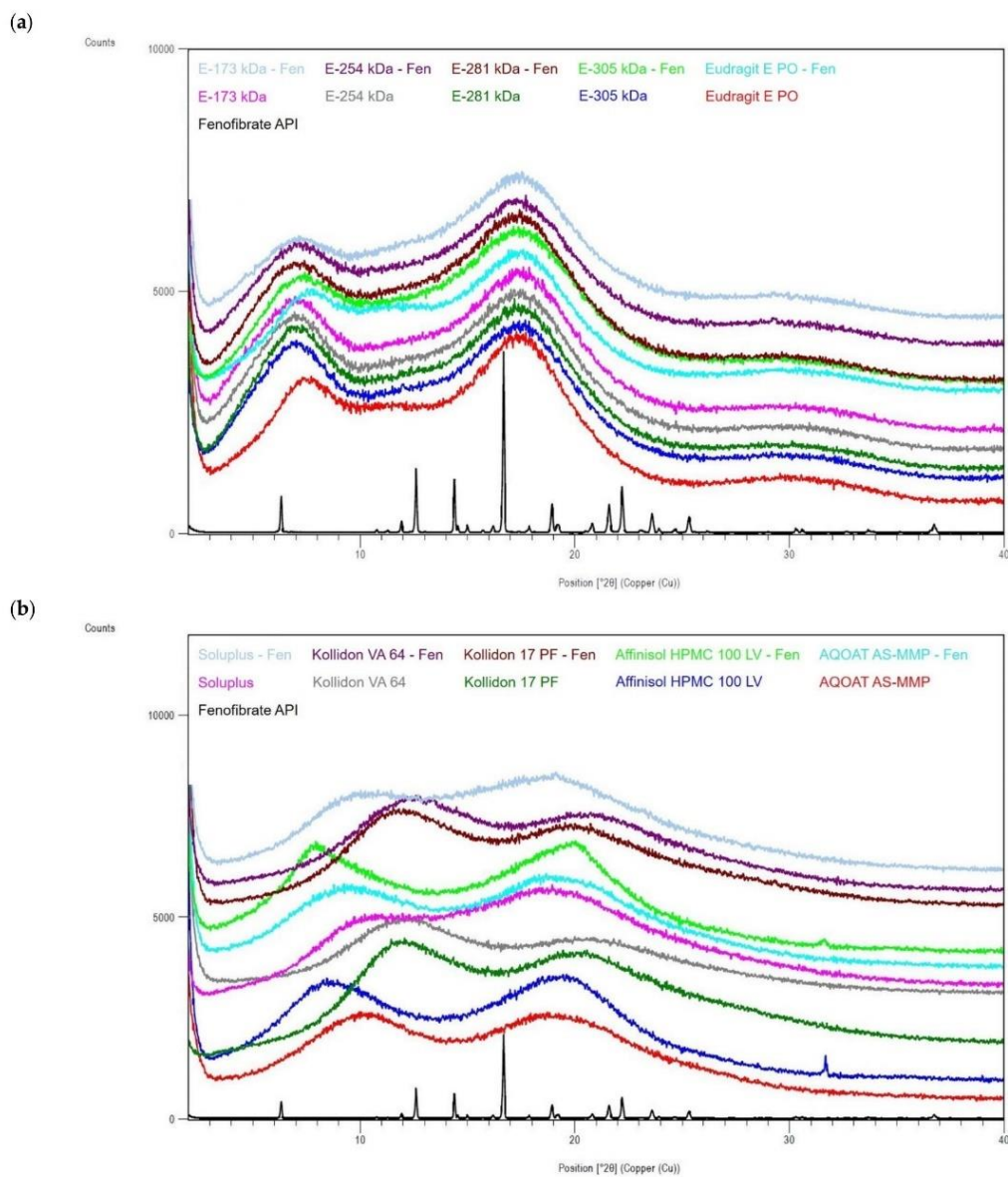
Figure 4. X-ray powder diffraction (XRPD) diffractograms of the drug substance fenofibrate, ModE copolymers, EPO and the corresponding ASDs (**a**), as well as fenofibrate drug substance, other marketed (co-)polymers (selection) and the corresponding ASDs (**b**).

Figure 5. *Cont.*

(c)
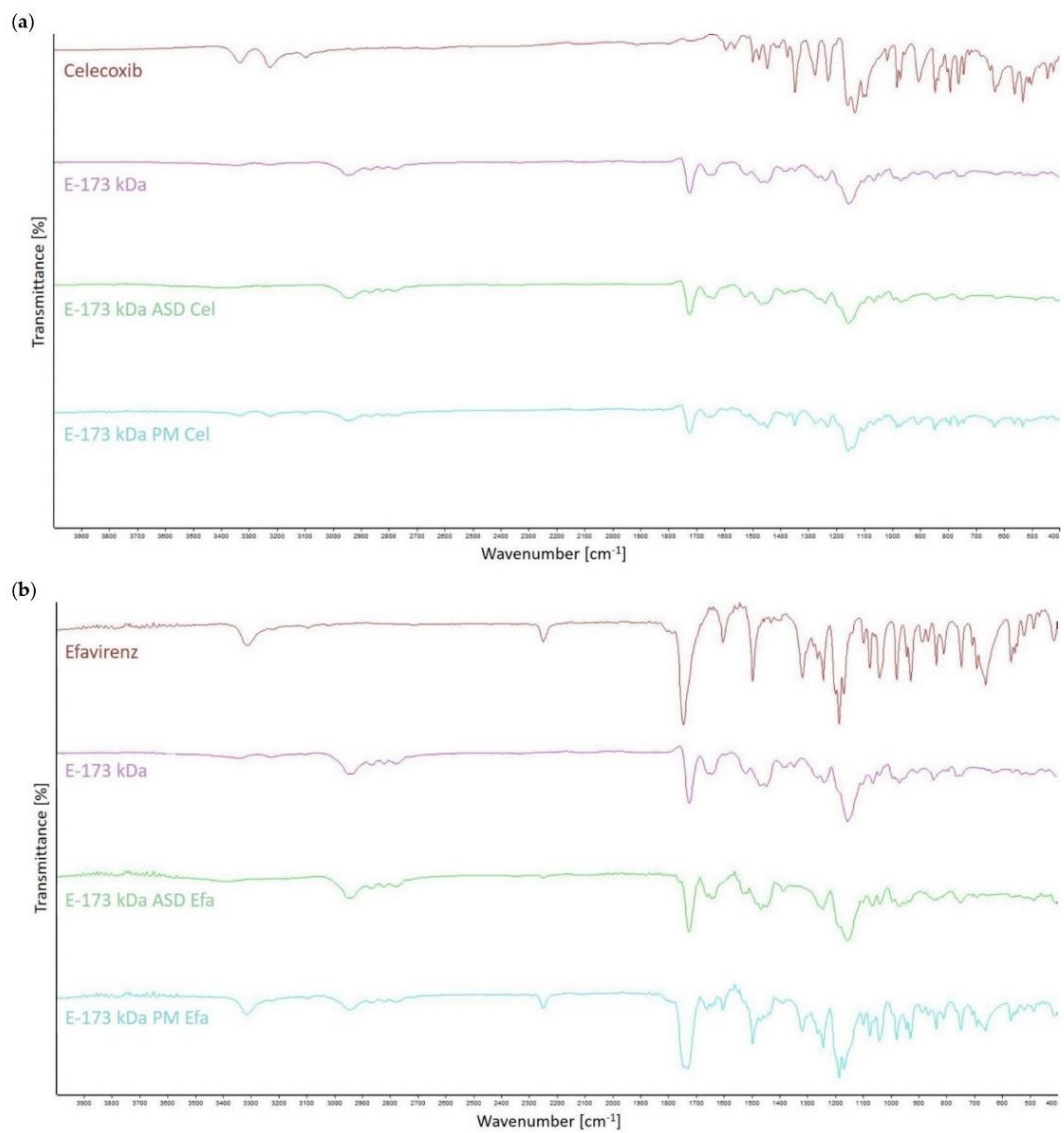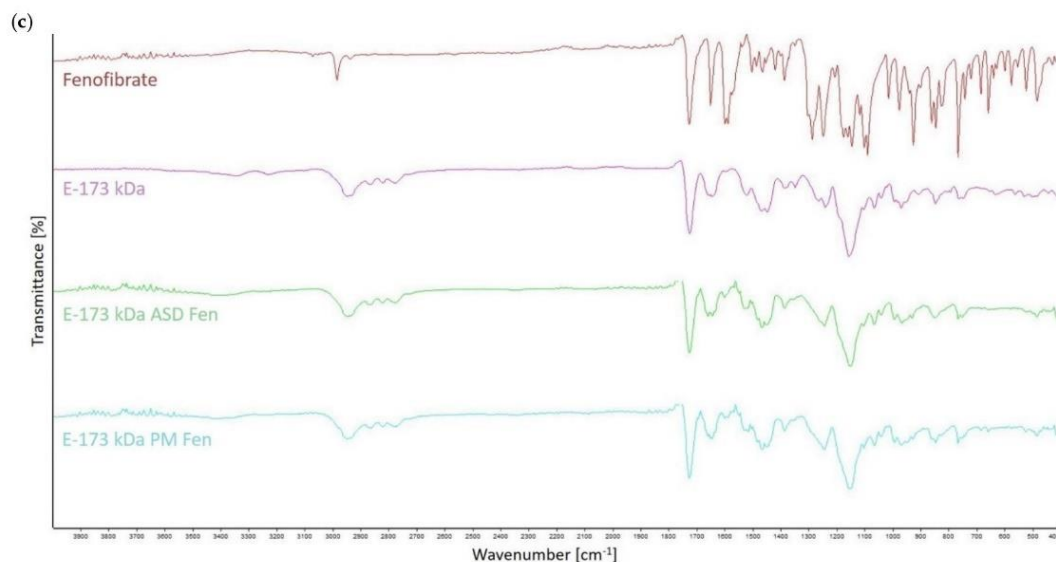
Figure 5. Fourier-transform infrared (FT-IR) spectrogram overlays of celecoxib (**a**), efavirenz (**b**), and fenofibrate (**c**), plotted together with E-173 kDa, a physical mixture (PM) of the specific drug and E-173 kDa, as well as the corresponding ASD processed via hot melt extrusion (HME).

3.10. Saturation Solubility Studies

The saturation solubility (48 h, 20 °C) of celecoxib, efavirenz, and fenofibrate in water was determined for the pure drugs and all ASDs (Table 7). Since the three compounds exhibit pH-independent solubility under physiological conditions of the gastrointestinal tract, solubility tests in water were considered sufficient for initial screening and assessment of the suitability of different polymers for the preparation of ASDs with the desired performance [27,28]. Results of the solubility studies indicated very low aqueous solubilities for the pure drugs (Table 7). By contrast, in most cases, the preparation of ASDs succeeded in considerably improving the water solubility of the drugs. However, some ASDs did not present the desired solubility improvement. The AQOAT® AS-MMP ASD, for instance, presented with low saturation solubilities of all three drugs (Table 7). The ASDs based on Kollidon® 17 PF showed solubility-enhancing effects in the case of fenofibrate only. High saturation solubilities for celecoxib and efavirenz were achieved with Soluplus® ASDs, while in the case of Kollidon® VA 64 ASDs, the highest solubilities of efavirenz and fenofibrate were observed. The solubility enhancing effect of ModE or EPO in ASDs was not as pronounced as that of Soluplus® in the case of celecoxib, and in the case of efavirenz or fenofibrate, they were also not as pronounced as that of Kollidon® VA 64 (Table 7), but was well within the range of results observed for Affinisol® HPMC 100 LV ASDs of the three drugs.

Table 7. Saturation solubility (48 h) of celecoxib, efavirenz, and fenofibrate pure drugs and ASDs in water at 20 °C. Each value designates the mean ± S.D. (n = 3).

Sample	Saturation Solubility of Celecoxib [μg/mL]	Saturation Solubility of Efavirenz [μg/mL]	Saturation Solubility of Fenofibrate [μg/mL]
Drug substance	0.6 ± 0.1	0.7 ± 0	0.1 ± 0
Soluplus® ASD	34.4 ± 0.3	8.8 ± 0	1.0 ± 0
Kollidon® VA 64 ASD	2.5 ± 0.1	15.5 ± 0.1	8.5 ± 0
Kollidon® 17 PF ASD	0.6 ± 0	0.5 ± 0	2.3 ± 0
AQOAT® AS-MMP ASD	0.7 ± 0	0.4 ± 0	0.1 ± 0
E-173 kDa ASD	3.5 ± 0.3	2.1 ± 0.2	0.9 ± 0.3
E-254 kDa ASD	3.0 ± 0.1	1.9 ± 0.1	1.2 ± 0.4
E-281 kDa ASD	2.7 ± 0.2	1.8 ± 0.2	0.8 ± 0.2
E-305 kDa ASD	2.1 ± 0.2	1.1 ± 0.1	0.6 ± 0.1
Affinisol® HPMC 100 LV ASD	3.6 ± 0.2	1.7 ± 0.1	1.7 ± 0
EUDRAGIT® E PO ASD	2.6 ± 0.3	1.8 ± 0.1	0.4 ± 0

3.11. Dissolution Studies

To get a first idea about the later in vivo performance of the formulations, dissolution of the drug-loaded ASDs was studied in USP apparatus II using 500 mL of 0.1 M hydrochloric acid (HCl) as the dissolution medium. For comparison, dissolution of the unprocessed drug substances was studied in the same test setup.

Looking first at the results of the release studies with celecoxib, the ASD formulations based on EPO, Soluplus® and E-173 kDa showed the highest drug release of 90% after 120 min (Figure 6a,b). The ASD formulation prepared with Kollidon® VA 64 released 65% of the incorporated celecoxib dose during the same test period, while all other ASDs showed significantly ($p < 0.05$) lower celecoxib release after 120 min (Figure 6a,b).
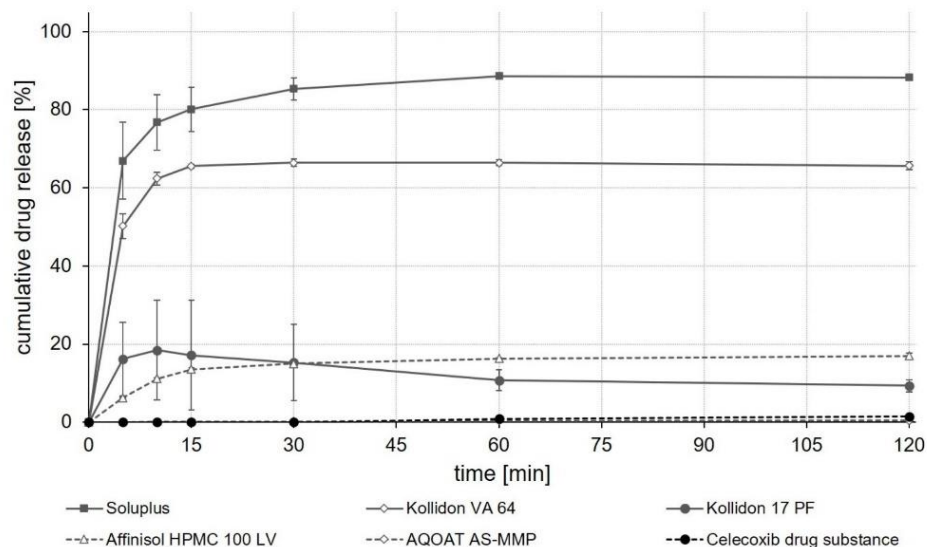
(**a**)

Figure 6. *Cont.*

(**b**)

Figure 6. Dissolution profiles of celecoxib drug substance and celecoxib ASDs based on ModE and EPO (**a**), as well as celecoxib drug substance and celecoxib ASDs based on other marketed (co-)polymers (**b**) in 500 mL 0.1 M HCl in USP apparatus II. Each value designates the mean $\pm$ S.D. (n = 3).

As with the celecoxib ASDs, the highest drug release was achieved when EPO, Soluplus® and E-173 kDa copolymers were used to prepare ASDs (Figure 7a,b). These ASDs released 80% to 85% of the incorporated efavirenz dose within 120 min. The Kollidon® VA 64-based ASD formulation showed, by contrast, a typical "spring and parachute" dissolution behavior, as the drug concentration in the medium started to slowly decrease again after a rapid release of about 55% of the efavirenz dose contained in the Kollidon® VA 64 ASD (Figure 7b).

In the case of fenofibrate, a significantly ($p < 0.05$) higher fenofibrate release was observed after a test duration of 120 min for the E-173 kDa ASD than for all other ASDs (Figure 8a). Whereas within the same test duration, without an apparent equilibrium already having been reached, about 30% of the incorporated fenofibrate dose was released from the E-173 kDa ASD, not more than 10% of the fenofibrate dose was released from all other ASDs (Figure 8a,b). In contrast to the ASDs prepared from Soluplus®, EPO and Affinisol® HPMC 100 LV—which showed pronounced supersaturation effects shortly after the start of the release experiment but also precipitation quickly after reaching the supersaturated state—no supersaturation occurred, but robust fenofibrate release was observed for the E-173 kDa formulation.

(**a**)

(**b**)
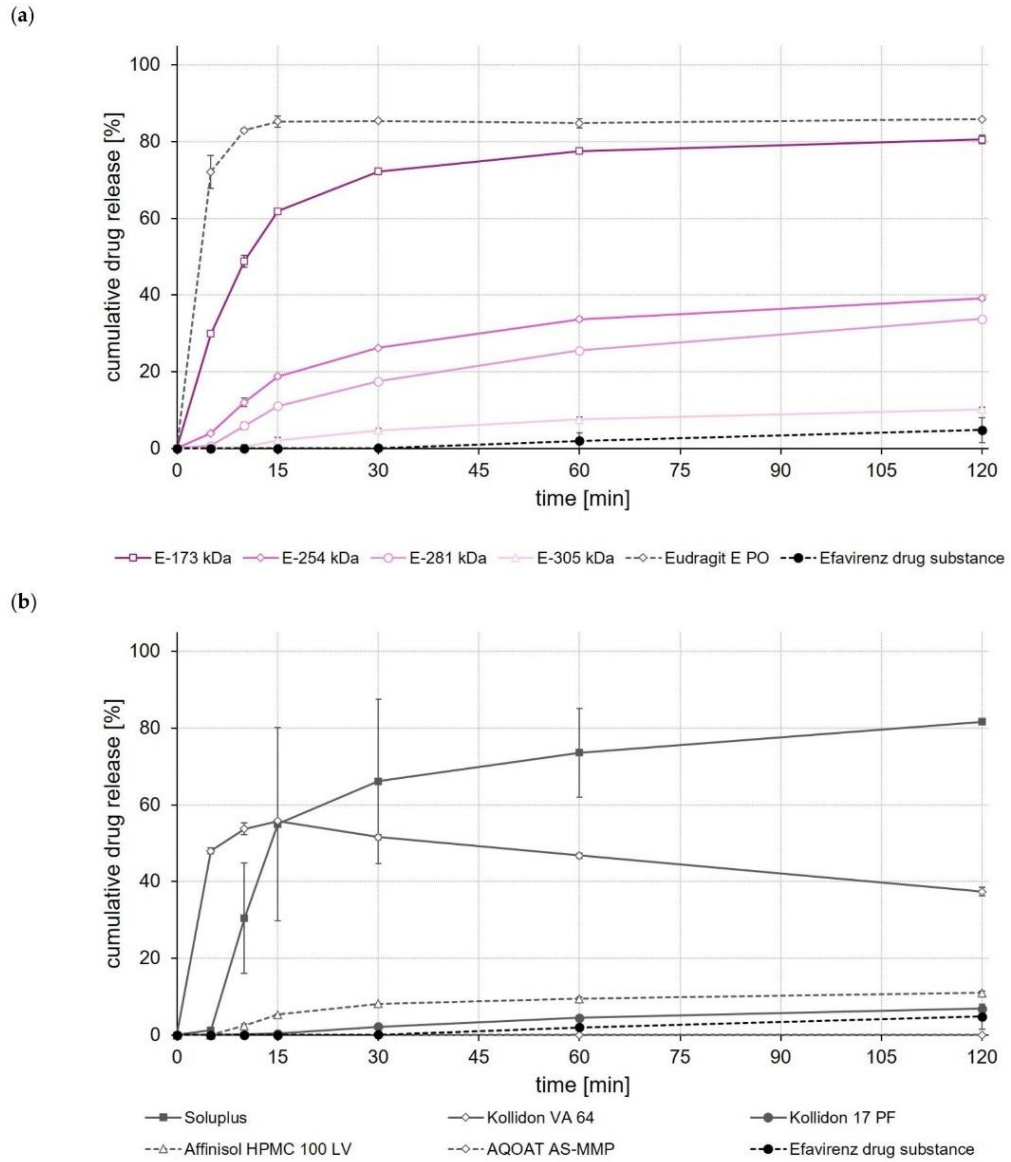
Figure 7. Dissolution profiles of efavirenz drug substance and efavirenz ASDs based on ModE and EPO (**a**), as well as efavirenz drug substance and efavirenz ASDs based on other marketed (co-)polymers (**b**) in 500 mL 0.1 M HCl in USP apparatus II. Each value designates the mean ± S.D. (n = 3).

86

(**a**)

(**b**)
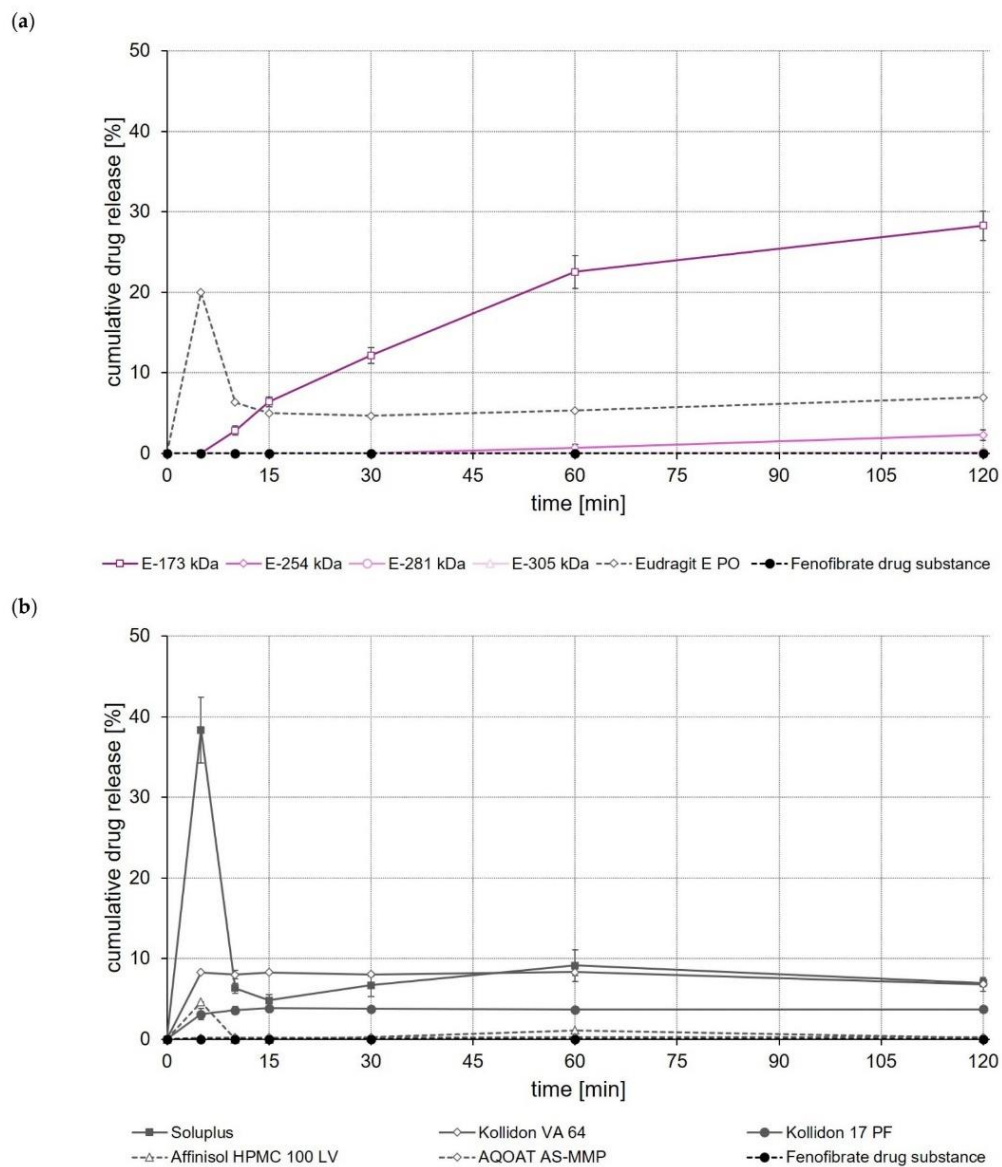
Figure 8. Dissolution profiles of fenofibrate drug substance and fenofibrate ASDs based on ModE and EPO (**a**), as well as fenofibrate drug substance and fenofibrate ASDs based on other marketed (co-)polymers (**b**) in 500 mL 0.1 M HCl in USP apparatus II. Each value designates the mean ± S.D. (n = 3).

When comparing the rate and extent of drug release of the ASDs prepared from different ModE types, the release of celecoxib, efavirenz, and fenofibrate was found to decrease with the higher M_w or higher T_g of the copolymer used (Figures 6a, 7a and 8a). An impact of the copolymers' M_w on celecoxib release (dissolution rate of the drug substance

was inversely proportional with M_w of the polymer used for ASD preparation) was also observed by Knopp et al. [29] using ASDs based on polyvinylpyrrolidone of different M_w. With decreasing M_w, the flexibility of a (co-)polymer usually increases while its viscosity decreases [29]. Both effects can make a positive contribution to the solubilization of a drug [29]. Results obtained in the present study suggest that the higher flexibility of the polymer chains in the E-173 kDa copolymer resulted in a good solubilization of the drugs. Overall, the E-173 kDa copolymer proved to be the most promising candidate for improving the solubility of poorly water-soluble drugs of all the (co-)polymers studied. In the case of celecoxib and efavirenz, approximately equal amounts of the drug (~80–90% of the total dose) were released from the E-173 kDa-, EPO-, and Soluplus®-based ASDs at the end of the experiment. However, in the case of fenofibrate, only the E-173 kDa formulation released a significant amount of the drug (~30% of the dose), while the other formulations released no more than 10% of the fenofibrate dose over the same time period; alternatively, in the case of the Soluplus® formulation, although 40% of the dose was released after 5 min, this resulted in precipitation due to supersaturation and therefore only less than 10% of the fenofibrate dose remained dissolved after 10 min. In addition to the reasons already mentioned, the observed differences in drug release from ASDs prepared from different ModE copolymers could be due to the fact that the protonation of the amino groups and thus the dissolution of the copolymers takes longer with increasing M_w, since longer polymer chains result in steric effects that could limit or impede access to the amino groups.

The results of this first set of screening experiments are quite promising. Since previous studies have shown that the drugs celecoxib, efavirenz, and fenofibrate exhibit pH-independent solubility [27,28], it could be assumed that the pH of the dissolution medium should not have a notable effect on the dissolution behavior of the drugs. For this initial set of dissolution experiments, 0.1 M HCl was selected to simulate pH conditions in the empty stomach at which all three model drugs would dissolve poorly but the new copolymers would dissolve. The addition of synthetic surfactants or bile salts, such as sodium lauryl sulfate or polyoxyethylene(20)sorbitan monooleate, as has been used in previous studies for screening drug release of enabling formulations celecoxib [29,30], fenofibrate [26,31,32] and efavirenz [23,24], was deliberately omitted in order to create worst-case conditions for the drugs under investigation and to be able to clearly map the effect of the polymers used to prepare the ASDs upon drug release. A comparison with data from the cited studies should not be made at this point because both the experimental conditions in the release studies and often also the drug loading of the formulations investigated were different.

3.12. Stability Studies

3.12.1. Visual Appearance

After three months of storage under defined and constant conditions (30 °C/65% RH), most ASD samples did not show any significant agglomeration and could easily be shaken up again. Only Kollidon® VA 64- and EPO-based ASDs were no longer easy to fluff up and, compared to all other ASDs, showed significantly larger agglomerates irrespective of the incorporated drug substance.

3.12.2. Thermal Characterization of ASD via DSC Analysis after Three Months of Storage

The applied storage conditions did not have any significant impact on the T_g of the pure (co-)polymers (Tables 6 and 8). Apart from Kollidon® VA 64 and EPO-based ASDs incorporating fenofibrate, after three months of storage, all ASD formulations were still amorphous. Fenofibrate loaded Kollidon® VA 64 and EPO-based ASDs demonstrated slight evidence of recrystallization of fenofibrate in the thermogram of the corresponding first heating cycle (data not shown here). The T_g of all stored ASDs was (slightly) impacted by the storage conditions (Figures S2–S7); however, except the two formulations mentioned, all others remained amorphous. The ASDs made of EPO showed low T_gs of 40 °C, 38 °C and 34 °C, which are close to the temperature conditions applied in the storage stability studies

(Table 8). These low T_gs may allow a better movement of the polymer chains, enabling a higher motility of the drug substance and, as particularly has been seen for fenofibrate, presenting with a higher risk of recrystallization, especially when formulations are stored at elevated temperatures. After three months of storage compared to the thermograms recorded immediately after the ASDs were manufactured, significantly lower T_gs (more than 10° C below the initial value) were observed for some of the ASDs, such as those made of celecoxib or fenofibrate and Kollidon® 17 PF (Figures S5b and S7b), efavirenz and Kollidon® VA 64, efavirenz or fenofibrate with AQOAT® AS-MMP (Figures S6b and S7b), as well as fenofibrate with E-305 kDa (Figure S7a) (Tables 6 and 8). By contrast, for some ASDs, such as those of efavirenz and Kollidon® 17 PF (Figure S6b), and efavirenz or fenofibrate and Affinisol® HPMC 100 LV (Figures S6b and S7b), T_gs were higher after three months of storage (Tables 6 and 8), indicating that at lower temperatures the mobility of the polymer chains was somewhat more restricted than before storage.

Table 8. Glass transition temperature (T_g) of ASDs incorporating celecoxib, efavirenz or fenofibrate after three months of storage. Each value designates the mean $\pm$ S.D. (n = 3).

Polymer	T_g (Polymer) [°C]	T_g (Celecoxib ASD) [°C]	T_g (Efavirenz ASD) [°C]	T_g (Fenofibrate ASD) [°C]
Soluplus®	70 ± 1	66 ± 2	65 ± 1	62 ± 3
Kollidon® VA 64	106 ± 0	99 ± 3	86 ± 2	92 ± 0
Kollidon® 17 PF	135 ± 2	88 ± 1	103 ± 0	78 ± 2
AQOAT® AS-MMP	111 ± 1	103 ± 2	84 ± 2	86 ± 2
E-173 kDa	78 ± 1	78 ± 3	74 ± 1	70 ± 1
E-254 kDa	84 ± 1	79 ± 2	77 ± 0	77 ± 0
E-281 kDa	89 ± 1	85 ± 1	82 ± 1	78 ± 3
E-305 kDa	91 ± 0	85 ± 2	80 ± 1	70 ± 1
Affinisol® HPMC 100 LV	103 ± 3	91 ± 1	98 ± 2	94 ± 2
EUDRAGIT® E PO	41 ± 1	40 ± 2	38 ± 2	34 ± 1

3.12.3. Dissolution Studies after Three Months of Storage

After three months of storage at 30 °C/65% RH, most of the ASDs showed slightly different dissolution performance (Figures 9–11).

With the exception of the EPO-based ASDs (Figure 9a) and Kollidon® VA 64 (Figure 9b) celecoxib, for which the amount of celecoxib released after a test duration of 120 min was significantly ($p < 0.05$) lower, after three months of storage, all other celecoxib ASDs (Figure 9a,b) showed approximately the same release behavior as immediately after manufacture. Similarly, after three months of storage, the EPO-based ASD formulation incorporating efavirenz (Figure 10a) after a test duration of 120 min revealed a significantly ($p < 0.05$) lower in vitro drug release than at the time of manufacture. In addition, the initial burst-like release of efavirenz observed within the first 10–15 min for Kollidon® VA 64 ASD (Figure 10b) immediately after preparation was not as pronounced after storage. However, all other ASDs containing efavirenz (Figure 10a,b) demonstrated similar dissolution behavior as at the time of manufacture. As already suspected from the visual appearance, as well as the results of the thermal analysis after three months of storage, the Kollidon® VA 64 (Figure 11b) and EPO-based (Figure 11a) ASDs showed a significantly ($p < 0.05$) lower drug release after the test period of 120 min. This may have resulted both from a reduction in the overall surface area of the formulation due to agglomeration, and from the storage-related tendency for recrystallization of fenofibrate in ASDs with the copolymers Kollidon® VA 64 and EPO. An influence of storage conditions on drug release was also observed for some other fenofibrate ASDs. In particular, supersaturation effects observed for some ASD formulations in the first minutes of the release experiments were no longer as pronounced as immediately after preparation. In contrast, the dissolution profile of the ASD prepared from the E-173 kDa copolymer (Figure 11a) remained almost unchanged and still indicated a significantly ($p < 0.05$) higher amount of fenofibrate released (28% of the

contained dose) than all other ASDs after an experimental period of 120 min (Figure 11b). Differences in T_gs of all other drug–(co-)polymer combinations before and after storage were much lower, i.e., less than 5 °C in all cases.

(**a**)

(**b**)
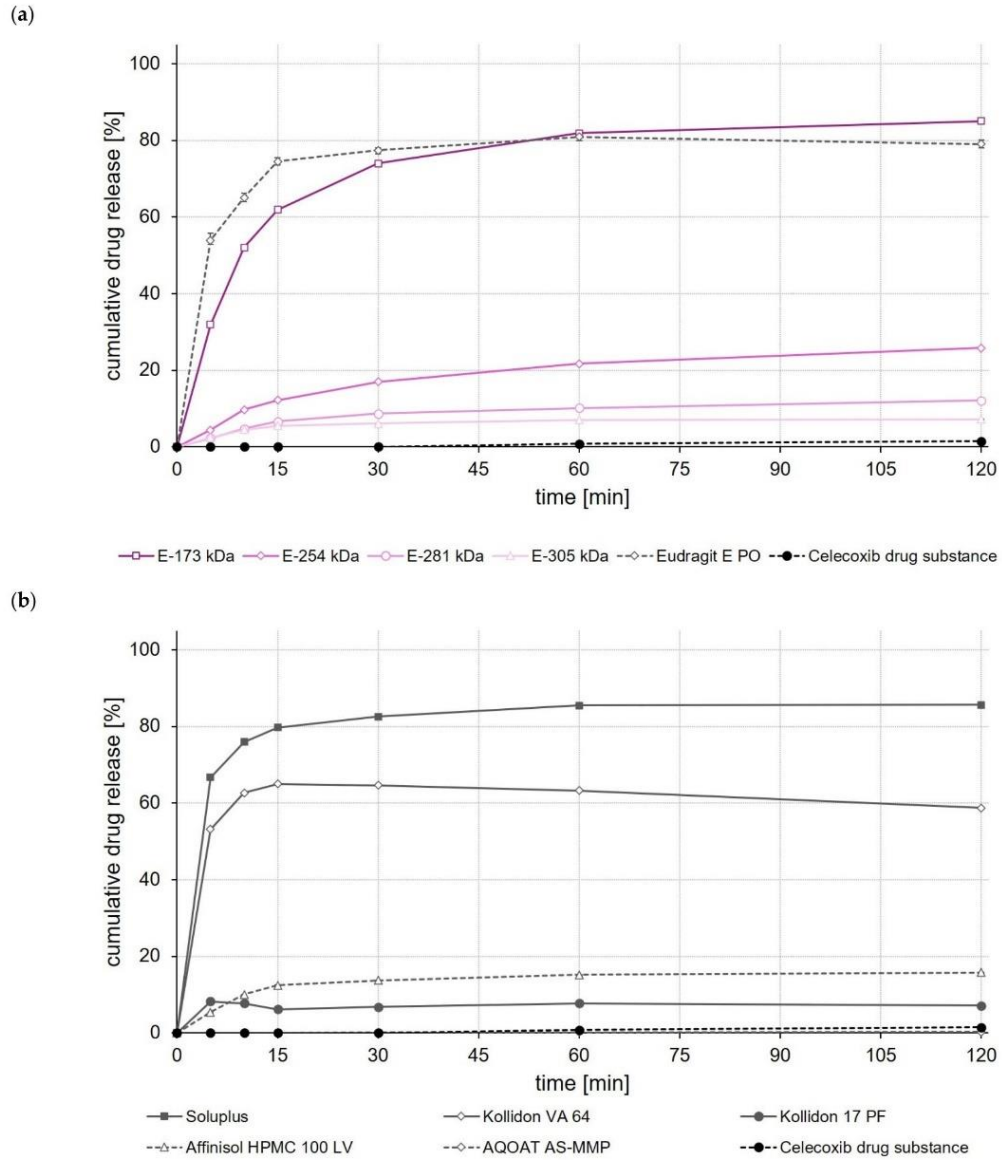
Figure 9. Dissolution profiles of celecoxib drug substance and celecoxib ASDs based on ModE and EPO (**a**), as well as celecoxib drug substance and celecoxib ASDs based on other marketed (co-)polymers (**b**) (after three months of storage at 30 °C/65% RH) in 500 mL 0.1 M HCl in USP apparatus II. Each value designates the mean ± S.D. (n = 3).

(**a**)

(**b**)
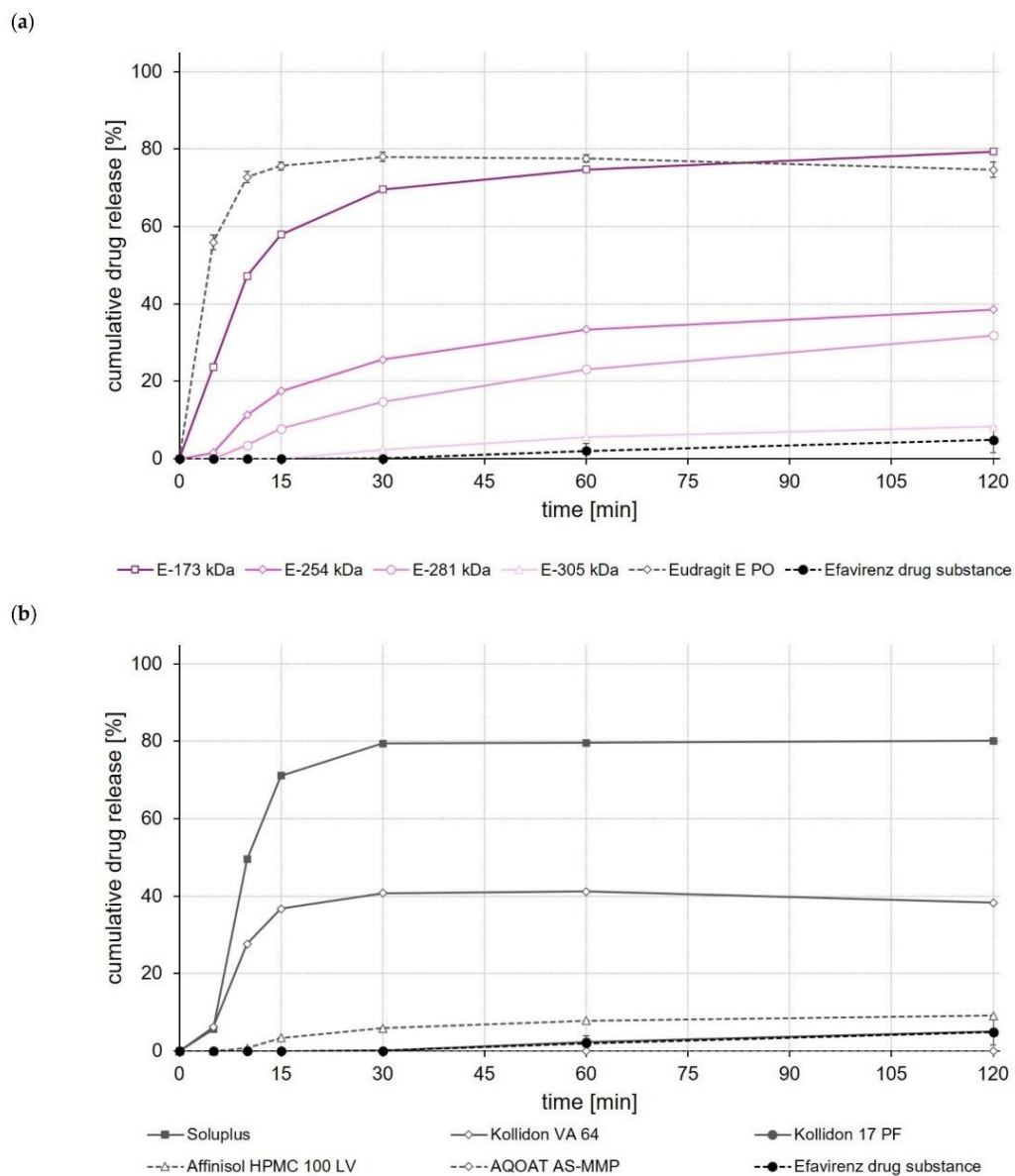
Figure 10. Dissolution profiles of efavirenz drug substance and efavirenz ASDs based on ModE and EPO (**a**), as well as efavirenz drug substance and efavirenz ASDs based on other marketed (co-)polymers (**b**) (after three months of storage at 30 °C/65% RH) in 500 mL 0.1 M HCl in USP apparatus II. Each value designates the mean ± S.D. (n = 3).

(**a**)

(**b**)
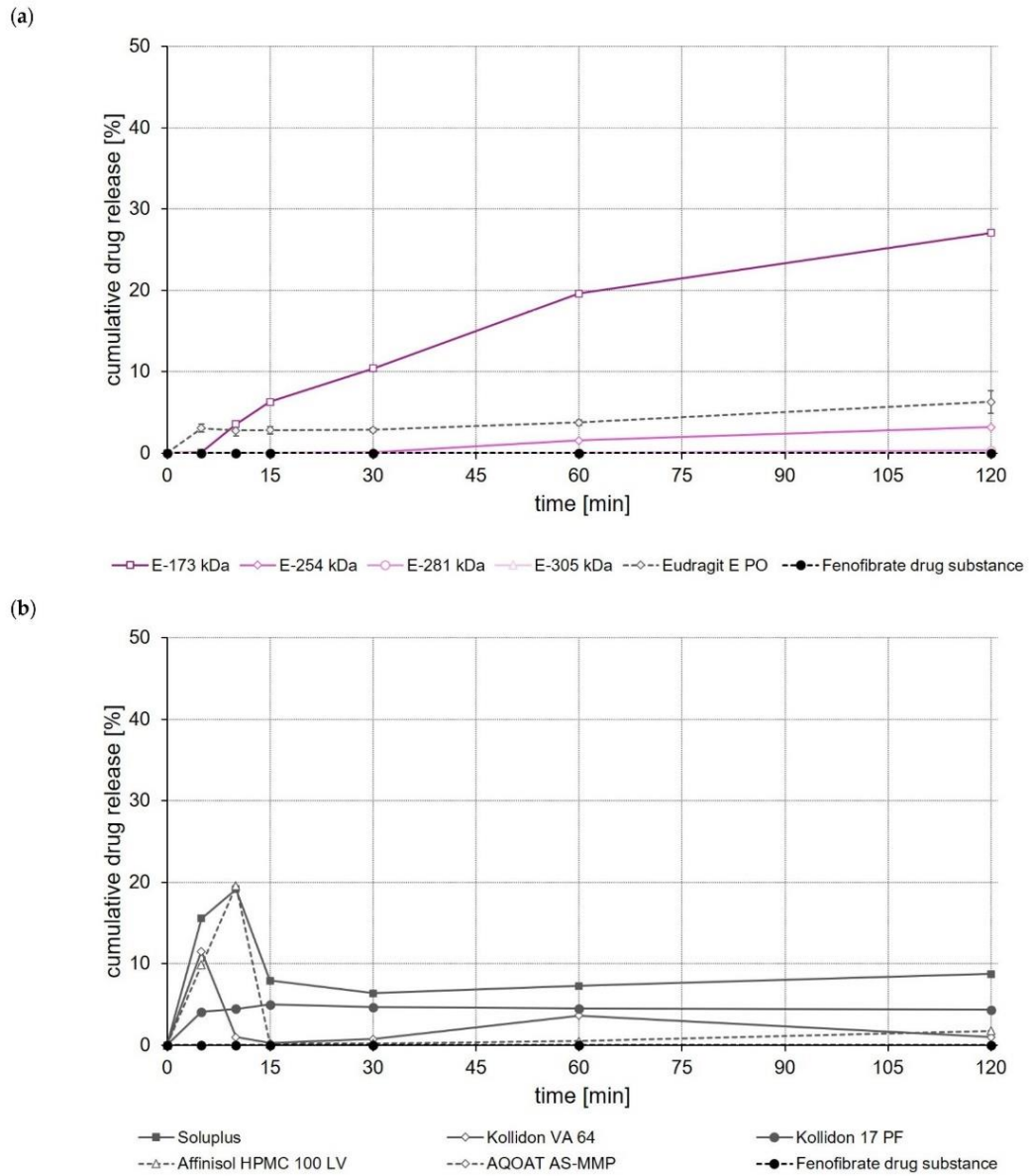
Figure 11. Dissolution profiles of fenofibrate drug substance and fenofibrate ASDs based on ModE and EPO (**a**), as well as fenofibrate drug substance and fenofibrate ASDs based on other marketed (co-)polymers (**b**) (after three months of storage at 30 °C/65% RH) in 500 mL 0.1 M HCl in USP apparatus II. Each value designates the mean ± S.D. (n = 3).

4. Conclusions

By means of radical polymerization using two specific radical initiators and n-dodecylmercaptan as CTA, a novel dimethylaminopropyl methacrylamide-butyl methacrylate-

methyl methacrylate copolymer (ModE) with different molecular weights was synthesized, characterized and investigated for its suitability to improve solubility and drug release of the poorly water-soluble model substances celecoxib, efavirenz and fenofibrate. For this purpose, drug-loaded ASDs were prepared with the new ModE copolymers, EPO, and several other polymers that have previously been successfully used for solubility enhancement. Based on the detailed investigation of the ASDs prepared from ModE copolymers, it can be concluded that M_w and T_g appear to have a significant impact on the drug release efficiency of poorly water-soluble drugs. The novel E-173 kDa copolymer proved to be the best candidate for improving the drug release of the chosen model drug substances. In a first set of stability experiments, ASDs prepared from this copolymer showed good storage stability, and were superior to ASDs prepared employing any other polymer used in the study with respect to the properties investigated here. Results from the present screening study therefore indicate the potential of the novel ModE copolymer for application in the field of solubility enhancement. Future studies will focus on employing several more poorly water-soluble drugs, including drugs with pH-dependent solubility, as well as increasing the drug load of the ASDs. Moreover, in vitro screening will also cover the use of biorelevant in vitro models that will allow for better estimation of the in vivo performance of the formulations.

Supplementary Materials: The following supporting information can be downloaded at: https://www.mdpi.com/article/10.3390/polym14071281/s1. Figure S1. Results from isothermal TGA of ModE copolymers at 150 °C (a) and 165 °C (b); Figure S2. DSC thermograms of celecoxib, ModE copolymers, EPO and the corresponding ASDs (a), and celecoxib and other marketed (co-)polymers used in the study, and the corresponding ASDs (b); Figure S3. DSC thermograms of efavirenz, ModE copolymers, EPO and the corresponding ASDs (a), and efavirenz and other marketed (co-)polymers used in the study, and the corresponding ASDs (b); Figure S4. DSC thermograms of fenofibrate, ModE copolymers, EPO and the corresponding ASDs (a), and fenofibrate and other marketed (co-)polymers used in the study, and the corresponding ASDs (b); Figure S5. DSC thermograms (after three months of storage at 30 °C/65% RH) of celecoxib, ModE copolymers, EPO and the corresponding ASDs (a), and celecoxib and other marketed (co-)polymers used in the study, and the corresponding ASDs (b); Figure S6. DSC thermograms (after three months of storage at 30 °C/65% RH) of efavirenz, ModE copolymers, EPO and the corresponding ASDs (a), and efavirenz and other marketed (co-)polymers used in the study, and the corresponding ASDs (b); Figure S7. DSC thermograms (after three months of storage at 30 °C/65% RH) of fenofibrate, ModE copolymers, EPO and the corresponding ASDs (a), and fenofibrate and other marketed (co-)polymers used in the study, and the corresponding ASDs (b).

Author Contributions: F.-P.S.: Methodology, Validation, Formal analysis, Investigation, Data Curation, Writing—Original Draft Preparation, Visualization. A.B.: Methodology, Formal analysis, Resources, Supervision, Project administration. C.M. (Christian Moers): Conceptualization, Methodology, Resources. C.M. (Christian Meier): Methodology, Investigation, Resources, Project administration. T.E.: Methodology, Resources, Project administration. S.K.: Writing—Review and Editing, Supervision, Project administration. All authors have read and agreed to the published version of the manuscript.

Institutional Review Board Statement: Not applicable.

Informed Consent Statement: Not applicable.

Data Availability Statement: Not applicable.

Conflicts of Interest: The authors declare no disclosure of potential conflict of interest.

References

1. Kalepu, S.; Nekkanti, V. Insoluble drug delivery strategies: Review of recent advances and business prospects. *Acta Pharm. Sin. B* **2015**, *5*, 442–453. [CrossRef] [PubMed]
2. Kamble, R.N.; Mehta, P.P.; Kumar, A. Efavirenz self-nano-emulsifying drug delivery system: In vitro and in vivo evaluation. *AAPS PharmSciTech* **2016**, *17*, 1240–1247. [CrossRef] [PubMed]
3. Kawabata, Y.; Wada, K.; Nakatani, M.; Yamada, S.; Onoue, S. Formulation design for poorly water-soluble drugs based on biopharmaceutics classification system: Basic approaches and practical applications. *Int. J. Pharm.* **2011**, *420*, 1–10. [CrossRef] [PubMed]
4. Raina, S.A.; Zhang, G.G.; Alonzo, D.E.; Wu, J.; Zhu, D.; Catron, N.D.; Gao, Y.; Taylor, L.S. Enhancements and limits in drug membrane transport using supersaturated solutions of poorly water soluble drugs. *J. Pharm. Sci.* **2014**, *103*, 2736–2748. [CrossRef]
5. Ullrich, A.; Schiffter, H.A. The influence of polymer excipients on the dissolution and recrystallization behavior of ketoconazole: Application, variation and practical aspects of a pH shift method. *Eur. J. Pharm. Biopharm.* **2018**, *133*, 20–30. [CrossRef]
6. Lipinski, C.A. Drug-like properties and the causes of poor solubility and poor permeability. *J. Pharmcol. Toxicol. Methods* **2000**, *44*, 235–249. [CrossRef]
7. Ueda, K.; Higashi, K.; Yamamoto, K.; Moribe, K. The effect of HPMCAS functional groups on drug crystallization from the supersaturated state and dissolution improvement. *Int. J. Pharm.* **2014**, *464*, 205–213. [CrossRef]
8. Williams, H.D.; Trevaskis, N.L.; Charman, S.A.; Shanker, R.M.; Charman, W.N.; Pouton, C.W.; Porter, C.J. Strategies to address low drug solubility in discovery and development. *Pharmacol. Rev.* **2013**, *65*, 315–499. [CrossRef]
9. Wyttenbach, N.; Janas, C.; Siam, M.; Lauer, M.E.; Jacob, L.; Scheubel, E.; Page, S. Miniaturized screening of polymers for amorphous drug stabilization (SPADS): Rapid assessment of solid dispersion systems. *Eur. J. Pharm. Biopharm.* **2013**, *84*, 583–598. [CrossRef]
10. Wegiel, L.A.; Mauer, L.J.; Edgar, K.J.; Taylor, L.S. Crystallization of amorphous solid dispersions of resveratrol during preparation and storage-Impact of different polymers. *J. Pharm. Sci.* **2013**, *102*, 171–184. [CrossRef]
11. Song, Y.; Zemlyanov, D.; Chen, X.; Su, Z.; Nie, H.; Lubach, J.W. Acid-base interactions in amorphous solid dispersions of lumefantrine prepared by spray-drying and hot-melt extrusion using X-ray photoelectron spectroscopy. *Int. J. Pharm.* **2016**, *514*, 456–464. [CrossRef] [PubMed]
12. Lin, X.; Su, L.; Li, N.; Hu, Y.; Tang, G.; Liu, L. Understanding the mechanism of dissolution enhancement for poorly water-soluble drugs by solid dispersions containing Eudragit. *J. Drug Deliv. Sci. Technol.* **2018**, *48*, 328–337. [CrossRef]
13. Calahan, J.L.; Zanon, R.L.; Alvarez-Nunez, F.; Munson, E.J. Isothermal microcalorimetry to investigate the phase separation for amorphous solid dispersions of AMG 517 with HPMC-AS. *Mol. Pharm.* **2013**, *10*, 1949–1957. [CrossRef] [PubMed]
14. Park, J.; Baek, M.J.; Choi, H.W.; Kim, H.S.; Lee, D.W. Development of poly(methyl methacrylate)-based copolymers with improved heat resistance and reduced moisture absorption. *Langmuir* **2019**, *35*, 15880–15886. [CrossRef]
15. Al-Odayni, A.B.; Saeed, W.S.; Ahmed, A.Y.B.H.; Alrahlah, A.; Al-Kahtani, A.; Aouak, T. New monomer based on eugenol methacrylate, synthesis, polymerization and copolymerization with methyl methacrylate-Characterization and thermal properties. *Polymers* **2020**, *12*, 160. [CrossRef]
16. Liang, C.; Wang, B.; Chen, J.; Huang, Y.; Fang, T.; Wang, Y.; Liao, B. The effect of acrylamides copolymers on the stability and rheological properties of yellow iron oxide dispersion. *Colloids Surf. A Physicochem. Eng. Asp.* **2017**, *513*, 136–145. [CrossRef]
17. Harrisson, S. The chain length distribution of an ideal reversible deactivation radical polymerization. *Polymers* **2018**, *10*, 887. [CrossRef]
18. Liao, J.; Peng, B.; Tan, S.; Tian, X.; Zhang, Z. Grafting PMMA onto P(VDF-TrFE) by C-F activation via a Cu(0) mediated controlled radical polymerization process. *Macromol. Rapid Commun.* **2020**, *41*, 1–5. [CrossRef]
19. Affinisol HPMC HME. Available online: https://www.pharma.dupont.com/content/dam/dupont/amer/us/en/nutrition-health/general/pharmaceuticals/documents/Download_Affinisol%20HPMC%20HME%20Brochure.pdf (accessed on 15 March 2022).
20. Hot Melt Extrusion with BASF Pharma Polymers. Available online: https://pharmaceutical.basf.com/global/images/03_120803_hot_melt_extrusion_with_basf_pharma_polymers.pdf (accessed on 15 March 2022).
21. Moseson, D.E.; Jordan, M.A.; Shah, D.D.; Corum, I.D.; Alvarenga, B.R., Jr.; Taylor, L.S. Application and limitations of thermo-gravimetric analysis to delineate the hot melt extrusion chemical stability processing window. *Int. J. Pharm.* **2020**, *590*, 119916. [CrossRef]
22. Hanada, M.; Jermain, S.V.; Williams, R.O., III. Enhanced dissolution of a porous carrier-containing ternary amorphous solid dispersion system prepared by a hot melt method. *J. Pharm. Sci.* **2018**, *107*, 362–371. [CrossRef]
23. Pawar, J.; Suryawanshi, D.; Moravkar, K.; Aware, R.; Shetty, V.; Maniruzzaman, M. Study the influence of formulation process parameters on solubility and dissolution enhancement of efavirenz solid solutions prepared by hot-melt extrusion: A QbD methodology. *Drug Deliv. Transl. Res.* **2018**, *8*, 1644–1657. [CrossRef] [PubMed]
24. Pawar, J.; Tayade, A.; Gangurde, A.; Moravkar, K.; Amin, P. Solubility and dissolution enhancement of efavirenz hot melt extruded amorphous solid dispersions using combination of polymeric blends: A QbD approach. *Eur. J. Pharm. Sci.* **2016**, *88*, 37–49. [CrossRef]
25. Silva, L.A.D.; Almeida, S.L.; Alonso, E.C.; Rocha, P.B.; Martins, F.T.; Freitas, L.A.; Taveira, S.F.; Cunha-Filho, M.S.; Marreto, R.N. Preparation of a solid self-microemulsifying drug delivery system by hot-melt extrusion. *Int. J. Pharm.* **2018**, *541*, 1–10. [CrossRef]

26. Wen, T.; Niu, B.; Wu, Q.; Zhou, Y.; Pan, X.; Quan, G.; Wu, C. Fenofibrate solid dispersion processed by hot-melt extrusion: Elevated bioavailability and its cell transport mechanism. *Curr. Drug Deliv.* **2019**, *16*, 538–547. [CrossRef] [PubMed]

27. Cristofoletti, R.; Nair, A.; Abrahamsson, B.; Groot, D.W.; Kopp, S.; Langguth, P.; Polli, J.E.; Shah, V.P.; Dressman, J.B. Biowaiver monographs for immediate release solid oral dosage forms: Efavirenz. *J. Pharm. Sci.* **2013**, *102*, 318–329. [CrossRef] [PubMed]

28. Schmied, F.P.; Bernhardt, A.; Engel, A.; Klein, S. A customized screening tool approach for the development of a self-nanoemulsifying drug delivery system (SNEDDS). *AAPS PharmSciTech* **2022**, *23*, 39. [CrossRef] [PubMed]

29. Knopp, M.M.; Nguyen, J.H.; Becker, C.; Francke, N.M.; Jørgensen, E.B.; Holm, P.; Holm, R.; Mu, H.; Rades, T.; Langguth, P. Influence of polymer molecular weight on in vitro dissolution behavior and in vivo performance of celecoxib: PVP amorphous solid dispersions. *Eur. J. Pharm. Biopharm.* **2016**, *101*, 145–151. [CrossRef]

30. Homayouni, A.; Sadeghi, F.; Nokhodchi, A.; Varshosaz, J.; Garekani, H.A. Preparation and characterization of celecoxib solid dispersions; Comparison of poloxamer-188 and PVP-K30 as carriers. *Iran. J. Basic Med. Sci.* **2014**, *17*, 322–331.

31. Kawakami, K.; Sato, K.; Fukushima, M.; Miyazaki, A.; Yamamura, Y.; Sakuma, S. Phase separation of supersaturated solution created from amorphous solid dispersions: Relevance to oral absorption. *Eur. J. Pharm. Biopharm.* **2018**, *132*, 146–156. [CrossRef]

32. Nguyen, C.N.; Pham, C.V.; Le Thien, G.; Ngoc, B.T.; Le Thi, H.; Huyen, C.P.T.; Thi, T.N. Immediate-released pelletized solid dispersion containing fenofibrate: Formulation, in vitro characterization, and bioequivalence studies in experimental beagle dogs. *Int. J. Pharm.* **2019**, *570*, 118661. [CrossRef]

Supplementary materials

A Novel Aminomethacrylate-Based Copolymer for Solubility Enhancement—From Radical Polymer Synthesis to Manufacture and Characterization of Amorphous Solid Dispersions

Fabian-Pascal Schmied [1,2], **Alexander Bernhardt** [2], **Christian Moers** [2], **Christian Meier** [3], **Thomas Endres** [2] **and Sandra Klein** [1,*]

[1] University of Greifswald, Department of Pharmacy, Institute of Biopharmaceutics and Pharmaceutical Technology, Felix-Hausdorff-Straße 3, 17489 Greifswald, Germany; fabian-pascal.schmied@stud.uni-greifswald.de (F.-P.S.); sandra.klein@uni-greifswald.de (S.K.)

[2] Evonik Operations GmbH, Research, Development & Innovation, Kirschenallee, 64293 Darmstadt, Germany; fabian-pascal.schmied@evonik.com (F.-P.S.); alexander.bernhardt@evonik.com (A.B.); christian.moers@evonik.com (C.M.); thomas.endres@evonik.com (T.E.)

[3] Evonik Operations GmbH, Research, Development & Innovation, Rodenbacher Chaussee 4, 63457 Hanau, Germany; christian.meier@evonik.com (C.M.)

[*] Correspondence: sandra.klein@uni-greifswald.de; Tel.: +49-3834-420-4897
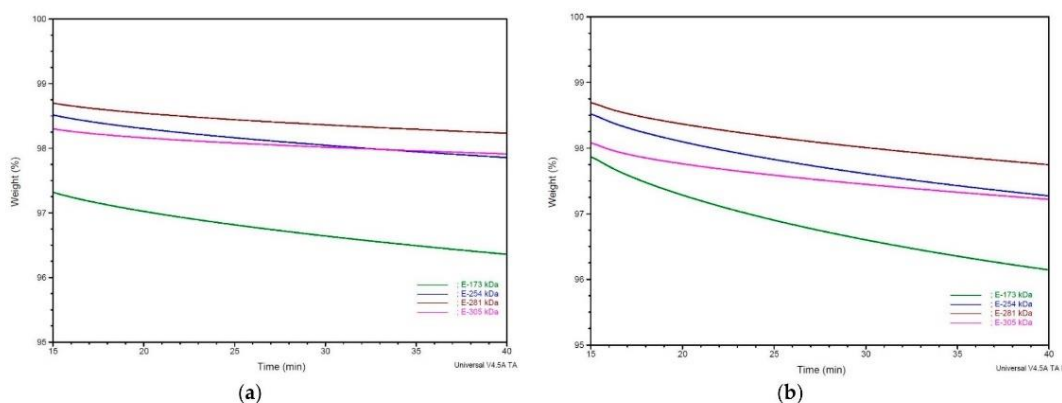
Figure S1. Results from isothermal TGA of ModE copolymers at 150 °C (**a**) and 165 °C (**b**).

(a)

(b)

Figure S2. DSC thermograms of celecoxib, ModE copolymers, EPO and the corresponding ASDs (**a**), and celecoxib and other marketed (co-)polymers used in the study, and the corresponding ASDs (**b**).

Figure S3. DSC thermograms of efavirenz, ModE copolymers, EPO and the corresponding ASDs (**a**), and efavirenz and other marketed (co-)polymers used in the study, and the corresponding ASDs (**b**).

(a)

(b)

Figure S4. DSC thermograms of fenofibrate, ModE copolymers, EPO and the corresponding ASDs (**a**), and fenofibrate and other marketed (co-)polymers used in the study, and the corresponding ASDs (**b**).

(**a**)

(**b**)

Figure S5. DSC thermograms (after three months of storage at 30 °C/65% RH) of celecoxib, ModE copolymers, EPO and the corresponding ASDs (**a**), and celecoxib and other marketed (co-)polymers used in the study, and the corresponding ASDs (**b**);.

(a)

(b)

Figure S6. DSC thermograms (after three months of storage at 30 °C/65% RH) of efavirenz, ModE copolymers, EPO and the corresponding ASDs (**a**), and efavirenz and other marketed (co-)polymers used in the study, and the corresponding ASDs (**b**).

(**a**)

(**b**)

Figure S7. DSC thermograms (after three months of storage at 30 °C/65% RH) of fenofibrate, ModE copolymers, EPO and the corresponding ASDs (**a**), and fenofibrate and other marketed (co-)polymers used in the study, and the corresponding ASDs (**b**).

6.4 Preparation of solid self-nanoemulsifying drug delivery systems (S-SNEDDS) by co-extrusion of liquid SNEDDS and polymeric carriers – a new and promising approach to improve the solubility of poorly water-soluble drugs*

(*Pharmaceuticals*, 2022, 15(9): 1135)

This final part of the work focused on establishing a new formulation approach to enhance the solubility of poorly water-soluble drugs. Drug-loaded S-SNEDDS formulations were successfully prepared applying a HME process, more precisely, a co-extrusion of different polymeric carriers in combination with L-SNEDDS, which had been developed in a preceding study. Maintaining or even improving the rapid and complete drug release behavior of the corresponding celecoxib, efavirenz or fenofibrate loaded L-SNEDDS was one of the major objectives for the development of S-SNEDDS via HME processing. A selection of (co-)polymers was evaluated for their suitability regarding co-extrusion with L-SNEDDS using HME technology. Individual HME process parameters were determined for the different (co-)polymers used depending on their material properties and melting behavior. S-SNEDDS were prepared via HME using a number of marketed (co-)polymers as well as the different variants of ModE copolymer and were analyzed regarding their *in vitro* drug release performance and storage stability. Stable drug-loaded S-SNEDDS, which showed a good drug release performance in an acidic dissolution medium (pH 1) were obtained considering some different (co-)polymer variants. In particular, the drug-loaded S-SNEDDS formulation using the recently developed aminomethacrylate-based copolymer "ModE" with a M_w of 173 kDa revealed high drug releases for the drug substances celecoxib, efavirenz and fenofibrate. Still largely unexplored, the novel concept for the preparation of drug-loaded S-SNEDDS formulations via HME proved its high potential for a growing technology platform and will be certainly refined by future experiments.

Own contributions:
Development of the scientific concept, performance of the laboratory experiments and the calculations, preparation of the manuscript

Alexander Bernhardt:
Contribution in the development of the scientific concept

Prof. Dr. Sandra Klein:
Contribution in the development of the scientific concept, revision of the manuscript

_____   _____

Fabian-Pascal Schmied   Prof. Dr. Sandra Klein

Article

Preparation of Solid Self-Nanoemulsifying Drug Delivery Systems (S-SNEDDS) by Co-Extrusion of Liquid SNEDDS and Polymeric Carriers—A New and Promising Formulation Approach to Improve the Solubility of Poorly Water-Soluble Drugs

Fabian-Pascal Schmied [1,2], **Alexander Bernhardt** [2] **and Sandra Klein** [1,*]

[1] Institute of Biopharmaceutics and Pharmaceutical Technology, Department of Pharmacy, University of Greifswald, Felix-Hausdorff-Straße 3, 17489 Greifswald, Germany
[2] Research, Development & Innovation, Evonik Operations GmbH, Kirschenallee, 64293 Darmstadt, Germany
[*] Correspondence: sandra.klein@uni-greifswald.de; Tel.: +49-3834-420-4897

Abstract: The present study focused on a new formulation approach to improving the solubility of drugs with poor aqueous solubility. A hot melt extrusion (HME) process was applied to prepare drug-loaded solid self-nanoemulsifying drug delivery systems (S-SNEDDS) by co-extrusion of liquid SNEDDS (L-SNEDDS) and different polymeric carriers. Experiments were performed with L-SNEDDS formulations containing celecoxib, efavirenz or fenofibrate as model drugs. A major objective was to identify a polymeric carrier and process parameters that would enable the preparation of stable S-SNEDDS without impairing the release behavior and storage stability of the L-SNEDDS used and, if possible, even improving them further. In addition to commercially available (co)polymers already used in the field of HME, a particular focus was on the evaluation of different variants of a recently developed aminomethacrylate-based copolymer (ModE) that differed in M_w. Immediately after preparation, the L-SNEDDS and S-SNEDDS formulations were tested for amorphicity by differential scanning calorimetry. Furthermore, solubility and dissolution tests were performed. In addition, the storage stability was investigated at 30 °C/65% RH over a period of three and six months, respectively. In all cases, amorphous formulations were obtained and, especially for the model drug celecoxib, S-SNEDDS were developed that maintained the rapid and complete drug release of the underlying L-SNEDDS even over an extended storage period. Overall, the data obtained in this study suggest that the presented S-SNEDDS approach is very promising, provided that drug-loaded L-SNEDDS are co-processed with a suitable polymeric carrier. In the case of celecoxib, the E-173 variant of the novel ModE copolymer proved to be a novel polymeric carrier with great potential for application in S-SNEDDS. The presented approach will, therefore, be pursued in future studies to establish S-SNEDDS as an alternative formulation to other amorphous systems.

Keywords: copolymer; amorphous formulations; poorly soluble drug; drug release; hot melt extrusion; nanoemulsion; celecoxib; fenofibrate; efavirenz

1. Introduction

Poor water solubility is one of the most important reasons for the limited and variable oral bioavailability of drugs [1]. While about 40% of orally administered drugs currently on the market are affected by poor water solubility, this problem is increasing significantly for newer drugs. Among drugs under development, an estimated 75% of

drug substances suffer from poor aqueous solubility [2]. Moreover, this proportion is expected to increase further in the future. This clearly demonstrates the importance of developing effective strategies to improve drug solubility when aiming to develop safe and effective oral drug products.

In recent decades, several formulation strategies have been developed that can increase the apparent solubility of poorly water-soluble drugs in gastrointestinal fluids and, provided they are drugs that can readily permeate the intestinal mucosa, also enhance oral bioavailability [3]. The individual formulation approaches used can be very different and usually are directed by the properties of the drug substance to be formulated. For lipophilic drugs, the development of lipid-based drug delivery systems (LBDDS) represents a valuable means of addressing solubility and bioavailability issues. In particular, self-nanoemulsifying drug delivery systems (SNEDDS), which are multicomponent systems containing a lipophilic drug in a mixture of an oil or a lipid and a surfactant or a mixture of surfactants and, optionally also a co-solvent, represent an interesting option to improve the limited water solubility of drugs [4–6]. When in contact with gastrointestinal fluids and under the influence of digestive, gastrointestinal motility, SNEDDS spontaneously form transparent nanoemulsions in which the formulated drug is solubilized [7]. The formulations commonly known as SNEDDS are usually liquid formulations, which are also known as Liquid-SNEDDS (L-SNEDDS). L-SNEDDS allow high loading with poorly water-soluble drugs and can be prepared rather quickly and by simple means. However, the fact that they are liquid formulations also presents some disadvantages [5,8]. To obtain administrable dosage forms, L-SNEDDS usually require cost-intensive processing into soft capsules, as can be seen in the example of Neoral® or Fortovase® [8,9]. However, this formulation step does not always guarantee a stable dosage form, as L-SNEDDS can interact with and, in the worst case, even leak out of the capsule shell [4,10,11]. In addition, drug precipitation can occur during storage for a variety of reasons. The development of an innovative solid dosage form that preserves the advantages of the L-SNEDDS formulation, but eliminates its disadvantages as much as possible, could hence be beneficial [8,10,12]. Various commonly described manufacturing technologies, such as adsorption to a solid carrier, wet granulation, spray drying, freeze drying, and supercritical fluid processes, can be used to convert L-SNEDDS into Solid-SNEDDS (S-SNEDDS) [4,8,13]. At present, the most common formulation approach currently used to produce S-SNEDDS is the adsorption of L-SNEDDS to a solid carrier [13,14].

Hot melt extrusion (HME) may be another option for S-SNEDDS production [10]. HME is a process that in the pharmaceutical industry has been used for quite some time, mainly for producing solid amorphous dispersions (ASDs) [15,16]. The process is solvent-free, easy to scale up, and can be used for continuous production. Since it is also less time-consuming than many of the other technologies used for S-SNEDDS preparation, it represents an interesting alternative for the development of S-SNEDDS. To date, HME has not been studied for the purpose of S-SNEDDS production. However, very recently first attempts to utilize this technology in the preparation of solid self-microemulsifying drug delivery systems (S-SMEDDS) were reported [10].

A successful HME process requires the input of both thermal and mechanical energy. To enable the conversion of the solid polymeric material into a flowable melt, a process temperature above the glass transition temperature (T_g) of the respective polymer(s) is required. Due to the thermal input when aiming to formulate S-SNEDDS via HME, the process temperature might be an essential parameter. It will need to be kept below the decomposition temperatures of the individual components in order to prevent changes in material properties, the formation of toxic by-products and the possible loss of active ingredients. In addition to this, the HME of a multicomponent system containing solid and liquid components can be challenging because premature leakage of the liquid components from the matrix during the HME process must be avoided to ensure the correct mixing ratio of the individual components and their uniform distribution in the

final solid product. For the polymeric material used in the HME process, in addition to T_g [17–19], molecular weight (M_w) [17,20], absorption and binding capacity for oily formulations (e.g., L-SNEDDS), solubilizing capacity [18], decomposition temperature, flexibility, hardness, and brittleness may be important.

The present study aimed to develop drug-loaded S-SNEDDS by the co-extrusion of L-SNEDDS and a polymeric carrier using an HME process. Experiments were performed with celecoxib-, efavirenz-, and fenofibrate L-SNEDDS formulations established in earlier studies [21]. A further objective was to identify a (co)polymer that would enable the preparation of stable S-SNEDDS without impairing the release behavior and storage stability of the L-SNEDDS used and, if possible, even improve them further. In addition to commercially available (co)polymers already used in the field of HME, a particular focus was on the evaluation of different variants of a recently developed aminomethacrylate-based copolymer that differed in M_w [22].

2. Results and Discussion

2.1. L-SNEDDS Composition

The qualitative and quantitative composition of celecoxib-, efavirenz-, and fenofibrate L-SNEDDS formulations prepared by applying the screening approach developed in a preceding study [21] is shown in Table 1. With 25%, particularly for the efavirenz L-SNEDDS, a high drug load was obtained. Drug loads for the celecoxib- and the fenofibrate L-SNEDDS were 17% and 14%, respectively.

Table 1. Composition of Liquid-SNEDDS (L-SNEDDS) incorporating celecoxib, efavirenz or fenofibrate.

Drug Substance	Miglyol® 812 (%)	Tween® 80 (%)	Gelucire® 44/14 (%)	d-TPGS (%)	IPM-100 (%)	Transcutol® HP (%)	Brij® 35 (%)	Drug (%)
Celecoxib	27.64	45.52	4.15	5.69	-	-	-	17.00
Efavirenz	-	23.94	-	2.99	19.45	28.42	-	25.20
Fenofibrate	17.20	50.16	-	10.04	-	-	8.60	14.00

All L-SNEDDS formulations shown in Table 1 provided good emulsification properties resulting in small droplet sizes and a narrow PDI (celecoxib L-SNEDDS: 24.4 ± 0.2 nm, 0.11 ± 0.01 [21], efavirenz L-SNEDDS: 36.7 ± 0.3 nm, 0.08 ± 0 and fenofibrate L-SNEDDS: 18.6 ± 0.3 nm, 0.06 ± 0.01 [21]) and thus were selected for subsequent HME processing.

2.2. S-SNEDDS Composition and Manufacture

After preparation and characterization of the different L-SNEDDS formulations (Table 1), a variety of S-SNEDDS formulations was prepared from each of the L-SNEDDS formulations and marketed (co)polymers commonly used in the field of solubility enhancement, as well as the different novel ModE copolymer types, referred to as E-173 kDa, E-254 kDa, E-281 kDa, and E-305 kDa according to their average molecular weight. Table 2 shows the L-SNEDDS and drug loads of the individual S-SNEDDS formulations, as well as the process parameters (extrusion temperature, screw speed, and torque) used for their preparation. The extrusion temperature, as well as the screw speed, were chosen individually for each (co)polymer–L-SNEDDS combination based on its melt viscosity when subjected to mechanical and thermal input in the HME process. The torque was recorded during HME for each composition and increased with higher melt viscosities. When selecting suitable extrusion parameters, care was taken to ensure that these resulted in torque values that did not exceed 200 Ncm. Torque values > 200 Ncm typically correlated with a pronounced melt viscosity, which could complicate the processing by clogging the extruder die. Compared to a previous study in which drug-loaded ASDs were prepared and in which the same active ingredients and similar amounts of active

ingredients were used [22], S-SNEDDS could be prepared at lower extrusion temperatures than the corresponding ASDs due to the plasticizing effect of the incorporated L-SNEDDS. This facilitated overall processing and resulted in substantially lower torque values than in the preceding study [22].

Table 2. Composition and hot melt extrusion process parameters of Solid-SNEDDS (S-SNEDDS) incorporating celecoxib/efavirenz/fenofibrate.

Polymer	L-SNEDDS Load (%)	Drug Load (%)	Extrusion Temperature (°C)	Screw Speed (rpm)	Torque (Ncm)
Soluplus®	20/16.67/20	3.4/4.2/2.8	130/130/130	200	50/40/45
Kollidon® VA 64	30/25/30	5.1/6.3/4.2	150/150/150	200	45/45/35
Kollidon® 17 PF	30/25/30	5.1/6.3/4.2	170/170/170	200	40/40/35
E-173 kDa	30/25/30	5.1/6.3/4.2	150/150/150	200	75/65/50
E-254 kDa	30/25/30	5.1/6.3/4.2	150/150/155	200	75/70/70
E-281 kDa	30/25/30	5.1/6.3/4.2	155/155/150	200	70/65/75
E-305 kDa	30/25/30	5.1/6.3/4.2	155/155/155	200	60/90/85
Affinisol® HPMC 100 LV	30/25/30	5.1/6.3/4.2	160/160/160	100	85/120/95

Affinisol® HPMC 100 LV was extruded at a lower screw speed than all other (co)polymers, as it would otherwise have clogged the extruder die or led to a loss of the integrity of the polymer when further increasing the extrusion temperature. Individual extrusion temperatures were used for each L-SNEDDS (co)polymer combination, while all extrusion temperatures were in the range of reported extrusion temperatures of the corresponding polymers [2,10,15,16,23].

In order to enable a good comparison of formulations, the same L-SNEDDS load and drug content was targeted for each individual S-SNEDDS formulation. Except for the Soluplus®-based S-SNEDDS, this could be realized, whereas for reasons of processability, a slightly lower L-SNEDDS load had to be applied when working with Soluplus®. When co-processed with the Soluplus® copolymer, an L-SNEDDS load of higher than 20% (celecoxib and fenofibrate) or 16.67% (efavirenz) did not provide a solid strand. Reasons for these limitations could be the lower T_g of Soluplus® compared to all other (co)polymers processed by HME in this study, as well as a possibly insufficient binding capacity for oily formulations. However, since the manufacture of S-SNEDDS via HME is largely unexplored, this can only be speculated since data for comparing the process parameters as well as the properties of obtained S-SNEDDS is lacking.

2.3. Thermal Characterization of the Pure Drugs, (Co)Polymers, and S-SNEDDS via DSC Analysis

Immediately after processing, the thermal characterization of celecoxib- (Figure S1a,b), efavirenz- (Figure S2a,b), and fenofibrate S-SNEDDS (Figure S3a,b), as well as the individual (co)polymers, was conducted via DSC. Without exception, the thermograms indicated amorphous properties (no melting peaks) for all S-SNEDDS formulations, irrespective of the L-SNEDDS, drug substances, and (co)polymers used (Table 3 and Figures S1–S3), while the crystalline character of the pure drug substances was revealed by a characteristic endothermic peak in the respective melting range of the individual drug substances (Figures S1–S3). Due to the plasticizing effect of the L-SNEDDS used, in comparison to the corresponding (co)polymers, a lower T_g could be measured for all S-SNEDDS (Table 3). The lowest T_g (31 °C), which was close to the storage temperature (30 °C) chosen for the stability studies, was determined for the Soluplus®-based fenofibrate S-SNEDDS. The chosen storage conditions might, therefore, allow for increased movement of the polymer chains, which could result in higher mobility of the respective drug combined with an increased risk of (re-)crystallization and thus result in lower drug release.

Table 3. Glass transition temperature (T_g) of pure (co)polymers and S-SNEDDS incorporating celecoxib, efavirenz, or fenofibrate. Each value designates the mean ± S.D. ($n = 3$).

	T_g (°C)			
	Polymer	Celecoxib S-SNEDDS	Efavirenz S-SNEDDS	Fenofibrate S-SNEDDS
Soluplus®	70 ± 0	39 ± 2	42 ± 2	31 ± 2
Kollidon® VA 64	107 ± 1	67 ± 3	43 ± 0	47 ± 1
Kollidon® 17 PF	136 ± 3	88 ± 1	60 ± 1	74 ± 2
E-173 kDa	77 ± 1	43 ± 0	38 ± 1	48 ± 0
E-254 kDa	85 ± 2	44 ± 1	37 ± 1	41 ± 0
E-281 kDa	89 ± 0	45 ± 2	38 ± 0	48 ± 1
E-305 kDa	91 ± 1	42 ± 0	42 ± 2	44 ± 1
Affinisol® HPMC 100 LV	103 ± 2	45 ± 1	43 ± 2	36 ± 0

2.4. Saturation Solubility Studies

The saturation solubility (48 h, 20 °C) of celecoxib, efavirenz, and fenofibrate in water was determined for the pure drugs and all L-SNEDDS and S-SNEDDS (Table 4). Since the three drug compounds exhibit pH-independent solubility under physiological conditions of the gastrointestinal tract, as a first estimate, solubility tests in water were considered sufficient for an initial screening and assessment of the suitability of different (co)polymers for the preparation of S-SNEDDS with the desired performance [21,24]. Very low aqueous solubilities were determined for all pure drug compounds (Table 4).

Table 4. Saturation solubility (48 h) of celecoxib, efavirenz, and fenofibrate pure drug substances, L-SNEDDS, and S-SNEDDS in water at 20 °C. Each value designates the mean ± S.D. ($n = 3$).

	Saturation Solubility (µg/mL)		
	Celecoxib	Efavirenz	Fenofibrate
Drug substance	0.6 ± 0.1	0.7 ± 0	0.1 ± 0
L-SNEDDS	31.3 ± 1.2	34.7 ± 2.4	17.4 ± 1.8
Soluplus® S-SNEDDS	140 ± 0.9	347 ± 2.3	70 ± 0.4
Kollidon® VA 64 S-SNEDDS	252 ± 1.3	99 ± 0.9	144 ± 1.1
Kollidon® 17 PF S-SNEDDS	197 ± 0.6	226 ± 1.4	125 ± 0.4
E-173 kDa S-SNEDDS	87 ± 0.8	46 ± 0.2	60 ± 0.5
E-254 kDa S-SNEDDS	50 ± 0.1	18 ± 1.0	47 ± 0.3
E-281 kDa S-SNEDDS	26 ± 0.2	16 ± 0.5	43 ± 0.4
E-305 kDa S-SNEDDS	21 ± 0.1	8 ± 0.4	50 ± 0.2
Affinisol® HPMC 100 LV S-SNEDDS	423 ± 6.1	281 ± 3.1	314 ± 3.6

As can be seen from the results in Table 4, it was possible to significantly ($p < 0.05$) improve the solubility of the model drugs used by preparing L-SNEDDS. The results also indicate that by processing L-SNEDDS to S-SNEDDS, it may be possible to further improve the solubility of the drug compounds. However, whether such an effect is achieved depends very much on the composition of the respective formulation. S-SNEDDS based on all commercial polymers used in the study resulted in improved solubility for all drugs compared to that obtained with the underlying L-SNEDDS formulation. For celecoxib and fenofibrate, the largest solubility-enhancing effect was observed for S-SNEDDS based on Affinisol® HPMC 100 LV, whereas for efavirenz S-SNEDDS, this was the case for the Soluplus®-based S-SNEDDS (Table 4). The effect of solubility enhancement of the S-SNEDDS prepared with ModE was not as pronounced as for the those based on the marketed (co)polymers. Independent of the drug compound, among the ModE-based S-SNEDDS, those made with E-173 kDa presented with higher drug solubilities than the underlying L-SNEDDS formulation. Particularly with the celecoxib- and the efavirenz S-SNEDDS, there was a clear trend toward decreasing drug

solubility with the increasing M_w of the polymer, and solubilities were, in several cases, lower than those obtained with the L-SNEDDS formulation. However, with all ModE-based S-SNEDDS, the saturation solubility of all three drug compounds was still tremendously higher than that of the pure drug substances.

One explanation for the limited solubility of celecoxib, efavirenz, and fenofibrate in water when formulated as S-SNEDDS with the ModE copolymer could be the limited water solubility of ModE itself. Based on the observation that ModE does not dissolve properly in water, L-SNEDDS containing any of the above poorly water-soluble active ingredients may not be released to the same extent as in the case of S-SNEDDS based on commercially available, pH-independent, soluble (co)polymers.

2.5. Dissolution Studies

To get a first impression of the drug release behavior of L- and S-SNEDDS formulations, dissolution studies of drug-loaded L- and S-SNEDDS were performed in USP apparatus II using 500 mL of 0.1 M hydrochloric acid (HCl) as a dissolution medium. For comparative purposes, corresponding doses of the unprocessed drug substances were also investigated in the same test setup.

The dissolution of the unprocessed drug substances was very poor, i.e., within the test duration of 120 min, in all cases, less than 5% of the tested dose was released. In contrast, the L-SNEDDS formulations, regardless of whether they contained celecoxib, efavirenz, or fenofibrate (Figures 1–3), showed rapid and complete drug release within 15 to 30 min. In the case of celecoxib, S-SNEDDS preparation did not affect the release rate of the L-SNEDDS formulation when the E-173 kDa copolymer was used. (Figure 1a), i.e., drug release was still fast and complete. Similar observations were made for the S-SNEDDS made with the Soluplus® copolymer (Figure 1b). Within the same time period, the S-SNEDDS formulations prepared with Kollidon® VA 64, Affinisol® HPMC 100 LV, and E-254 kDa released about 80% to 85% of the incorporated celecoxib dose, while celecoxib release from all other S-SNEDDS formulations was slower in most cases, with markedly less celecoxib released within 120 min (Figure 1a,b). Similarly, for efavirenz, the drug release performance of the S-SNEDDS made of the E-173 kDa or the Soluplus® copolymer was fast and complete and similar to that of the L-SNEDDS (Figure 2a,b). Within the same test duration, the S-SNEDDS made of the E-254 kDa showed a slightly lower efavirenz release (about 90% of the dose released) (Figure 2a), whereas all other S-SNEDDS formulations presented with a much lower amount of drug release in this time period (Figure 2a,b). Observations made with the fenofibrate S-SNEDDS were slightly different. Of the S-SNEDDS formulations, those made with Kollidon® VA 64 presented the best in vitro performance (about 90% of the dose released) (Figure 3b). Within the same time period, approximately the same total amount of fenofibrate (~90%) was released from the E-173 kDa S-SNEDDS, but at a lower release rate (Figure 3a). S-SNEDDS based on Soluplus® (~85%), Affinisol® HPMC 100 LV (~80%), and Kollidon® 17 PF (~76%) also released a large proportion of the contained fenofibrate dose within the test duration of 120 min (Figure 3b). Overall, the amount of fenofibrate released from all S-SNEDDS formulations studied was a little lower than that observed for the underlying L-SNEDDS formulation. In summary, the results of the release studies show that, by using a suitable (co)polymer as well as a suitable manufacturing process, it is possible to convert L-SNEDDS into S-SNEDDS while barely changing the original release behavior.

(**a**)
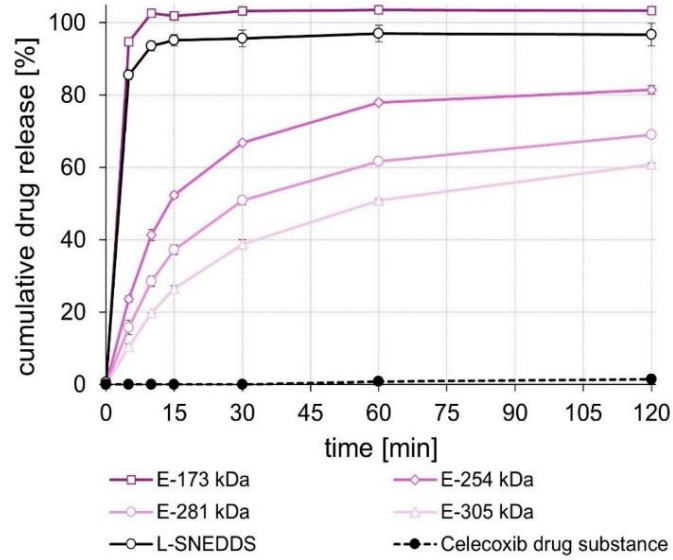
(**b**)
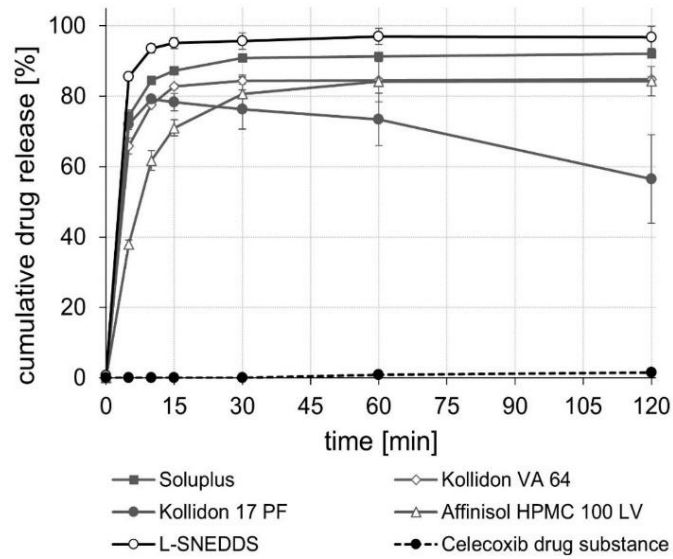
Figure 1. Dissolution profiles of the celecoxib drug substance and celecoxib L- and S-SNEDDS based on ModE (**a**), as well as the celecoxib drug substance and celecoxib L- and S-SNEDDS based on other marketed (co)polymers (**b**) in 500 mL 0.1 M HCl in USP apparatus II. Each value designates the mean ± S.D. (*n* = 3).
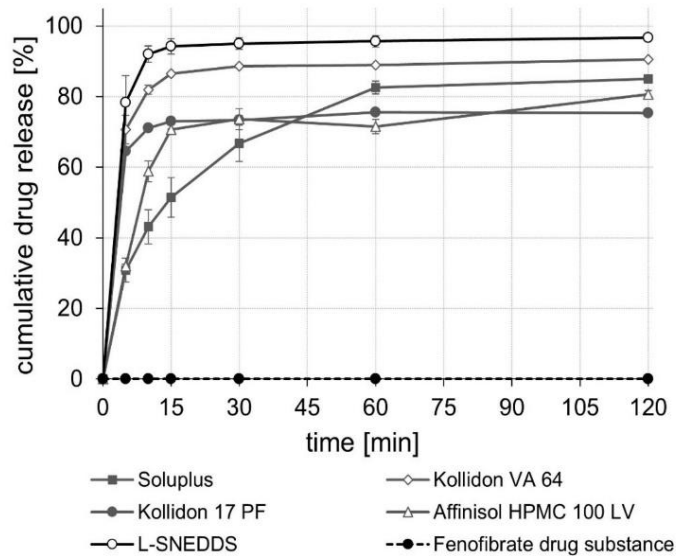
(**a**)
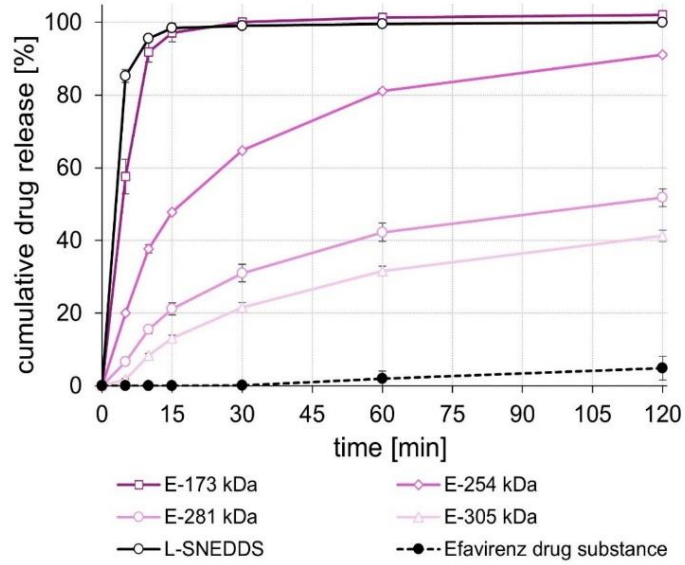
(**b**)
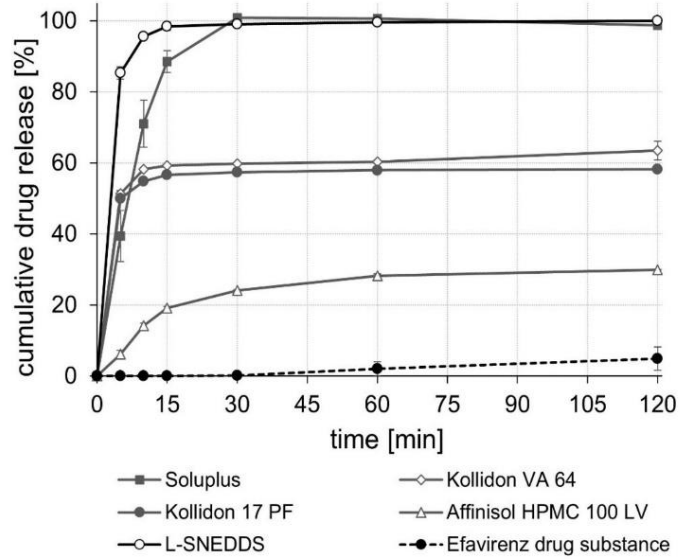
Figure 2. Dissolution profiles of the efavirenz drug substance and efavirenz L- and S-SNEDDS based on ModE (**a**), as well as the efavirenz drug substance and efavirenz L- and S-SNEDDS based on other marketed (co)polymers (**b**) in 500 mL 0.1 M HCl in USP apparatus II. Each value designates the mean ± S.D. ($n = 3$).

(**a**)
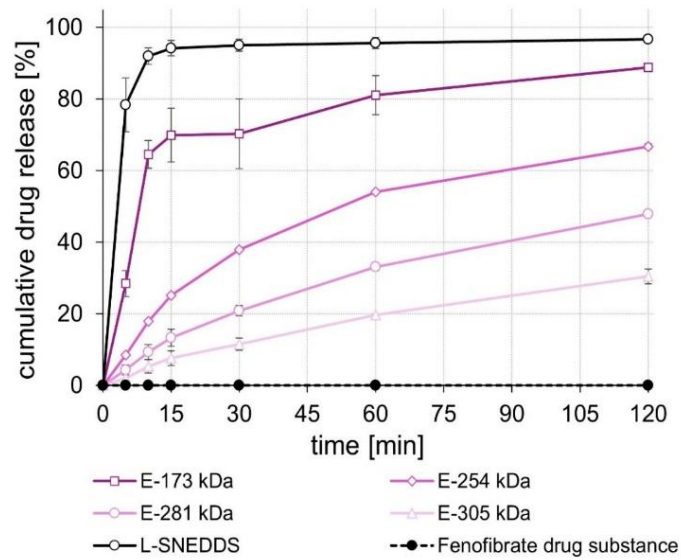
(**b**)

Figure 3. Dissolution profiles of the fenofibrate drug substance and fenofibrate L- and S-SNEDDS based on ModE (**a**), as well as the fenofibrate drug substance and fenofibrate L- and S-SNEDDS based on other marketed (co)polymers (**b**) in 500 mL 0.1 M HCl in USP apparatus II. Each value designates the mean ± S.D. (*n* = 3).

A comparison of the rate and extent of drug release of the S-SNEDDS prepared from different ModE types showed that a higher M_w or a higher T_g of the ModE copolymer used resulted in a decrease, both in the rate and extent of celecoxib-, efavirenz-, and fenofibrate

112

release within the test period of 120 min (Figures 1a, 2a and 3a). These observations correlate with those made when ModE was used in the preparation of ASD [22]. The observed effect of M_w and T_g on drug release performance (dissolution rate of the drug substance was inversely proportional with M_w and T_g of a copolymer) was also determined by Knopp et al. [25], who studied polyvinylpyrrolidone-based ASDs incorporating the drug substance celecoxib. Further, for these formulations, a decrease in the (co)polymer's M_w was accompanied by decreasing viscosity and increasing flexibility of polymeric chains [25]. These effects are likely to contribute to better solubilization of poorly water-soluble drug substances [25]. Concluding from these observations on the release performance obtained when E-173 kDa was used in the S-SNEDDS technology, it can be assumed that the higher flexibility of the polymer chains in the E-173 kDa copolymer resulted in good solubilization of the drugs celecoxib, efavirenz, and fenofibrate, respectively. As already stated, the trend regarding an improved drug release performance of S-SNEDDS containing ModE with lower M_w observed in the present study was in good agreement with that observed in a previous study [22]. In both studies, the drug release of celecoxib-, efavirenz- and fenofibrate formulations with the same drug dose was investigated. Comparing the results, the S-SNEDDS formulations provide significantly ($p < 0.05$) better in vitro release performance than the ASD formulations. This is particularly clear from the example of fenofibrate, where the E-173 kDa ASD formulation released 30% [22] and the corresponding S-SNEDDS formulation almost 90% of the fenofibrate dose within a period of 120 min under the same test conditions.

This first set of dissolution studies was performed using 0.1 M HCl as the dissolution medium to simulate the pH conditions of the fasting stomach, in which the ModE copolymer is also soluble. By not adding artificial surfactants, such as sodium lauryl sulfate or polysorbate 20, to the dissolution medium, which were used in previous studies to screen drug release from formulations containing celecoxib [25,26], efavirenz [15,23], and fenofibrate [16,27,28], worst-case conditions should be established to clearly highlight the effects of the S-SNEDDS technology on drug release. For the same reason, the use of physiologically relevant amounts of bile salts was refrained from. Since the pH-independent solubility of all three agents used in the present series of tests has been demonstrated in previous studies [21,24], it can be assumed that the dissolution behavior of celecoxib, efavirenz, and fenofibrate will be the same or similar in media at other pH values.

Comparison with other dissolution data related to S-SNEDDS prepared by HME is not (yet) possible at this time because of the lack of studies in this field. Silva et al. [10] have recently published preliminary results from a similar study. They chose hydroxypropyl methylcellulose acetate succinate (HPMCAS) for the preparation of S-SMEDDS by HME. However, they did not develop an S-SNEDDS formulation, they used a different active ingredient as well as a different loading level, and the experimental conditions in the release studies performed were also different from those used in the present study. Therefore, if one wants to discuss the formulation's influence on drug release, it must remain at this point for the corresponding drug when comparing L-SNEDDS, S-SNEDDS, and ASDs.

2.6. Stability Studies

2.6.1. Appearance (after Three and Six Months of Storage)

After three months of storage under defined and constant conditions (30 °C/65% RH), the appearance of all L-SNEDDS formulations remained unchanged regardless of the drug substance incorporated. The stored samples of most S-SNEDDS formulations showed no significant agglomeration and could be easily shaken up. Only S-SNEDDS prepared using the copolymer Soluplus® were found to have larger agglomerates in samples containing the active ingredients celecoxib as well as efavirenz. After a further three months, i.e., after a total of six months of storage under the same conditions (30

°C/65% RH), very slight turbidity was observed in the L-SNEDDS. As before, most of the stored S-SNEDDS formulations could be easily shaken up again. Agglomeration was observed for the celecoxib S-SNEDDS prepared using Soluplus® and Kollidon® 17 PF. Larger agglomerates were also evident in efavirenz S-SNEDDS based on the (co)polymers Soluplus®, Kollidon® VA 64, and Affinisol® HPMC 100 LV. In the case of fenofibrate S-SNEDDS, agglomeration was observed exclusively with Soluplus®-based S-SNEDDS. There was a fairly clear correlation between the agglomeration tendency and the T_gs of the corresponding S-SNEDDS formulations, which will be discussed in the following section. Overall, the agglomeration tendency was increased when the temperature of the storage conditions and the T_g were close to each other.

2.6.2. Thermal Characterization of S-SNEDDS via DSC Analysis (after Six Months of Storage)

Thermal characterization of the pure (co)polymers after six months of storage revealed that the applied storage conditions did not have any significant impact on the T_g of the pure (co)polymers (Tables 3 and 5). Furthermore, although storage conditions affected the T_g of all S-SNEDDS, regardless of the drug substance used, these still exhibited an amorphous state when the corresponding thermograms of the first heating cycle were analyzed (Figures S1–S6, Tables 3 and 5). In some cases, after storage, the T_gs of S-SNEDDS were even closer to the elevated storage temperature of 30 °C as before storage. Substantial decreases in T_g (more than 5 °C below the initial value) were observed for celecoxib S-SNEDDS based on Kollidon® VA 64, efavirenz S-SNEDDS based on Soluplus® and E-305 kDa, and fenofibrate S-SNEDDS prepared using different ModE copolymer types (Tables 3 and 5). Interestingly, none of the corresponding thermograms showed evidence for crystallization. This may be due, in particular, to the special formulation concept of the S-SNEDDS. The fact that the active ingredients used were completely dissolved in L-SNEDDS before conversion to S-SNEDDS seems to substantially contribute to the stabilization of the amorphous state and the lack of crystallization tendency.

Table 5. Glass transition temperature (T_g) of the pure (co)polymers and S-SNEDDS incorporating celecoxib, efavirenz, or fenofibrate after six months of storage. Each value designates the mean ± S.D. (*n* = 3).

	T_g (°C)			
	Polymer	Celecoxib S-SNEDDS	Efavirenz S-SNEDDS	Fenofibrate S-SNEDDS
Soluplus®	69 ± 1	39 ± 2	32 ± 2	29 ± 1
Kollidon® VA 64	105 ± 1	60 ± 2	38 ± 1	47 ± 0
Kollidon® 17 PF	135 ± 0	88 ± 1	59 ± 2	75 ± 1
E-173 kDa	77 ± 1	45 ± 1	36 ± 0	38 ± 1
E-254 kDa	83 ± 0	39 ± 1	35 ± 1	33 ± 0
E-281 kDa	88 ± 1	44 ± 0	33 ± 1	32 ± 1
E-305 kDa	91 ± 1	46 ± 2	35 ± 0	30 ± 0
Affinisol® HPMC 100 LV	69 ± 1	39 ± 2	32 ± 2	29 ± 1

2.6.3. Dissolution Studies after Three and Six Months of Storage

After three months of storage at 30 °C/65% RH, there was hardly any change in the release profiles for the drug-loaded L-SNEDDS. After six months of storage, a trend toward a slightly lower amount of released dose (approx. 91–92% of the applied dose) was observed for all active ingredients used when compared with results obtained from release studies directly after the preparation of the individual drug-loaded L-SNEDDS, which could indicate potential stability issues for the L-SNEDDS under these storage conditions.

After storage of the drug-loaded S-SNEDDS at 30 °C/65% RH for three and six months, most of the S-SNEDDS showed slightly different dissolution performance (Figures S7–S9 and 4–6). Whereas the rate and extent of drug release of some of the formulations marginally changed, for some of the S-SNEDDS formulations, a substantial change in drug release performance, particularly with regard to the extent of drug release, could be observed.

(**a**)
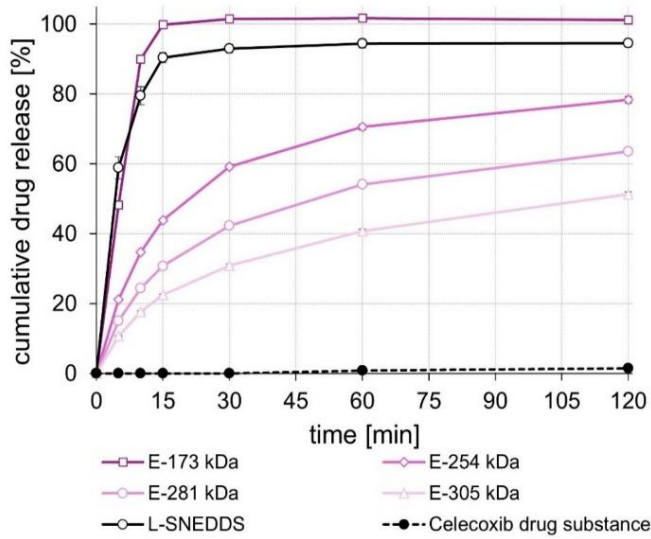
(**b**)
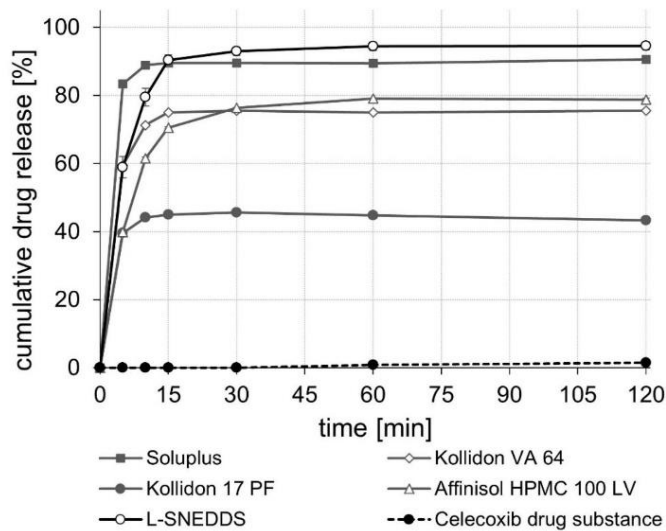
Figure 4. Dissolution profiles of the celecoxib drug substance and celecoxib L- and S-SNEDDS based on ModE (**a**), as well as the celecoxib drug substance and celecoxib L- and S-SNEDDS based on other

marketed (co)polymers (**b**) after six months of storage at 30 °C/65% RH in 500 mL 0.1 M HCl in USP apparatus II. Each value designates the mean ± S.D. (*n* = 3).

(**a**)
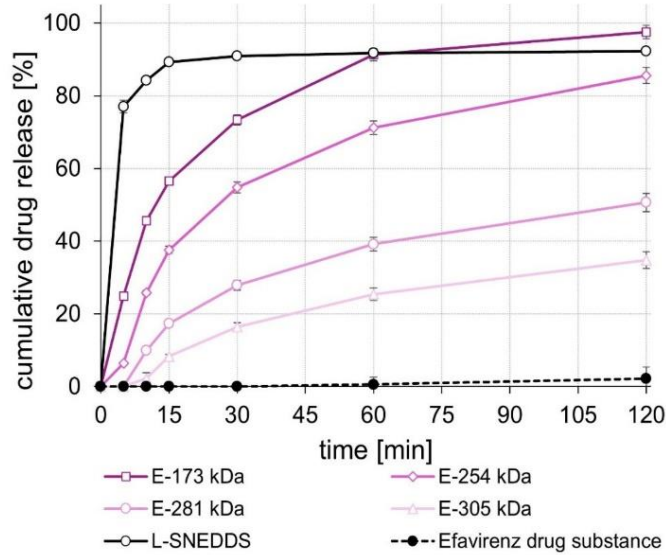
(**b**)
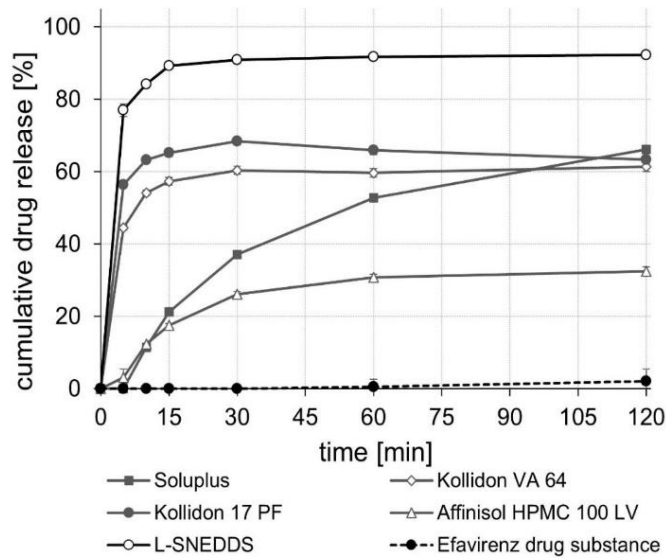
Figure 5. Dissolution profiles of the efavirenz drug substance and efavirenz L- and S-SNEDDS based on ModE (**a**), as well as the efavirenz drug substance and efavirenz L- and S-SNEDDS based on other marketed (co)polymers (**b**) after six months of storage at 30 °C/65% RH in 500 mL 0.1 M HCl in USP apparatus II. Each value designates the mean ± S.D. (*n* = 3).

(**a**)

(**b**)
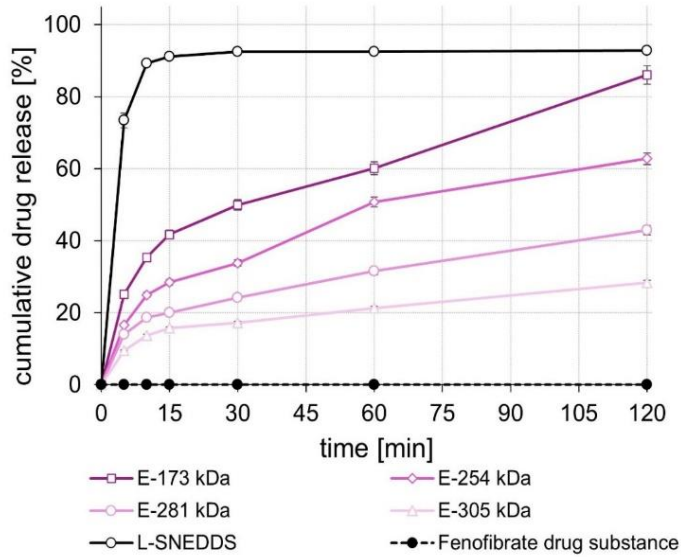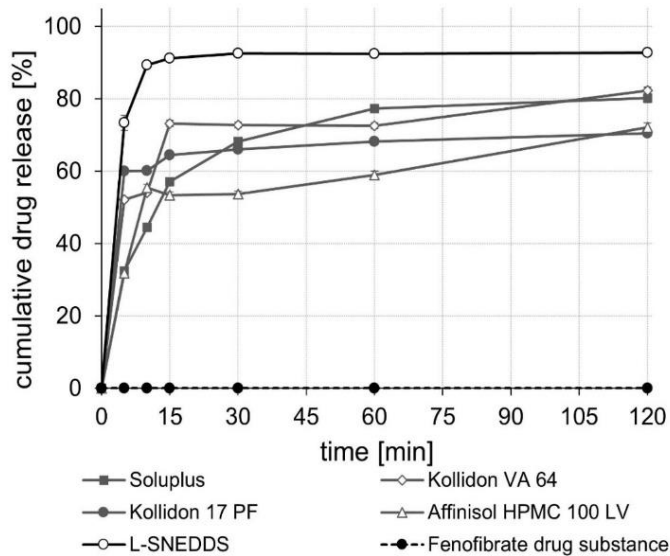
Figure 6. Dissolution profiles of the fenofibrate drug substance and fenofibrate L- and S-SNEDDS based on ModE (**a**), as well as the fenofibrate drug substance and fenofibrate L- and S-SNEDDS based on other marketed (co)polymers (**b**) after six months of storage at 30 °C/65% RH in 500 mL 0.1 M HCl in USP apparatus II. Each value designates the mean ± S.D. (*n* = 3).

For the celecoxib S-SNEDDS, a marked decrease in the total amount of drug released was observed for the Kollidon® 17 PF- and the E-305 kDa-based S-SNEDDS after only three months of storage (Figures S7a,b). For the Kollidon® 17 PF-based S-SNEDDS, this

trend continued during the remaining storage time (Figure 4b). For the Kollidon® VA 64-based S-SNEDDS, which showed an almost complete drug release immediately after preparation, both the release rate and the amount of drug released at 120 min after a storage period of six months were noticeably different (Figure 4b). In good agreement with this observation, substantially lower T_gs were also measured for these S-SNEDDS after six months of storage, suggesting that there may be a correlation between changes in T_g and drug release.

For the efavirenz S-SNEDDS, a major decrease in drug release after the test duration of 120 min was noticed for E-305 kDa-based S-SNEDDS after three months of storage (Figure S8a). Similar observations were made for the efavirenz S-SNEDDS prepared with Soluplus® after six months of storage (Figure 5b). As observed in the case of celecoxib-loaded S-SNEDDS, the results obtained with the efavirenz S-SNEDDS formulations based on E-305 kDa and Soluplus® may support the hypothesis of a possible correlation between changes in T_g and drug release. Similar to the above-discussed celecoxib S-SNEDDS, these efavirenz S-SNEDDS presented with a pronounced decrease in T_g after six months of storage and, correspondingly, provided a significantly ($p < 0.05$) lower amount of drug released after a test duration of 120 min compared to their release performance immediately after manufacture.

Results from dissolution studies with fenofibrate S-SNEDDS based on Soluplus®, Kollidon® VA 64, Kollidon® 17 PF, E-281 kDa, and Affinisol® HPMC 100 LV (Figure S9a,b) showed a considerable decrease in fenofibrate release already after three months of storage. However, when these formulations were stored for another three months under the same conditions, this had little effect, and the fenofibrate release profiles remained almost unchanged (Figure 6a,b).

Several S-SNEDDS formulations, particularly many of those prepared with celecoxib or efavirenz, demonstrated good storage stability. The corresponding L-SNEDDS also presented good stability data, especially when stored for three months. When L-SNEDDS were stored for an additional three months, the amount of drug released after 120 min of testing decreased by approximately 8%. A decrease in drug release in the same range, as determined for L-SNEDDS, was also observed for several S-SNEDDS formulations. However, comparing the stability data of the S-SNEDDS with those of the L-SNEDDS collected after six months of storage indicates that, depending on the copolymer used for the preparation of the S-SNEDDS, in some cases, an effect could be obtained with respect to further stabilization of the L-SNEDDS. Overall, the results for the drug release of S-SNEDDS indicate that the type of polymer carrier used for the preparation of S-SNEDDS has a major influence on maintaining the initial release behavior of the L-SNEDDS formulations both immediately after preparation of the S-SNEDDS, but also over a longer storage period under "stress conditions". Overall, the results of the release studies indicated that fenofibrate appears to be the most challenging model compound to formulate among the three drugs used for the S-SNEDDS formulation approach since fenofibrate-loaded S-SNEDDS showed a markedly reduced drug release already after three months of storage in the case of almost all S-SNEDDS regardless of the polymeric carrier used. In contrast, very good results were obtained for celecoxib, in particular when the new E-173 kDa was used for S-SNEDDS preparation. In this case, an almost unchanged, rapid, and complete release of the investigated drug dose could be observed both shortly after preparation and after a three-month storage period at 30 °C/65% RH.

3. Materials and Methods

3.1. Materials

Celecoxib (purity of 99.7%) was obtained from Aarti Drugs Ltd. (Mumbai, India), efavirenz (purity of 99.3%) was purchased from Angene International Ltd. (London, UK), and fenofibrate (purity of 99.1%) was obtained from D.K. Pharma Chem PVT Ltd. (Maharashtra, India). Polyoxyethylene (80) sorbitan monooleate (Tween® 80), d-α-

Tocopherol polyethylene glycol 1000 succinate (d-TPGS), isopropyl myristate (IPM-100), and polyoxyethylene (23) lauryl ether (Brij® 35) were purchased from Sigma Aldrich Chemie GmbH (Steinheim, Germany). Lauroyl polyoxyl-32 glycerides (Gelucire® 44/14) and diethylene glycol monoethyl ether (Transcutol® HP) were kindly donated by Gattefossé S.A.S (Saint Priest, France). Medium-chain triglycerides (Miglyol® 812) were obtained from Caesar & Loretz GmbH (Hilden, Germany). Polyvinyl caprolactam–polyvinyl acetate–polyethylene glycol graft copolymer (Soluplus®, M_w = 90,000–140,000 g/mol), polyvinylpyrrolidone-polyvinyl acetate copolymer (Kollidon® VA 64, M_w = 45,000–70,000 g/mol) and polyvinylpyrrolidone (Kollidon® 17 PF, M_w = 7000–11,000 g/mol) were purchased from BASF SE (Ludwigshafen, Germany). Hydroxypropyl methylcellulose (Affinisol® HPMC 100 LV, M_w = 179,000 g/mol) was provided by Dow Chemical Company (Schwalbach am Taunus, Germany). Dimethylaminopropyl methacrylamide-butyl methacrylate-methyl methacrylate copolymer (2:1:1, ratios by weight), a modified Eudragit® E copolymer (ModE) in different M_ws, i.e., E-173 kDa, E-254 kDa, E-281 kDa, and E-305 kDa, is an in-house product of Evonik Operations GmbH (Darmstadt, Germany) and was synthesized as described in [22]. All other chemicals and solvents were of analytical grade and purchased commercially.

3.2. Methods

3.2.1. Development and Preparation of L-SNEDDS

L-SNEDDS incorporating the drug substances celecoxib, efavirenz, or fenofibrate were developed according to a systematic screening approach established by Schmied et al. [21]. The optimal excipient composition and mixing ratio for L-SNEDDS resulted from meeting the following self-imposed specifications: After the dispersion of L-SNEDDS in water, a nanoemulsion with a droplet size < 50 nm, a PDI < 0.15, and transmission of >99% was supposed to result (data not shown) [21]. It should be noted here that these limits were deliberately chosen and very strict but explicitly self-imposed and did not represent regulatory quality criteria.

3.2.2. Preparation of S-SNEDDS via HME

Following their preparation and characterization, drug-loaded L-SNEDDS were co-extruded with different (co)polymers in individual HME processes. Marketed (co)polymers already established for the purpose of solubility enhancement, such as Soluplus®, Kollidon® VA 64, Kollidon® 17 PF, and Affinisol® HPMC 100 LV, as well as various ModE copolymers with different M_w were used as polymeric carriers. Extrudates were prepared as follows: First, 15 g of a mixture of each of the individual (co)polymers and an L-SNEDDS formulation containing one of the poorly soluble model compounds was prepared at a predetermined mixing ratio by mixing the components in a 100-mL jar sealed with a screw cap for 10 min using a turbula mixer (TURBULA®, WAB Group, Nidderau, Germany). Subsequently, this mixture was processed into S-SNEDDS by HME using a co-rotating HAAKE MiniLab twin screw extruder with a conical screw design (Thermo Fisher Scientific, Dreieich, Germany). The HME process was defined by the set parameters screw speed and process temperature as well as by the torque recorded during the process. The die diameter was 2 mm, and the strand leaving the extruder was allowed to cool during transport via a conveyor belt before it was finally ground to coarse granules by a small chopper with a rotating metal gear. These coarse granules were then pulverized using a ZM 200 ultra-centrifugal mill from Retsch GmbH (Haan, Germany) (mesh size: 0.25 mm). The obtained powders were used for all subsequent experiments.

3.2.3. Differential Scanning Calorimetry (DSC) Analysis

All S-SNEDDS formulations were analyzed via DSC (DSC 3+ (DSC-HC01), Mettler Toledo, Giessen, Germany) to determine whether the incorporated drug was in the amorphous (glass transition) or crystalline (melting/crystallization peak) state. The DSC

119

method used was the same as in a preceding study [22]. Briefly, a 5–10 mg sample was weighed into a small aluminum pan that was cold sealed with a perforated lid and exposed to a heating–cooling–heating cycle in a temperature range of 0 to 200 °C. A nitrogen flow of 50 mL/min was applied while running the experiments. The heating and cooling rates were both set at 10 °C/min. The melting point of the pure drug substances, as well as the glass transition temperature of the individual (co)polymers were investigated. For all analyzed samples, T_g was taken from the thermogram obtained from the second heating cycle, and the indicated value represents the mean of $n = 3$.

3.2.4. Saturation Solubility Assessments

The saturation solubility of celecoxib, efavirenz, and fenofibrate in water was studied for the pure drug substances and the corresponding L-SNEDDS and S-SNEDDS immediately after preparation. For this purpose, about 25 mg of the drug substance or an amount of S-SNEDDS equivalent to this amount was added to a volume of 25 mL of distilled water and stirred (100 rpm) at a controlled temperature of 20 °C for 48 h. The resulting suspensions were filtered via a 0.22 μm polytetrafluoroethylene (PTFE) membrane filter (25 mm diameter) from Global Biomed Scientific (Forest, VA, USA). The suitability of the filter material was validated for each of the active ingredients before use. All filtrates were diluted in a specific ratio with acetonitrile before quantification of the amount of dissolved celecoxib, efavirenz, and fenofibrate by high-performance liquid chromatography (HPLC).

3.2.5. Dissolution Studies

Dissolution experiments were conducted in triplicate with 25 mg drug substance or an equivalent amount of L-SNEDDS or S-SNEDDS using USP apparatus II (DT 800 LH, ERWEKA GmbH, Langen, Germany). The paddle speed was set to 100 rpm to avoid coning effects, and all experiments were performed in 500 mL of 0.1 M hydrochloric acid at 37 ± 0.5 °C. The test duration was 120 min. All samples were withdrawn via a fraction collector, equipped with cannula filters of 10 μm pore size and, after sampling, were manually diluted in a 1:1 ratio (*v:v*) with acetonitrile before HPLC analysis.

3.2.6. HPLC Analysis

An Agilent 1260 Infinity HPLC system was used for the quantification of the different model drug substances. The system consisted of a quaternary pump (G1311B), an autosampler (G1329B), a column oven (G1316A), and a UV detector (G1314C), all from Agilent Technologies (Frankfurt am Main, Germany). The HPLC methods used to quantify celecoxib, efavirenz, and fenofibrate were the same as described by Schmied et al. [22] and, prior to use, had been validated according to USP requirements.

HPLC Method for Celecoxib

The separation of all samples containing celecoxib was achieved using a Knauer Nucleosil 100-7 C18 (125 × 4.6 mm, 7 μm) column maintained at 40 °C. The mobile phase consisted of an acetonitrile:water:triethylamine mixture (300:300:0.9 *v/v*), adjusted topH 3.00 with phosphoric acid. The flow rate was set to 1.8 mL/min. An injection volume of 5 μL was applied and celecoxib was detected at 254 nm. In the concentration range of 0.13–542 μg/mL, the analytical curve was linear ($r^2 = 0.999995$). The method was found to be accurate (100.2–102.1%) and precise (CV 2.46%) with a quantification limit of 0.05 μg/mL. The total run time was 7 min [22].

HPLC Method for Efavirenz

Separation of the samples containing efavirenz was achieved on a Symmetry 300 C18 (250 × 4.6 mm, 5 μm) column maintained at 22 °C. The mobile phase consisted of an acetonitrile:buffer solution (disodium hydrogen phosphate/phosphoric acid adjusted to

pH 3.60) mixture (290:210 *v/v*). The flow rate was set to 1.5 mL/min. An injection volume of 20 μL was applied, and efavirenz was detected at 247 nm. In the concentration range of 0.13–515 μg/mL, the analytical curve was linear (r^2 = 0.999894). The method was found to be accurate (101.4–103.0%) and precise (CV 4.05%) with a quantification limit of 0.05 μg/mL. The total run time was 10 min [22].

HPLC Method for Fenofibrate

The separation of all samples containing fenofibrate was achieved using a Symmetry 300 C18 (150 × 4.6 mm, 5 μm) column maintained at 22 °C. The mobile phase consisted of an acetonitrile:water mixture (70:30 *v/v*), adjusted to pH 2.50 with phosphoric acid. The flow rate was set to 2.0 mL/min. An injection volume of 20 μL was applied, and fenofibrate was detected at 286 nm. In the concentration range of 0.13–526 μg/mL, the analytical curve was linear (r^2 = 0.999992). The method was found to be accurate (101.2–101.4%) and precise (CV 2.42%) with a quantification limit of 0.05 μg/mL. The total run time was 7 min [22].

For all HPLC methods, the selectivity for the respective drug substances was determined (formulation excipients), and no interference was observed at the retention time of the specific drug. Moreover, the peak area of the drug did not change in the presence of all excipients used in the study.

3.2.7. Stability Studies

A quantity of approximately 10 g of each L-SNEDDS and S-SNEDDS formulation was added to a 30 mL amber glass jar, closed with a screw cap, and stored at constant and controlled conditions (30 °C/65% RH) in a climatic chamber (Model KBF 720, Binder GmbH, Tuttlingen, Germany) for six months. After three and six months, S-SNEDDS were first visually inspected to check whether they could be easily fluffed up again or stuck together (formation of larger agglomerates), whereas L-SNEDDS were analyzed for separation of their constituents and precipitation of the incorporated drug substance. Subsequently, all formulations were subjected to dissolution experiments. In addition, after six months of storage, DSC analyses were performed with the S-SNEDDS formulations. All results obtained in the stability studies were compared with those obtained immediately after manufacture.

3.2.8. Data Analysis

All reported data originated from at least three independent experiments. Significance tests were conducted with SigmaPlot 14.0 from Systat Software GmbH (Erkrath, Germany) using a one-way analysis of variance (ANOVA) followed by the Holm–Sidak test. Significances are indicated with $p < 0.05$ in brackets.

4. Conclusions

In the present study, the preparation of S-SNEDDS from L-SNEDDS and polymeric carrier materials using HME was successfully established as a novel technology concept for the preparation of solid lipid-based formulations for improving the solubility of poorly water-soluble drugs. In particular, for the model drug celecoxib, S-SNEDDS could be developed that maintained the rapid and complete drug release of the underlying L-SNEDDS even over an extended storage period. Overall, the data obtained in the study indicate that the presented S-SNEDDS approach is very promising, provided one combines L-SNEDDS with a suitable polymeric carrier. In the case of celecoxib, the E-173 variant of the new ModE copolymer was revealed to be a novel polymeric carrier with potential for application in S-SNEDDS. Overall, the results obtained in the present study indicate that the presented S-SNEDDS formulation approach represents a novel alternative for the development of solid oral dosage forms for poorly soluble drug candidates. It is believed that this formulation approach also offers great potential for the development of stable solid formulations with improved oral bioavailability for other

poorly soluble drug candidates. It merits, therefore, strong pursuit, with particular emphasis on experiments that provide more clarity on the expected in vivo behavior. Overall, therefore, it is likely to see more research addressing this formulation approach in the near future.

Supplementary Materials: The following supporting information can be downloaded at: https://www.mdpi.com/article/10.3390/ph15091135/s1. Figure S1. DSC thermograms of celecoxib, ModE copolymers, and the corresponding S-SNEDDS (a), celecoxib and other marketed (co)polymers used in the study, and the corresponding S-SNEDDS (b); Figure S2. DSC thermograms of efavirenz, ModE copolymers, and the corresponding S-SNEDDS (a), efavirenz and other marketed (co)polymers used in the study, and the corresponding S-SNEDDS (b); Figure S3. DSC thermograms of fenofibrate, ModE copolymers, and the corresponding S-SNEDDS (a), fenofibrate and other marketed (co)polymers used in the study, and the corresponding S-SNEDDS (b); Figure S4. DSC thermograms (after six months of storage at 30 °C/65% RH) of celecoxib, ModE copolymers, and the corresponding S-SNEDDS (a), celecoxib and other marketed (co)polymers used in the study, and the corresponding S-SNEDDS (b); Figure S5. DSC thermograms (after six months of storage at 30 °C/65% RH) of efavirenz, ModE copolymers, and the corresponding S-SNEDDS (a), efavirenz and other marketed (co)polymers used in the study, and the corresponding S-SNEDDS (b); Figure S6. DSC thermograms (after six months of storage at 30 °C/65% RH) of fenofibrate, ModE copolymers, and the corresponding S-SNEDDS (a), fenofibrate and other marketed (co)polymers used in the study, and the corresponding S-SNEDDS (b); Figure S7. Dissolution profiles of celecoxib drug substance and celecoxib L- and S-SNEDDS based on ModE (a), as well as celecoxib drug substance and celecoxib L- and S-SNEDDS based on other marketed (co)polymers (b) (after three months of storage at 30 °C/65% RH) in 500 mL 0.1 M HCl in USP apparatus II. Each value designates the mean ± S.D. ($n = 3$); Figure S8. Dissolution profiles of efavirenz drug substance and efavirenz L- and S-SNEDDS based on ModE (a), as well as efavirenz drug substance and efavirenz L- and S-SNEDDS based on other marketed (co)polymers (b) (after three months of storage at 30 °C/65% RH) in 500 mL 0.1 M HCl in USP apparatus II. Each value designates the mean ± S.D. ($n = 3$); Figure S9. Dissolution profiles of fenofibrate drug substance and fenofibrate L- and S-SNEDDS based on ModE (a), as well as fenofibrate drug substance and fenofibrate L- and S-SNEDDS based on other marketed (co)polymers (b) (after three months of storage at 30 °C/65% RH) in 500 mL 0.1 M HCl in USP apparatus II. Each value designates the mean ± S.D. ($n = 3$).

Author Contributions: Methodology, F.-P.S. and A.B.; validation, F.-P.S.; investigation, F.-P.S.; resources, A.B.; data curation, F.-P.S.; writing—original draft preparation, F.-P.S.; writing—review and editing, S.K.; visualization, F.-P.S.; supervision, A.B. and S.K.; project administration, A.B. and S.K. All authors have read and agreed to the published version of the manuscript.

Funding: This research received no external funding.

Institutional Review Board Statement: Not applicable.

Informed Consent Statement: Not applicable.

Data Availability Statement: Data is contained within the article and Supplementary Material.

Conflicts of Interest: The authors declare no conflict of interest.

References

1. Kalepu, S.; Nekkanti, V. Insoluble drug delivery strategies: Review of recent advances and business prospects. *Acta Pharm. Sin. B.* **2015**, *5*, 442–453. https://doi.org/10.1016/j.apsb.2015.07.003.
2. Hanada, M.; Jermain, S.V.; Williams, R.O., III. Enhanced dissolution of a porous carrier-containing ternary amorphous solid dispersion system prepared by a hot melt method. *J. Pharm. Sci.* **2018**, *107*, 362–371. https://doi.org/10.1016/j.xphs.2017.09.025.
3. Williams, H.D.; Trevaskis, N.I.; Charman, S.A.; Shanker, R.M.; Charman, W.N.; Pouton, C.W.; Porter, C.J. Strategies to address low drug solubility in discovery and development. *Pharmacol. Rev.* **2013**, *65*, 315–499. https://doi.org/10.1124/pr.112.005660.
4. Dokania, S.; Joshi, A.K. Self-microemulsifying drug delivery system (SMEDDS)—Challenges and road ahead. *Drug Deliv.* **2015**, *22*, 675–690. https://doi.org/10.3109/10717544.2014.896058.
5. Porter, C.J.H.; Pouton, C.W.; Cuine, J.F.; Charman, W.N. Enhancing intestinal drug solubilisation using lipid-based delivery systems. *Adv. Drug Deliv. Rev.* **2008**, *60*, 673–691. https://doi.org/10.1016/j.addr.2007.10.014.
6. Pouton, C.W. Lipid formulations for oral administration of drugs: Non-emulsifying, self-emulsifying and 'self-microemulsifying' drug delivery systems. *Eur. J. Pharm. Sci.* **2000**, *11*, 93–98. https://doi.org/10.1016/s0928-0987000167-6.

7.   Thomas, N.; Holm, R.; Mullertz, A.; Rades, T. In vitro and in vivo performance of novel supersaturated self-nanoemulsifying drug delivery systems (super-SNEDDS). *J. Control. Release.* **2012**, *160*, 25–32. https://doi.org/10.1016/j.jconrel.2012.02.027.

8.   Vithani, K.; Hawley, A.; Jannin, V.; Pouton, C.; Boyd, B.J. Inclusion of digestible surfactants in solid SMEDDS formulation removes lag time and influences the formation of structured particles during digestion. *AAPS J.* **2017**, *19*, 754–764. https://doi.org/10.1208/s12248-016-0036-6.

9.   Chatterjee, B.; Almurisi, S.H.; Dukhan, A.A.M.; Mandal, U.K.; Sengupta, P. Controversies with self-emulsifying drug delivery system from pharmacokinetic point of view. *Drug Deliv.* **2016**, *23*, 3639–3652. https://doi.org/10.1080/10717544.2016.1214990.

10. Silva, L.A.D.; Almeida, S.L.; Alonso, E.C.; Rocha, P.B.; Martins, F.T.; Freitas, L.A.; Taveira, S.F.; Cunha-Filho, M.S.; Marreto, R.N. Preparation of a solid self-microemulsifying drug delivery system by hot-melt extrusion. *Int. J. Pharm.* **2018**, *541*, 1–10. https://doi.org/10.1016/j.ijpharm.2018.02.020.

11. Vithani, K.; Hawley, A.; Jannin, V.; Pouton, C.; Boyd, B.J. Solubilisation behaviour of poorly water-soluble drugs during digestion of solid SMEDDS. *Eur. J. Pharm. Biopharm.* **2018**, *130*, 236–246. https://doi.org/10.1016/j.ejpb.2018.07.006.

12. Yetukuri, K.; Sudheer, P. Approaches to development of solid-self micron emulsifying drug delivery system: Formulation techniques and dosage forms: A review. *Int. J. Pharm. Sci. Res.* **2012**, *3*, 3550–3558.

13. Sander, C.; Holm, P. Porous magnesium aluminometasilicate tablets as carrier of a cyclosporine self-emulsifying formulation. *AAPS PharmSciTech* **2009**, *10*, 1388–1395. https://doi.org/10.1208/s12249-009-9340-0.

14. Kim, D.S.; Yang, E.S.; Yong, C.S.; Youn, Y.S.; Oh, K.T.; Li, D.X.; Kim, J.O.; Jin, S.G.; Choi, H.G. Effect of inorganic mesoporous carriers on 1-palmitoyl-2-linoleoyl-3-acetyl-rac-glycerol-loaded solid self-emulsifying drug delivery system: Physicochemical characterization and bioavailability in rats. *Colloids Surf. B. Biointerfaces.* **2017**, *160*, 331–336. https://doi.org/10.1016/j.colsurfb.2017.09.041.

15. Pawar, J.; Tayade, A.; Gangurde, A.; Moravkar, K.; Amin, P. Solubility and dissolution enhancement of efavirenz hot melt extruded amorphous solid dispersions using combination of polymeric blends: A QbD approach. *Eur. J. Pharm. Sci.* **2016**, *88*, 37–49. https://doi.org/10.1016/j.ejps.2016.04.001.

16. Wen, T.; Niu, B.; Wu, Q.; Zhou, Y.; Pan, X.; Quan, G.; Wu, C. Fenofibrate solid dispersion processed by hot-melt extrusion: Elevated bioavailability and its cell transport mechanism. *Curr. Drug Deliv.* **2019**, *16*, 538–547. https://doi.org/10.2174/1567201816666190122123044.

17. Rumondor, A.C.F.; Dhareshwar, S.S.; Kesisoglou, F. Amorphous solid dispersions or prodrugs: Complementary strategies to increase drug absorption. *J. Pharm. Sci.* **2016**, *105*, 2498–2508. https://doi.org/10.1016/j.xphs.2015.11.004.

18. Wegiel, L.A.; Mauer, L.J.; Edgar, K.J.; Taylor, L.S. Crystallization of amorphous solid dispersions of resveratrol during preparation and storage-Impact of different polymers. *J. Pharm. Sci.* **2013**, *102*, 171–184. https://doi.org/10.1002/jps.23358.

19. Wyttenbach, N.; Janas, C.; Siam, M.; Lauer, M.E.; Jacob, L.; Scheubel, E.; Page, S. Miniaturized screening of polymers for amorphous drug stabilization (SPADS): Rapid assessment of solid dispersion systems. *Eur. J. Pharm. Biopharm.* **2013**, *84*, 583–598. https://doi.org/10.1016/j.ejpb.2013.01.009.

20. Jain, S.; Patel, N.; Lin, S. Solubility and dissolution enhancement strategies: Current understanding and recent trends. *Drug Dev. Ind. Pharm.* **2015**, *41*, 875–887. https://doi.org/10.3109/03639045.2014.971027.

21. Schmied, F.P.; Bernhardt, A.; Engel, A.; Klein, S. A customized screening tool approach for the development of a self-nanoemulsifying drug delivery system (SNEDDS). *AAPS PharmSciTech* **2022**, *23*, 39. https://doi.org/10.1208/s12249-021-02176-7.

22. Schmied, F.P.; Bernhardt, A.; Moers, C.; Meier, C.; Endres, T.; Klein, S. A novel aminomethacrylate-based copolymer for solubility enhancement—From radical polymer synthesis to manufacture and characterization of amorphous solid dispersions. *Polymers* **2022**, *14*, 1281. https://doi.org/10.3390/polym14071281.

23. Pawar, J.; Suryawanshi, D.; Moravkar, K.; Aware, R.; Shetty, V.; Maniruzzaman, M. Study the influence of formulation process parameters on solubility and dissolution enhancement of efavirenz solid solutions prepared by hot-melt extrusion: A QbD methodology. *Drug Deliv. Transl. Res.* **2018**, *8*, 1644–1657. https://doi.org/10.1007/s13346-018-0481-0.

24. Cristofoletti, R.; Nair, A.; Abrahamsson, B.; Groot, D.W.; Kopp, S.; Langguth, P.; Polli, J.E.; Shah, V.P.; Dressman, J.B. Biowaiver monographs for immediate release solid oral dosage forms: Efavirenz. *J. Pharm. Sci.* **2013**, *102*, 318–329. https://doi.org/10.1002/jps.23380.

25. Knopp, M.M.; Nguyen, J.H.; Becker, C.; Francke, N.M.; Jørgensen, E.B.; Holm, P.; Holm, R.; Mu, H.; Rades, T.; Langguth, P. Influence of polymer molecular weight on in vitro dissolution behavior and in vivo performance of celecoxib: PVP amorphous solid dispersions. *Eur. J. Pharm. Biopharm.* **2016**, *101*, 145–151. https://doi.org/10.1016/j.ejpb.2016.02.007.

26. Homayouni, A.; Sadeghi, F.; Nokhodchi, A.; Varshosaz, J.; Garekani, H.A. Preparation and characterization of celecoxib solid dispersions; Comparison of poloxamer-188 and PVP-K30 as carriers. *Iran. J. Basic Med. Sci.* **2014**, *17*, 322–331.

27. Kawakami, K.; Sato, K.; Fukushima, M.; Miyazaki, A.; Yamamura, Y.; Sakuma, S. Phase separation of supersaturated solution created from amorphous solid dispersions: Relevance to oral absorption. *Eur. J. Pharm. Biopharm.* **2018**, *132*, 146–156. https://doi.org/10.1016/j.ejpb.2018.09.014.

28. Nguyen, C.N.; Pham, C.V.; Le Thien, G.; Ngoc, B.T.; Le Thi, H.; Huyen, C.P.T.; Thi, T.N. Immediate-released pelletized solid dispersion containing fenofibrate: Formulation, in vitro characterization, and bioequivalence studies in experimental beagle dogs. *Int. J. Pharm.* **2019**, *570*, 118661. https://doi.org/10.1016/j.ijpharm.2019.118661.
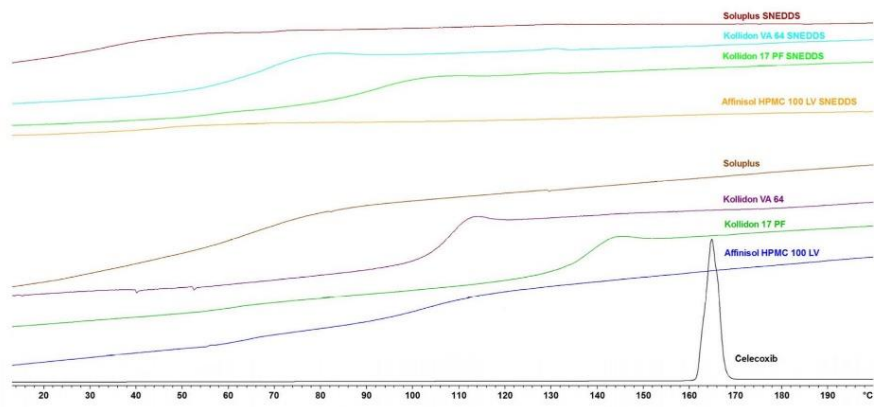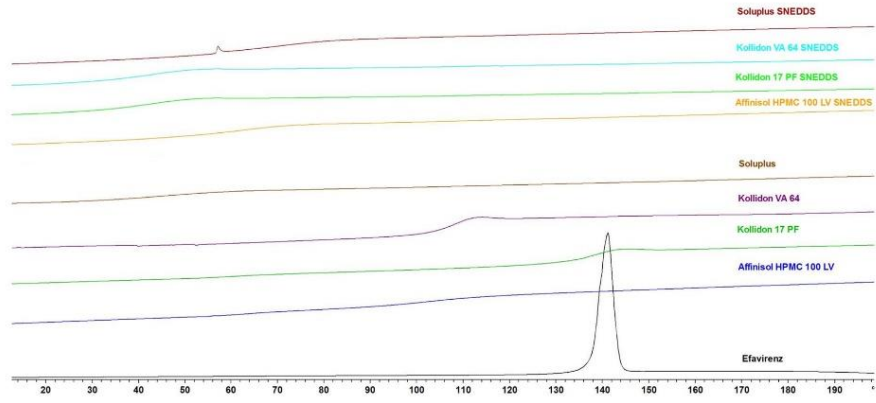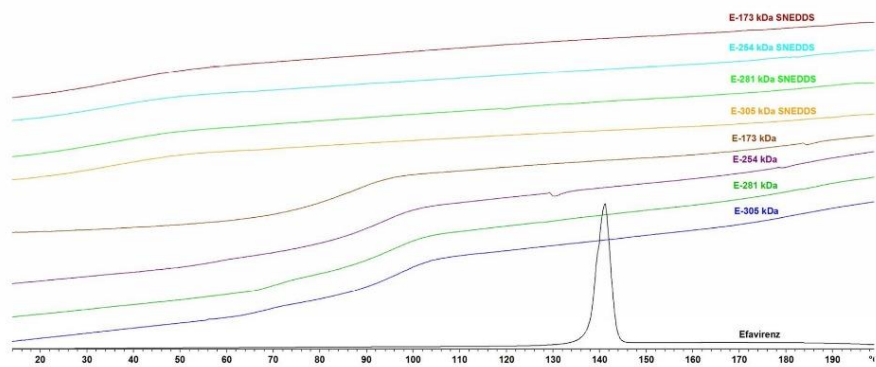
(a)
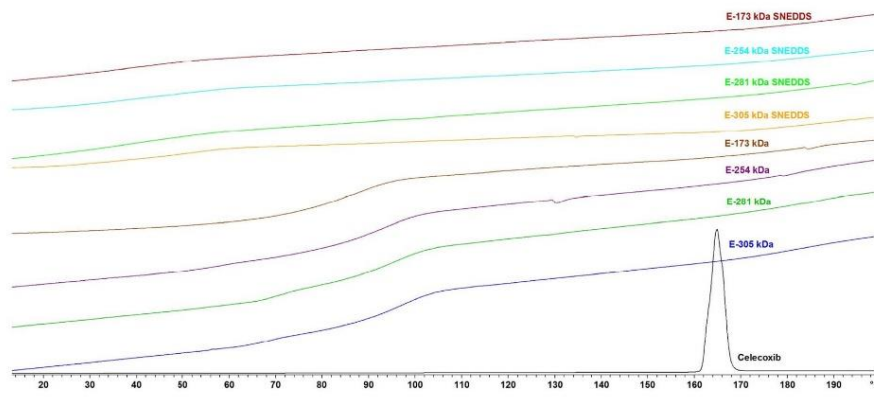
(b)

Figure S1. DSC thermograms of celecoxib, ModE copolymers, and the corresponding S-SNEDDS (a), celecoxib and other marketed (co)polymers used in the study, and the corresponding S-SNEDDS (b).

1

(a)

(b)

Figure S2. DSC thermograms of efavirenz, ModE copolymers, and the corresponding S-SNEDDS (a), efavirenz and other marketed (co)polymers used in the study, and the corresponding S-SNEDDS (b)
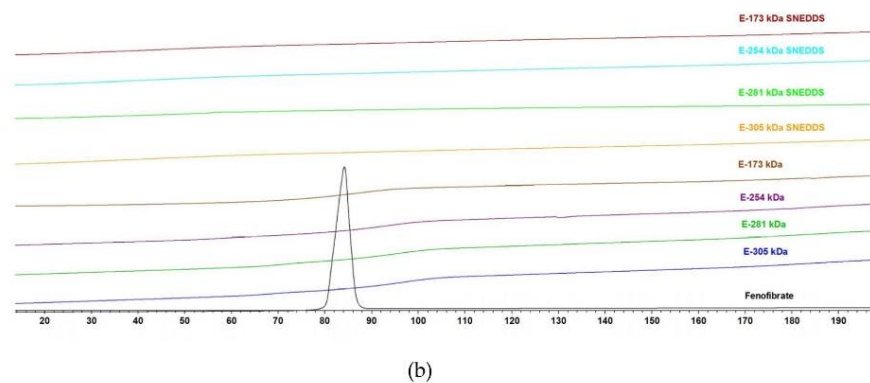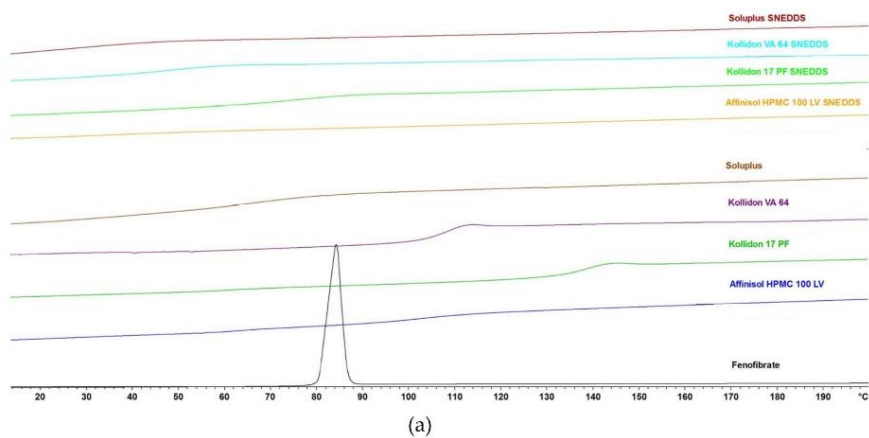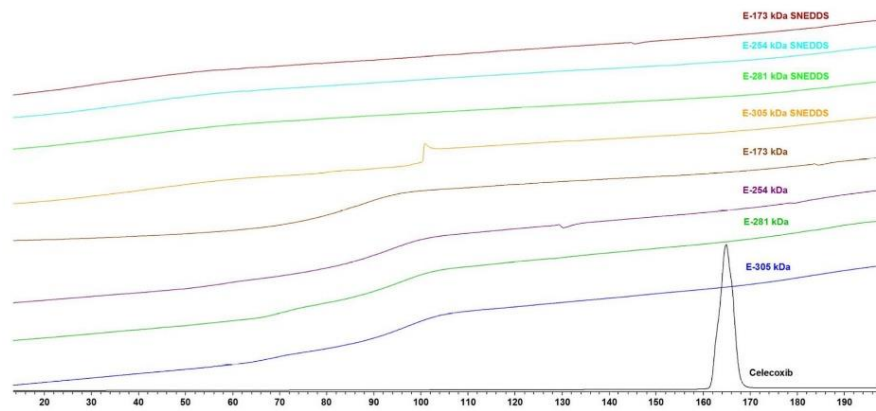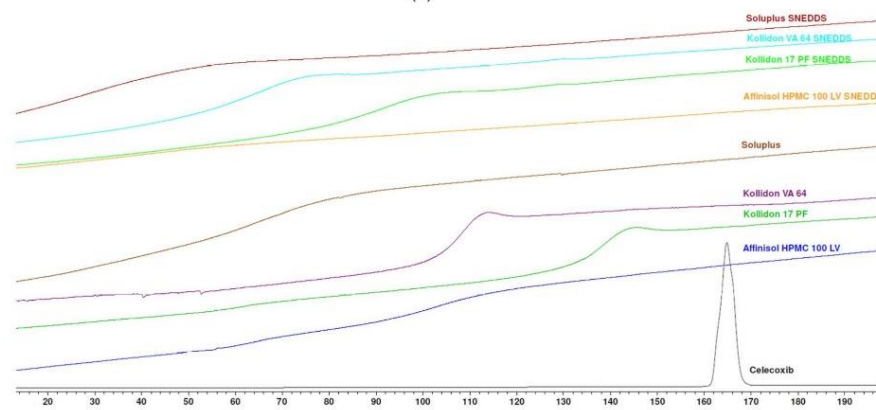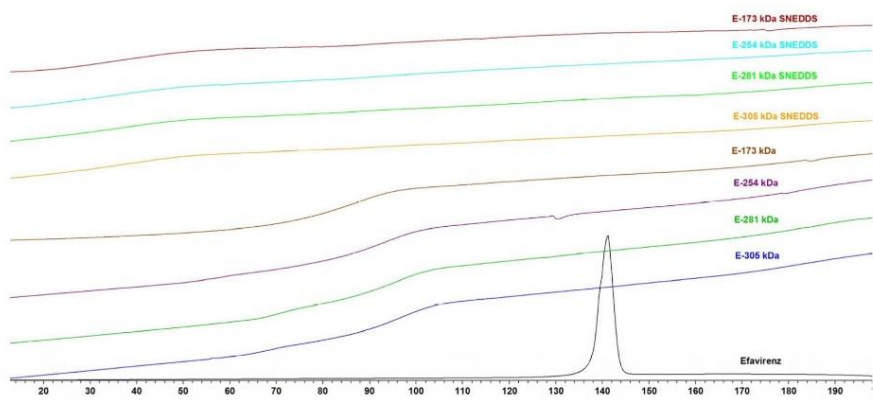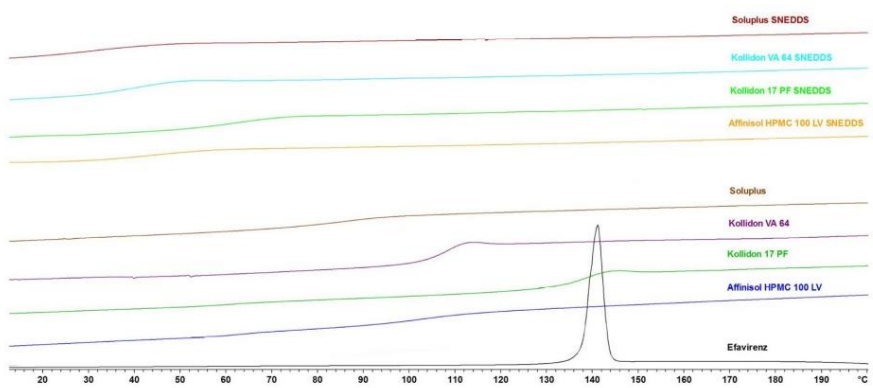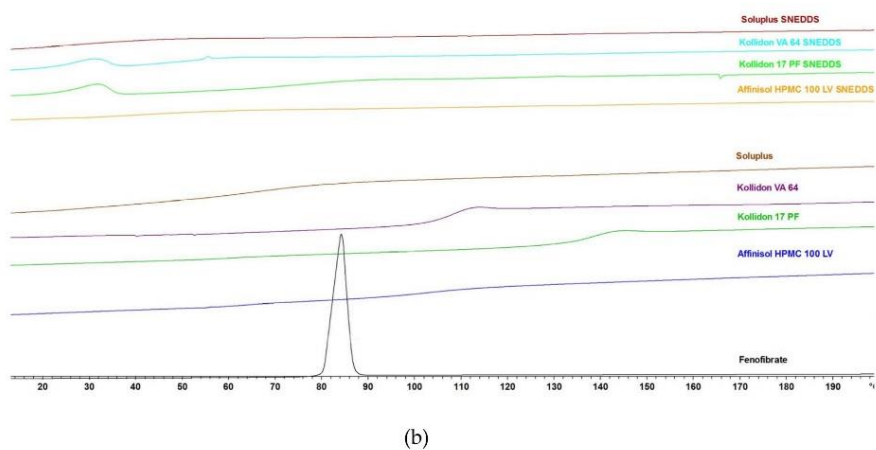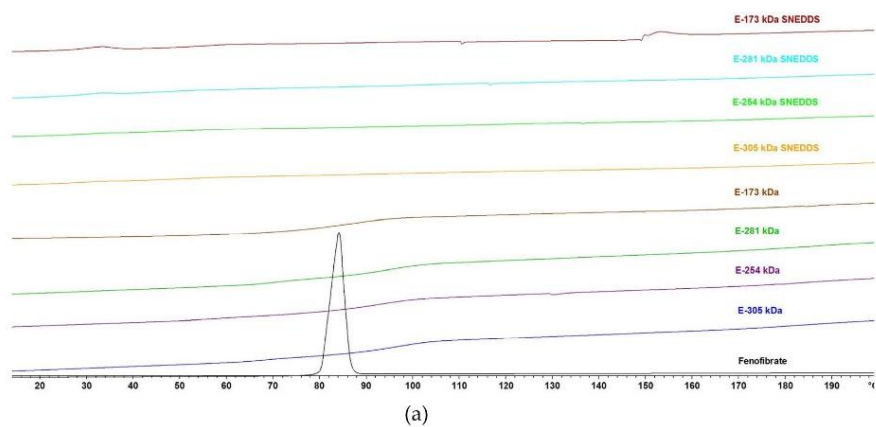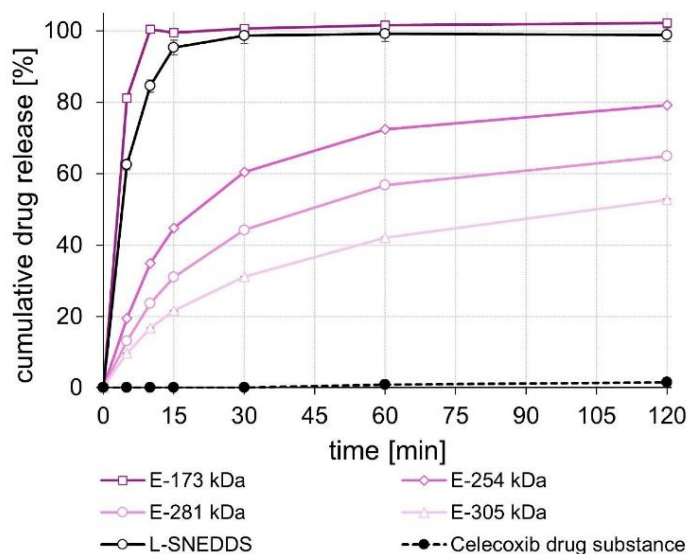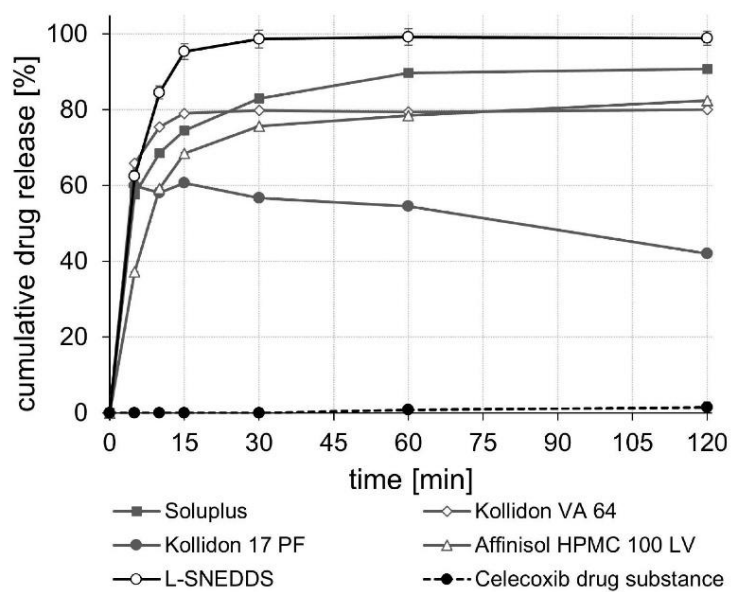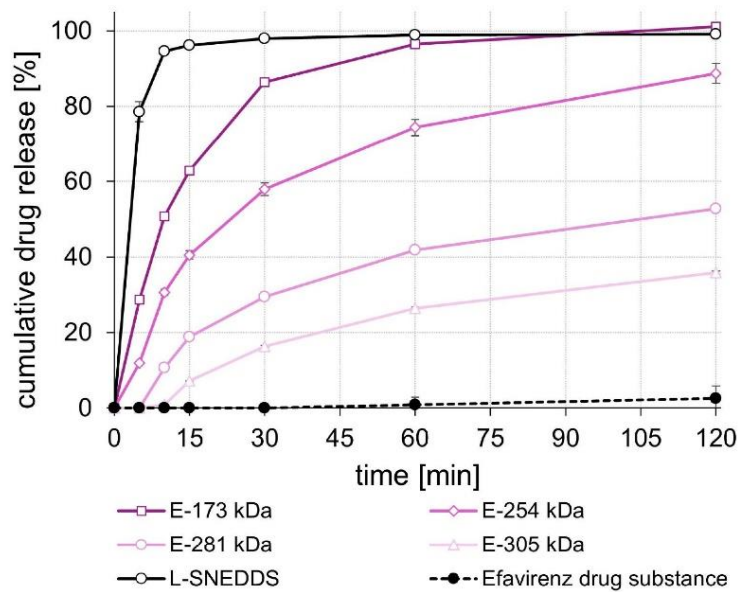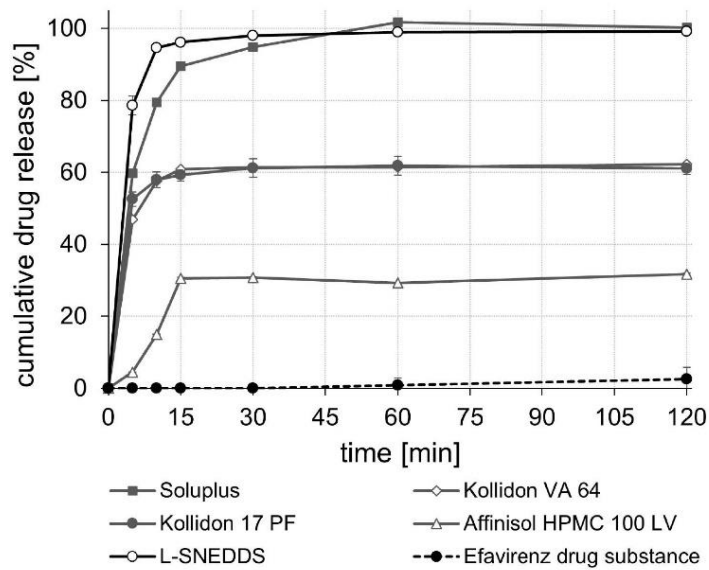
2

(a)

(b)

Figure S3. DSC thermograms of fenofibrate, ModE copolymers, and the corresponding S-SNEDDS (a), fenofibrate and other marketed (co)polymers used in the study, and the corresponding S-SNEDDS (b).

(a)

(b)

Figure S4. DSC thermograms (after six months of storage at 30 °C/65% RH) of celecoxib, ModE copolymers, and the corresponding S-SNEDDS (a), celecoxib and other marketed (co)polymers used in the study, and the corresponding S-SNEDDS (b).

4

(a)

(b)

Figure S5. DSC thermograms (after six months of storage at 30 °C/65% RH) of efavirenz, ModE copolymers, and the corresponding S-SNEDDS (a), efavirenz and other marketed (co)polymers used in the study, and the corresponding S-SNEDDS (b).

5

(a)

(b)

Figure S6. DSC thermograms (after six months of storage at 30 °C/65% RH) of fenofibrate, ModE copolymers, and the corresponding S-SNEDDS (a), fenofibrate and other marketed (co)polymers used in the study, and the corresponding S-SNEDDS (b).

6

(a)

(b)

Figure S7. Dissolution profiles of celecoxib drug substance and celecoxib L- and S-SNEDDS based on ModE (a), as well as celecoxib drug substance and celecoxib L- and S-SNEDDS based on other marketed (co)polymers (b) (after three months of storage at 30 °C/65% RH) in 500 mL 0.1 M HCl in USP apparatus II. Each value designates the mean ± S.D. (n = 3).

7

(a)

(b)

Figure S8. Dissolution profiles of efavirenz drug substance and efavirenz L- and S-SNEDDS based on ModE (a), as well as efavirenz drug substance and efavirenz L- and S-SNEDDS based on other marketed (co)polymers (b) (after three months of storage at 30 °C/65% RH) in 500 mL 0.1 M HCl in USP apparatus II. Each value designates the mean ± S.D. ($n = 3$).

8

(a)

(b)

Figure S9. Dissolution profiles of fenofibrate drug substance and fenofibrate L- and S-SNEDDS based on ModE (a), as well as fenofibrate drug substance and fenofibrate L- and S-SNEDDS based on other marketed (co)polymers (b) (after three months of storage at 30 °C/65% RH) in 500 mL 0.1 M HCl in USP apparatus II. Each value designates the mean ± S.D. ($n = 3$).

9

Index of publications

Manuscripts

F-P. Schmied, A. Bernhardt, A. Engel, S. Klein. A customized screening tool approach for the development of a self-nanoemulsifying drug delivery system (SNEDDS). *AAPS PharmSciTech*, 2022, 23(1): 39. DOI: 10.1208/s12249-021-02176-7.

F-P. Schmied, A. Bernhardt, V. Baudron, B. Beine, S. Klein. Development and characterization of celecoxib solid self-nanoemulsifying drug delivery system (S-SNEDDS) prepared using novel cellulose-based microparticles as adsorptive carriers. *AAPS PharmSciTech*, 2022, 23(6): 213. DOI: 10.1208/s12249-022-02347-0.

F-P. Schmied, A. Bernhardt, C. Moers, C. Meier, T. Endres, S. Klein. A novel aminomethacrylate-based copolymer for solubility enhancement – from radical polymer synthesis to manufacture and characterization of amorphous solid dispersions. *Polymers*, 2022, 14(7): 1281. DOI: 10.3390/polym14071281.

F-P. Schmied, A. Bernhardt, S. Klein. Preparation of solid self-nanoemulsifying drug delivery systems (S-SNEDDS) by co-extrusion of liquid SNEDDS and polymeric carriers – a new and promising approach to improve the solubility of poorly water-soluble drugs. *Pharmaceuticals*, 2022, 15(9): 1135. DOI: 10.3390/ph15091135.

Conferences

Poster presentations:

F-P. Schmied, A. Bernhardt, A. Engel, S. Klein. Self-microemulsifying drug delivery system (SMEDDS) for solubility enhancement – adsorption to a solid carrier.
3rd European Conference on Pharmaceutics, 2019 (Bologna, Italy)

F-P. Schmied, V. Baudron, B. Beine. Novel cellulose-based particles as an innovative, adsorptive carrier material for Solid-SNEDDS development.
12th World Meeting on Pharmaceutics, Biopharmaceutics and Pharmaceutical Technology, 2021 (Vienna, Austria (online))

F-P. Schmied, A. Bernhardt, A. Engel, S. Klein. A customized screening tool approach for the development of a self-nanoemulsifying drug delivery system (SNEDDS).
12th World Meeting on Pharmaceutics, Biopharmaceutics and Pharmaceutical Technology, 2021 (Vienna, Austria (online))

F-P. Schmied, A. Bernhardt, S. Klein. A new amino methacrylate copolymer for solubility improvement – from copolymer synthesis to development and characterization of amorphous solid dispersions.
13th World Meeting on Pharmaceutics, Biopharmaceutics and Pharmaceutical Technology, 2022 (Rotterdam, Netherlands)

F-P. Schmied, A. Bernhardt, S. Klein. Solid self-nanoemulsifying drug delivery system (S-SNEDDS) for solubility enhancement prepared by hot melt extrusion using a novel amino methacrylate copolymer.
13th World Meeting on Pharmaceutics, Biopharmaceutics and Pharmaceutical Technology, 2022 (Rotterdam, Netherlands)

Oral presentations:

F-P. Schmied. Self-microemulsifying drug delivery system (SMEDDS) for solubility enhancement – adsorption to a solid carrier.
Evonik conference entitled: Advanced Formulation Strategies and Manufacturing Approaches for Challenging Drugs, 2019 (Darmstadt, Germany)

F-P. Schmied, S. Klein. Solid self-nanoemulsifying drug delivery system (S-SNEDDS) for solubility enhancement.
Evonik conference entitled: Functional solid oral dosage forms, 2021 (Paris, France (online))

Patents

Solid particles containing solid primary particles of essentially native cellulose and optionally a binder, their production and use (EP3818974A1; WO2021094192A1).
Priority: 2019 – F-P. Schmied, G. Dürr, J. Tschernjaew, S. Schlegel-Kachel, J. Öhrlein

Solid self-nanoemulsifying drug delivery system (S-SNEDDS) (EP3915543A1; WO2021239798A1).
Priority: 2020 – F-P. Schmied, A. Engel, A. Bernhardt, T. Endres, C. Moers

Novel methacrylate copolymer and compositions comprising it (EP3916029A1; WO2021239787A1).
Priority: 2020 – F-P. Schmied, C. Moers, T. Endres, J.H. Schattka, K. Nollenberger

Solid SNEDDS based on a specific mixture of acrylic polymers (WO2022184549A1).
Priority: 2021 – F-P. Schmied, C. Moers, A. Bernhardt, M. Seibel

Solid SNEDDS based on salts of methacrylic copolymers (TBP).
Priority: 2021 – F-P. Schmied, C. Moers, A. Bernhardt

Eigenständigkeitserklärung

Hiermit erkläre ich, dass diese Arbeit bisher von mir weder an der Mathematisch-Naturwissenschaftlichen Fakultät der Universität Greifswald noch einer anderen wissenschaftlichen Einrichtung zum Zwecke der Promotion eingereicht wurde.

Ferner erkläre ich, dass ich diese Arbeit selbstständig verfasst und keine anderen als die darin angegebenen Hilfsmittel und Hilfen benutzt und keine Textabschnitte eines Dritten ohne Kennzeichnung übernommen habe.

_____

Fabian-Pascal Schmied

Acknowledgement

the present community, cross-thematic exchange of experimental knowledge, organizing and providing materials, introduction to the procedure of mentoring pharmaceutical students in the university laboratories as well as several great evenings in Greifswald.

Last but not least, very special thanks go to my lovely family, who supported me in every way at all times and encouraged me along the progress until the finalization of my PhD thesis.